

DOCTORAL THESIS

System Level Optimizations in Wearable Wireless Networks

Rida Khan

TALLINN UNIVERSITY OF TECHNOLOGY
DOCTORAL THESIS
10/2021

System Level Optimizations in Wearable Wireless Networks

RIDA KHAN



TALLINN UNIVERSITY OF TECHNOLOGY

School of Information Technologies

Thomas Johann Seebeck Department of Electronics

The dissertation was accepted for the defence of the degree of Doctor of Philosophy in Electronics and Telecommunication on 01 February 2021

Supervisor: Professor Muhammad Mahtab Alam,
Thomas Johann Seebeck Department of Electronics,
Tallinn University of Technology
Tallinn, Estonia

Opponents: Muhammad Ali Imran, Ph.D.,
Professor, James Watt School of Engineering,
Dean University of Glasgow UESTC
Glasgow, United Kingdom

Christos Verikoukis, Ph.D.,
Fellow Researcher
Telecommunications Technological Centre of Catalonia
Av. Carl Friedrich Gauss 7, 08860 Castelldefels, Spain

Defence of the thesis: 26 February 2021, Tallinn

Declaration:

Hereby I declare that this doctoral thesis, my original investigation and achievement, submitted for the doctoral degree at Tallinn University of Technology, has not been submitted for any academic degree elsewhere.

Rida Khan

signature



European Union
European Regional
Development Fund



Investing
in your future

Copyright: Rida Khan, 2021

ISSN 2585-6898 (publication)

ISBN 978-9949-83-662-8 (publication)

ISSN 2585-6901 (PDF)

ISBN 978-9949-83-663-5 (PDF)

Printed by Koopia Niini & Rauam

TALLINNA TEHNIKAÜLIKOOL
DOKTORITÖÖ
10/2021

Kantavate seadmete võrkude süsteemi tasemel optimeerimine

RIDA KHAN



Contents

List of Publications	7
Author's Contributions to the Publications	8
Abbreviations	9
List of Figures	11
List of Tables	12
1 Introduction	13
1.1 Background and Motivation	13
1.1.1 WBAN Standards and Technologies	13
1.1.2 Applications of WBAN	14
1.1.3 WBAN Application Requirements and Challenges	15
1.2 Problem Statement and Research Questions	17
1.3 Thesis Contributions	17
1.4 Thesis Organization	18
2 ETSI SmartBAN Performance Evaluation	20
2.1 Overview of ETSI SmartBAN	20
2.2 ETSI SmartBAN PHY-MAC Layer	20
2.2.1 ETSI SmartBAN Slot Structure	21
2.2.2 Slot Reassignment in ETSI SmartBAN	24
2.3 Performance Analysis of ETSI SmartBAN	25
2.3.1 Use-case Description	25
2.3.2 Channel Model Description	25
2.3.3 Numerical Results	27
3 Throughput and Channel Aware MAC ETSI SmartBAN	30
3.1 Dynamic MAC Scheduling Algorithms for ETSI SmartBAN	30
3.2 ETSI SmartBAN Complaint TCA MAC	31
3.2.1 Baseline TCA MAC Algorithm	31
3.2.2 TCA Implementation in ETSI SmartBAN	32
3.3 Modifications in Primary TCA MAC	34
3.3.1 Enhanced TCA MAC for ETSI SmartBAN	34
3.3.2 Channel Prediction based TCA MAC for ETSI SmartBAN	36
3.4 Performance Analysis	38
3.4.1 Packet Reception Rate	38
3.4.2 Energy Consumption	39
4 Flexible Enhanced Throughput and Reduced Overhead MAC for ETSI SmartBAN	41
4.1 Throughput Management Techniques in ETSI SmartBAN	41
4.1.1 Energy Consumption for PHY-MAC Overhead Transmission	42
4.1.2 Energy Consumption for Overhead Transmission in Slot Re-assignment	43
4.1.3 Energy Consumption for Payload Transmission	44
4.2 FETRO MAC Algorithm	44
4.2.1 Implementation of FETRO MAC in ETSI SmartBAN	44
4.2.2 IBI data transmission in FETRO MAC	45

4.3	Performance Evaluation	47
4.3.1	Throughput Analysis	49
4.3.2	Normalized Energy Consumption Analysis	49
5	Body-to-body Communication Channel Modeling	50
5.1	Limitations in Body-to-body Communication Channel Modeling	50
5.2	Biomechanical Mobility Modeling of Body-to-body Communication Channel	50
5.2.1	Static Channel Model	51
5.2.2	Biomechanical mobility model	52
5.2.3	Radio link model	53
5.3	Performance Analysis	54
5.3.1	Packet Reception Results	56
6	Conclusion	57
6.1	Future Work	57
	References	59
	Acknowledgements	63
	Abstract	64
	Kokkuvõte	66
	Appendix 1	69
	Appendix 2	85
	Appendix 3	103
	Appendix 4	121
	Appendix 5	137
	Appendix 6	145
	Appendix 7	163
	Appendix 8	171
	Curriculum Vitae	175
	Elulookirjeldus	177

List of Publications

- Publication I:** R. Khan and M. M. Alam. SmartBAN performance evaluation for diverse applications. In *EAI International Conference on Body Area Networks*, pages 239–251. Springer, 2019
- Publication II:** M. Hämäläinen, L. Mucchi, M. G. Genet, T. Paso, J. Farserotu, H. Tanaka, D. Anzai, L. Pierucci, R. Khan, M. M. Alam, and P. Dallemagne. ETSI SmartBAN architecture: the global vision for smart body area networks. *IEEE Access*, 7(10):100–107, 2020
- Publication III:** R. Khan and M. M. Alam. Joint throughput and channel aware MAC scheduling for SmartBAN. In *EAI International Conference on Body Area Networks*, pages 49–64, 2018
- Publication IV:** R. Khan, M. M. Alam, T. Paso, and J. Haapola. Throughput and channel aware MAC scheduling for SmartBAN standard. *IEEE Access*, 7:63133–63145, 2019
- Publication V:** R. Khan, M. M. Alam, and A. Kuusik. Channel prediction based enhanced throughput and channel aware MAC in SmartBAN standard. In *2019 16th International Symposium on Wireless Communication Systems (ISWCS)*, pages 463–468. IEEE, 2019
- Publication VI:** R. Khan, M. M. Alam, and M. Guizani. A flexible enhanced throughput and reduced overhead (FETRO) MAC protocol for ETSI SmartBAN (Accepted). *IEEE Transactions on Mobile Computing (Early Access)*
- Publication VII:** R. Khan and M. M. Alam. Joint PHY-MAC realistic performance evaluation of body-to-body communication in IEEE 802.15. 6 and SmartBAN. In *12th International Symposium on Medical Information and Communication Technology (ISMICT)*, pages 1–6. IEEE, 2018
- Publication VIII:** R. Khan and M. M. Alam. Body-to-body communication: Applications, system design aspects and performance evaluation. In *12th International Symposium on Medical Information and Communication Technology (ISMICT)*, pages 1–2. IEEE, 2018

Author's Contributions to the Publications

The author's contributions to the publications in this thesis are:

1. The author characterized the wireless body area networks (WBANs) use-cases into three categories according to their respective throughput requirements, as low, medium and high data rate applications. The author investigated the ETSI SmartBAN physical (PHY) and medium access control (MAC) layers to handle the variations in data rate requirements of these WBAN use-cases, while satisfying the other quality of service (QoS) parameters like packet reception rate (PRR) and latency. The author performed simulations for the ETSI SmartBAN PHY and MAC layers and provided the performance analysis for various WBAN applications in 2 and 2. The author wrote the 2 and was a co-author in the 2 while the supervisor helped with the revision by giving feedback.
2. The author proposed the ETSI SmartBAN complaint throughput and channel aware (TCA) MAC algorithm to improve the PRR and energy efficiency in ETSI SmartBAN. The algorithm is based on the dynamic scheduling of the WBAN traffic according to the channel quality and data rate of WBAN nodes. Moreover the author proposed several enhancements in the existing TCA algorithm to further improve the energy consumption profile. Finally, channel prediction was also introduced in baseline ETSI SmartBAN TCA MAC, to improve the PRR and energy efficiency performance. To comprehend these contributions, the author wrote the 3, 3 and 3. The supervisor helped with the revision by giving feedback.
3. The author investigated the two primary methods of throughput management in ETSI SmartBAN MAC, namely extra slot allocation and slot reassignment, to handle the massive data rate variations in the WBAN sensor nodes traffic. The author proposed an innovative and "flexible" enhanced throughput and reduced overhead (FETRO) scheduled access MAC protocol with variable slot length. In FETRO MAC algorithm, the assigned slot durations are distinctive to the data rate requirements of the individual sensors. The author performed the MATLAB simulations for the performance evaluation of both the fixed slot length MAC strategies and the variable slot duration FETRO MAC. The author wrote the 4 and the supervisor provided feedback to improve the paper quality.
4. The author also integrated the existing body-to-body (B2B) communication channel model with the bio-mechanical mobility model. In the available literature, the B2B channels were modeled assuming the restricted mobility scenarios using the measurement campaigns. The author generated the mobility traces for multiple co-located WBANs which provide dynamic distances with space-time variations. These dynamic distances serve to provide the realistic path-losses for B2B links under different mobility profiles. The bio-mechanical mobility modeling of the B2B channels helped in the realistic joint PHY-MAC performance evaluation of IEEE 802.15.6 and ETSI SmartBAN. The author performed the simulations and wrote 5 and 5. The supervisor helped by providing feedback to improve the paper quality.

Abbreviations

WBAN	Wireless Body Area Network
WSN	Wireless Sensor Network
BLE	Bluetooth Low Energy
ETSI	European Telecommunication Standards Institute
MBAN	Medical Body Area Network
CSMA-CA	Carrier Sense Multiple Access with Collision Avoidance
MAC	Medium Access Control layer
MUA	Multi-use Channel Access
ECG	Electrocardiogram
EEG	Electroencephalogram
EMG	Electromyogram
QoS	Quality-of-Service
BER	Bit Error Rate
PER	Packet Error Rate
API	Application Programming Interface
ISM	Industrial,Scientific and Medical Band
CCH	Control Channel
DCH	Data Channel
C-Beacon	Control Channel Beacon
D-Beacon	Data Channel Beacon
GFSK	Gaussian Frequency Shift Keying
BCH	Bose-Chaudhuri Hocquenghem
BT	Bandwidth-bit Period Product
CM	Control and Management
IBI	Inter-Beacon Interval
SAP	Scheduled Access Period
IFS	Inter-Beacon Interval
PPDU	Physical-Layer Protocol Data Unit
PSDU	Physical-Layer Service Data Unit
PLCP	Physical-Layer Convergence Protocol
MPDU	MAC-Layer Protocol Data Unit
AWGN	Additive White Gaussian Noise
LOS	Line of Sight
NLOS	Non-Line of Sight
PRR	Packet Reception Rate
MAP	Managed Access Phase
RAP	Random Access Phase
TCA	Throughput and Channel Aware MAC
ISDM	Improved Supplementary Downlink Mode
LEDM	Limited Exhaustive Downlink Mechanism
FEDM	Fully Exhaustive Downlink Mechanism
SNR	Signal-to-Noise Ratio
AR	Autoregressive
ACF	Autocorrelation Function

FETRO	Flexible Enhanced Throughput and Reduced Overhead MAC
B2B	Body-to-Body Communication
LT	Long Term Fading
ST	Short Term Fading
DBPSK	Differential Binary Phase Shift Keying
DQPSK	Differential Quadrature Phase Shift Keying

List of Figures

1	WBAN Architecture	13
2	Thesis Organization	19
3	IBI Format without PPDU Repetitions	22
4	IBI Format with two PPDU Repetitions	22
5	Slot reassignment in SmartBAN	24
6	Packet reception rate (%) analysis of ETSI SmartBAN w.r.t transmission power (dBm).	28
7	Throughput (kbps) analysis of ETSI SmartBAN w.r.t transmission power (dBm).	28
8	TCA MAC Algorithm	32
9	TCA Execution in SmartBAN	33
10	Enhanced TCA MAC	34
11	Channel Prediction based Enhanced TCA MAC	37
12	Packet reception rate (%) comparison of baseline TCA MAC with ETSI SmartBAN reference MAC.	38
13	Packet reception rate (%) analysis of TCA MAC variants.	39
14	Energy consumption per successful transmission (mJ) for TCA MAC variants.	39
15	Hub energy consumption per successful transmission (mJ) for TCA MAC variants.	40
16	FETRO MAC Connection Initialization	46
17	IBI Transmission in FETRO MAC	46
18	Throughput analysis of ETSI SmartBAN MAC and FETRO MAC	47
19	Node energy consumption (mJ) per kbps analysis of ETSI SmartBAN MAC and FETRO MAC	48
20	Hub energy consumption (mJ) per kbps analysis of ETSI SmartBAN MAC and FETRO MAC	48
21	Mobility, channel and radio link modeling for B2B communication	53
22	Packet reception rate (%) w.r.t transmission power level in body-to-body communication	56

List of Tables

1	Comparison of WBAN-specific Standard	15
2	Requirements for WBAN Sensors	16
3	ETSI SmartBAN PHY-MAC Parameters	23
4	Payload size (bytes) in ETSI SmartBAN	23
5	SmartBAN use-cases	26
6	Packet Reception Rate for B2B channels	55

1 Introduction

Recent advancements in wireless communication and miniaturization of sensor devices have led to the emergence of wearable and implanted sensors as well as their derivative technologies like Wireless Body Area Network (WBAN). The WBANs are a specific case of the Wireless Sensor Networks (WSNs) that deal with human body-centric medical or consumer electronics [22] applications. A typical WBAN consists of inter-connected battery-powered, invasive or non-invasive and light-weight tiny nodes such as sensors which can gather specific data like vital signs, body posture and environmental parameters in real time (requires timely access of sensor data) or non-real time (the sensor information can be transmitted later for data analysis). The sensor nodes have wireless communication capabilities and send the obtained information to a sink node, known as network coordinator, gateway or the hub node. The WBAN coordinator forwards this information to the remote server via an access point or base station for continuous long term monitoring. Moreover the coordinator also executes the control and management functions of a given WBAN. Further information analysis of the WBAN data is performed at the remote server and an optional feedback is generated accordingly [54]. Other than sensor nodes, there are WBAN actuators as well which perform specific actions according to the perceived WBAN data and the generated feedback. The WBAN includes optional relay nodes as well which assist in forwarding the sensor data to the coordinator if the direct on-body link is shadowed. Fig. 1 depicts the general WBAN architecture as explained in the text above.

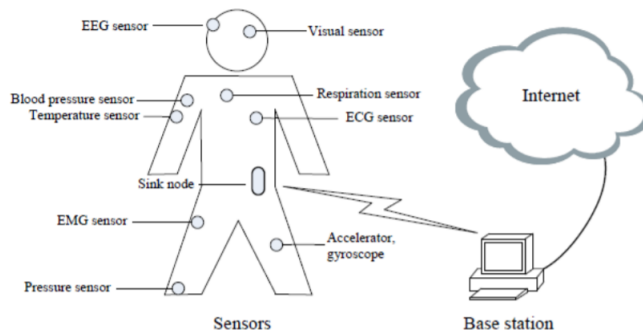


Figure 1 - WBAN Architecture [35].

1.1 Background and Motivation

Wireless technologies have a great potential to be implemented in future healthcare systems which introduce the vision of remote health monitoring and telemedicine. Many diseases and their detrimental after effects can be prevented by providing proactive healthcare systems, employing wearable monitoring systems with low-power, miniaturized and resource constrained sensor devices for early detection of abnormal conditions.

1.1.1 WBAN Standards and Technologies

The existing radio technologies for wireless personal area networks (WPANs), such as Bluetooth (IEEE 802.15.1), Zigbee (IEEE 802.15.4) and UWB (IEEE 802.15.4a), are not well-suited to be implemented in wearable systems because of their substantially higher levels of power consumption and the consequently reduced battery life. In addition, Bluetooth low

energy (BLE) dominates the existing implemented standards in WBANs but the standard allows the star-bus type of topology with a size of up to eight devices per Piconet, power consumption of the order of 10mW and no particular channel access mechanism for emergency traffic [23]. In order to address these shortcomings, IEEE introduced the first WBAN-specific standard named IEEE 802.15.6 in 2012 [2]. Later in 2015, European Telecommunication Standards Institute (ETSI) proposed another set of guidelines for WBAN, known as ETSI SmartBAN standard [5]. Medical BAN (MBAN) provides another set of instructions for WBAN functioning.

MBAN standard, though being dedicated to medical applications and being functional in quiet ISM band, has only fifteen available channels and low data rate. These attributes make MBAN inefficient for dense WBAN deployments and high data rate sensors. Moreover, the MBAN application environment ought to be far away from the application of e.g. wireless sensors used for machine automation in a factory environment [1]. IEEE 802.15.6 standard has a rather complicated channel access mechanism with different beacon and non-beacon modes [2] which impedes the development and availability of the standard compliant devices. Furthermore, IEEE 802.15.6 standard has significantly high synchronization overhead and physical layer header. The provision of carrier sense multiple access with collision avoidance (CSMA-CA) for channel access at the medium access control (MAC) layer in both MBAN and IEEE 802.15.6 standards also may lead to higher power consumption and shorter battery life time. In comparison, ETSI SmartBAN standard provides the best data payload to physical and MAC overhead ratio in comparison to MBAN and IEEE 802.15.6 standards. The specifications for IEEE 802.15.6, ETSI SmartBAN and MBAN standards are indicated in the table 1 in terms of different physical (PHY) and MAC layer parameters.

1.1.2 Applications of WBAN

Among the prospective WBAN applications, healthcare is the most promising field. Several non-intrusive sensors deployed inside or on the human body allow the patients and the doctors to sample continuous waveform of biomedical signals in a remote and continuous fashion. Events that require prompt assistance like heart attack and epileptic seizure, can be detected and even foreseen through the continuous monitoring of the heart and brain activity, respectively. WBANs cannot only detect fatal events and anomalies, they can also improve the life style of hearing and visually impaired people by means of cochlear implant and artificial retina, respectively. The following is a non-exhaustive list of applications that can benefit from WBAN usage: electrocardiogram (ECG), electroencephalogram (EEG), electromyogram (EMG), pulse oximetry, drugs delivery, post operative and temperature monitoring, glucose level, toxins, blood pressure, etc. [41], [27]. A real-time log of vital parameters like blood pressure, heart beat, blood oximetry and posture can improve fitness and sport experiences. In this way users can gather information concerning their sport activity and utilize that information for preventing injuries and planning future training to improve their performance. WBANs bring more realism to the user experience in the field of entertainment as well. Motion capturing techniques make it possible to track the position of different body parts by means of a network of gyroscopes and accelerometers, wirelessly connected to a central node and worn by the user. The real-time information about the motion allows the user to utilize ones body as a controller in video games. Moreover, film industry takes advantage of motion capture along with post production techniques to realise highly realistic digital movies where actors play the role of non-human subjects [21]. New capabilities added by a WBAN will enhance the performance, at both individual and squad level, of soldiers engaged in mil-

Table 1 – Comparison of IEEE 802.15.6, MBAN and ETSI SmartBAN standards

Parameters	IEEE 802.15.6 (Narrowband)	MBAN	ETSI SmartBAN
Network Topology	One-hop/two-hop star topology	Star and peer-to-peer	Star and relay
Hub-to-hub Communication	Not specified	Allowed	Allowed
Operating Frequency [MHz]	2360-2400, 2400-2483.5	2360-2400	2401-2481
PHY-layer Overhead [bits]	121	48	56
MAC-layer Overhead [bits]	72	40-312	72
Channel Bandwidth [MHz]	1	2	2
No: of Channels	39 and 79	15	40 (3 control, 37 data)
Repetition/Spreading	2x/4x spreading and interleaving	Direct sequence spread spectrum	2x/4x repetition
Modulation	$\pi/2$ -DBPSK, $\pi/4$ -DQPSK	OQPSK	GMSK (BT=0.5, h=0.5)
Information Rate [kbps]	91.9-971.4	250	220-1000
Channel Access	CSMA/CA, Scheduled and Unscheduled, Type I/II Polling Access	Slotted CSMA/CA, ALOHA, Guaranteed time slot (for emergency traffic)	Scheduled TDMA, Slotted ALOHA, Multiuse Channel Access (MUA)
MAC Payload	256 bytes	127 bytes	Up to 2430 bytes

itary operations. At individual level, a set of sensors can monitor vital parameters and communicate information about the surrounding environment in order to avoid threats. Whereas the information retrieved at the squad level will enable the commander to coordinate the squad actions and tasks more effectively. Spatial localisation techniques and communication between different WBANs (inter-WBAN communications) also play a vital role in this field as well as provide security in order to prevent sensitive information from being caught by the enemies [48].

1.1.3 WBAN Application Requirements and Challenges

Developing a WBAN is a challenging task because of the broad range of requirements imposed by the above mentioned applications. The bit rate requirements vary significantly depending on the application and on the type of data to be transmitted. The required data rate ranges from a few bits per second (e.g., temperature monitoring) to 10 Mbps (e.g., video streaming). The bit rate can refer to a single link or to multiple links, when several devices transmit/receive information to/from one coordinator at the same time (e.g., multiple leads ECG). High level of QoS and reliability should also be guaranteed in medical and military applications. Appropriate error correction and interference-avoidance methods should be implemented at MAC and PHY layers to reduce the bit error rate (BER). The li-

cense free industrial, scientific and medical (ISM) band utilized by WBAN is overcrowded and the standards like Wi-Fi (IEEE 802.11), Bluetooth (IEEE 802.15.1), ZigBee (IEEE 802.15.4) and other standards operate in this band. Many WBAN applications (e.g., medical applications) require very high reliability especially when an emergency or alarm traffic has to be established, therefore techniques to avoid or reduce interference should be studied and implemented [40]. Other important parameters also include the end-to-end delay, delay variations and the capability to provide fast and reliable reaction to emergency situations [55]. The communication range should not be larger than few meters for most of the applications. Therefore a simple star topology is usually enough for WBAN transmissions but the human body can represent an obstacle itself for the radio propagation, especially for the implanted nodes. In this case, a multi-hop communication must be established and a relaying technique should be accounted for in order to exploit node spatial diversity. The number of nodes forming the WBAN ranges from two (e.g., glucose meter) to ten and can vary at run time [20]. Therefore, the network should implement reliable association and disassociation procedures to facilitate the nodes join and leave the network as needed by the application. The power consumption requirement is also very dependent on the nature of the application. However, WBAN devices are generally battery-powered and in case of implants, the battery lifetime is required to be up to several years for implanted devices. A common technique for energy conservation at the expense of end-to-end delay is lowering the duty cycle, which allows devices to be in sleep mode (transceiver and CPU shut down) for most of the time. This solution is effective for applications that require infrequent transmissions, however, a proper trade-off between delay and power consumption should be found. A good radio channel characterization is also important in WBAN performance evaluation since the WBAN channels are mainly dominated by the human body shadowing. Security in WBAN communication is also of primary importance, especially for medical and military applications. The WBAN security should be addressed in terms of privacy, confidentiality, authorisation, and integrity [43]. Table 2 sums up the bit-rate and delay requirements for different WBAN sensor types.

Table 2 – Requirements for WBAN Sensor.

Application	Bit Rate	Delay
Deep brain stimulation	< 320 kbps	< 250 ms
Drug delivery	< 16 kbps	< 250 ms
Capsule endoscope	1 Mbps	< 250 ms
ECG	192 kbps	< 250 ms
EEG	86.4 kbps	< 250 ms
EMG	1.536 Mbps	< 250 ms
Glucose level monitor	< 1 kbps	< 250 ms
Audio streaming	1 Mbps	< 20 ms
Video streaming	< 10 Mbps	< 100 ms
Voice	50 - 100 kbps	< 100 ms

1.2 Problem Statement and Research Questions

The WBAN application requirements and operating scenarios, as discussed in the previous sub-section impose a unique set of challenges in WBAN design and implementation, given as follows:

- A good radio channel characterization is mandatory in the context of WBAN communication since the presence of human body and on-body node position affect WBAN channel characteristics. WBAN channels are highly dominated by the impact of human body shadowing and therefore, the channel properties not only vary significantly from one super-frame to the other but for the different on-body links as well. So far, the current literature covers the on-body communication channel modeling in detail but the research work on body-to-body channel modeling is insufficient and does not consider the realistic human mobility patterns.
- There are massive variations in the bit rate requirements in the prospective WBAN applications. The data rates are determined by the sensor type, sample rate and bit resolution of each data sample to be transmitted. For example, in “Rescue and Emergency Monitoring” use case, both low data rate measurements like GPS and pulse monitoring (few bps data rate) as well as high data rate voice communication (upto 100 Kbps) are required [31]. It becomes difficult to manage the different sensor rates while facilitating reliable transmission through the existing WBAN technologies.
- WBAN devices are generally battery-powered and the battery lifetime is supposed to be up to several years, especially for implanted devices. Therefore, for energy preservation, the maximum allowed transmission power level in WBAN communications is 0dBm. It becomes quite challenging to provide reliable WBAN communication given the adverse channel conditions and low transmission power levels.

These challenges narrow-down the PhD thesis investigation to answer the following research questions:

1. How to design a flexible MAC protocol for addressing the variety of data rate requirements from different WBAN applications?
2. How to improve the WBAN throughput and reliability for different applications while ensuring the low energy consumption?
3. How to optimize re-transmissions and packet overheads?
4. How to manage the impact of human mobility on channel and radio link modeling?
5. How to ensure ultra low power communication under different data transmission rates and packet sizes?

1.3 Thesis Contributions

In order to derive the solution for the aforementioned problems in WBAN and answer the related research questions, this thesis makes the following contributions.

1. At first, a comprehensive discussion about the ETSI proposed WBAN standard, i.e. SmartBAN, is provided in terms of its PHY-MAC structure and specifications. Then, a detailed performance evaluation of ETSI SmartBAN PHY-MAC is carried out using the realistic channel models for different WBAN use-cases, categorized by their

data rate requirements [Publication I and Publication II]. This contribution helps in comprehending the key parameters and settings of ETSI SmartBAN PHY-MAC that are required to achieve a certain QoS for the given use-case.

2. For improving the WBAN communication reliability at lower transmission power levels, a SmartBAN compliant throughput and channel aware (TCA) MAC algorithm is presented which is easily applicable to the ETSI SmartBAN PHY-MAC structure. The algorithm examines the WBAN channels conditions and the data packet availability/node priority before allocating the MAC resources for the packet transmission by WBAN sensor nodes. The primary TCA algorithm is also modified to make several improvements which lead to the higher energy efficiency and transmission reliability. By improving the reliability during the first packet transmission, the re-transmissions of the identical data are also reduced, decreasing the energy consumption in packet re-transmissions [Publication III, Publication IV and Publication V]. The results provided in this contribution indicate a significant performance gain of the SmartBAN-compliant TCA algorithm in terms of packet reception rate (PRR) and energy efficiency over the reference SmartBAN MAC scheduling. The average improvement in PRR results is approximately 40% whereas a maximum enhancement of 66% is observed in terms of energy efficiency, while satisfying the throughput and latency requirements of the use-case considered during simulations.
3. Another contribution of this thesis is the design of a novel and flexible MAC protocol which is based on the variation of the transmission slot sizes as per the data rate requirements of the individual sensor nodes. The proposed MAC algorithm, flexible enhanced throughput and reduced overhead (FETRO) MAC, is shown to both improve the attainable throughput and the decrease the energy wasted in overheads transmission [Publication VI]. The FETRO MAC algorithm proposed in this contribution gives an average reduction of 65.5% and 59.16%, respectively, in the normalized overhead energy consumption per Kbps outcomes at both the hub and nodes, as compared to the de-facto ETSI SmartBAN MAC scheduling strategies.
4. The last and the secondary contribution of this thesis is the biomechanical mobility-based channel modeling of the body-to-body (B2B) communication links under the unrestricted mobility scenarios. After the channel modeling, the PHY-MAC performance evaluation of both the IEEE 802.15.6 and ETSI SmartBAN is also elaborated for B2B channels [Publication VII and Publication VIII]. Consequently, transmission power, packet length and data rate variations are investigated and the obtained results of PRR identify “head” as the best position to place the coordinator nodes for B2B communication.

1.4 Thesis Organization

The rest of this thesis is structured as follows:

Chapter 2: The second chapter details the ETSI smartBAN standard specifications and the functional description as well as its PHY-MAC performance evaluation.

Chapter 3: The third chapter describes the TCA MAC for ETSI SmartBAN standard with full compliance to the standard specifications. Moreover, the detailed information about the several enhancements in the primary TCA algorithm and PHY-MAC performance results are also depicted.

Chapter 4: This chapter includes the explanation of the FETRO MAC algorithms and its implement in the ETSI SmartBAN standard along with the performance results.

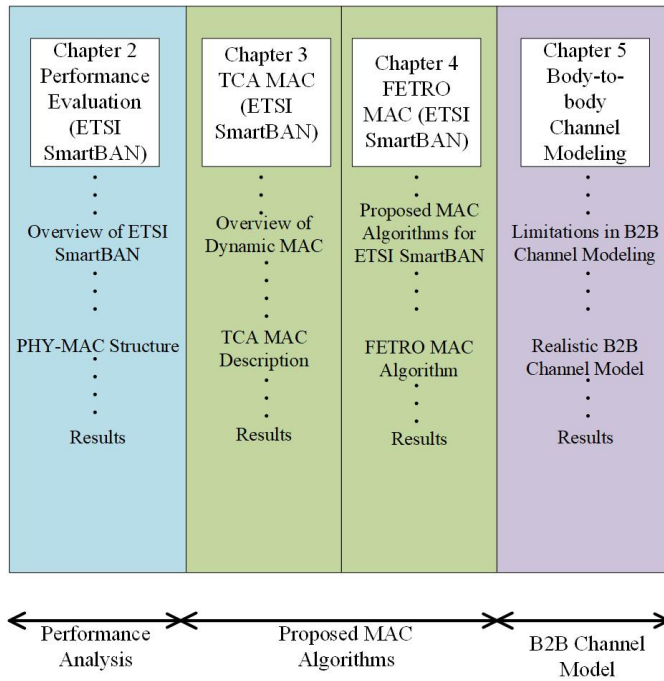


Figure 2 - Thesis Organization.

Chapter 5: The fifth chapter provides the explanation about the realistic channel modeling for B2B communication scenarios and the related PHY-MAC performance.

Chapter 6: This chapter concludes the thesis with the final remarks about each contribution.

Fig 2 shows the pictorial representation of the main contributions and primary topics as progressed chapter-wise in the thesis.

2 ETSI SmartBAN Performance Evaluation

In this chapter, ETSI SmartBAN standard specifications, the functional details at PHY-MAC layers and the PHY-MAC performance evaluation are described. At first, a brief overview of the main features enabled in ETSI SmartBAN standard is presented and then ETSI SmartBAN PHY and MAC layer operations are explained in detail. Finally, the performance evaluation of ETSI SmartBAN is carried on using the standardized WBAN channel model descriptions and considering the implemented WBAN use-case.

This chapter is based on the following publications.

- R. Khan and M. M. Alam. SmartBAN performance evaluation for diverse applications. In *EAI International Conference on Body Area Networks*, pages 239–251. Springer, 2019
- M. Hämäläinen, L. Mucchi, M. G. Genet, T. Paso, J. Farserotu, H. Tanaka, D. Anzai, L. Pierucci, R. Khan, M. M. Alam, and P. Dallemagne. ETSI SmartBAN architecture: the global vision for smart body area networks. *IEEE Access*, 7(10):100–107, 2020

2.1 Overview of ETSI SmartBAN

The primary WBAN features addressed in ETSI SmartBAN standard contain unified data representation formats and semantics, heterogeneity and interoperability management, RF environment measurement and modeling, low complexity MAC layer and enhanced ultra-low power PHY layer. An extensive view of WBANs is included in ETSI SmartBAN standard from lower layer (such as PHY and MAC layers) to higher level user-interface and end-to-end connectivity [5]. SmartBAN semantic open data model, unified data representation formats and corresponding ontology are determined along with the extensible semantic metadata for SmartBAN entities. The standard draft also covers other related information such as the description about sensor/actuator/relay/hub as well as their measured data values. The standardized SmartBAN end-to-end architecture depends upon the SmartBAN semantic data model this reliance facilitates the WBAN smart control, neighboring WBAN discovery, and inter-networking functionalities. The SmartBAN end-to-end architecture design also encompasses the specification and perception of the application programming interfaces (APIs) which allow data access and monitoring, regardless of the radio technologies implemented at the lower layers [25].

SmartBAN proposes star topology-based WBAN architecture with the sensor nodes centralized around a hub, which can be a hand-held device or smart watch with enhanced functionalities. A central hub is the core device in SmartBAN, which controls and manages all the WBAN functioning. SmartBAN can be envisioned as a smart solution in the sense that it merges most of its operations to hub, allowing node implementation to be very straightforward. This also leads to a reduced implementation cost and energy consumption for the battery-powered sensor nodes. The options for multi-hop relay and hub-to-hub communications are also being considered to improve the usability of the SmartBAN devices in the upcoming standard revision(s).

2.2 ETSI SmartBAN PHY-MAC Layer

The SmartBAN PHY layer specification includes two different channel categories operating in the 2.4 GHz unlicensed industrial, scientific and medical (ISM) frequency band; Control Channels (CCH) and Data Channels (DCH). The broadcasting of control channel beacon (C-Beacon) by the Hub is accomplished using the CCH. The sensor data as well as the control

and management (CM) information between the Hub and the sensor nodes are transmitted using the DCH. Both the DCH and CCH channels are implemented in a single RF chain. The provision of separate CCH and DCH sets up faster channel acquisitions and simplifies the MAC layer operations. The CCH only supports in the discovery of neighbouring WBANs by a sensor node and once the sensor node joins a SmartBAN, all the communication between the hub and node occurs on data channel. In ETSI SmartBAN standard, the entire spectrum allocated for WBAN operation is divided into 40 individual channels of 2 MHz bandwidth. The center frequencies for all the channels are equally distributed between 2.402 GHz and 2.480 GHz. Three of these channels are reserved for CCHs and the remaining 37 channels are allocated for DCHs communication. A SmartBAN utilizes a single CCH and DCH, chosen by the Hub, unless the communication channel is modified by the Hub. In other words, all communications between the nodes and the Hub is carried out using the identical DCH. Currently, different DCHs are implemented by different (i.e., neighboring) Hubs/SmartBANs for coexistence management. Frequency hopping is not supported in ETSI SmartBAN PHY, which deviates it from Bluetooth or Bluetooth low energy (BLE) standards [3][17].

ETSI SmartBAN implements Gaussian frequency shift keying (GFSK) with modulation index $h = 0.5$ and a bandwidth-bit period duration $BT = 0.5$. SmartBAN utilizes forward error control coding and repetition coding for improving the transmission channel reliability. The standard specifies a mandatory Bose-Chaudhuri Hoc-quenghem (BCH)-(36,22,2) channel coding to protect the PHY Layer header from errors. Whereas the MAC layer information is optionally encoded using BCH (127,113,2) while being transmitted at the PHY layer. There are three options in SmartBAN for repetition coding: no repetition and 2- or 4-times repetitions of the physical unit block [3][17]. This distinguishes SmartBAN, e.g., from the IEEE802.15.6 standard which uses more commonly employed bit-level scrambling. The highest information rate supported at the SmartBAN PHY layer is upto 1000kbps [52].

The transmission on inter-beacon interval (IBI) is provided in terms of IBI and the entire IBI is divided into "time slots". Each transmission IBI begins with the D-Beacon, followed by the scheduled access period (SAP), CM and inactive durations. SAP includes the data transmission by sensor nodes and the reception of respective acknowledgements from hub. CM period is employed for other WBAN management functions such as connection establishment, connection modification and connection termination. The SAP implements TDMA (time division multiple access) for contention free channel access for sensor data transmissions while the CM duration applies contention-based slotted ALOHA channel access method for WBAN management. Furthermore, if SAP does not provide sufficient channel resources for data transmission, CM period may serve as the additional channel resource for transmitting the sensor data. Inactive period is provided to enable the sleep mode and duty cycling for facilitating power saving in SmartBAN [3], [42].

2.2.1 ETSI SmartBAN Slot Structure

Every time slot in the SAP or CM duration is partitioned into physical-layer protocol data unit (PPDU) transmissions and the corresponding PPDU acknowledgements separated by inter-frame spacing (IFS). The sensor data or control information payload are located in MAC frame body, that is appended with MAC header and frame parity to create a MAC-layer protocol data unit (MPDU). An MPDU can simply be a physical-layer service data unit (PSDU) for uncoded transmissions while for the channel coded transmission, the MPDU is optionally encoded using BCH codes to generate the PSDU. PSDU, along with physical-layer convergence protocol (PLCP) header and preamble, constitutes a complete PPDU. The PPDU transmission is repeated twice or four times in scheduled access mode with

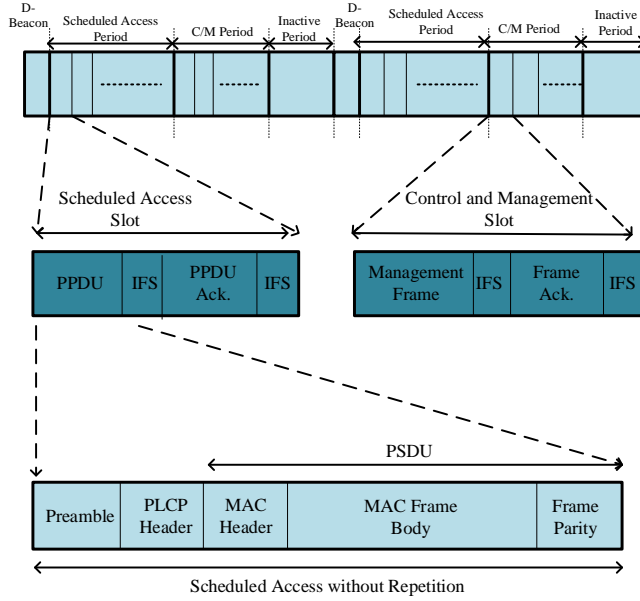


Figure 3 – IBI format with no PPDU repetitions in scheduled access duration.

two and four repetitions respectively. This PPDU repetition within the assigned time slot duration leads to a decrease of the maximum allowed payload size for each slot transmission [4][42]. Fig. 3 and Fig. 4 respectively illustrate the IBI formats for no repetition and 2-repetition transmission scenarios.

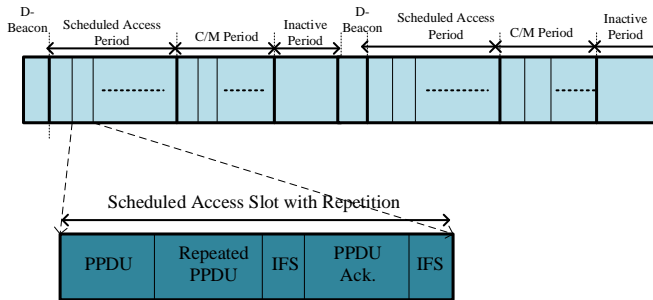


Figure 4 – IBI format with two PPDU repetitions in scheduled access duration.

The slot duration T_{slot} for each slot in the IBI on DCH is defined by the parameter L_{slot} through the relation $T_{slot} = L_{slot} \times T_{min}$, where $L_{slot} = \{1, 2, 4, 8, 16, 32\}$ and T_{min} is the minimum slot duration. A minimum slot size of $T_{min} = 0.625$ ms is allowed in ETSI SmartBAN and the maximum possible slot duration is 20 ms. The slot duration is broadcast in C-beacon by the central hub and all the sensor nodes after connection establishment transmit their data at this pre-defined slot length in each IBI. Smaller slot sizes are more reasonable for low latency applications with smaller payloads because of the shorter IBIs

duration, given the similar number of slots in IBI. Whereas longer slot durations facilitate higher throughput due to the transmission of more payload at once. Since each slot comprises of PPDU transmission duration T_{tx} , two IFS of length T_{IFS} and acknowledgement duration T_{ack} , therefore

$$T_{tx} = \frac{T_{slot} - T_{ack} - 2 \times T_{IFS}}{REP}, \quad (1)$$

where REP is the number of times an identical PPDU is repeated. The PHY and MAC overheads are accommodated along with the data payload within T_{tx} . Hence, the effective payload size in bits for a single slot becomes

$$PL = T_{tx} \times R_{sym} - K_{overhead}, \quad (2)$$

where R_{Sym} is the symbol rate. For uncoded SmartBAN transmissions, $K_{overhead} = K_{preamble} + K_{PHY} + K_{parity} + K_{MAC}$. $K_{preamble}$, K_{PHY} , K_{parity} and K_{MAC} respectively indicate the number of bits in preamble, PHY header, frame parity and MAC header [4][42]. All the relevant ETSI SmartBAN PHY-MAC parameters, mentioned in this section, are further summarized in Table 3. Table 4 provides more details about the payload size (in bytes) for all the L_{slot} values and repetition scenarios specified in the SmartBAN, calculated using (1) and (2). The minimum slot length T_{min} provides the PPDU transmissions only once. PPDU repetitions are not possible because with 0.625ms slot duration, the amount of related PHY-MAC overheads to constitute a complete PPDU cannot be transmitted more than once.

Table 3 – ETSI SmartBAN PHY-MAC Parameters.

Minimum slot length (T_{min})	625 μ s
Interframe spacing (T_{IFS})	150 μ s
Acknowledgement Duration (T_{ack})	128 μ s
Symbol Rate (R_{Sym})	10 ⁶
MAC header (K_{MAC})	7 octets
PHY header (K_{PHY})	5 octets
Preamble ($K_{preamble}$)	2 octets
Frame Parity (K_{parity})	2 octets

Table 4 – Payload size (bytes) for different L_{slot} values and repetition modes.

L_{slot}	Field Value in C-Beacon	T_{slot} (ms)	Payload (bytes) No Repetition	Payload (bytes) 2 Repetitions	Payload (bytes) 4 Repetitions
1	000	0.625	8	NA	NA
2	001	1.25	86	35	9
4	010	2.5	243	113	48
8	011	5	555	269	126
16	100	10	1180	582	283
32	101	20	2430	1207	595

The MAC throughput for each sensor node is defined by its total number of bits transmitted per second. The theoretical MAC throughput TP_{th} is determined using the IBI duration T_{IBI} and the total data payload size PL sent by the given node in each IBI, as

$$TP_{th} = \frac{1}{T_{IBI}} \times PL. \quad (3)$$

The IBI duration for the SmartBAN includes the D-Beacon transmission duration T_{Beacon} , SAP duration T_{SA} , CM period T_{CM} and inactive duration T_{IA} . The entire IBI duration T_{IBI} is also divided into the slots of equal size T_{slot} , so T_{IBI} becomes

$$T_{IBI} = T_{Beacon} + N_{SA} \times T_{slot} + N_{CM} \times T_{slot} + N_{IA} \times T_{slot}, \quad (4)$$

where N_{SA} , N_{CM} and N_{IA} are the number of slots in SAP, CM and inactive durations respectively. N_{slot} is the total number of slots in the entire IBI duration. Substituting T_{IBI} from (4) in (3), the expression for TP_{th} can be written as

$$TP_{th} = \frac{1}{\left(T_{Beacon} + N_{SA} \times T_{slot} + N_{CM} \times T_{slot} + N_{IA} \times T_{slot} \right)} \times PL, \quad (5)$$

2.2.2 Slot Reassignment in ETSI SmartBAN

Slot reassignment operation in ETSI SmartBAN MAC is performed to notify sensor nodes of their newly allocated slots in scheduled access duration. In order to perform slot reassignment, the hub indicates in D-Beacon about the execution of slot reassignment during the CM period and the list of nodes for which slot re-assignment would be carried out. The hub then sends slot reassignment frame in the CM period with the highest level user priority employing the slotted ALOHA channel access mechanism. The procedure is repeated again in the next IBI if the transmission of slot reassignment frame is not successful in the current IBI. The slot reassignment frame contains the timing information specifying the starting and ending time slot allocated to the node. The nodes, upon successful reception of slot re-assignment frame during the CM period, acknowledge hub in the MAC header of the data frame during the following IBI. The complete procedure of slot reassignment in SmartBAN is depicted in Fig. 5. The new slot allocation comes into practice for data transmission by nodes in the next IBI, having the slot reassignment procedure completed un at least two successive IBIs.

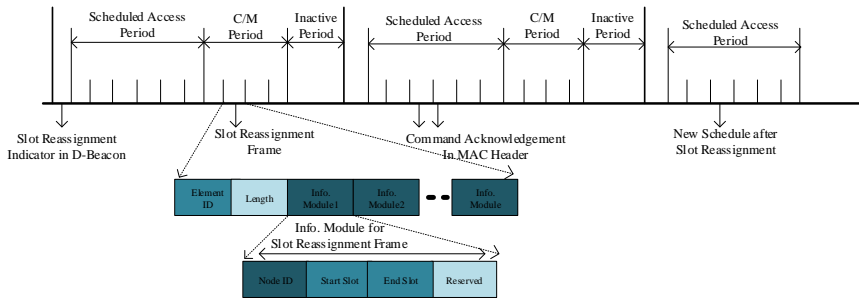


Figure 5 – Slot reassignment procedure in SmartBAN

2.3 Performance Analysis of ETSI SmartBAN

This sub-section explains the performance analysis of the ETSI SmartBAN PHY-MAC layer for the given WBAN use-cases, at the wireless channels derived for WBAN communication.

2.3.1 Use-case Description

A number of medical and consumer electronics use-cases can be identified as potential scenarios for ETSI SmartBAN PHY and MAC layer implementation. Each use-case has its own reliability, data rate and latency requirements that are peculiar to the number of nodes, sampling rates, quantization levels, urgency of the data delivery and types of the nodes present in the given use-case. ETSI SmartBAN typically supports a nominal data rate of 100 kbps and a maximum transmission rate of up to 1 Mbps at the PHY layer. The maximum node capacity is 16 nodes per WBAN but in most cases, up to 8 nodes are present in a SmartBAN. For real time high priority traffic, 10 ms latency can be facilitated while for regular traffic 125 ms latency is required [5].

Three different use-cases, classified according to their throughput requirements as low, medium and high data rate applications, are considered. A safety and fall monitoring medical use-case is referred as a low rate application in which patch-type sensors are attached on an elderly adult body. An alert signal is transmitted to the data server when the elder feels physically sick or falls during the regular everyday activities. A rescue and emergency management use-case is adverted as medium data rate WBAN application in which sensor data is used to monitor the physical conditions, surrounding environment and location of the rescue workers. A precise athlete monitoring use-case is assumed as a high rate application to measure the electrical activity of the muscles and for checking the pitching form in an athlete [5]. All the relevant information about these use-cases is summarized in Table 5. According to Table 5, all example applications require a maximum 10 ms latency whereas the aggregated throughput requirements range from 2.56 kbps-64 kbps, 52.656 kbps-164.096 kbps and 62.56 kbps-664 kbps for low, medium and high data rate applications respectively. The packet reception rate (PRR) should be above 90% for all the given use-cases.

2.3.2 Channel Model Description

Two different channel models are considered for calculating the pathloss values which include static IEEE CM3B (S-CM3B) channel with additive white Gaussian noise (AWGN) [51] and realistic IEEE CM3B (R-CM3B) channel with AWGN [9]. The distances associated with each on-body link between the sensor node and hub remain the same in static CM3B model and pathloss is computed for those constant distances. In the realistic channel model with AWGN, dynamic distances and link types are generated for different on-body links using a biomechanical mobility trace file. Dynamic distances and link types, as defined by a specific mobility scenario like walking, running or sit-stand, are considered as inputs for pathloss estimation. The space-time varying link types identify a particular on-body link as either line of sight (LOS) or non-line of sight (NLOS). An additional NLOS factor of 13% is added to the resultant pathloss value with time-varying distances, for NLOS link status, otherwise the pathloss remains unchanged [9].

After calculating the static as well as realistic pathloss values, radio link modeling is performed which includes signal-to-noise ratio (SNR), bit error ratio (BER) and packet error ratio (PER) computations. The theoretical expression for the GFSK BER calculation at SmartBAN PHY layer is given in [29] for a single PPDU transmission scenario. Whereas, for finding BER with two and four PPDU repetitions, SNR calculations are performed according to the diversity technique used for contributing the repetition gain. The maximal ratio

Table 5 – Low, medium and high data rate example use-cases [5, 12, 15]

Safety and fall monitoring (low-data rate)				
Sensor type	Sampling rate /Quantization	Data rate	Number of sensors	Real time /Non-real time
Pulse Wave /ECG	10-16 bit, 64 Hz-1 kHz	640 bps-16 kbps	1	Real time
Accelerometer /Gyroscopic sensor	10-16 bit, 64 Hz-1 kHz	640 bps-16 kbps	3	Real time
Rescue and emergency management (medium-data rate)				
Sensor type	Sampling rate /Quantization	Data rate	Number of sensors	Real time /Non-real time
Pulse Wave	10-16 bit, 64 Hz-1 kHz	640 bps-16 kbps	1	Real time
Accelerometer /Gyroscopic sensor	10-16 bit, 64 Hz-1 kHz	640 bps-16 kbps	2	Real time
Voice Command	-	50 kbps-100 kbps	1	Real time
Ambient sensor	10-16 bit, 64 Hz-1 kHz	640 bps-16 kbps	1	Real time
GPS node	-	96 bps	1	Real time
Precise athlete monitoring (high-data rate)				
Sensor type	Sampling rate /Quantization	Data rate	Number of sensors	Real time /Non-real time
EMG	6-12 bit, 10 kHz-50 kHz	60 kbps-600 kbps	1	Real time
Accelerometer /Gyroscopic sensor	10-16 bit, 64 Hz-1 kHz	640 bps-16 kbps	4	Real time

combining (MRC) diversity scheme is employed with statistically independent channels for repetition scenarios, therefore, the resulting SNR is the summation of instantaneous link SNRs during each round of the identical PPDU transmission [49]. Subsequently, BER for the repeated PPDU transmissions is computed using the similar BER expression, as mentioned in [9].

2.3.3 Numerical Results

For numerical performance evaluation, the transmission power levels from -10dBm to 0dBm, receiver sensitivity levels of -92.5dBm and time slot durations of 0.625ms, 1.25ms and 2.5ms are considered.

Packet Reception Rate Analysis: For low data rate use-case, the smallest slot duration of 0.625 ms can provide a PRR above 90% at all transmission power levels, with single uncoded PPDU transmission and under both the S-CM3B and R-CM3B channel models. While for 1.25ms and 2.5ms slot durations, the transmission power should be -7.5dBm or above to attain the required PRR with single uncoded transmission while with PPDU repetitions, all transmission power levels result in the targeted PRR.

For medium and high data rate use-cases, the PRR values are not significantly affected by the PPDU repetition scheme or transmission power levels at S-CM3B WBAN channel. The transmission power levels above -2.5dBm are mostly required with uncoded PPDU to achieve the targeted PRR for all slot durations and repetition schemes under R-CM3B channel model. Furthermore larger slot durations, despite carrying more payload with less PHY-MAC overheads, can have decreased PRR because of the increase in overall packet size. The reason for lower PRR values, with R-CM3B channel is that the R-CM3B model integrates the NLOS or human body shadowing losses as well in radio link modeling, while computing the pathloss, SNR, BER and PER values. The channel losses due to human body shadowing or NLOS conditions are not considered in S-CM3B channel model and pathloss calculations are performed only for the fixed hub-node link distances. Consequently, the impact of human mobility on PRR performance is not evident with the S-CM3B channel model. The PRR results for medium and high data rate use-cases follow the similar patterns since the PPDU repetitions also improve the PRR performance over the uncoded single transmission, specially with R-CM3B channel.

In order to overcome the impact of human body shadowing, BCH coded transmissions can be performed in SmartBAN. The coded PPDU transmission significantly enhances the PRR performance over the uncoded single and repeated PPDU transmissions, particularly in medium and high data rate use-cases. The channel coding gain is not very significant in low data rate use-case over the uncoded transmissions because in this use-case, the PRR performance is satisfactory even without channel coding in single and repetitive PPDU transmissions. Fig. 6 depicts the comparison of ETSI SmartBAN PHY-MAC layer performance with channel coded, uncoded and repetition-based transmission for high data rate precise athlete monitoring use-case. The required PRR of greater than 90% is achieved at -7.5dBm and above transmission power levels with 0.625ms and 1.25ms slot sizes. Whereas with 2.5ms slot duration, a transmission power of greater than -7.5dBm is required to achieve a PRR of 90%.

Throughput Analysis: Considering the low data rate use-case and uncoded transmission, the smallest slot duration 0.625ms is sufficient to satisfy the throughput QoS requirement. However for medium data rate use-case, which requires 52kbps-148.2kbps data rate, 1.25ms and 2.5ms slot durations are more appropriate with single uncoded PPDU transmission and two PPDU repetitions. Finally, 2.5ms slot duration with single uncoded PPDU transmission and two PPDU repetitions serves as the best option for high data rate

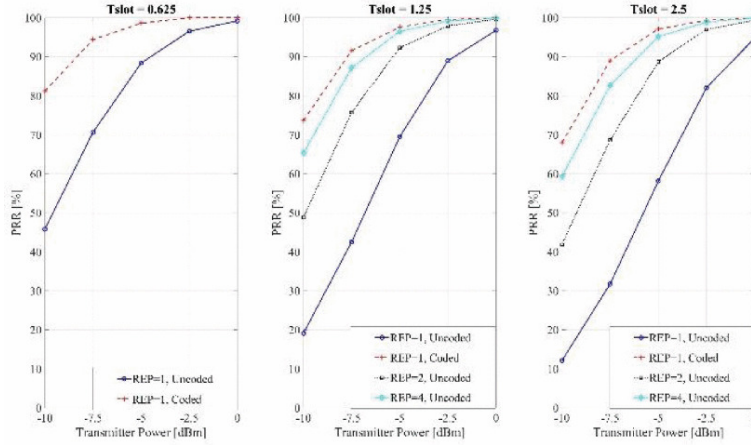


Figure 6 – PRR (%) w.r.t transmission power (dBm) for Precise Athlete Monitoring application.

use-case throughput requirements because it enables the transmission of more payload at once. The increase in throughput with the increase in slot duration (T_{slot}) can be explained by the phenomenon that larger T_{slot} values allow the transmission of more payload with the same PHY-MAC overheads, as compared to the smaller T_{slot} values, in a single transmission. Also PPDU repetitions degrade the throughput because the identical payload is transmitted multiple times. The BCH coded transmission considerably improves the throughput performance over the repeated PPDU transmissions, particularly for medium and high data rate use-cases. With coded transmission, the throughput requirements of the medium and high data rate applications can be satisfied at 1.25ms and 2.5ms slot durations, even at low transmission power levels. With BCH coded PPDU transmissions, the required throughput can be obtained at the transmission power level of -5dBm for precise athlete monitoring application as shown in Fig. 7.

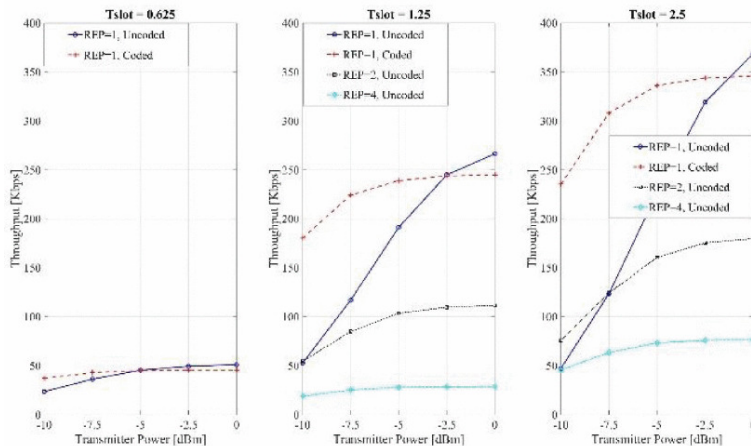


Figure 7 – Throughput (kbps) w.r.t transmission power (dBm) for Precise Athlete Monitoring application.

Latency Analysis: The latency values increase with the larger time slot durations as well as the number time slots in IBI because of the relative increase in IBI durations. The highest latency values are observed for the medium data rate use-case since it has the largest number of sensor nodes and the assigned scheduled access slots, and consequently longest IBI duration. For low data rate use-case, the PRR and throughput requirements are met with the 0.625ms slot duration, so using this slot duration can guarantee the minimum possible latency for this real time application. The minimum latency can be ensured for medium data rate use-caes with 1.25ms slot size while satisfying the PRR and throughput demands. Finally, for high data rate use-case, a slight compromise in latency is observed since only 2.5ms slot can support the required throughput. Concisely, smaller slot durations are more suitable for low data rate real-time applications as they provide improved PRR, reduced latency while satisfying the throughput requirements. While for high data rate applications, longer slot durations should be considered since they help attaining better throughput results with a slight trade-off in latency constraints. Moreover, the BCH coded transmission helps improving the PRR and throughput when longer slot durations are used for PPDU transmission.

3 Throughput and Channel Aware MAC ETSI SmartBAN

The SmartBAN standard specifies low complexity PHY and MAC layers for transmitting both the periodic and emergency WBAN traffic. SmartBAN PHY layer designates separate channels for control signals and data packet transmissions. The communication on data channel involves IBI transmission. All IBIs are partitioned into distinct time slots that constitute D-Beacon period, SAP duration, CM duration and inactive duration. D-Beacon marks the IBI boundaries and is broadcast by hub for communicating specific information about SmartBAN. SAP duration is reserved for data transmission by sensor nodes and CM period contains control information exchange between the SmartBAN hub and sensor nodes. Finally inactive duration serves to implement duty cycling in SmartBAN for energy preservation. This chapter provides insights about the throughput and channel aware (TCA) MAC algorithm which is in compliance with ETSI SmartBAN PHY-MAC layers along with the performance analysis.

This chapter is based on the following publications.

- R. Khan and M. M. Alam. Joint throughput and channel aware MAC scheduling for SmartBAN. In *EAI International Conference on Body Area Networks*, pages 49–64, 2018
- R. Khan, M. M. Alam, T. Paso, and J. Haapola. Throughput and channel aware MAC scheduling for SmartBAN standard. *IEEE Access*, 7:63133–63145, 2019
- R. Khan, M. M. Alam, and A. Kuusik. Channel prediction based enhanced throughput and channel aware MAC in SmartBAN standard. In *2019 16th International Symposium on Wireless Communication Systems (ISWCS)*, pages 463–468. IEEE, 2019

3.1 Dynamic MAC Scheduling Algorithms for ETSI SmartBAN

TCA MAC falls under the category of scheduled access MAC but it is based on the dynamic resource allocation. Dynamic MAC scheduling techniques are proposed to optimize and/or enhance the reliability, delay, energy efficiency and throughput performance of a network. There has been a fraction of research efforts that is related to the dynamic MAC scheduling in ETSI SmartBAN. Authors in [36] suggest a time-optimized MAC architecture in which the IBI, SAP duration, CM period and duration are optimized for minimizing both delay and energy consumption. Authors in [44] introduce a resource allocation scheme for ETSI SmartBAN in which both IBI duration and single slot durations are optimized depending upon the delay requirements of periodic uplink transmissions. The proposed optimization also allows sensor nodes to remain in the longest possible sleep mode to minimize the energy consumption while maintaining the delay constraints. The work in [45] presents an ETSI SmartBAN PHY and MAC configuration that prolongs sensors battery lifespan by reducing the energy consumed on transceivers. This link adaptation scheme is integrated with a resource allocation algorithm for deriving the IBI duration and the sensor transmission period. The resulting IBI structure fulfills the traffic delay constraints and minimizes sensors transceivers energy consumption concurrently. Furthermore, the presented algorithm has the ability to group several instances of data generation at sensor nodes in order to obtain the longest possible IBI period that satisfies the emergency and scheduled traffic delay requirements.

ETSI SmartBAN MAC framework proposes contention based MAC techniques as well. A few research endeavours are also made in the domain of dynamic contention based MAC techniques for ETSI SmartBAN. In order to improve the channel utilization and better throughput management in ETSI SmartBAN, a contention based MAC algorithm is pro-

vided in [24]. The MAC algorithm suggests the utilization of managed access phase (MAP) and random access phase (RAP) for pre-allocated and un-allocated time slots respectively. In MAP, the emergency data is sent by high priority sensor nodes immediately without the prior channel sensing. If no transmissions are detected for emergency traffic upon channel sensing, slot owner nodes execute their transmissions. If none of the priority nodes and allocated nodes send data, the remaining sensor nodes in WBAN contend for data transmission. The similar procedure takes place only between high priority sensor nodes and other transmission entities in RAP with unassigned time slots. A downlink transmission framework to reduce the delay and energy consumption for downlink dominated SmartBANs in [47]. At first, the delay of the supplementary downlink mode (SDM) specified in the SmartBAN MAC protocol is formulated and then an improved supplementary downlink mode (ISDM) is proposed, validating that reordering the access periods in the SmartBAN MAC frame can effectively reduce the delay. To address the delay bottleneck in SDM and ISDM, limited-exhaustive (LEDM) and fully-exhaustive (FEDM) downlink mechanisms are also proposed. In LEDM, once the downlink buffer becomes empty during CM period, the remaining CM duration becomes part of inactive duration. The downlink transmission in FEDM ends only when CM ends in an IBI which means that the hub does not start inactive period immediately, rather, it will continue to wait and transmit any new arrivals until CM ends. However the contention based methods require channel sensing and contention at subsequent slots which in turn increases the energy consumption of the network. This leads to the perception that scheduled access methods yield better outcomes in terms of energy efficiency.

3.2 ETSI SmartBAN Complaint TCA MAC

Based on the discussion provided in the previous sub-section, it can be stated that the scheduling algorithms with dynamic allocations are the most suitable candidate for channel access in WBANs. Therefore a throughput and channel aware (TCA) dynamic MAC protocol is elaborated in this sub-section for ETSI SmartBAN.

3.2.1 Baseline TCA MAC Algorithm

TCA algorithm exploits the principle of m -periodic scheduling recommended by IEEE 802.15.6 standard. M -periodic allocation is concerned with the assignment of scheduled access time slots in every m th beacon period for servicing low duty cycle periodic traffic [2]. The priority nodes, which are generally high data rate or emergency nodes, are assigned time slots at consecutive IBIs while low data rate nodes are assigned scheduled access slots m -periodically only when a new data packet is generated [6]. TCA employs the primary concept of m -periodic allocation along with the information about the channel conditions between the hub and sensor nodes. TCA algorithm comprises of two steps: 1) slot allocation based on the SNR conditions at WBAN links and 2) a final slot assignment based on m -periodicity. The input of the algorithm incorporates estimated pathloss values (obtained using the experimental traces of the motion capture system and bio-mechanical modeling [7]), transmission power, noise level and packet generation intervals at each sensor node. The estimated pathloss is used for the calculation of signal-to-noise ratio (SNR) threshold during the first step. In the first step, the SNR or channel quality at each node-hub link is examined and if the link SNR is higher than the pre-defined threshold value, the particular node is included into the list of candidate nodes for the final slot assignment in the next step. The sensor nodes with poor channel quality or low SNR are checked in the upcoming time slots for improvement at their node-hub link SNR. During the second step, the resulting batch of sensor nodes is checked for priority node presence. If there priority

node exists among the candidate sensor nodes with data packet available, it is assigned the given time slot. If priority node does not have favorable SNR value at the radio link or is already allocated the slot, other low priority nodes are assigned the time slot based on their data packet status. The flow chart representation of TCA algorithm is depicted in Fig. 8. Each stage of the algorithm is also explained in more detail in **Algorithm 1**.

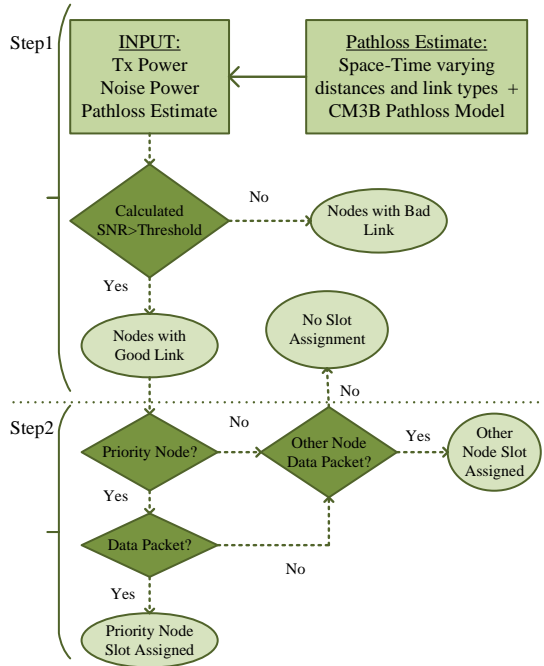


Figure 8 – Throughput and channel aware MAC algorithm.

3.2.2 TCA Implementation in ETSI SmartBAN

TCA is applied to ETSI SmartBAN MAC by implementing the slot reassignment procedure at the alternate IBIs. At first, the hub executes the TCA algorithm and creates an array of the assigned slots for all the nodes present in WBAN with suitable channel quality and data packet available for transmission. At the IBI beginning in D-Beacon, hub notifies all the sensor nodes about the possibility of slot reassignment frame transmission during the CM period. Later in the CM period, hub transmits the slot reassignment frame, with the highest priority, to all the nodes that shall perform packet transmissions. If the hub fails to carry out the slot reassignment frame transmission within the current IBI, it attempts to send the slot reassignment frame in the successive IBI [4] for TCA scheduling. All the sensor nodes, which receive slot reassignment frame, reply with a mandatory command acknowledgement in the frame MAC header transmitted during the scheduled access period of the subsequent IBI, with or without data payload from MAC layer. The new slot assignment, as recommended by the hub, is implemented in the next IBI. The hub simultaneously investigates the current WBAN links' SNR values to perform the TCA scheduling via slot reassignment procedure again. Fig. 9 summarizes the description of the TCA execution and the relevant frame exchange in SmartBAN.

```

input :  $P_{Tx}$  [dBm],  $PL_i^j$  [dB],  $P_{Noise}$  [dBm], Packet Generation Interval
output: Time Slot allocated to sensor nodes
for  $j \leftarrow 2$  to  $N_{SA}$  do
    /* j is the time slot index */
    for  $i \leftarrow 2$  to  $N$  do
        /* i is the sensor node index */
         $SNR_i^j = P_{Tx} - PL_i^j + P_{Noise}$ ;
        if  $SNR_i^j > \text{Threshold SNR}$  then
             $i$ th node has good channel at the  $j$ th slot;
            if  $i$  is priority node and has data then
                Time slot  $j$  is assigned to sensor node  $i$ ;
            else
                if  $i$  node has data then
                    Time slot  $j$  is assigned to sensor node  $i$ ;
                else
                    No packet assignment in  $j$ th time slot;
                end
            end
        end
    else
         $i$ th node is checked at the  $(j+1)$ th slot for link SNR;
    end
end
end

```

Algorithm 1: TCA MAC Algorithm details.

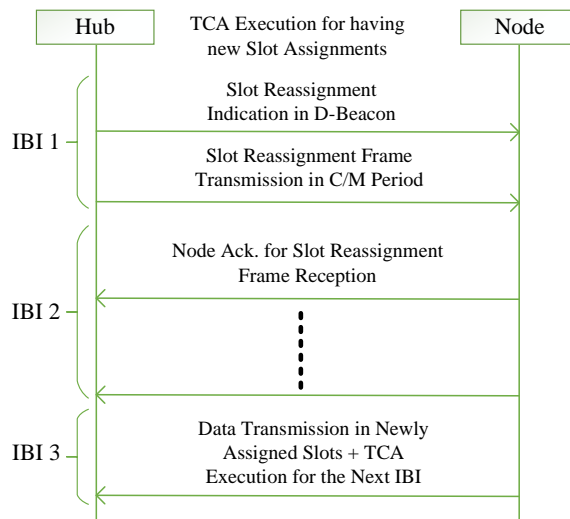


Figure 9 – TCA execution in SmartBAN.

3.3 Modifications in Primary TCA MAC

The baseline TCA algorithm involves the slot reassignment implementation at each alternate IBI after generating the array of assigned slots. This periodic execution of slot reassignment increases the energy consumption of the ETSI SmartBAN-compliant baseline TCA. The periodic transmission of slot reassignment frame at alternate IBIs can be decreased by executing TCA and recreating the assignment array only when required, depending upon the channel states and the data packet status of the past slot allocations.

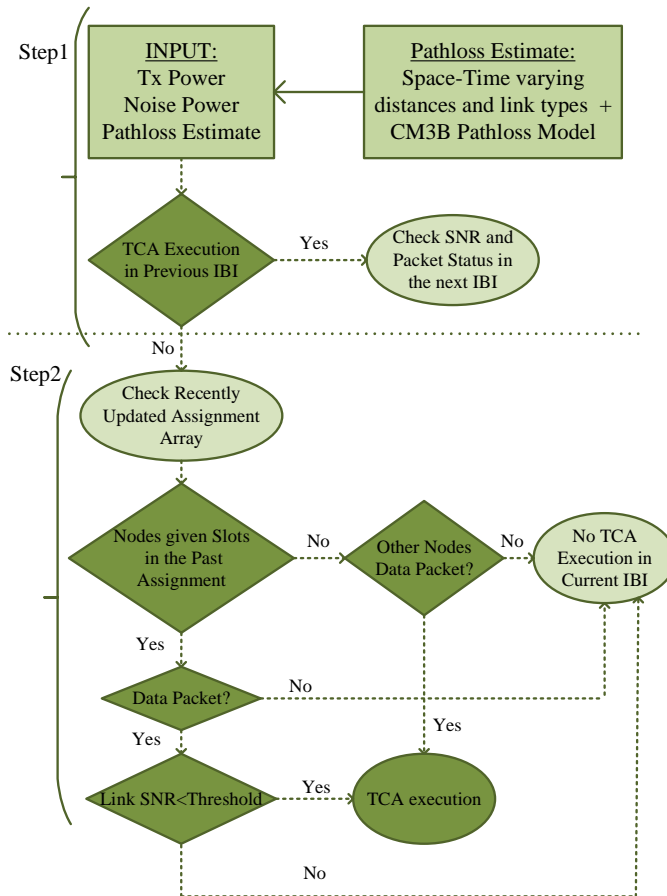


Figure 10 – Enhanced TCA MAC modifications.

3.3.1 Enhanced TCA MAC for ETSI SmartBAN

The enhanced TCA algorithm comprises of some additional steps before skipping to the TCA execution through slot reassignment at alternate IBIs. Fig. 10 shows the modifications made in the TCA algorithm for performance enhancements. At first, the hub checks that whether TCA was executed and slot reassignment frame was sent in the preceding IBI or not because TCA execution through slot reassignment is not allowed at the consecutive IBIs. If TCA execution was performed in the previous IBI, the algorithm stops and repeats

the similar procedure during the next IBI, else the algorithm proceeds to the next step. The hub then examines the past assignment array provides the details of the assigned slots to sensor nodes. The hub proceeds with the conventional TCA execution and the implementation of slot reassignment if i) SNR values of all the nodes in the past assignment array, having data packet to send, go below the pre-defined threshold for the current IBI. In other words, the channel quality degrades for the nodes which have allocated slots in the previous assignment array. OR ii) Some other sensor nodes have data packet to send but were not allocated any time slot in the previous assignment array. Otherwise the next IBI is checked for potential changes in the channel conditions of the hub-node links or packet status of the sensor nodes. Algorithm 2 explains the details about the modifications specified in Enhanced TCA MAC.

```

input :  $P_{Tx}$  [dBm],  $PL_i^j$  [dB],  $P_{Noise}$  [dBm], Packet Generation Interval
output: TCA Execution in current IBI
if TCA Execution in pervious IBI then
    | No TCA execution in current IBI;
    | break;
else
    | while TCA execution is true OR  $i \leq N$  do
    | | /* i is the sensor node index */
    | | /* j is the time slot index for node i from previous slot
    | | allocation */
    | | /* Recently updated assignment array is check */
    | |  $SNR_i^j = P_{Tx} - PL_i^j + P_{Noise}$ ;
    | | if i has a slot in the recent assignment array then
    | | | if i has data packet in current IBI then
    | | | | if  $SNR_i^j < \text{Threshold SNR}$  then
    | | | | | TCA Execution is true;
    | | | | else
    | | | | | Repeat the loop;
    | | | | end
    | | | else
    | | | | Repeat the loop;
    | | | end
    | | else
    | | | if i has data packet in current IBI then
    | | | | TCA Execution is true;
    | | | else
    | | | | Repeat the loop;
    | | | end
    | | end
    | |  $i = i + 1$ ;
    | end
    end

```

Algorithm 2: Enhanced TCA MAC Algorithm details.

3.3.2 Channel Prediction based TCA MAC for ETSI SmartBAN

The primary TCA MAC as well as the enhanced TCA MAC are implemented in ETSI SmartBAN using the slot reassignment method. Albeit enhanced TCA MAC reduces the recurrence of periodic slot reassignment frame transmission at alternate IBIs and the corresponding node acknowledgements, it still includes the flaws of the mandatory node acknowledgements upon slot reassignment frame reception and a delayed execution of the updated slot assignments. This delay in the TCA execution by slot reassignment and node acknowledgement might lead to the changes in channel quality or link SNR, decreasing the effectiveness of TCA MAC algorithm. In order to overcome these issues, a channel prediction based enhanced TCA MAC for ETSI SmartBAN is introduced in which the channel prediction is performed using the auto-regressive (AR) modeling. It is based on the assumption that the channel characteristics on the WBAN links are highly correlated due to the repetitive human body movements such as respiration, walking, running and sit-stand mobilities and predominantly include human body shadowing. Therefore, AR modeling offers the most relevant approach for utilizing the space-time dependent behavior of WBAN channels [18]. AR modeling generates the time series related to the on-body channel traces using the auto-correlation function (ACF) for on-body channels. The ACFs for different mobility scenarios additionally give insight into the time-dependency of on-body propagation and a theoretical basis for WBAN channel prediction. Algorithm 3 further elaborates the channel prediction based enhanced TCA MAC.

Estimation of AR Coefficients: The WBAN channel is considered as an AR process of order p in which the current channel tap $x(t)$ is a function of the past p inputs at equidistant time instants t . The estimated output process $\hat{x}(t)$ can be represented as an AR(p) process by

$$\hat{x}(t) = \sum_{i=1}^p \alpha_i \times \hat{x}(t-i) + \sigma(t), \quad (6)$$

where $\{\alpha_1, \alpha_2, \dots, \alpha_p\}$ are the AR coefficients or parameters of the previous channel samples and σ is a zero mean uncorrelated Gaussian noise process. Multiplying (6) by $\hat{x}(t)$ at time lag k and taking the expectation yields

$$\delta(k) = \sum_{i=1}^p \alpha_i \times \delta(k-i), \quad (7)$$

where $\delta(k) = E[\hat{x}(t)\hat{x}(t+k)]$ and $k > 0$. The auto-correlation at time lag k can be found using the relation $\rho_k = \frac{\delta(k)}{\delta(0)}$ which transforms (7) into the form (for $k > 0$)

$$\rho_k = \sum_{i=1}^p \alpha_i \times \rho_{k-1}. \quad (8)$$

Replacing $k = 1, 2, \dots, p$ for the selected order of AR model produces Yule-Walker equations [14]. These Yule-Walker equations are recursively solved using the Levinson-Durbin algorithm [18] for acquiring the weighted AR coefficients α_i .

Channel Prediction based TCA MAC: Initially, filter coefficients are generated using the above mentioned procedure to build the necessary AR model for predicting the on-body channel. Once the channel states for the given WBAN links are estimated for the upcoming IBI, these predicted channel states are followed by the pathloss computations which helps in obtaining the SNR conditions of the individual WBAN links. As depicted in Fig. 11, if the SNR value corresponding to any of the WBAN links goes below the pre-defined threshold level, TCA algorithm is executed at the hub and new channel assignments are broadcast in

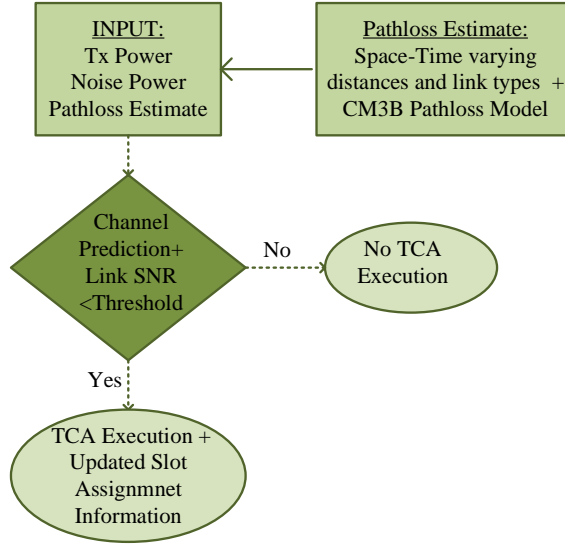


Figure 11 – Channel prediction based enhanced TCA MAC.

input : $\alpha_1^i(j), \alpha_2^i(j), \dots, \alpha_p^i(j); x_{t-1}^i(j), x_{t-2}^i(j), \dots, x_{t-p}^i(j)$

output: TCA Execution in current IBI

while TCA execution is true OR $i \leq N$ **do**

```

    /* i is the sensor node index */
    /* j is the time slot index for node i from previous slot
    allocation */
    /* P Order of the AR process for WBAN channels */
    /* t Time instant for the current IBI */
    /* Channel Prediction for each sensor node, given the
    previous slot allocation */
     $x_t^i(j) = \sum_{p=1}^P \alpha_p^i(j) \times x_{t-p}^i(j) + \sigma_t^i(j);$ 
    Estimation of  $PL_i^j$ ;
     $SNR_i^j = P_{Tx} - PL_i^j + P_{Noise};$ 
    if  $SNR_i^j < \text{Threshold SNR}$  then
    | TCA Execution is true;
    | Downlink information about the updated slot allocation is broadcast;
    else
    | Repeat the loop;
    end
     $i = i + 1;$ 
  
```

end

Algorithm 3: Channel Prediction based TCA MAC Algorithm details.

the form of downlink information to all sensor nodes in a pre-allocated (fixed) scheduled access slot. The execution of channel prediction based enhanced TCA using the downlink information broadcast during the SAP, rather than the generic slot reassignment method, eliminates the requirement of sending the node acknowledgements in response to the slot reassignment frame. This not only decreases the WBAN energy consumption but also allows the TCA execution at consecutive IBIs if WBAN channel conditions change rapidly at successive IBIs. This channel prediction based technique it effective in enhancing the error performance of TCA variants executed using the slot reassignment method.

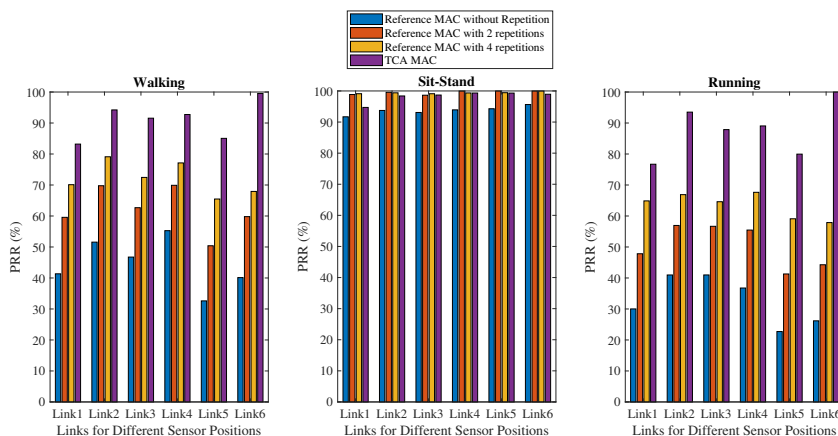


Figure 12 – Packet reception rate (PRR) (%) comparison of baseline TCA MAC with ETSI SmartBAN reference MAC under: walking, sit-stand and running mobility profiles.

3.4 Performance Analysis

In this sub-section, the conventional ETSI SmartBAN MAC performance is compared with the SmartBAN-compliant TCA MAC (and its variants), taking the packet reception rate (PRR) and energy consumption per successful transmission as the key performance indicators (KPIs). A transmission power of -10.9dBm and a slot duration of 1.25ms are assumed in the simulations. For providing the diversity gain with PPDU repetitions, maximal ratio combining (MRC) is utilized.

3.4.1 Packet Reception Rate

In terms of PRR results, the TCA MAC scheduling in ETSI SmartBAN outperforms the reference SmartBAN MAC schemes with and without repetition under walking and running scenarios. Despite using packet repetitions with MRC technique, a significant improvement in performance is not observed because of data transmission under poor channel conditions with fixed scheduling. However, SmartBAN reference MAC scheduling gives good performance under sit-stand posture for all the links due to the reduction mobility and rather stable channels. On average under walking conditions, SmartBAN-compliant TCA gives a respective PRR performance gain of about 40%, 25% and 12% over the reference SmartBAN without repetition, SmartBAN MAC with 2-repetitions and 4-repetitions, as shown in Fig. 12. The similar trends in performance enhancement can be seen under running mobility scenario.

Fig. 13 demonstrates the PRR analysis of baseline TCA MAC, enhanced TCA MAC and

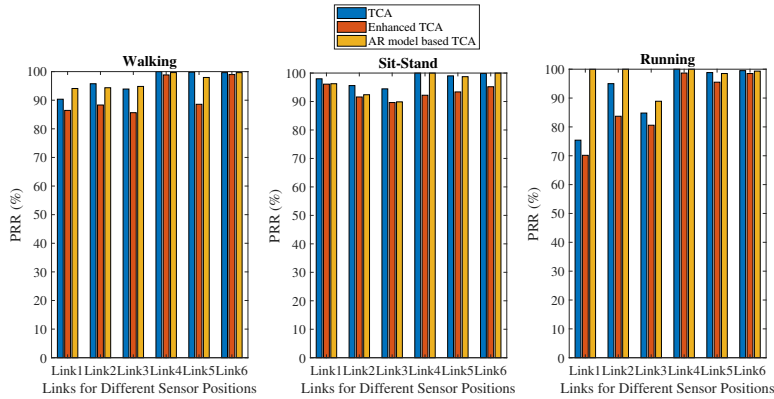


Figure 13 – Packet reception rate (PRR) (%) analysis of TCA MAC variants under: walking, sit-stand and running mobility profiles.

channel prediction based TCA in ETSI SmartBAN. The PRR performance of enhanced TCA is equivalent to the primary TCA for most of the links related to the different sensor positions under consideration. Under walking scenario, channel prediction based enhanced TCA scheduling outperforms all the TCA variants for majority of the links and maintains a desired PRR above 90% for all the sensor nodes. The channel conditions under sit-stand mobility are generally static, so the performance gain for channel prediction based TCA is not quite obvious, yet the suggested TCA variant preserves the PRR requirement of greater than 90%. Whereas under the running mobility, the severe degradation in PRR performance at some node-hub links is mitigated by the channel prediction based TCA technique which results in a maximum PRR performance gain of about 25%.

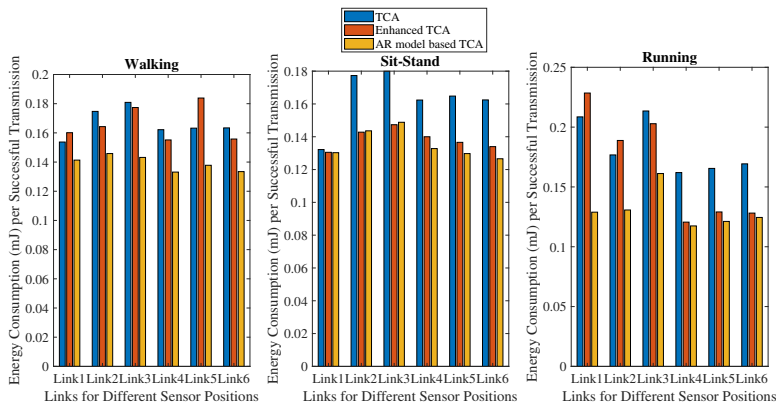


Figure 14 – Energy consumption per successful transmission (mJ) for TCA MAC variants under: walking, sit-stand and running mobility profiles.

3.4.2 Energy Consumption

SmartBAN-compliant primary TCA MAC cuts down the node energy consumption per successful transmission by 50% and 60% on average as compared to the reference MAC with no repetitions, under walking and running mobility scenarios respectively. TCA MAC also

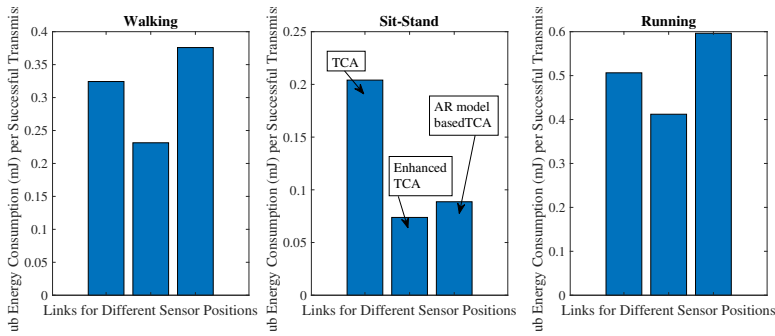


Figure 15 – Hub energy consumption per successful transmission (mJ) for TCA MAC variants under: walking, sit-stand and running mobility profiles.

decreases the energy consumption per successful transmission at the hub by 60% and 66% in comparison with the reference MAC with no repetitions subsequently under the walking and running conditions.

Fig. 14 provides the energy consumption per successful transmission outcomes for all the TCA MAC variants in ETSI SmartBAN. An average decrease of 11.7% in energy consumption per successful transmission can be observed under the walking scenario with enhanced TCA MAC as compared to the conventional TCA. For sit-stand and running mobilities, enhanced TCA reduces the energy consumption by 13% on average. This decrease in energy consumption is due to the selective execution of TCA via slot reassignment procedure only when the hub-node link SNR goes below the appropriate SNR threshold or sensors' packet availability status changes. The channel prediction based TCA variant imparts a maximum 44.44% reduction of energy consumption over the other the conventional TCA MAC at the sensor nodes. Fig. 15 illustrates the energy consumption per successful transmission evaluation of TCA MAC variants at hub. Under the walking and running scenario, enhanced TCA MAC decreases the energy consumption per successful transmission by 11% while under sit-stand position, both the basic and enhanced TCA give almost identical energy consumption performance. The channel prediction based TCA MAC slightly increases the hub energy consumption under walking and running mobilities due to rapid changes in transmission channel and hence, more frequent transmissions of downlink information frames.

4 Flexible Enhanced Throughput and Reduced Overhead MAC for ETSI SmartBAN

ETSI SmartBAN MAC specifies a parameter L_{slot} to indicate a single time slot duration within every IBI. L_{slot} is broadcast in the C-Beacon by hub and it remains essentially the same in each upcoming IBI. The connected sensor nodes transmit their data at this predefined slot duration, irrespective of their particular data rate requirements. The MAC time slot duration is altered only when the coordinator node broadcasts a different L_{slot} value in its C-Beacon and the connection is re-established with all the sensor nodes [4] to communicate at the modified time slot. A longer time slot can accommodate more payload, with the same PHY-MAC and acknowledgement overheads, and facilitates higher throughput. On the contrary, shorter slot duration is sufficient to support low data rate sensor nodes. The allocation of fixed longer time slots in the presence of low data rate sensor nodes leads to the inefficient usage of scheduled access time slot resources. Whereas the throughput requirements of high data rate sensors cannot be fulfilled with fixed smaller slot durations.

For better throughput management in existing ETSI SmartBAN standard with scheduled access, additional slots can be allocated to high data rate sensor nodes. Another option for handling data traffic with scheduled access method is slot re-assignment in which the dedicated but available time slots of low data rate sensor nodes are reassigned to high data rate sensor nodes within an IBI. The main issues with the conventional scheduled access MAC are: i) Allocating extra slots to high data rate sensor nodes for throughput management not only decreases the throughput (due to long T_{IBI}) but also increases energy consumption related to the PHY-MAC overhead and acknowledgement transmissions, ii) Performing slot reassignment periodically between the sensor nodes also results in the extra overhead energy consumption due to slot reassignment frame transmission, and iii) Increasing the overall slot duration to accommodate the high data rate sensor nodes also increases the IBI duration which in turn results in the throughput saturation. These issues in the basic ETSI SmartBAN structure motivate the design of a MAC algorithm in which the time slot durations could be adjusted according to the data rate requirements of the sensor nodes. Therefore, to overcome these problems with fixed slot duration scheduled access MAC in ETSI SmartBAN, this chapter elaborates the structural and performance details about flexible enhanced throughput and reduced overhead (FETRO) MAC protocol in ETSI SmartBAN. The variable slot length execution in the ETSI SmartBAN decreases the PHY-MAC and slot reassignment overheads as well as frequent acknowledgement transmissions for subsequently enhancing the throughput at a reduced overhead energy consumption.

This chapter is based on the following publication.

- R. Khan, M. M. Alam, and M. Guizani. A flexible enhanced throughput and reduced overhead (FETRO) MAC protocol for ETSI SmartBAN (Accepted). *IEEE Transactions on Mobile Computing (Early Access)*

4.1 Throughput Management Techniques in ETSI SmartBAN

The MAC throughput associated with each sensor node is characterized by its total number of bits transmitted per second. The theoretical MAC throughput TP_{th} can be found by the multiplication of the number of IBIs sent in one second N_{IBI} and the total data payload size PL transmitted by the given node in each IBI, as

$$TP_{th} = N_{IBI} \times PL. \quad (9)$$

The first term is defined as the reciprocal of the IBI duration T_{IBI} , therefore (9) can also be written as

$$TP_{th} = \frac{1}{T_{IBI}} \times PL. \quad (10)$$

The IBI duration for the SmartBAN consists of the D-Beacon, scheduled access period, CM period and inactive duration and can be described as

$$T_{IBI} = T_{Beacon} + T_{SA} + T_{CM} + T_{IA}, \quad (11)$$

where T_{Beacon} is the duration of D-Beacon slot which equals T_{slot} . T_{SA} , T_{CM} and T_{IA} are scheduled access, CM and inactive durations respectively. Since the entire IBI duration T_{IBI} is divided into the slots of equal size T_{slot} , therefore the T_{IBI} becomes

$$T_{IBI} = T_{Beacon} + N_{SA} \times T_{slot} + N_{CM} \times T_{slot} + N_{IA} \times T_{slot}, \quad (12)$$

or

$$T_{IBI} = N_{slot} \times T_{slot}, \quad (13)$$

where N_{SA} , N_{CM} and N_{IA} are the number of slots in scheduled access, CM and inactive durations respectively. N_{slot} is the total number of slots in the entire IBI duration. Substituting T_{IBI} from (12) or (13) in (10), the TP_{th} can also be represented as

$$TP_{th} = \frac{1}{\left(T_{Beacon} + N_{SA} \times T_{slot} + N_{CM} \times T_{slot} + N_{IA} \times T_{slot} \right)} \times PL, \quad (14)$$

or

$$TP_{th} = \frac{1}{N_{slot} \times T_{slot}} \times PL. \quad (15)$$

The PL can be calculated using (1) and (2) and the details are already mentioned in chapter II of this thesis. The amount of payload transmitted in a single slot decreases as the time slot duration decreases. The minimum slot length T_{min} provides the PPDU transmissions only once and no PPDU repetitions are possible with 0.625ms time slot. It because with 0.625ms slot duration, the amount of necessary PHY-MAC overheads to generate a complete PPDU cannot be transmitted more than once. According to (14) and (15), there is a reduction in TP_{th} with the increase in IBI duration and the IBI increases either due to the higher number of slots N_{slot} and/or longer time slot duration T_{slot} . Moreover, larger slot durations allow the transmission of more payload in a single round and hence, the MAC throughput theoretically improves for longer time slots, given the equal number of N_{slot} in the IBI.

4.1.1 Energy Consumption for PHY-MAC Overhead Transmission

The total energy consumed during the active transmission and reception at both the sensor nodes and hub is the summation of energies utilized in the data payload and overheads communication. While the energy consumed during the data payload transmission leads to the enhanced effective throughput, the frequent transmission of PHY-MAC overheads and data acknowledgements results in high overhead energy consumption. The primary source of overheads in each scheduled access time slot consists of PHY-MAC layer headers

and the subsequent acknowledgements sent by the hub. Therefore, the resulting energy consumption at each sensor node due to overheads in scheduled access time slot can be written as

$$E_{OHnode} = 3V \times T_B \times I_{mA}^{rx} + 3V \times \frac{K_{overhead}}{R_{sym}} \times I_{mA}^{tx} + 3V \times T_{ack} \times I_{mA}^{rx}, \quad (16)$$

where I_{mA}^{tx} and I_{mA}^{rx} are the current consumptions in mA at the transmission and reception respectively. T_B , $K_{overhead}$, R_{sym} and T_{ack} respectively denote the beacon transmission duration, number of bits in PHY-MAC overheads, PHY layer symbol rate and acknowledgement transmission duration. The first term in (16) represents the energy consumption due to the reception of D-Beacon at the IBI beginning. The second term corresponds to the energy consumption during the PHY-MAC layer overheads transmission by the sensor node. The third term represents the energy consumption due to the reception of packet acknowledgement sent by the hub. $3V$ represents the hub or sensor node's supply voltage. In the similar way, the overhead energy consumption at the hub during the scheduled access communication is due to the transmission of D-Beacon and data packet acknowledgements and the reception of PHY-MAC layer overheads appended with the payload. It can be mentioned as

$$E_{OHhub} = 3V \times T_B \times I_{mA}^{tx} + \sum_{N_{SA}} \left\{ 3V \times \frac{K_{overhead}}{R_{sym}} \times I_{mA}^{rx} + 3V \times T_{ack} \times I_{mA}^{tx} \right\}. \quad (17)$$

According to (16) and (17), each time a node is allocated an extra slot for data transmission, the related PHY-MAC headers, preamble and acknowledgement overhead energy is also consumed by both the hub as well as the sensor nodes.

4.1.2 Energy Consumption for Overhead Transmission in Slot Re-assignment

One of the procedures for managing the throughput requirements, without allocating the additional slots to high data rate sensor nodes and increasing the IBI size as well as the frequent transmissions of PHY-MAC overheads and acknowledgements, is slot reassignment. Slot reassignment refers to the periodic re-allocation of the unused slots of low data rate sensor nodes to the high data rate sensor nodes. The slot reassignment frames are also transmitted as information units appended with PHY-MAC overhead, from the hub to the sensor nodes, as discussed in sub-section 2.2. During slot reassignment procedure, the hub first informs all the sensor nodes of possible slot re-allocations in D-Beacon and then transmits the slot re-assignment frame during the CM period of the IBI [4]. Therefore, the extra energy consumption at each sensor node because of the slot reassignment during the run time can be described as

$$E_{SRAstnode} = 3V \times \frac{\left(K_{overhead} + K_{ID} + K_L + N_{SRas} \times K_{SRas} \right)}{R_{sym}} \times I_{mA}^{rx}, \quad (18)$$

where K_{ID} , K_L , K_{SRas} and N_{SRas} represent the element ID field size in bits, information unit length field in bits, slot re-assignment information module size in bits and the number of sensor nodes which receive the slot reassignment frame [4] respectively. In a similar manner, the related extra energy consumption at the hub due to slot reassignment frame

transmission becomes

$$E_{SRaShub} = 3V \times \frac{\left(K_{overhead} + K_{ID} + K_L + N_{SRas} \times K_{SRas} \right)}{R_{sym}} \times I_{mA}^{ex}. \quad (19)$$

Consequently the execution of slot reassignment also leads to extra energy consumption at both the sensor nodes and the hub.

4.1.3 Energy Consumption for Payload Transmission

The energy consumptions at the nodes and the hub associated with the payload transmission during the scheduled access period are given as

$$E_{PLnode} = 3V \times T_{PL} \times I_{mA}^{ex}, \quad (20)$$

and

$$E_{PLhub} = \sum_{N_{SA}} 3V \times T_{PL} \times I_{mA}^{ex}, \quad (21)$$

where T_{PL} is the time duration for payload transmission and equals $\frac{PL}{R_{sym}}$.

4.2 FETRO MAC Algorithm

In the proposed FETRO MAC scheme, the slot durations are allocated by the hub based on the amount of payload every node intends to send. For this purpose, each sensor node provides its own required L_{slot} value at the time of connection establishment. The requested L_{slot} depends upon the sensor node's data rate requirement, sampling rate and bit resolution. The hub sends its response, indicating the acceptance (grant) of the requested L_{slot} , retainment of its own L_{slot} or the suggestion of another L_{slot} value. The hub decision and response in this context is again determined by the duty cycling status, number of connected sensor nodes and the presence of relay node. It should be noted that the existing connection request or connection assignment frames can only notify about the number of allocated slots, whose duration T_{slot} is already defined and broadcast in C-Beacon. The existing frame format cannot modify T_{slot} depending upon the sensor node data rate requirements on the run-time.

4.2.1 Implementation of FETRO MAC in ETSI SmartBAN

FETRO MAC is implemented by granting the few necessary adaptations in the primary ETSI SmartBAN MAC frame format which include: i) Rather than broadcasting the number of slots in IBI N_{slot} within C-Beacon and D-Beacon at the beginning, the number of minimum slot duration T_{min} units, i.e., N_{min} should be broadcast by the hub, ii) The connection request information module should specify the number of minimum slot units (of length T_{min}) requested by the sensor node while initializing the hub-node connection request for data transmissions, iii) The connection assignment information module should also indicate the numbers at which the minimum slot unit allocation starts and ends. These modifications will ensure the necessary synchronization between the hub and the sensor nodes when the individual time slot duration of each sensor node is different, iv) The L_{slot} value, respective to the sensor data rate requirements, should be mutually agreed between the node and hub at the time of connection request and connection assignment.

Algorithm 4 elaborates information about the implementation of FETRO MAC algorithm in ETSI SmartBAN. The initialization of connection between sensor node and hub

```

input :  $L_{slot}^{sensor}$ ,  $L_{slot}^{hub}$ 
output: FETRO MAC Execution in ETSI SmartBAN
  /*  $L_{slot}^{sensor}$  is the slot parameter required by the sensor node */
  /*  $L_{slot}^{hub}$  is the slot parameter predefined by the hub */
while C-Req received is true do
  | Node sends C-Req;
  | if C-Req received then
  | | Hub sends ACK;
  | else
  | | Hub sends NACK;
  | | Repeat the loop;
  | end
end
Hub checks  $L_{slot}^{sensor}$ ;
if  $L_{slot}^{sensor}$  granted then
  | Hub sends C-Assgn;
  | Time slot duration modified for the sensor as requested;
else
  | Hub suggests another  $L_{slot}^{sensor}$  or retains  $L_{slot}^{hub}$ ;
  | Hub sends C-Assgn;
end
Node sends ACK or NACK for C-Assgn;

```

Algorithm 4: Enhanced TCA MAC Algorithm details.

takes place in the similar manner as the default connection establishment method in ETSI SmartBAN. The node trying to establish connection, monitors the C-Beacon over the control channel and obtains the information about the data channel and other network parameters. Following that, the sensor node monitors the data channel and D-Beacon to acquire the CM period start for sending its connection request frame. The node requests the L_{slot} value suitable for its payload size, in the modified connection request frame which is acknowledged by the hub. Then the hub responds with connection assignment frame within the CM period. The hub also informs that whether the requested L_{slot} has been granted or another L_{slot} value is suggested for transmission by the node or the L_{slot} value broadcast in C-Beacon is to be retained. The received connection assignment frame by the node is acknowledged and the communication starts taking place from the mutually agreed IBI between the sensor node and the hub. The entire procedure for connection establishment in FETRO MAC with variable slot length is embodied in Fig. 16.

4.2.2 IBI data transmission in FETRO MAC

The execution of IBI with variable slot durations would be difficult to manage in terms of synchronization. However, the synchronization among other sensor nodes and the hub in FETRO MAC can be maintained with the help of the fact that the slot durations T_{slot} for the increasing L_{slot} values are the integer multiples of the T_{min} , as was mentioned in Table 4 (Chapter 2). The proposed idea in FETRO MAC focuses on having a flexible and dynamic T_{slot} assignment by keeping intact the existing integer multiple characteristic of slot durations represented by L_{slot} values. For example, 2.5ms slot duration is the twice of 1.25ms slot duration and so on. Therefore, a single 2.5ms slot lasts as long as the two slots of 1.25ms time duration but sends more data payload at once with less PHY-MAC and

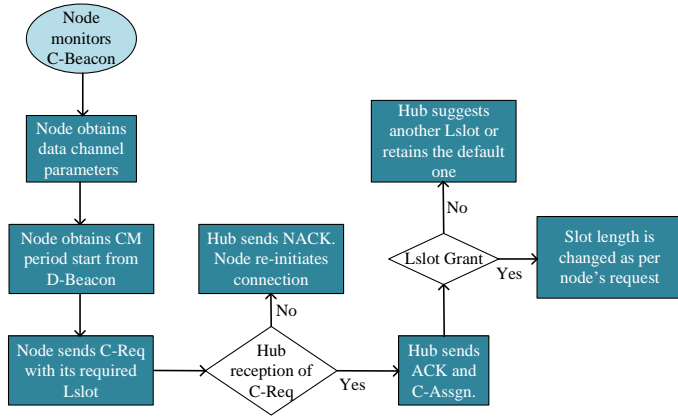
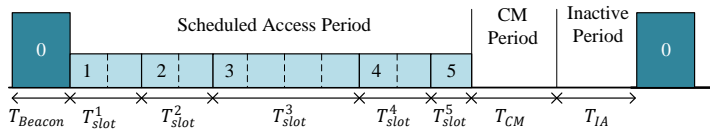


Figure 16 – Connection initialization in FETRO MAC protocol. The modified connection request frame by the node indicates the desired L_{slot} and the modified connection assignment frame by the hub responds with the grant or refusal of the requested L_{slot} .



0: D-Beacon sends the number of units of length T_{min} in its inter-beacon interval field.

1: Slot Length with the broadcast L_{slot} .

2: Slot Length with the broadcast L_{slot} .

3: Slot Length double the default slot length.

4: Slot Length with the broadcast L_{slot} .

5: Slot Length equal to T_{min} .

Figure 17 – IBI transmission with different slot lengths in FETRO MAC. Each slot has frame transmission duration and acknowledgement duration separated by IFS in scheduled access period. The duration of each slot T_{slot} is an integer multiple of T_{min} for retaining the synchronization at each node.

acknowledgement overheads. The strategy here is that the D-beacon would broadcast the number of minimum length T_{min} units, that are present within the IBI, in its “inter-beacon interval field”, where T_{min} is the minimum time slot duration possible in ETSI SmartBAN MAC. In other words, rather than broadcasting the N_{slot} which represents the number of equal length slots in an IBI, N_{min} should be broadcast in D-Beacon which indicates the IBI duration in terms of the number of minimum length units. This would allow the sensor nodes to adjust their wake-up intervals irrespective of the L_{slot} broadcast in the C-Beacon and the remaining slot lengths which are exclusively requested by the other sensor nodes. An illustration of the IBI in the FETRO MAC scheme is shown in Fig. 17 in which the slots “1”, “2” and “4” follow the L_{slot} broadcast in the C-Beacon whereas the slot number “3” has a duration equal to the twice of default slot length. Slot “5” has the duration equal to T_{min} . The duration of each scheduled access slot is an integer multiple of T_{min} and every slot has the frame transmission duration, acknowledgement duration and two IFS. The D-Beacon broadcasts the N_{min} , i.e. the number of minimum time slot duration T_{min} units in its “inter-beacon interval field” for the sensor nodes to adjust their wake-up intervals accordingly.

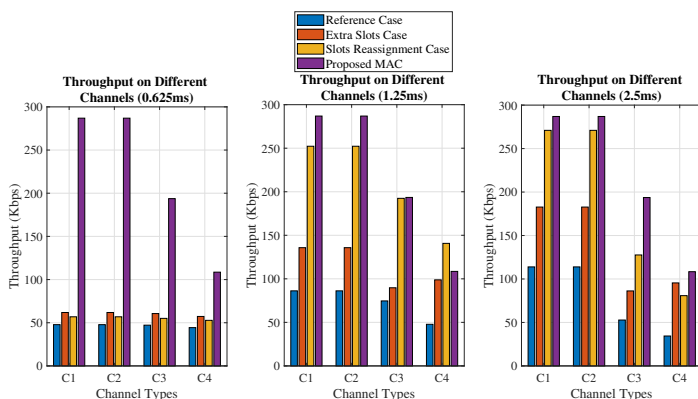


Figure 18 – Throughput on different channel types (kbps), health and fitness monitoring applications. C1: Static AWGN channel, C2: Deterministic AWGN channel, C3: Static fading channel, C4: Deterministic fading channel.

4.3 Performance Evaluation

For performance evaluation, four different channel models are taken i.e., static IEEE CM3B model with additive white Gaussian noise (AWGN) [50], dynamic IEEE CM3B (deterministic) channel model with AWGN [8], static IEEE CM3B model with fading [50] and deterministic channel model with fading. The trace file that generates space-time varying distances and link types for the deterministic channel models (with and without fading) assessment of this application scenario is about 59 seconds long and contains several mobility patterns such as walking, sitting and hand motions. Three different values of fixed time slot durations are considered in the conventional SmartBAN MAC which are 0.625ms, 1.25ms and 2.5ms. For each considered slot duration, three different conventional SmartBAN MAC scheduling strategies are assumed to analyze the throughput performance of a health monitoring application scenario. The first one is the reference scheme, in which each channel/node is allocated a single scheduled access slot. In the second strategy, extra slots are provided to the high data rate sensor node. With 0.625ms, 1.25ms and 2.5ms slot

durations, the high data rate sensor is allocated three, one and one extra slots whereas the slot allocation for other nodes remains the same. The slot reassignment strategy has the similar IBI duration as the reference SmartBAN MAC scheme but the unused slots of low data rate sensor nodes are strategically reassigned to manage the high data rate sensor transmissions. In the proposed FETRO MAC with variable slot length, a slot duration of 2.5ms is assumed for high data rate channel while the remaining nodes retain a slot length of 0.625ms since this slot length is enough to manage their throughput requirements. The transmission power assumed is 0dBm while the receiver sensitivity is -96dBm. The IBI is assumed to include two slots in CM duration and one slot in inactive period.

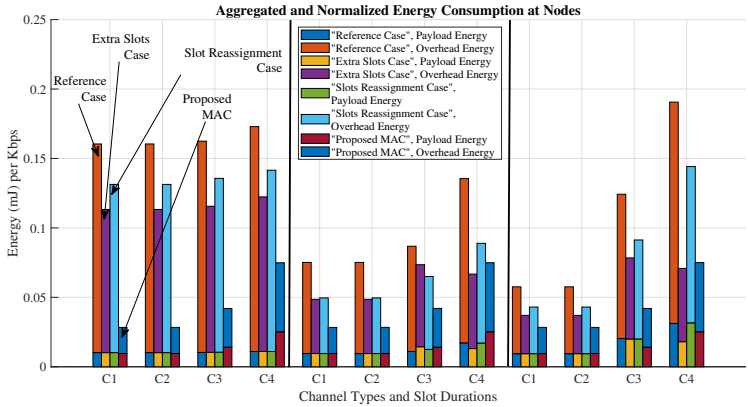


Figure 19 – Node energy consumption (mJ) per kbps, health monitoring and fitness applications. C1: Static AWGN channel, C2: Deterministic AWGN channel, C3: Static fading channel, C4: Deterministic fading channel.

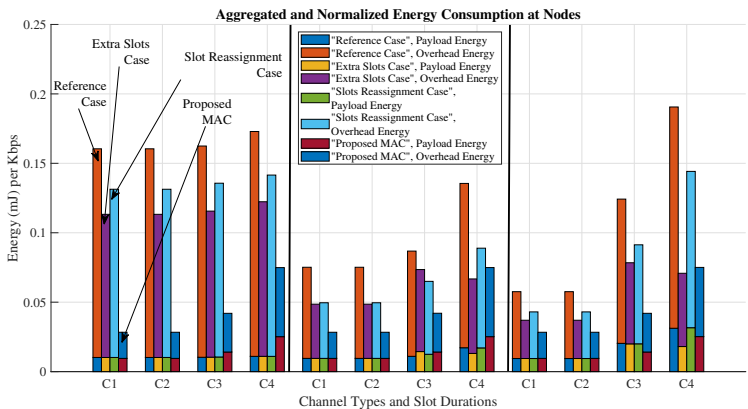


Figure 20 – Hub energy consumption (mJ) per kbps, health monitoring and fitness applications. C1: Static AWGN channel, C2: Deterministic AWGN channel, C3: Static fading channel, C4: Deterministic fading channel.

4.3.1 Throughput Analysis

The aggregated throughput results of all the sensor nodes in the given health and fitness monitoring use-case are depicted in Fig. 18. The “static AWGN channel” is referred as “C1”, deterministic AWGN channel” as “C2”, “static fading channel” as “C3” and the “deterministic fading model” as “C4” in all the performance evaluation results. The throughput results of the extra slot and the slot reassignment cases are better than the reference SmartBAN case under all channel conditions and MAC slot durations. For 1.25ms slot duration, the reference SmartBAN MAC and the SmartBAN MAC with extra slots fail to fulfil the throughput requirements under all the channel conditions because of the transmission of insufficient payload and increased IBI duration respectively. However the throughput is significantly improved with slot reassignment strategy under the static and deterministic AWGN channels. It is because the unused slots of other nodes/channels are re-allocated to the high data rate node for maximum resource utilization within the smaller IBI duration. The same trends in throughput can be observed with 2.5ms slot duration under the static and deterministic AWGN channels.

4.3.2 Normalized Energy Consumption Analysis

Fig. 19 represents the aggregated and normalized energy consumption per kbps for all the sensor nodes. With 0.625ms time slot duration and under all the given channel types, the application of FETRO MAC decreases the overhead energy consumption per kbps by 84.6%, 80.9% and 83% in comparison with the reference, extra slot allocation and slot reassignment SmartBAN MAC schemes respectively on average. The overhead energy consumption per kbps is significantly decreased in all three conventional ETSI SmartBAN MAC schemes (reference, extra slot, slot reassignment) with 1.25ms and 2.5ms slot durations because of the transmission of relatively higher payload with less overheads. Nevertheless, the proposed FETRO MAC reduces the mean energy consumption per kbps by 65%, 53.3% and 49% as compared to the reference, extra slot allocation and slot reassignment SmartBAN MAC scheduling methods respectively with 1.25ms slot length. With 2.5ms slot, the proposed FETRO MAC results in an average decrease of 42.8% in overhead energy consumption per kbps outcomes in contrast to the conventional SmartBAN MAC scheduling methods. The payload and overhead energy consumption per kbps outcomes for the hub follow a similar pattern as the aggregated and normalized energy consumption per kbps results for the nodes. The energy consumption at the hub is summed up for the entire trace duration and normalized to the effective throughput. Implementing the FETRO MAC reduces the overhead energy consumption per kbps by 75%, 62.5% and 40% as compared to the conventional SmartBAN scheduling methods with 0.625ms, 1.25ms and 2.5ms slot durations respectively, as shown in Fig. 20.

5 Body-to-body Communication Channel Modeling

WBANs have different types of communication scenarios based on the relative positions of WBAN nodes. The placement of communicating BAN nodes on multiple bodies is attributed to body-to-body (B2B) networks [10]. B2B networks provide innovative solutions for a wide range of applications such as remote health care, precision monitoring of athletes, search and rescue operations in disastrous situations and coordination of soldiers on a battlefield [10]. The channel modeling in B2B networks is different from the on-body communication channel modeling because there is mobility and human body shadowing involved at both ends of the communication. This thesis chapter provides explanation about the B2B channel modeling, utilizing the biomechanical mobility channel traces over a dedicated frequency channel with realistic channel models, using IEEE 802.15.6 and SmartBAN standards specifications.

This chapter is based on the following publications.

- R. Khan and M. M. Alam. Joint PHY-MAC realistic performance evaluation of body-to-body communication in IEEE 802.15.6 and SmartBAN. In *12th International Symposium on Medical Information and Communication Technology (ISMICT)*, pages 1-6. IEEE, 2018
- R. Khan and M. M. Alam. Body-to-body communication: Applications, system design aspects and performance evaluation. In *12th International Symposium on Medical Information and Communication Technology (ISMICT)*, pages 1-2. IEEE, 2018

5.1 Limitations in Body-to-body Communication Channel Modeling

Most of the efforts in channel characterization of WBANs have been dedicated to on-body communications and the contribution of research efforts in B2B channel modeling is quite limited. Since WBAN communication is dominated by the human body posture, therefore the channel modeling in WBAN also integrates the mobility. A comprehensive analysis of the MAC layer performance evaluation is presented in [46] for on-body communication scenario, after measuring the channel characteristics when the nodes are placed on a walking subject. The notion of integrating realistic mobility traces with IEEE 802.15.6 channel models for accurate performance analysis of on-body communication at the MAC layer was proposed in [9]. Considering other co-located WBAN signals as interference and jointly exploiting on-body and B2B realistic channel models, a comprehensive MAC level performance analysis of intra-BAN communication is given in [37, 8]. Many noteworthy contributions exist in the literature which attempt to discuss B2B channel characteristics as well [19, 53, 13]. But these channel models assume very limited mobility scenarios and for the realistic performance evaluation of B2B networks on the higher layers such as MAC and network, accurate mobility and radio link modeling should be taken into account. So far, there is no research work that has been dedicated to study the joint PHY-MAC layer performance evaluation of inter-BAN communication systems under realistic/unrestricted mobility scenarios.

5.2 Biomechanical Mobility Modeling of Body-to-body Communication Channel

In order to perform the B2B channel modeling under realistic channel, three main steps are required which consist of: i) Static channel modeling, ii) Biomechanical mobility modeling, and iii) Radio link modeling. The static channel model provides the pathloss expression with the static distance whereas the biomechanical mobility modeling generates

space-time varying distances and link types. The pathloss with space-time varying channels is computed by integrating the space-time varying distances and link types into the static channel models. The radio link modeling is performed at the end to transform the dynamic pathloss values into the packet reception rate (PRR) performance.

5.2.1 Static Channel Model

For computing the static channel pathloss, B2B channel model derived in [38] and [39] is utilized. This channel model is developed using real time measurement campaigns under restricted mobility scenarios. The B2B channel model provides channel gain, long term (LT) and short term (ST) fading components to estimate the path-loss values and the channel characteristics are a function of inter-body distance (d) and mutual body orientation (α) for various inter-BAN links. These links include head-to-head, belt-to-belt, wrist-to-wrist, head-to-belt, head-to-wrist, belt-to-wrist inter-BAN channels and are in-line with the links investigated in [38], [39]. In this model, shadowing effects by the bodies are primarily dealt with the distance and orientation-dependent channel gain, LT effects caused by the environment are represented by LT fading and ST fading is the outcome of the constructive and destructive interference resulting from multi-path propagation. According to [39], the distance (d) and orientation (α) dependent channel gain can be stated in dB as

$$G(d, \alpha) = G_0(\alpha) - 10n(\alpha)\log_{10}\left(\frac{d}{d_0}\right), \quad (22)$$

where n represents the path-loss exponent and G_0 corresponds to the gain at the reference distance d_0 , equal to 1m. $G_0(\alpha)$ and $n(\alpha)$ show different characteristics for various links between the relative node positions over different BANs. For example, n and G_0 do not exhibit mutual orientation dependence for head-to-head links between two different BANs so, distance-based channel gain can be calculated with the fixed values of n and G_0 . But mutual orientation α is crucial in determining n and G_0 values for other links mentioned previously. Further information about $G_0(\alpha)$ and $n(\alpha)$ calculations for obtaining the channel gains corresponding to other links can be found in [39].

The LT fading component in dB scale can be characterized with a zero-mean normal distribution [39] as

$$f(z_{LT}) = \frac{1}{\sigma_{LT}\sqrt{2\pi}}\exp\left(\frac{-z_{LT}^2}{2\sigma_{LT}^2}\right), \quad (23)$$

where z_{LT} is the LT fading component in dB and σ_{LT} is the standard deviation, whose values for different B2B links are indicated in [38, Table 5]. The ST fading envelope can be typically represented by Rice distribution [38], [39], as given

$$f(z_{ST}) = \frac{z_{ST}}{\sigma^2}\exp\left(\frac{-z_{ST}^2 - A^2}{2\sigma^2}\right)I_0\left(\frac{z_{ST}A}{\sigma^2}\right), \quad (24)$$

where z_{ST} is the ST fading envelope, A is the non-centrality parameter and σ represents the scale parameter. The Rician channel K -factor is the power ratio between the direct path and the multi-paths and is calculated as $K = \frac{A^2}{2\sigma^2}$. The characteristics of head-to-head links again do not show mutual orientation-dependence in estimating A and σ values whereas for other links, A and σ values are mainly described by mutual orientation α [38], [39]. A comprehensive discussion of ST fading properties for other B2B links is presented in [38], [39].

5.2.2 Biomechanical mobility model

The space-time variations of wireless links under unrestricted mobility are often not fully considered while developing pathloss models using measurement campaigns in [38] and [39]. The B2B channel model proposed assumes restricted mobility scenarios (close and far crossing and parallel walking) and can be enhanced to give more practical inter-BAN performance by the integration of dynamic distances with unrestricted mobility. This can be accomplished by exploiting real-time body motion capture traces which include various mobility scenarios (walking, running, sitting, exercising etc.) [7]. This real-time motion capture data when combined with geometrical transformation and analysis methods helps in actual performance evaluation of WBANs and B2B networks. The procedure for biomechanical mobility modeling includes the following steps as mentioned below

- At first, the motion capture trace file is extracted which contains the mobility traces for various postures.
- The trace file is imported to MATLAB for capturing the human body skeleton which includes markers at the joints. These markers/joints provide the space-time varying distances between the two WBAN links.
- A cylinder is applied on the body for modeling different body parts like head, torso and arms as well as for categorizing the link types as line of sight (LOS) or non-line of sight (NLOS). The determined body constructed by motion capture traces is replicated in multiple human bodies for simulating dynamic inter-BAN links
- Geometrical transformations are applied for scaling the marker dimensions into average human size.
- Geometrical analysis is performed to distinguish the inter-BAN link types as LOS or NLOS. The wrist-related channels, which include wrist-to-wrist, head-to-wrist, belt-to-wrist links, can be LOS or NLOS for the same body orientation. This is because for the same α or orientation angle, the two nodes may either be shadowed or not shadowed by the torso [39], [38]. Therefore, geometrical analysis is applied to ensure the accuracy of link types in inter-BAN wrist-related channels. In this case, the intersection of the link with single or multiple human body torso cylinders declares the given B2B link as NLOS for the wrist-related channels. The static channel modeling for the links between the other relative node positions including: head-to-head, belt-to-belt, and head-to-belt links, considers the impact of body shadowing in the distance and orientation-dependent channel gain calculation. Therefore, the geometrical analysis is not important to characterize such links as LOS or NLOS.
- Space-time varying inter-BAN links and mobility traces are generated to give the appropriate dynamic distances for the B2B channels mentioned above. The mutual orientation between two separate BANs are identical throughout the mobility trace duration since a coordinated movement scenario is simulated and the variations in α are within a range of 10° . Furthermore, the classification of dynamic link types as LOS or NLOS is performed for B2B wrist-related channels.

After obtaining the dynamic distances and link types for the given inter-BAN scenario, the channel behavior is accurately modeled with unrestricted mobility. The inter-BAN dynamic distances and mutual orientation are used to obtain channel gain values while ST fading parameters for different links are a function of mutual orientation only. The channel gain, LT fading and ST fading for wrist-related channels are computed differently for LOS

and NLOS link types so, the knowledge of dynamic link types is important in this context. It should be noted that mobility modeling provides higher and more accurate space-time variations which help in estimating more accurate path-loss results in comparison to the restricted mobility based channel models [38], [39] for B2B channels. Subsequently, the obtained path-loss values are utilized in radio link modeling to calculate the signal-to-noise ratio (SNR), bit error rate (BER) and packet error rate (PER). The entire system model with mobility modeling, B2B channel modeling and radio link modeling is illustrated in Fig. 21.

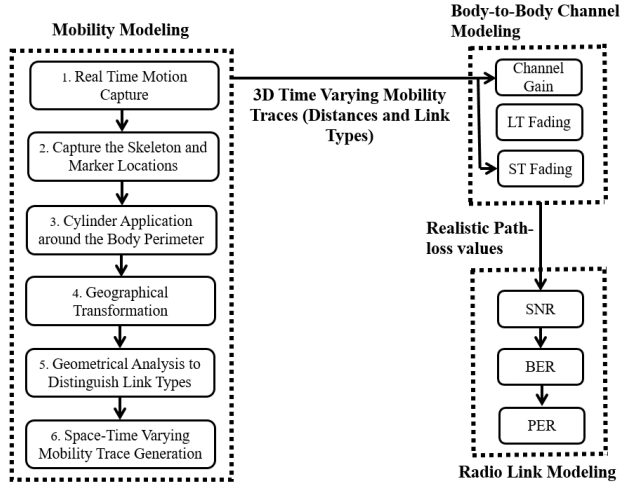


Figure 21 – Mobility, channel and radio link modeling for B2B communication.

5.2.3 Radio link model

The realistic mobility modeling of inter-BAN communication and the resultant space-time varying channels are followed by the significance of accurate radio link modeling, which includes SNR, BER and PER evaluation. The SNR between the two nodes i and j on two different BANs over the time index t can be written as

$$SNR_{i,j,t}^{dB} = P_{Tx}^{dBm} + PL_{i,j,t}^{dB} - P_N^{dBm}, \quad (25)$$

where P_{Tx} is the transmit power, P_N is the noise power and $PL_{i,j,t}^{dB}$ is the path-loss between i and j over the time t .

The exact formulation of the energy per bit to noise power spectral density ratio E_b/N_0 and BER is done depending upon the frequency and exact data rate at the physical layer. According to IEEE 802.15.6 physical layer specifications, differential binary phase shift keying (DBPSK) modulation is used for low data rates and differential quadrature phase shift keying (DQPSK) modulation is employed for high data rates at 2.45 GHz frequency [2]. The value of E_b/N_0 in dB, based on the current $SNR_{i,j,t}^{dB}$, bandwidth BW in Hz and data rate R in bps can be written as

$$E_b/N_0[dB] = SNR_{i,j,t}^{dB} + 10\log_{10}\left(\frac{BW}{R}\right), \quad (26)$$

Since Rice type ST fading is assumed in the channel model, therefore the corresponding DBPSK BER for low data rate between the inter-BAN links i and j over the time t can be

calculated as

$$BER_{i,j,t}^{DBPSK} = \frac{K+1}{2(1+K+\Gamma)} \exp\left(-\frac{K\Gamma}{1+K+\Gamma}\right). \quad (27)$$

where Γ is the average SNR given as $\Gamma = E\{z_{ST}^2\} \frac{E_b}{N_0}$ [56]. The DQPSK BER expression for high data rate is derived using the Rice density equation as a function of instantaneous SNR γ_b and the DQPSK additive white Gaussian noise (AWGN) error equation which are respectively written as

$$p(\gamma_b) = \frac{K+1}{\Gamma} \exp\left(-\frac{\gamma_b(K+1)+K\Gamma}{\Gamma}\right) I_0\left(\sqrt{\frac{4(K+1)K\gamma_b}{\Gamma}}\right), \quad (28)$$

$$P_e(\gamma_b) = Q\left(\sqrt{1.112\gamma_b}\right). \quad (29)$$

Substituting $p(\gamma_b)$ and $P_e(\gamma_b)$ into the average error probability expression $P_e = \int_0^\infty P_e(\gamma_b)p(\gamma_b)d(\gamma_b)$ [56] and integrating using the Chernoff bound for Gaussian Q-function $Q(\gamma_b) \leq \frac{1}{2} \exp^{-\frac{\gamma_b}{2}}$ [16], the upper bound on the respective DQPSK BER for high data rate between the inter-BAN links i and j over the time t can be described as

$$BER_{i,j,t}^{DQPSK} \leq \frac{\Gamma}{2(1+K+0.556\Gamma)} \left(\frac{K+1}{\Gamma}\right) \exp\left(-K + \frac{K(K+1)}{1+K+0.556\Gamma}\right). \quad (30)$$

The ETSI SmartBAN standard defines the usage of Gaussian minimum shift keying (GMSK) with the bandwidth-bit period product (BT) of 0.5 and modulation index (h) of 0.5 as the key modulation technique at the physical layer [3]. The upper bound on GMSK BER under Rice fading is acquired using the procedure discussed above and taking $P_e(\gamma_b)$ as

$$P_e(\gamma_b) = Q\left(\sqrt{2\varepsilon\gamma_b}\right), \quad (31)$$

where ε is the GMSK constant and for BT of 0.5 is equal to 0.79 [11]. The upper bound on the corresponding GMSK BER between the given B2B links i and j over the time t is therefore mentioned as

$$BER_{i,j,t}^{GMSK} \leq \frac{\Gamma}{2(1+K+0.79\Gamma)} \left(\frac{K+1}{\Gamma}\right) \exp\left(-K + \frac{K(K+1)}{1+K+0.79\Gamma}\right). \quad (32)$$

Consequently, the PER is computed based on the packet length N in bits and the adequate $BER_{i,j,t}$ expression as

$$PER_{i,j,t} = 1 - (1 - BER_{i,i,t})^N. \quad (33)$$

Finally, the obtained PER values which are based on the dynamic space-time dependent channel measurements and the accurate radio link modeling, are given to the high level packet-oriented simulation environment for the MAC layer performance evaluation.

5.3 Performance Analysis

Three different BANs are assumed in the simulation setup. with the first BAN being the inter-BAN coordinator and the rest two receive information from the coordinator BAN over a dedicated frequency channel. A separate frequency channel utilized for on-body

communication on each WBAN. The node positions for all the BANs examined in simulations consist of head (H), belt (B) and right wrist (W). With the objective to understand the best location to place the coordinator node, each node on all the first BAN takes turn in the B2B communication with the nodes on the other two BANs. For IEEE 802.15.6 standard, MAC payload sizes (N) of 16, 128 and 256 bytes as well as both low data rate (LDR, 121.4 kbps) and high data rate (HDR, 971.4 kbps) are considered. Whereas ETSI SmartBAN standard assumes a data rate of 1000 kbps for all payload sizes of 16, 128 and 250 bytes and no data transmission repetition.

Table 6 – Packet Reception Rate (%) for B2B channels w.r.t transmission power level (dBm) in IEEE 802.15.6.

Transmission Power (dBm)	Packet size (bytes)	Data Rate (kbps)	Belt-to-Head Link (%)	Head-to-Head Link (%)	Wrist-to-Head Link (%)
-10	16	121.4	89.2	99.5	50.6
		971.4	25.2	87.5	1.24
	128	121.4	61.2	95.13	12.34
		971.4	3.5	65.21	0.65
	256	121.4	39.8	92.51	0.2
		971.4	0.5	64.71	0.01
-7.5	16	121.4	92.5	99.9	66.4
		971.4	43.5	93.21	5.51
	128	121.4	74.2	96.71	26.31
		971.4	10.1	78.24	0.99
	256	121.4	55.8	94.1	7.95
		971.4	2.5	64.85	0.5
-5	16	121.4	95.3	100	75.3
		971.4	60.9	95.56	14.38
	128	121.4	84.98	98.21	42.56
		971.4	24.97	86.32	1.43
	256	121.4	70.6	96.9	20.0
		971.4	10.4	78.35	1.14
-2.5	16	121.4	98.7	100	82.15
		971.4	76.1	98.68	28.74
	128	121.4	90.3	99.93	59.74
		971.4	40.15	91.47	11.09
	256	121.4	81.05	98.21	51.95
		971.4	22.3	85.19	4.49
0	16	121.4	99.4	100	98.13
		971.4	85.05	99.01	44.29
	128	121.4	95.25	99.9	69.95
		971.4	59.9	95.3	11.21
	256	121.4	89.1	99.14	51.48
		971.4	40.01	90.9	4.97

5.3.1 Packet Reception Results

Table 6 summarizes the PRR results for B2B communication channels in IEEE 802.15.6 standard. In terms of PRR versus transmitter power performance for IEEE 802.15.6 standard, head-to-head links outperform all the other links while wrist-to-head links give the worst performance. The PRR values degrade for all link types if the packet size and the data rate are increased. For belt-to-head links, the acceptable performance of equal or above 90% PRR is achieved only when 16 byte payload is sent with low data rate (121.4 Kbps) at any given transmission power level. 128 byte payload also gives adequate performance when transmitted at higher power levels (above -2.5 dBm) with low data rates. But for head-to-head links, the PRR performance is considerably improved in comparison to the belt-to-head links. For low data rate, the transmission of different payload sizes is permissible even at the lower transmission power levels for head-to-head link. High transmission power and small payload size should be used when data is transmitted at the high rate (971.4 Kbps). For wrist-to-head links, a PRR above 90 percent is achieved only at the higher transmission power levels (-2.5 dBm) with lower payload sizes (16 bytes) and low data rate.

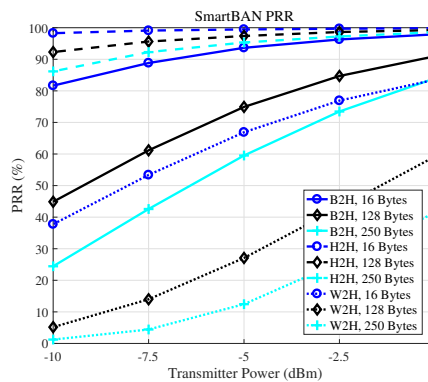


Figure 22 – PRR w.r.t transmission power level results for ETSI SmartBAN, $N = 16, 128$ and 250 bytes, belt-to-head (B2H), head-to-head (H2H) and wrist-to-head (W2H) links.

Fig. 22 illustrates the PRR performance for B2B communication results in ETSI SmartBAN standard. It is shown that the Head-to-head links again give the best results among all the link types. Data can be sent with all payload sizes at almost all transmission power levels over head-to-head links. For belt-to-head links, payload of 16 bytes can be transmitted at the transmission power level of above -5 dBm while the payload size of 128 bytes requires higher transmission power levels (0 dBm and above). Finally, wrist-to-head links do not contribute to any transmission with acceptable performance for any payload size or transmission power and might require encoded or repetitive transmissions. The presented results indicate that the placement of coordinators on the head for B2B communication significantly reduces the required transmission power levels (and hence energy consumption) for inter-BAN communication, even at high data rate and payload sizes

6 Conclusion

This PhD thesis is majorly focused on the MAC layer aspects of WBAN communication, with B2B channel modeling being the contribution at the PHY layer. At the MAC layer, ETSI SmartBAN PHY-MAC performance evaluation was carried out using different PHY-MAC parameters specified in the standard document and under various application scenarios. Moreover, a SmartBAN complaint TCA MAC algorithm was presented, implemented, and evaluated, along with several enhancements and modification to improve the baseline TCA performance. A novel FETRO MAC algorithm is also proposed to overcome the higher overhead energy consumption and considerable data rate variance issues in the WBAN use-cases. At the end, the channel for B2B communication in WBAN has been modeled using the biomechanical mobility channel traces which enables the channel modeling under unrestricted mobility scenarios and allows the realistic performance evaluation of the WBAN standards.

It is concluded that smaller slot durations are more suitable for low data rate real-time applications as they provide improved PRR, reduced latency while satisfying the throughput requirements. While for high data rate applications, longer slot durations should be considered since they help achieving better throughput results with a slight trade-off in latency constraints. Furthermore, channel coded transmissions in ETSI SmartBAN significantly improve the PRR performance over the uncoded single and repeated PPDU transmissions and also help in satisfying the high data rate throughput requirements even at low transmission power levels. The presented SmartBAN-complaint TCA MAC increases the PRR and reduces the energy consumption over the reference SmartBAN MAC while satisfying the latency and throughput constraints of the given application. Further improvements in the baseline SmartBAN-complaint TCA MAC are introduced by analyzing the channel and WBAN traffic patterns and using the AR channel modeling for channel prediction to decide the the possibility of TCA execution at each IBI. The innovative FETRO MAC technique with variable slot length counters the extra energy consumption by reducing the required transmission of several PHY-MAC overheads and offers the best trade-off between the effective throughput and overhead energy consumption outcomes. It is also determined the WBAN performance under the realistic channels is significantly affected by the node placements and for B2B communication, the placement of the coordinators on the head significantly reduces the required transmission power levels for inter-BAN communication, even at high data rate and payload sizes.

6.1 Future Work

Several directions in future can be taken to extend the work presented in this thesis. As mentioned previously, ETSI SmartBAN operates in the unlicensed spectrum and is prone to the interference issues if there are other neighbouring networks operating on the similar band. Although the channel modeling for ETSI SmartBAN under the interfered channels in hospital environments is already worked out but the interference management and co-existence strategies at the MAC layer are yet to be investigated in ETSI SmartBAN standard. IEEE 802.15.6 standard proposes three methods for co-existence which include beacon shifting, channel hopping and active superframe interleaving. These coexistence strategies can be employed in compliance with ETSI SmartBAN standard as well as several improvisations can also be proposed to further improve the performance of the primary interference mitigation and coexistence methods.

Another future contribution can be the introduction of network coding strategies in ETSI SmartBAN standard which has an ongoing work on the WBAN relaying techniques.

So far, the relevant literature about the provision of network coding in WBANs is very limited. Network Coding mainly requires the processing of incoming packets at the relay nodes such that the relay to destination packet error is reduced and the overall throughput is improved. But the WBAN sensors, including the relay nodes, are battery-powered and will require the proposal of low-complexity and highly efficient network coding schemes. This is a challenging task since the simple bit-wise XOR of the incoming WBAN packets at the relay node will not provide significant improvement in the error performance and the more sophisticated network coding techniques such as complex field network coding or Galois field network coding require a lot of computation for packet recovery at the destination node. Therefore, the proposed network coding technique for WBANs should follow a trade-off that allows an efficient error recovery mechanism even at low transmission power levels as well as does not involve heavy calculations.

Another future direction to investigate in the WBANs is the implementation of machine learning (ML) algorithms for an overall network management in scenarios that involve many individual WBANs operating in the vicinity and are being interfered by each other as well as by the other external networks operating in the similar ISM band. Since WBANs are resource-constrained, therefore the default supervised and unsupervised ML algorithms are not well suited. The focus should be turned to the Reinforcement Learning (RL) algorithms that require lesser computational complexity and memory resources. The RL algorithms learn from their previous experiences and do not require any training with the datasets, thereby saving time as well as computational resources. The RL based systems can not only be applied for the autonomous network management but also for the detection of abnormal behavior and generation of alerts.

References

- [1] Electromagnetic compatibility and radio spectrum matters (ERM); system reference document (SRdoc); medical body area network systems (MBAN) in the 1785 mhz to 2500 mhz range. Technical report, European Telecommunication Standards Institute (ETSI), 2012.
- [2] IEEE Standard for Local and metropolitan area networks - Part 15.6: Wireless Body Area Networks. *IEEE Std 802.15.6-2012*, pages 1–271, Feb 2012.
- [3] Smart body area network (SmartBAN); enhanced ultra-low power physical layer. Technical report, European Telecommunication Standards Institute (ETSI), 2015.
- [4] Smart body area network (SmartBAN); low complexity medium access control (MAC) for SmartBAN. Technical report, European Telecommunication Standards Institute (ETSI), 2015.
- [5] Smart body area networks (SmartBAN); system description. Technical report, European Telecommunication Standards Institute (ETSI), 2018.
- [6] M. M. Alam, D. Ben Arbia, and E. Ben Hamida. Joint throughput and channel aware (TCA) dynamic scheduling algorithm for emerging wearable applications. In *2016 IEEE Wireless Communications and Networking Conference*, pages 1–6, April 2016.
- [7] M. M. Alam and E. Ben Hamida. Towards accurate mobility and radio link modeling for IEEE 802.15.6 wearable body sensor networks. In *2014 IEEE 10th International Conference on Wireless and Mobile Computing, Networking and Communications (WiMob)*, pages 298–305, Oct 2014.
- [8] M. M. Alam, E. Ben Hamida, D. Ben Arbia, M. Maman, F. Mani, B. Denis, and R. D’Errico. Realistic simulation for body area and body-to-body networks. *Sensors*, 16(4):561, 2016.
- [9] M. M. Alam and E. B. Hamida. Performance evaluation of IEEE 802.15.6 MAC for wearable body sensor networks using a space-time dependent radio link model. In *2014 IEEE/ACS 11th International Conference on Computer Systems and Applications (AICCSA)*, pages 441–448. IEEE, 2014.
- [10] M. M. Alam and E. B. Hamida. Surveying wearable human assistive technology for life and safety critical applications: Standards, challenges and opportunities. *Sensors*, 14(5):9153–9209, 2014.
- [11] R. Anane, M. Bouallegue, K. Raoof, and R. Bouallegue. Achieving energy efficient and reliable communication in WSN with coded GMSK system under various channel conditions. In *2015 International Wireless Communications and Mobile Computing Conference (IWCMC)*, pages 769–775. IEEE, 2015.
- [12] S. Arnon, D. Bhasdekar, D. Kedar, and A. Tauber. A comparative study of wireless communication network configurations for medical applications. *IEEE Wireless Communications*, 10(1):56–61, 2003.
- [13] N. Bhargav, S. L. Cotton, and D. B. Smith. An experimental-based analysis of inter-ban co-channel interference using the k-u fading model. *IEEE Transactions on Antennas and Propagation*, 65(2):983–988, 2016.

- [14] G. E. Box, G. M. Jenkins, G. C. Reinsel, and G. M. Ljung. *Time series analysis: forecasting and control*. John Wiley & Sons, 2015.
- [15] C. Chakraborty, B. Gupta, and S. K. Ghosh. A review on telemedicine-based WBAN framework for patient monitoring. *Telemedicine and e-Health*, 19(8):619–626, 2013.
- [16] S.-H. Chang, P. C. Cosman, and L. B. Milstein. Chernoff-type bounds for the gaussian error function. *IEEE Transactions on Communications*, 59(11):2939–2944, 2011.
- [17] W. H. Chin, H. Tanaka, T. Nakanishi, T. Paso, and M. Hämmäläinen. An overview of ETSI TC SmartBAN's ultra low power physical layer. In *9th International Symposium on Medical Information and Communication Technology (ISMICT)*, pages 6–9, 2015.
- [18] S. L. Cotton, G. A. Conway, and W. G. Scanlon. A time-domain approach to the analysis and modeling of on-body propagation characteristics using synchronized measurements at 2.45 ghz. *IEEE Transactions on Antennas and Propagation*, 57(4):943–955, April 2009.
- [19] S. L. Cotton and W. G. Scanlon. Channel characterization for single-and multiple-antenna wearable systems used for indoor body-to-body communications. *IEEE Transactions on Antennas and Propagation*, 57(4):980–990, 2009.
- [20] R. D'Errico, R. Rosini, and M. Maman. A performance evaluation of cooperative schemes for on-body area networks based on measured time-variant channels. In *2011 IEEE International Conference on Communications (ICC)*, pages 1–5. IEEE, 2011.
- [21] F. Dijkstra. Requirements for BAN and BAN standardization from the point of view of gaming. In *BODYNETS2012, 7th Int. Conf. on Body Area Networks*, 2012.
- [22] D. Fernandes, A. G. Ferreira, R. Abrishambaf, J. Mendes, and J. Cabral. Survey and taxonomy of transmissions power control mechanisms for wireless body area networks. *IEEE Communications Surveys Tutorials*, 20(2):1292–1328, 2018.
- [23] E. Ferro and F. Potorti. Bluetooth and wi-fi wireless protocols: a survey and a comparison. *IEEE Wireless Communications*, 12(1):12–26, 2005.
- [24] J. Haapola, P. Tuomas, and R. Kohno. Method of improving channel utilization, Feb. 7 2017. US Patent 9,565,692.
- [25] M. Hämmäläinen, T. Paso, L. Mucchi, M. Girod-Genet, J. Farserotu, H. Tanaka, W. H. Chin, and L. N. Ismail. ETSI TC SmartBAN: Overview of the wireless body area network standard. In *2015 9th international symposium on medical information and communication technology (ISMICT)*, pages 1–5. IEEE, 2015.
- [26] M. Hämmäläinen, L. Mucchi, M. G. Genet, T. Paso, J. Farserotu, H. Tanaka, D. Anzai, L. Pierucci, R. Khan, M. M. Alam, and P. Dallemagne. ETSI SmartBAN architecture: the global vision for smart body area networks. *IEEE Access*, 7(10):100–107, 2020.
- [27] J. Y. Khan and M. R. Yuce. Wireless body area network (WBAN) for medical applications. *New developments in biomedical engineering*, 31:591–627, 2010.
- [28] R. Khan and M. M. Alam. Body-to-body communication: Applications, system design aspects and performance evaluation. In *12th International Symposium on Medical Information and Communication Technology (ISMICT)*, pages 1–2. IEEE, 2018.

- [29] R. Khan and M. M. Alam. Joint PHY-MAC realistic performance evaluation of body-to-body communication in IEEE 802.15. 6 and SmartBAN. In *12th International Symposium on Medical Information and Communication Technology (ISMICT)*, pages 1–6. IEEE, 2018.
- [30] R. Khan and M. M. Alam. Joint throughput and channel aware MAC scheduling for SmartBAN. In *EAI International Conference on Body Area Networks*, pages 49–64, 2018.
- [31] R. Khan and M. M. Alam. SmartBAN performance evaluation for diverse applications. In *EAI International Conference on Body Area Networks*, pages 239–251. Springer, 2019.
- [32] R. Khan, M. M. Alam, and M. Guizani. A flexible enhanced throughput and reduced overhead (FETRO) MAC protocol for ETSI SmartBAN (Accepted). *IEEE Transactions on Mobile Computing (Early Access)*.
- [33] R. Khan, M. M. Alam, and A. Kuusik. Channel prediction based enhanced throughput and channel aware MAC in SmartBAN standard. In *2019 16th International Symposium on Wireless Communication Systems (ISWCS)*, pages 463–468. IEEE, 2019.
- [34] R. Khan, M. M. Alam, T. Paso, and J. Haapola. Throughput and channel aware MAC scheduling for SmartBAN standard. *IEEE Access*, 7:63133–63145, 2019.
- [35] X. Lai, Q. Liu, X. Wei, W. Wang, G. Zhou, and G. Han. A survey of body sensor networks. *Sensors*, 13(5):5406–5447, 2013.
- [36] Lihua Ruan, M. P. I. Dias, and E. Wong. Time-optimized MAC for low latency and energy-efficient smartBANs. In *2016 IEEE Conference on Computer Communications Workshops (INFOCOM WKSHPS)*, pages 1089–1090, 2016.
- [37] M. Maman, F. Mani, B. Denis, and R. D’Errico. Evaluation of multiple coexisting body area networks based on realistic on-body and body-to-body channel models. In *2016 10th International Symposium on Medical Information and Communication Technology (ISMICT)*, pages 1–5. IEEE, 2016.
- [38] F. Mani and R. D’Errico. Short term fading spatial dependence in indoor body-to-body communications. In *2015 IEEE 26th Annual International Symposium on Personal, Indoor, and Mobile Radio Communications (PIMRC)*, pages 171–175, 2015.
- [39] F. Mani and R. D’Errico. A spatially aware channel model for body-to-body communications. *IEEE Transactions on Antennas and Propagation*, 64(8):3611–3618, 2016.
- [40] F. Martelli and R. Verdone. Coexistence issues for wireless body area networks at 2.45 ghz. In *European Wireless 2012; 18th European Wireless Conference 2012*, pages 1–6. VDE, 2012.
- [41] R. Negra, I. Jemili, and A. Belghith. Wireless body area networks: Applications and technologies. *Procedia Computer Science*, 83:1274–1281, 2016.
- [42] T. Paso, H. Tanaka, M. Hämäläinen, W. H. Chin, R. Matsuo, S. Subramani, and J. Haapola. An overview of ETSI TC SmartBAN MAC protocol. In *9th International Symposium on Medical Information and Communication Technology (ISMICT)*, pages 10–14, 2015.

- [43] M. Patel and J. Wang. Applications, challenges, and prospective in emerging body area networking technologies. *IEEE Wireless communications*, 17(1):80–88, 2010.
- [44] J. Ramis-Bibiloni and L. Carrasco-Martorell. An energy-efficient and delay-constrained resource allocation scheme for periodical monitoring traffic in smartBANs. In *2017 IEEE Biomedical Circuits and Systems Conference (BioCAS)*, pages 1–4, 2017.
- [45] J. Ramis-Bibiloni and L. Carrasco-Martorell. Energy-efficient and QoS-aware link adaptation with resource allocation for periodical monitoring traffic in smartBANs. *IEEE Access*, 8:13476–13488, 2020.
- [46] R. Rosini, F. Martelli, M. Maman, R. D’Errico, C. Buratti, and R. Verdone. On-body area networks: from channel measurements to MAC layer performance evaluation. In *European Wireless 2012; 18th European Wireless Conference 2012*, pages 1–7. VDE, 2012.
- [47] L. Ruan and E. Wong. SmartBAN downlink performance study: A novel transmission framework for reducing delay and energy consumption. *IEEE Internet of Things Journal*, 5(4):3151–3159, 2018.
- [48] S. Schillaci. BAN in defence applications. In *BODYNETS2012, 7th Int. Conf. on Body Area Networks*, 2012.
- [49] M. K. Simon and M.-S. Alouini. *Digital communication over fading channels*, volume 95. John Wiley & Sons, 2005.
- [50] D. Smith and L. W. Hanlen. *Channel Modeling for Wireless Body Area Networks*, pages 25–55. O1 2015.
- [51] D. B. Smith and L. W. Hanlen. Channel modeling for wireless body area networks. In *Ultra-Low-Power Short-Range Radios*, pages 25–55. Springer, 2015.
- [52] H. Viitala, L. Mucchi, M. Hämäläinen, and T. Paso. ETSI smartBAN system performance and coexistence verification for healthcare. *IEEE Access*, 5:8175–8182, 2017.
- [53] Y. Wang, I. B. Bonev, J. Ø. Nielsen, I. Z. Kovacs, and G. F. Pedersen. Characterization of the indoor multiantenna body-to-body radio channel. *IEEE Transactions on Antennas and Propagation*, 57(4):972–979, 2009.
- [54] G. Yi, D. Yu, and N. Kim. Adjusting control packet transmission intervals in low power sensor systems. *International Journal of Distributed Sensor Networks*, 10(8):1–8, 2014.
- [55] B. Zhen, M. Patel, S. Lee, E. Won, and A. Astrin. Tg6 technical requirements document (TRD) IEEE p802. 15-08-0644-09-0006. *Tech. Rep.*, 2008.
- [56] F. Ziong. *Digital Modulation Techniques*. Artech House Inc., 2006.

Acknowledgements

I would like to thank the Thomas Johann Seebeck Department of Electronics at Tallinn University of Technology for providing me this opportunity to pursue a PhD degree. I would like to thank my supervisor, Professor Muhammad Mahtab Alam who guided and assisted me as well as kept me motivated throughout my PhD studies. I am also thankful to my colleagues at Tallinn University of Technology, especially to Dr. Navuday Sharma, Dr. Hassan Malik, Hip Koiv, Dr. Sander Ulp, IT manager Fredrick Rang who was always willing to solve any IT related issues, staff member Eva Keerov and Senior Researcher Dr. Alar Kuusik who helped me translate thesis title and abstract in Estonian. I particularly thank my parents, brother and friends for all the support and encouragement that I received during my studies.

Finally, I express my gratitude to the following entities for their financial support during my PhD studies:

- This work has partly received funding from the European Union's Horizon 2020 research and innovation program under grant agreement No 668995 and partly supported by the Estonian Research Council under Grant PUT-PRG424.
- ICT Doctoral School at Tallinn University of Technology.
- IT Academy Scholarship at Tallinn University of Technology.
- ASTRA6-2 Project at Tallinn University of Technology.
- DoRa Programme.

Abstract

System Level Optimizations in Wearable Wireless Networks

The advances in the miniaturization of electronic equipment size have led to the emergence of inter-connected sensor nodes for realizing various types of physical data monitoring and medical/industrial/environment sensing applications. Among them, Wireless body area networks (WBANs) have gained considerable research efforts because of their potential applications in the contemporary era. The prospective WBAN applications range from the medical telemonitoring use-cases to the other embedded sensor-technology based sports, entertainment and military applications. These applications pose a broad range of quality of service (QoS) requirements related to the throughput, energy efficiency, latency and reliability. In order to realize the WBAN applications with their explicit QoS demands, three main WBAN standards were proposed, named as IEEE 802.15.6, ETSI SmartBAN and Medical BAN (MBAN). Among the WBAN-specific standards, IEEE 802.15.6 and MBAN have the constraints of high PHY-MAC layer overheads, intricate channel access mechanism and lower available bandwidths. On the contrary, the PHY-MAC structure defined by ETSI SmartBAN is rather simple and allows interoperability with the other low power sensor network standards.

WBANs are categorized by their unique set of implementation problems, mainly related to the WBAN channel modeling, massive variations in data rate requirements and energy efficiency. The human body-centric communication in WBANs poses various challenges related to the WBAN channel modeling, making it prone to the human body shadowing. A meager change in the body posture can lead to a considerable decrease in communication reliability since the transmission power levels are extremely low. WBAN devices are battery-powered, so the contention based MAC techniques for channel access are less efficient due to the additional energy consumed in channel sensing. Moreover, WBAN sensor data is heterogeneous which makes the fixed MAC scheduling less efficient. Therefore, traffic adaptive and dynamic MAC scheduling techniques ensure both the reliability and energy efficiency in WBAN channel access methods.

ETSI SmartBAN performance is thoroughly examined for the implementation of the diverse WBAN applications, categorized as low, medium and high data rate use-cases. For performance evaluation, packet reception rate (PRR), aggregated throughput and latency are taken as the primary QoS criteria. Two different channel models are assumed, namely static CM3B (S-CM3B) and realistic CM3B (R-CM3B), for the performance analysis and different slot durations allowed in ETSI SmartBAN are considered to further comprehend the results. The simulation results indicate that the smaller slot duration overperform in terms of PRR and latency while the longer slot durations are more effective to support high data rate application throughput requirements. Furthermore, the channel coding is shown to significantly enhance the error performance in ETSI SmartBAN compared to the repetition coding technique.

An ETSI SmartBAN-compliant Throughput and Channel Aware (TCA) MAC scheduling scheme is proposed and evaluated. TCA algorithm utilizes the channel signal-to-noise ratio (SNR) to choose the candidate transmission nodes in a given time slot during the first phase of the algorithm. During the second phase, the slot is assigned to one of the selected sensor nodes based on their priority level and data packet availability. The algorithm uses m-periodic scheduling in which the sensor nodes are envisaged for slot assignment (of time slot) according to their data packet generation rate during the second phase. TCA algorithm in ETSI SmartBAN is executed through slot reassignment during which the scheduling information is shared with the sensor nodes. But sending slot reassignment frames and their node acknowledgements for TCA execution at alternate inter-beacon in-

tervals (IBIs) may lead to poor energy efficiency. For curtailing the frequent occurrence of TCA execution due to slot reassignment frame transmission, further enhancements are introduced in the primary TCA algorithm in this thesis. These modified algorithms to provide improved performance include Enhanced TCA MAC and channel prediction based enhanced TCA MAC algorithms. The enhanced TCA MAC algorithm decreases the frequency of slot reassignment frame transmission at alternate IBIs by executing TCA and recreating the assignment array only when the channel states fluctuate or the data packet status of the past slot allocations varies. The channel prediction based enhanced TCA utilizes the auto-regressive (AR) modeling of the channel states in the upcoming time slots to make the decision about the execution of TCA and performs the TCA slot assignment using the downlink frame transmission.

An innovative and flexible enhanced throughput and reduced overhead (FETRO) MAC protocol for scheduled access is described to manage the sensor node data rate variations. In the proposed FETRO MAC scheme, the sensor node data rate requirements are considered while assigning the scheduled access time slot duration by allowing minimal changes in the base-line standard implementation. This infers the provision of scheduled access slots with variable slot durations within an IBI to accommodate various payload sizes from sensor nodes. The proposed FETRO MAC scheme results in optimizing both the overall throughput and normalized overhead energy consumption per Kbps at both the sensor nodes and the central hub.

There are some WBAN applications which utilize body-to-body (B2B) communication like rescue and emergency management as well as defence and military use-cases. In order to accurately model the B2B channels and incorporate the impact of B2B channels on the MAC layer, a joint PHY-MAC performance analysis of inter-BAN communication systems is elaborated. The performance evaluation utilizes the realistic B2B wireless channel models for IEEE 802.15.6 and ETSI SmartBAN standards. The time-varying distances for the space-time B2B link variations are generated by real-time motion capture traces which are then introduced into already established B2B wireless channel models to provide the actual pathloss values in dynamic environments. Using the proposed mobility and radio link models, a more tangible performance assessment of B2B networks with IEEE 802.15.6 and ETSI SmartBAN specifications is achieved.

Kokkuvõte

Kantavate seadmete võrkude süsteemi tasemel optimeerimine

Elektroonikasõlmede mõõtmete edukas vähendamine on tekitanud vajaduse omavahel ühenduvate sensormoodulite järele erinevate monitoorimisrakenduste realiseerimiseks. Juhtmevabad kehapiirkonna võrgud (wireless body area networks, WBANs) nende hulgast on osaks saanud märkimisväärsed teadustöö alaseid pingutusi seoses nende potentsiaalsete rakendustega käesoleval ajal. Võimalikud kehapiirkonna võrkude rakendused ulatu-vad meditsiinilise telemonitooringu kasutuslugudest muude sardssensorüsteemidel põ-hinevate spordi, meelelahutuse ja militaarrakendusteni. Nimetatud rakendused esitavad laia valiku nõudeid teenuskvaliteedile (quality of service, QoS), mis on seotud läbilaske-võimega, energiaefektiivsusega, hilistumise ja töökindlusega. Realiseerimaks juhtmeta ke-hapiirkonna võrkude rakendusi vastavalt kehtestatud teenuskvaliteedi nõuetele, on välja pakutud kolm peamist WBAN standardit: IEEE 802.15.6, ETSI SmartBAN ja Medical BAN (MBAN). Nende WBAN-spetsiifiliste standardite hulgast IEEE 802.15.6 ja MBAN omavad piiranguid füüsilise ja sidemeedia ligipääsu haldamise (physical - media access control, PHY-MAC) andmekihi ülekulu, keeruka sidekanali poole pöördumise mehhanismi ja ma-dalate kättesaadavate ribalaiuste tõttu. Vastupidiselt eelnevale on ETSI SmartBAN defi-neeritud PHY-MAC struktuur üsna lihtne ja lubab ühilduvust teiste madala energiatarbega sensorvõrkude standarditega.

Juhtmeta kehapiirkonna võrke lahterdatakse rakendusprobleemide unikaalse kogumi põhjal, mis on peamiselt seotud sidekanali modelleerimisega, massiivsete variatsioonidega andmeedastuskiiruse nõuetes ja energiaefektiivsuses. Nimkehakesksus WBAN sides loob mitmesuguseid keerukusi seoses sidekanali modelleerimisega, muutes selle mõju-tatuks kehaga varjamisest. Tühine muutus keha asendis võib põhjustada olulist side töö-kindluse vähenemist, sest saatevõimsused on erakordselt väikesed. Kehapiirkonna võr-guseadmed on patareitoitelised, seega võistlevat laadi sidemeediale ligipääsu haldamise (media access control, MAC) meetodikad kanali kasutamiseks on vähemefektiivsed, sest kulutavad lisaenergiat kanali jälgimiseks. Veel enam, sensorandmed juhtmevabades ke-hapiirkonna võrkudes on heterogeensed, mis teeb fikseeritud MAC ajaplaanuri väheefek-tiivseks. Seetõttu liiklusele kohanduv ja ajas dünaamiline sidemeediale ligipääsu planeeri-mine tagab samaaegselt töökindluse ja energiaefektiivsuse WBAN sidekanali poole pöör-dumisel.

ETSI SmartBAN jõudlust on põhjalikult analüüsitud selle rakendamiseks erinevates kehavõrkude rakendustes, mida klassifitseeritakse madala, keskmise ja kõrge sidekiirusega kasutusjuhtudeks. Jõudluse hindamiseks on sidepakettide vastuvõtmise määr (packet reception rate, RRR), agregeeritud läbilaskevõime ja hilistumine primaarsed teenuskvaliteedi hindamise kriteeriumid. Jõudluse hindamiseks eeldatakse kahte erinevat sidekanali mudelit, staatilist CM3B (S-CM3B) ja realistikku CM3B (R-CM3B) ja erinevate pikkustega ETSI SmartBAN-s lubatud ajapilud (slots) võetakse arvesse tulemuste paremaks analüü-siks. Simulatsiooni tulemused näitavad, et lühem ajapilu tagab paremad RRR ja hilistumise väärtused, samal ajal on pikemad ajapilud efektiivsemad toetamaks suuri andmekiirusi nõudvate rakenduste nõudeid. Edasi, on näidatud, et kanali kodeerimine parandab ETSI SmartBANi puhul oluliselt kvaliteeti vigade osas võrreldes korduste kodeerimise tehnika-ga.

ETSI SmartBAN-ga ühilduv läbilaskevõime- ja sidekanalitundlik (throughput and channel aware, TCA) sidemeediale ligipääsu planeerimise meetod on välja pakutud ning ana-lüüsitud. TCA algoritm kasutab esimeses faasis ära signaali-müra suhet (signal-to-noise ra-

tio, SNR) et valida kandidaatsõlm transmissiooniks konkreetsetes ajapilus. Teises faasis määratakse ajapilu ühele valitud sensorsõlmele vastavalt sõlmele prioriteedile ja andmepaketi olemasolule. Algoritm kasutab m-perioodilist ajastamist, mille puhul sensorsõlmele ajapilu määratakse vastavalt nende poolt andmepakettide genereerimise kiirusele teises faasis. ETSI SmartBAN-i puhul rakendatakse TCA algoritmi ajapilude ümberjagamise, mille jooksul jagatakse ajaplaneerimise infot sensorsõlmedega. TCA algoritmi rakendamiseks vajalikud ajapilude ümberjagamise sõnumid ja sõlmele saadetud kinnitused neile võivad vahelduvate taktsignaali intervallide (inter-beacon interval, IBI) korral lõppeda aga puuduliku energiaefektiivsusega. Piiramaks TCA sagedast rakendamist ajapilu ümberjagamise paketi edastamisel esitatakse käesolevas töös täiendavad parendusi TCA baasalgoritmile. Need jõudlust parendavad modifitseeritud algoritmid sisaldavad täiustatud TCA MAC ja sidekanali ennustamisel põhinevat täiustatud TCA MAC algoritme. Täiustatud TCA MAC algoritm lühendab ajapilu saatepaketi perioodilisi transmissioone vahelduva taktsignaali perioodi korral rakendades TCA-d ja taasluues määramismassiivi üksnes juhul kui kanali olekud muutuvad või kui andmepaketi staatus varasemast ajapilu määramisest on muutunud. Kanali ennustamisel põhinev täiustatud TCA kasutab auto-regressiivset kanali olekute mudeldamist järgnevate ajapilude jooksul, et otsustada TCA rakendamine ja teostab TCA ajapilude määramist kasutades selleks allalaadimissuunalisi sidepakette.

Kirjelatud on innovatiivset ja paindlikku parendatud läbilaskevõime ja side vähendatud ülekuluga (FETRO) MAC protokolliga ajastatud kanali ligipääsuks, mis võimaldab hallata sensorsõlme andmevahetuskiruse muutusi. Välja pakutud FETRO MAC lahenduses arvestatakse sensorsõlme sidekiiruse nõudeid kanalit plaanikohaselt kasutatavate ajapilude kestvuse määramisel, lubades seejuures minimaalseid erinevusi baasstandardi rakendamisel. Sellest tulenevad sidekanalit planeeritult kasutavad muutuva pikkusega ajapilud taktsignaali intervallide raames, eesmärgiga mahutada erinevaid andmemahte erinevatest sensorssõlmedest. Pakutud FETRO MAC lahendus optimeerib nii üldist läbilaskevõimet kui ka normaliseeritud ülevaluenergiat kb/s kohta sensorsõlmedes ja keskseadmes.

On olemas mõningaid WBAN rakendusi, mis kasutavad kehalt kehale (body-to-body, B2B) sidet nagu näiteks pääste- ja hädaabi operatsioonid, samuti kaitse- ja militaarrakendused. Selleks, et täpselt mudeldada B2B kanaleid ja tuua sisse B2B kanalite mõjud MAC kihti, töötati välja ühine PHY-MAC sooritusanalüüs keha lähiala võrkudele. Sooritusanalüüs kasutab realistlikke B2B raadiokanali mudeleid IEEE 802.15.6 ja ETSI SmartBAN standarditele. Ajas muutuvad distantsid B2B side asukoha-aja variatsioonide tarbeks on genereeritud reaalsajas liikumise kohutud jälgedest, mis seejärel on sisse viidud juba eksisteerivatesse B2B sidekanali mudelitesse kirjeldamiseks tegelikke signaalikadusid dünaamilises keskkonnas. Kasutades mobiilsust ja välja pakutud raadiolingi mudeleid, on saavutatud käega katsutavam B2B võrkude võimekuse hindamine IEEE 802.15.6 ja ETSI SmartBAN spetsifikatsioonide baasil.

Appendix 1

R. Khan and M. M. Alam. SmartBAN performance evaluation for diverse applications. In *EAI International Conference on Body Area Networks*, pages 239–251. Springer, 2019

SmartBAN Performance Evaluation for Diverse Applications*

Rida Khan, and Muhammad Mahtab Alam

Thomas Johann Seebeck Department of Electronics, Tallinn University of
Technology, Tallinn, Estonia
{rikhan, muhammad.alam}@ttu.ee

Abstract. Wireless Body Area Networks (WBANs) envision the realization of several applications which involve the physiological monitoring and/or feedback generations according to the monitored vital signs. These applications range from telehealth or telemedicine to sports and entertainment. SmartBAN provides the physical (PHY) and medium access control (MAC) layer specifications for a simplified and efficient execution of these applications. This paper provides an overview of the existing WBAN use-cases and categorizes them according to their data rate requirements. The SmartBAN performance is thoroughly investigated for the implementation of these diverse applications. For performance evaluation, packet reception rate (PRR), aggregated throughput and latency are taken as the primary quality of service (QoS) criteria. We assume two different channel models, namely static CM3B (S-CM3B) and realistic CM3B (R-CM3B), and different options for the slot durations to further comprehend the results. The simulation results indicate that smaller slot duration performs better in terms of PRR and latency while longer slot durations are more effective to support high data rate application throughput requirements.

Keywords: Wireless body area network (WBAN) · SmartBAN · data rate · packet reception rate (PRR) · throughput · latency.

1 Introduction

Telemedicine and telehealth monitoring systems require the collection of vital information, and in some cases transmission of appropriate feedback, from/to remote patients or subjects through a central hub. Wireless body area network (WBAN) is a set of sensor nodes placed on/inside the subject body for collecting physiological information, actuators for receiving the feedback information and a central hub for managing WBAN functioning and communicating with the

* This research was supported in part by the European Unions Horizon 2020 Research and Innovation Program under Grant 668995, in part by the European Union Regional Development Fund through the framework of the Tallinn University of Technology Development Program 20162022, and in part by the Estonian Research Council under Grant PUT-PRG424.

gateway [1]. Initially, some generic mesh-topology based low power and reduced data rate standards, like IEEE 802.15.4 [2,3], were considered as potential candidates for WBAN applications. But the first attempt to standardize the WBAN physical (PHY) and medium access control (MAC) layer operations was made by IEEE, resulting in the release of IEEE 802.15.6 WBAN standard [4]. European Telecommunication Standard Institute (ETSI) later introduced another WBAN specific standard, called SmartBAN, with rather simplified and energy efficient network structure [5]. Other important features exclusively provided by SmartBAN include faster channel acquisitions, interoperability with other network nodes, hub-to-hub communication or inter-hub relay and coexistence management by coordinator [5].

WBAN can expedite several medical and non-medical applications such as stress monitoring, cardiac monitoring, sports and entertainment [1]. The application requirements vary according to the types of sensor nodes employed, number of nodes, urgency of data delivery, information sampling rate and bit resolution. Some use-cases require only few kilo bits per second (kbps) of data rate while some use-cases demand a throughput as high as hundreds of kbps. A SmartBAN is designed to handle these high variations in data transmission rates while satisfying the other quality of service (QoS) parameters like packet reception rate (PRR) and latency.

In the view of the above discussion, we aim to make the following contributions in this paper:

- We categorize the WBAN use-cases into three categories according to their respective throughput requirements, as low, medium and high data rate applications.
- We evaluate each of these use-cases in terms of PRR, attainable throughput and latency as key performance indicators.
- For a better analysis of associated results, we take static IEEE CM3B (S-CM3B) [6] as well as realistic IEEE CM3B (R-CM3B) [7] channel models. Moreover, different options for slot durations in SmartBAN are also considered for performance evaluation.

The remaining paper is organized in the following way: section II describes the SmartBAN PHY and MAC layer specifications and section III explains the inherent system model. In section IV, numerical results are investigated and section V concludes the paper along with the future work.

2 SmartBAN PHY and MAC Layer Specifications

This section elaborates the ultra low power PHY layer and simplified scheduled access MAC layer structures in SmartBAN.

2.1 Ultra Low Power PHY Layer

SmartBAN operates on 2.4GHz unlicensed spectrum with 2MHz bandwidth for each individual channel. The employed modulation scheme is Gaussian Frequency Shift Keying (GSFK) with a bandwidth-bit period product $BT = 0.5$,

and modulation index $h = 0.5$. An optional systematic Bose-Chaudhuri Hocquenghem (BCH) code is also provided for the error correction control of MAC-layer protocol data unit (MPDU). SmartBAN proposes the utilization of one, two and four physical-layer protocol data unit (PPDU) repetitions for improving the PRR performance [8].

2.2 Scheduled Access MAC Layer

SmartBAN mainly supports star topology for communication between sensors and central hub. Separate control and data channels are used to enable faster channel acquisitions and simplify the MAC layer operation. Once a sensor node joins SmartBAN, all the communication between the hub and node takes place on data channel. Each inter-beacon interval (IBI) on data channel starts with the D-Beacon, followed by the scheduled access, control and management (C/M) and inactive durations. Scheduled access period involves the data transmission by sensor nodes and the reception of corresponding acknowledgements from hub. C/M period is used for other WBAN operations such as connection establishment, connection modification and connection termination. Inactive period is provided to enable the sleep mode and power saving in SmartBAN [9].

Each scheduled access or C/M slot consists of PPDU transmissions and PPDU acknowledgements separated by inter-frame spacing (IFS). The actual data or control information payload is present in MAC frame body, that is appended with MAC header and frame parity to generate an MPDU. For uncoded transmission, an MPDU becomes physical-layer service data unit (PSDU). PSDU, along with physical-layer convergence protocol (PLCP) header and preamble, constitutes a complete PPDU. In scheduled access mode with two and four repetitions, the transmitted PPDU is repeated twice and four times, respectively, within the assigned time slot duration for each node, resulting in a decrease of the maximum allowed payload size for each slot transmission. Figs. 1 and 2 respectively illustrate the IBI formats for no repetition and 2-repetition transmission scenarios [9].

The slot duration T_{slot} for each slot in the IBI on data channel is determined by the parameter L_{slot} as $T_{slot} = L_{slot} \times T_{min}$, where $L_{slot} = \{1, 2, 4, 8, 16, 32\}$ and T_{min} is the minimum slot duration. The slot duration is broadcast in control channel beacon and all the connected sensors transmit their data at this pre-defined slot length in each IBI, after connection establishment with their corresponding central hub. A longer slot length can accommodate more payload, with lesser PHY-MAC layer overheads and acknowledgement transmissions, and facilitates higher throughput whereas a shorter slot duration is sufficient to support low data rate applications. Further details about the SmartBAN PHY and MAC layer specifications are given in [8] and [9].

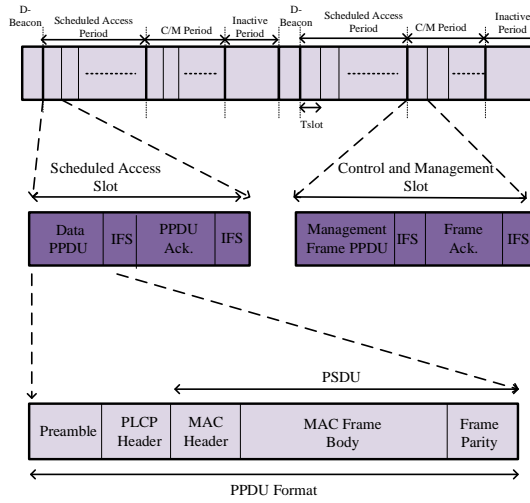


Fig. 1. IBI format with no PPDU repetitions in scheduled access and C/M durations.

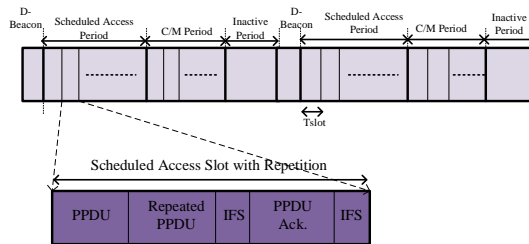


Fig. 2. IBI format with two PPDU repetitions in scheduled access duration.

3 System Model

This section explains the related physical channel and application-specific details of the system model, utilized for carrying out the simulations. Additionally, the simulation setup details are also provided.

3.1 Channel, Mobility and Radio Link Modeling

We take two different channel models for computing the pathloss values which include static IEEE CM3B (S-CM3B) channel with additive white Gaussian noise (AWGN) [6] and realistic IEEE CM3B (R-CM3B) channel with AWGN [7]. The distances related to each on-body link between the sensor node and hub remain the same in static CM3B model and pathloss is calculated for those constant distances. In the realistic channel model with AWGN, dynamic distances and link types are generated for different on-body links using a biomechanical mobility trace file. Dynamic distances and link types, as defined by a specific mobility scenario like walking, running or sit-stand, are taken as inputs for pathloss calculations. The space-time varying link types identify a particular on-body link as either line of sight (LOS) or non-line of sight (NLOS). An additional NLOS factor of 13% is added to the resultant pathloss value with time-varying distances, for NLOS link status, otherwise the pathloss remains unchanged [7].

After computing the static as well as realistic pathloss values, radio link modeling is performed which includes signal-to-noise ratio (SNR), bit error ratio (BER) and packet error ratio (PER) computations. The theoretical expression for the GFSK BER calculation at SmartBAN PHY layer is given in [10] for a single PPDU transmission scenario. Whereas, for finding BER with two and four PPDU repetitions, SNR calculations are performed according to the diversity technique used for integrating the repetition gain. We assume the maximal ratio combining (MRC) diversity scheme with statistically independent channels for repetition scenarios, therefore, the resulting SNR is the summation of instantaneous link SNRs during each round of the identical PPDU transmission [11]. Subsequently, BER for the repeated PPDU transmissions is computed using the similar BER expression, as mentioned in [7]. Further details about the inherent radio link modeling and the packet reception rate (PRR) analysis are provided in [7].

3.2 WBAN Application-Specific Requirements

A number of medical and consumer electronics use-cases can be identified as potential scenarios for SmartBAN PHY and MAC layer implementation. Each use-case has its own data rate and latency requirements that are peculiar to the number of nodes, sampling rate and quantization, urgency of the data delivery and types of the nodes present in the given use-case. Generally SmartBAN supports a nominal data rate of 100 kbps and a maximum transmission rate of up to 1 Mbps at the PHY layer. The maximum node capacity is 16 nodes per WBAN but typically up to 8 nodes are present in a SmartBAN. For real time

high priority traffic, 10 ms latency can be facilitated while for regular traffic 125 ms latency is required [5].

We take three different use-cases classified according to their throughput requirements as low, medium and high data rate applications. A safety and fall monitoring medical use-case is assumed as a low rate application in which patch-type sensors are attached on an elderly adult body. An alert signal is transmitted to the data server when the elder feels physically sick or falls during the regular everyday activities. A rescue and emergency management use-case is considered as medium data rate WBAN application in which sensor data is used to monitor the physical conditions, surrounding environment and location of the rescue workers. A precise athlete monitoring use-case is taken as a high rate application to measure the electrical activity of the muscles and for checking the pitching form in an athlete. All the relevant information about these use-cases is summarized in Table 1.

Table 1. Low, medium and high data rate example use-cases [5, 12, 13].

Safety and fall monitoring (low-data rate)				
Sensor type	Sampling rate /Quantization	Data rate	Number of sensors	Real time /Non-real time
Pulse Wave /ECG	10-16 bit, 64 Hz-1 kHz	640 bps-16 kbps	1	Real time
Accelerometer /Gyroscopic sensor	10-16 bit, 64 Hz-1 kHz	640 bps-16 kbps	3	Real time
Rescue and emergency management (medium-data rate)				
Sensor type	Sampling rate /Quantization	Data rate	Number of sensors	Real time /Non-real time
Pulse Wave	10-16 bit, 64 Hz-1 kHz	640 bps-16 kbps	1	Real time
Accelerometer /Gyroscopic sensor	10-16 bit, 64 Hz-1 kHz	640 bps-16 kbps	2	Real time
Voice Command	-	50 kbps-100 kbps	1	Real time
Ambient sensor	10-16 bit, 64 Hz-1 kHz	640 bps-16 kbps	1	Real time
GPS node	-	96 bps	1	Real time
Precise athlete monitoring (high-data rate)				
Sensor type	Sampling rate /Quantization	Data rate	Number of sensors	Real time /Non-real time
EMG	6-12 bit, 10 kHz-50 kHz	60 kbps-600 kbps	1	Real time
Accelerometer /Gyroscopic sensor	10-16 bit, 64 Hz-1 kHz	640 bps-16 kbps	4	Real time

According to Table 1, all example applications require a maximum 10 ms latency whereas the aggregated throughput requirements range from 2.56 kbps-64 kbps, 52.656 kbps-164.096 kbps and 62.56 kbps-664 kbps for low, medium and high data rate applications respectively. The PRR should be above 90% for all the given use-cases.

3.3 Simulation Setup

Table 2 mentions all the SmartBAN PHY and MAC layer parameters assumed during the simulation. We allocate a single scheduled access slot per sensor node while there are two slots in both the C/M period and inactive durations for all the given use-cases. Therefore, safety and fall monitoring application has four scheduled access slots in its IBI, rescue and emergency management application employs six scheduled access slots and precise athlete monitoring application requires five scheduled access slots. The trace file that provides space-time varying distances and link types for the R-CM3B channel model assessment of the safety and fall monitoring use-case is about 59 seconds long and contains walking, sitting and hand motions mobility patterns. For the rescue and emergency management and precise athlete monitoring use-cases, the mobility trace file is 63 seconds long and includes walking, sit-stand and running mobility scenarios. The pathloss values for the S-CM3B channel models are repeated for the similar durations to ensure the performance evaluation at a similar time span. The simulations with the given trace files are repeated 100 times to give performance outcomes with more certainty. All the simulations are carried out in the MATLAB run-time environment.

Table 2. Simulation setup parameters [8, 9].

RF parameters	
Transmitted Power (dBm)	-10, -7.5, -5, -2.5, 0
Receiver Sensitivity (dBm)	-92.5
Bandwidth per channel (MHz)	2
Information Rate (kbps)	1000
Modulation	GFSK ($BT=0.5$, $h=0.5$)
PHY/MAC parameters	
Minimum slot length (T_{min})	625 μ s
Slot duration (T_{slot})	0.625 ms, 1.25 ms, 2.5 ms
Interframe spacing (IFS)	150 μ s
Symbol Rate (R_{Sym})	10 ⁶ symbols/sec
MAC header (N_{MAC})	7 octets
Frame Parity (N_{par})	2 octets
PLCP header (N_{PLCP})	5 octets
PLCP Preamble ($N_{preamble}$)	2 octets
PPDU repetition	1, 2 and 4

4 Performance Evaluation

This section analyzes the simulation results to comprehend the QoS obtained using SmartBAN system specifications, for various use-cases.

4.1 Packet Reception Rate (PRR)

The average PRR results for low, medium and high data rate applications are illustrated in Figs. 3, 4 and 5. For low data rate use-case, the smallest slot duration of 0.625 ms, represented by $L_{slot} = 1$ in Fig. 3, can achieve a PRR above 90% under all transmission power levels, single PPDU transmission and both the channel models. PPDU repetitions with smallest slot duration are not possible because the amount of related PHY-MAC overheads to constitute a complete PPDU cannot be transmitted more than once. For 1.25 ms and 2.5 ms slot durations, respectively indicated by $L_{slot} = 2$ and $L_{slot} = 4$ in Fig. 3, the transmission power should be -7.5 dBm or above to obtain the required PRR for single transmission while with PPDU repetitions, all transmission power levels result in the target PRR. In Figs. 4 and 5 for medium and high data rate applications respectively, the PRR values are not significantly affected by the PPDU repetition scheme or transmission power levels for S-CM3B channel. However the transmission power levels above -2.5 dBm are generally required to achieve the target PRR for all slot durations and repetition schemes. Furthermore, larger slot durations, despite carrying more payload with less PHY-MAC overheads, can have decreased PRR because of the increase in overall packet size [10]. The reason for lower PRR values, with realistic CM3B (R-CM3B) channel model in Figs. 3, 4 and 5, is that the R-CM3B model integrates the NLOS or human body shadowing losses as well in radio link modeling, while computing the pathloss, SNR, BER and PER values. The channel losses due to human body shadowing or NLOS conditions are not considered in static CM3B (S-CM3B) channel model and pathloss calculations are performed only for the fixed hub-node link distances. Consequently, the impact of human mobility on PRR performance is not evident with the S-CM3B channel model.

4.2 Throughput

The effective throughput under the given static and realistic CM3B channel conditions can be computed as $Th_{pr} = \frac{N_{Rx}}{T_{trace}}$, where N_{Rx} is the total number of received bits for each node in the given time span and the T_{trace} is complete duration of the pathloss file, as mentioned in sub-section 3.3. We assume that the maximum allowed payload size, as determined by the slot duration (L_{slot}) is transmitted for each use-case or application. The aggregated throughput results of all the sensor nodes for all the considered use-cases are shown in Figs. 6, 7 and 8. We evaluate the throughput results for -2.5 dBm transmitter power since it ensures the PRR above 90% in almost all of the scenarios, as discussed in sub-section 4.1. Considering the safety and fall monitoring application, the smallest slot duration 0.625 ms would be enough to satisfy the throughput QoS

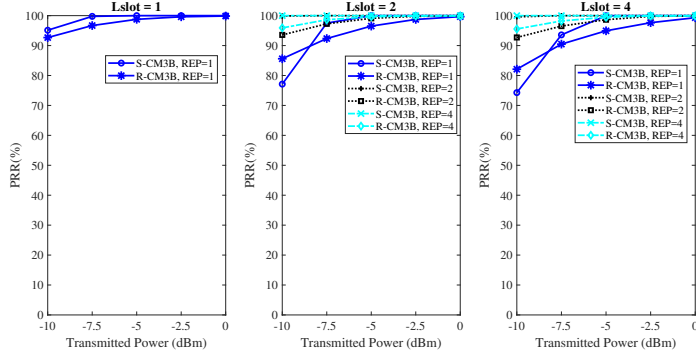


Fig. 3. Packet reception rate (PRR) (%) w.r.t transmission power (dBm) for safety and fall monitoring application (low-data rate), at (a) $L_{slot} = 1, 2, 4$ or $T_{slot} = 0.625\text{ms}, 1.25\text{ms}, 2.5\text{ms}$ (b) $REP = 1, 2, 4$ (c) static CM3B (S-CM3B) and realistic CM3B (R-CM3B).

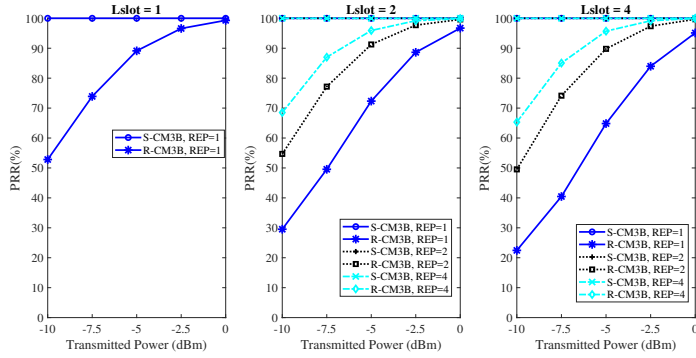


Fig. 4. Packet reception rate (PRR) (%) w.r.t transmission power (dBm) for rescue and emergency management application (medium-data rate), at (a) $L_{slot} = 1, 2, 4$ or $T_{slot} = 0.625\text{ms}, 1.25\text{ms}, 2.5\text{ms}$ (b) $REP = 1, 2, 4$ (c) static CM3B (S-CM3B) and realistic CM3B (R-CM3B).

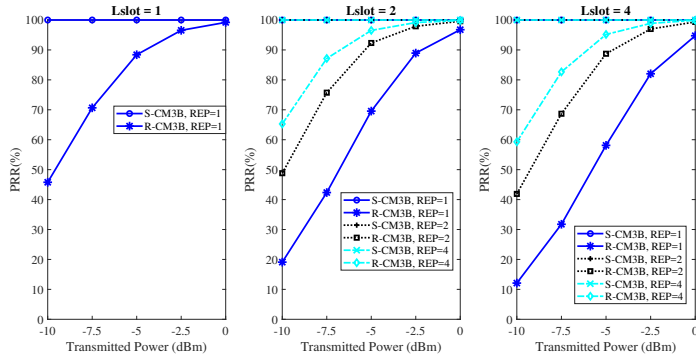


Fig. 5. Packet reception rate (PRR) (%) w.r.t transmission power (dBm) for precise athlete monitoring application (high-data rate), at (a) $L_{slot} = 1, 2, 4$ or $T_{slot} = 0.625\text{ms}, 1.25\text{ms}, 2.5\text{ms}$ (b) $REP = 1, 2, 4$ (c) static CM3B (S-CM3B) and realistic CM3B (R-CM3B).

requirements, as given in sub-section 3.2. However for medium data rate application, which requires 52.656 kbps-164.096 kbps data rate, 1.25 ms and 2.5 ms slot durations are more suitable with single PPDU transmission and two PPDU repetitions. Finally, for high data rate application throughput requirements, 2.5 ms slot duration with single PPDU transmission and two PPDU repetitions serves as the best option since it enables the transmission of more payload at once. The increase in throughput with the increase in slot duration (L_{slot}) can be explained by the phenomenon that larger L_{slot} values allow the transmission of more payload with the same PHY-MAC overheads, as compared to the smaller L_{slot} values, in a single transmission.

4.3 Latency

The packet latency is calculated as the time difference between the data packet generation and its successful reception. Table 3 enlists the latency values for all the given use-cases with different slot durations. It should be noted that the repetition scheme or the channel types do not affect the obtained latency values since the latency is computed only for the successfully received packets. The latency values increase with the increase in slot durations because larger slot durations have longer IBIs. Also the latency values are the highest for the rescue and emergency management application since it has the largest number of sensor nodes and the assigned scheduled access slots. For safety and fall monitoring application, the PRR and throughput requirements are met with the 0.625 ms slot duration, so using this slot duration can guarantee the minimum possible latency for this real time application. The minimum latency can be ensured for

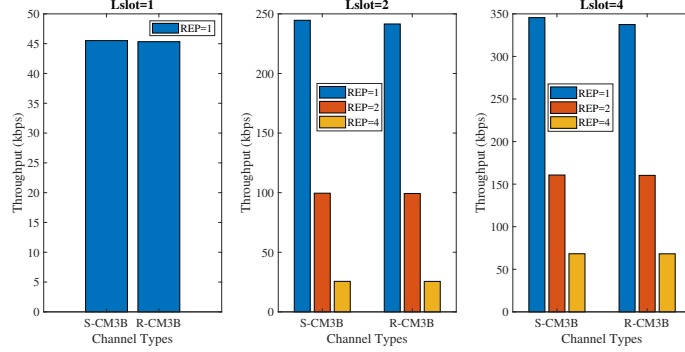


Fig. 6. Throughput (kbps) for safety and fall monitoring application (low-data rate), at (a) $L_{slot} = 1, 2, 4$ or $T_{slot} = 0.625\text{ms}, 1.25\text{ms}, 2.5\text{ms}$ (b) $REP = 1, 2, 4$ (c) static CM3B (S-CM3B) and realistic CM3B (R-CM3B) (d) -2.5dBm transmission power.

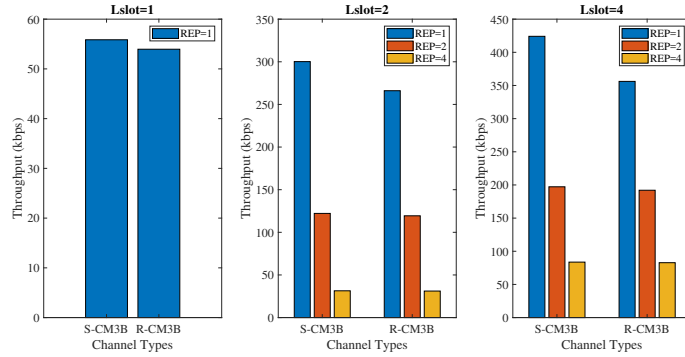


Fig. 7. Throughput (kbps) for rescue and emergency management application (medium-data rate), at (a) $L_{slot} = 1, 2, 4$ or $T_{slot} = 0.625\text{ms}, 1.25\text{ms}, 2.5\text{ms}$ (b) $REP = 1, 2, 4$ (c) static CM3B (S-CM3B) and realistic CM3B (R-CM3B) (d) -2.5dBm transmission power.

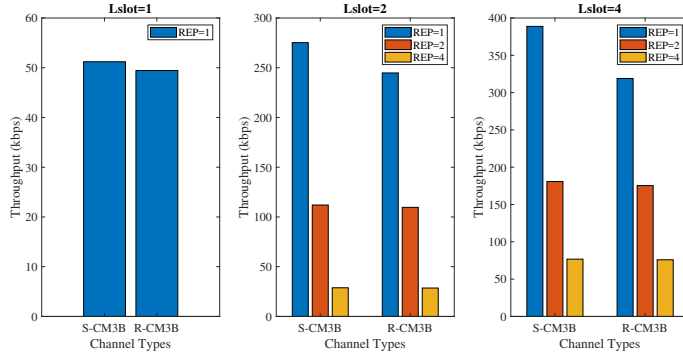


Fig. 8. Throughput (kbps) for precise athlete monitoring application (high-data rate), at (a) $L_{slot} = 1, 2, 4$ or $T_{slot} = 0.625\text{ms}, 1.25\text{ms}, 2.5\text{ms}$ (b) $REP = 1, 2, 4$ (c) static CM3B (S-CM3B) and realistic CM3B (R-CM3B) (d) -2.5dBm transmission power.

rescue and emergency management application with 1.25 ms slot size while satisfying the PRR and throughput demands. Finally, for precise athlete monitoring application, a slight compromise in latency is observed since only 2.5 ms slot can support the required throughput.

Table 3. Latency (ms) for low, medium and high data rate use-cases.

Safety and fall monitoring (low-data rate)		
$L_{slot}=1/T_{slot}=0.625\text{ms}$	$L_{slot}=2/T_{slot}=1.25\text{ms}$	$L_{slot}=4/T_{slot}=2.5\text{ms}$
2.5	5	10
Rescue and emergency management (medium-data rate)		
$L_{slot}=1/T_{slot}=0.625\text{ms}$	$L_{slot}=2/T_{slot}=1.25\text{ms}$	$L_{slot}=4/T_{slot}=2.5\text{ms}$
3.8	7.5	15
Precise athlete monitoring (high-data rate)		
$L_{slot}=1/T_{slot}=0.625\text{ms}$	$L_{slot}=2/T_{slot}=1.25\text{ms}$	$L_{slot}=4/T_{slot}=2.5\text{ms}$
3.1	6.3	12.5

5 Conclusion and Future Work

The paper evaluates the SmartBAN PHY and MAC layer performance to support the low, medium and high data rate applications in terms of PRR, aggregated throughput and latency. Smaller slot durations are more suitable for low data rate real-time applications as they provide improved PRR, reduced

latency while satisfying the throughput requirements. While for high data rate applications, longer slot durations should be considered since they help achieving better throughput results with a slight trade-off in latency constraints. As a future work, we aim to perform these evaluations with multi-use channel access mode and coded transmissions in SmartBAN.

References

1. Movassaghi, S., Abolhasan, M., Lipman, J., Smith, D., Jamalipour, A.: Wireless Body Area Networks: A Survey. *IEEE Commun. Surveys and Tutorials* **16**(3), 1658–1686 (2014)
2. Scazzoli, D., Kumar, A., Sharma, N., Magarini, M., Verticale, G.: Fault Recovery in Time-Synchronized Mission Critical ZigBee-Based Wireless Sensor Networks. *International Journal of Wireless Information Networks* **24**(3), 268–277 (2017)
3. Scazzoli, D., Kumar, A., Sharma, N., Magarini, M., Verticale, G.: A novel technique for ZigBee coordinator failure recovery and its impact on timing synchronization. In: *Proc. IEEE 27th Annual Int. Symp. on Personal, Indoor, and Mobile Radio Comm. (PIMRC)*, pp. 1–5. IEEE, Valencia (2016)
4. IEEE Standard for Local and metropolitan area networks - Part 15.6: Wireless Body Area Networks, <https://ieeexplore.ieee.org/document/6161600>. Last accessed 25 July 2019
5. Smart Body Area Networks (SmartBAN); System Description, http://www.etsi.org/deliver/etsi_tr/103300_103399/103394/01.01.01_60/tr_103394v010101p.pdf. Last accessed 25 July 2019
6. Smith, D. B., W. Hanlen, L. W.: Channel Modeling for Wireless Body Area Networks. In: Mercier P., Chandrakasan A. (eds) *Ultra-Low-Power Short-Range Radios. Integrated Circuits and Systems*. Springer, 25–55 (2015)
7. Alam, M. M., Hamida, E. B.: Performance evaluation of IEEE 802.15.6 MAC for Wearable Body Sensor Networks using a Space-Time dependent radio link model. In: *Proc. IEEE/ACS 11th Int. Conf. on Computer Systems and Applications (AICCSA)*, pp. 441–448. IEEE, Qatar (2014)
8. Smart Body Area Network (SmartBAN); Enhanced Ultra-Low Power Physical Layer, http://www.etsi.org/deliver/etsi_ts/103300_103399/103326/01.01.01_60/ts_103326v010101p.pdf. Last accessed 26 May 2018
9. Smart Body Area Network (SmartBAN); Low Complexity Medium Access Control (MAC) for SmartBAN, http://www.etsi.org/deliver/etsi_ts/103300_103399/103325/01.01.01_60/ts_103325v010101p.pdf. Last accessed 26 May 2018
10. Khan, R., Alam, M. M.: Joint PHY-MAC Realistic Performance Evaluation of Body-to-Body Communication in IEEE 802.15.6 and SmartBAN. In: *Proc. IEEE 12th Int. Symp. on Medical Info. and Commun. Tech., IEEE, Australia* (2018)
11. Simon, M. K., Alouini, M. S.: *Digital Communication over Fading Channel*. 2nd edn. John Wiley & Sons Inc., New York (2005)
12. Arnon, S., Bhastekar, D., Kedar, D., Tauber, A.: A comparative study of wireless communication network configurations for medical applications. *IEEE Wireless Communications* **10**(1), 56–61 (2003)
13. Chakraborty, C., Gupta, B., Ghosh, S.: A Review on Telemedicine-Based WBAN Framework for Patient Monitoring. *Telemedicine journal and e-health: the official journal of the American Telemedicine Association* **19**, (2013)

Appendix 2

M. Hämäläinen, L. Mucchi, M. G. Genet, T. Paso, J. Farserotu, H. Tanaka, D. Anzai, L. Pierucci, R. Khan, M. M. Alam, and P. Dallemagne. ETSI SmartBAN architecture: the global vision for smart body area networks. *IEEE Access*, 7(10):100–107, 2020

Received July 14, 2020, accepted August 4, 2020, date of publication August 14, 2020, date of current version August 26, 2020.

Digital Object Identifier 10.1109/ACCESS.2020.3016705

ETSI SmartBAN Architecture: The Global Vision for Smart Body Area Networks

MATTI HÄMÄLÄINEN¹, (Senior Member, IEEE), **LORENZO MUCCHI²**, (Senior Member, IEEE), **MARC GIROD-GENET³**, (Member, IEEE), **TUOMAS PASO¹**, **JOHN FARSEROTU⁴**, (Senior Member, IEEE), **HIROKAZU TANAKA⁵**, (Senior Member, IEEE), **DAISUKE ANZAI⁶**, **LAURA PIERUCCI²**, (Senior Member, IEEE), **RIDA KHAN⁷**, (Student Member, IEEE), **MUHAMMAD MAHTAB ALAM⁷**, (Senior Member, IEEE), **AND PHILIPPE DALLEMAGNE⁴**, (Member, IEEE)

¹Centre for Wireless Communications, University of Oulu, 90014 Oulu, Finland

²Department of Information Engineering, University of Florence, 511039 Florence, Italy

³Institut Mines-Télécom–Télécom SudParis, 91011 Evry Cedex, France

⁴Swiss Center for Electronics and Microtechnology, 2002 Neuchâtel, Switzerland

⁵Toshiba Research Europe, Bristol BS1 4ND, U.K.

⁶Friedrich-Alexander Universität Erlang-Nürnberg, 91054 Erlangen, Germany

⁷Thomas Johann Seebeck Department of Electronics, Tallinn University of Technology, 19086 Tallinn, Estonia

Corresponding author: Matti Hämäläinen (matti.hamalainen@oulu.fi)

This work was supported in part by the Academy of Finland 6Genesis Flagship under Grant 318927, and in part by the European Union's Horizon 2020 Programme under the Marie Skłodowska-Curie grant under Grant 872752.

ABSTRACT This paper presents a condensed review of the European smart body area network (BAN) standardization work and its already published standards. The work is carried out under the ETSI Technical Committee (TC) SmartBAN. The goal of ETSI TC SmartBAN is to define and develop new European BAN standards; fostering the successful market adoption of wireless BAN technology by providing a standardized way to bring new interoperable products into the health, medical, sport, leisure and IoT markets, targeting to global exploitation. TC SmartBAN covers wireless communications, especially the physical and medium access control layers, associated security, semantic interoperability and open data representation, which are necessary features in the data transmissions, as well as building blocks of the future smart coordinator. The use of smart coordinator centralizes the network intelligence to the hub, which enables implementation of simple nodes. The SmartBAN approach will be computationally light, and it supports reliable operations across heterogeneous networks. Due to the semantic approach in all functional levels, SmartBAN also supports high interoperability. For emergency traffic, SmartBAN provides different priority classes and fast channel access associated with a low latency. Novel concept adopted in the SmartBAN for high-priority traffic is a multi-use channel access, which can also improve the spectral efficiency. Not only on-body nodes and applications, TC SmartBAN is considering in-body communications for capsule endoscopy. In addition, SmartBAN collaborates with other standardization groups, such as oneM2M and AIOTI, to widen the impact of its work.

INDEX TERMS Interoperability, medium access control, open data format, physical layer, semantic interoperability, wireless.

I. INTRODUCTION

The Internet of Things (IoT) business is currently growing exponentially and the use of wearable electronics and body sensors/devices is expanding rapidly along with it. It is not only growth though in terms of the number of devices, but also with respect to the type of devices, their functionality,

The associate editor coordinating the review of this manuscript and approving it for publication was Pietro Savazzi¹.

services and the richness of connectivity. More and more, our personal systems must support not only wireless connectivity, but the ability to seamlessly interact with our environment and communicate in a secure, privacy preserving and dependable manner. This sets new and increasing demands on wireless part.

Today, there are various standards available which are suitable for wireless body area network (BAN), IoT and industrial applications. The most prominent ones are Bluetooth Low

Energy (BLE), IEEE 802.15.4 and IEEE 802.15.6. In addition to those, there are several proprietary technologies available. The use of BANs offers easy connectivity that can facilitate data sharing, interoperability and basic interaction in various environments, from homes and offices to automobiles, industrial and aerospace environments. However, as processing moves increasingly to the edge, our simple BAN devices will also become smarter and more capable. The capabilities that were once in a desktop may, for example, be found in a handset or even in a watch or wristband device in our current BAN. Interaction with the environment and cooperation between heterogeneous systems will become the norm. Accordingly, we will need BAN solutions capable of efficiently operating in the smart, hyper-connected environments of tomorrow, with embedded intelligence on the one hand, while co-existing with legacy systems on the other. This is the environment of future smart BAN's. It is the environment of increasingly smart personal edge devices in the IoT.

As can be seen, e.g., from [1]–[4], the use of BAN has been proposed for wearables quite a long time. As the wireless technology has become more mature and the miniaturization of components and devices has evolved, we assume that the BAN exploitation will grow fast during the coming years.

In order to realize our “Smart BAN” of the future, a number of design and implementation challenges must be addressed; including, the growing need for seamless interoperability with both new and existing radio standards sharing an increasingly crowded spectrum. Further, BAN use cases are expected to increasingly demand secure and privacy preserving solutions, jointly optimized for low power, low latency, robust operations, and the ability to interact with embedded intelligence and heterogeneous environments.

The European Telecommunications Standards Institute's (ETSI) Technical Committee (TC) SmartBAN was approved in March 2013. ETSI TC SmartBAN seeks to help pave the way towards a new generation of BAN's capable of efficiently supporting and operating in smart IoT environments of the future. TC SmartBAN is a vertical technical committee with responsibilities for development and maintenance of ETSI standards, specifications, reports, guides and other deliverables to support the development and implementation of Smart Body Area Network technologies (Wireless BAN, Personal BAN, Personal Networks, etc.)

This paper is organized as follows. Chapter II shortly links SmartBAN to the existing technology map. Chapter III introduces the SmartBAN physical (PHY) and medium access control (MAC) layers. Chapter IV describes the SmartBAN interoperability. Chapter V presents examples of SmartBAN performance measures. Chapter VI discusses the open work items and future development plans. Finally, Chapter VII provides a summary and concluding remarks.

II. PRESENT WORK

SmartBAN covers wireless communications, and especially, the associated MAC [9], [10], PHY [11], [12] and network layers. SmartBAN is currently working to improve and tailor

the performance of the PHY-MAC support of various popular applications, such as health, sport and leisure [1]. It also takes into account security, quality-of-service (QoS), and the need for easy adjustments for more generic applications and services.

The original SmartBAN system and operational environment are described in [6], [7]. The use of a star network is envisioned around a “smart” hub, which could be, e.g., a hand-held device or a smart watch. An option for a multi-hop relay and hub-to-hub communications is also considered to improve the usability of the SmartBAN devices in the coming standard revision(s). Compared to its main short-range BAN competitors, such as Bluetooth[®] or IEEE 802.15.6 Std., SmartBAN provides new MAC layer and PHY layer functionalities, which improve its performance and also provides very low latency emergency messaging with low energy consumption.

Rapid initial setup time and a channel reassignment help to reduce energy consumption and enable faster network deployment. In addition, SmartBAN provides semantic and data analytic enablers, e.g., semantic discovery and reasoning/rules. In the future, such features will become part of the smart coordinator or hub (e.g., handset, watch or even wristband). A smart coordinator may be viewed as a smart edge device that is capable of controlling and coordinating the operation of our BAN in an efficient and transparent manner. The key functionalities in smart coordinator include, e.g., 1) coordination/interface/ interoperability (in wireless and system levels), 2) security, privacy and trust, 3) interaction/cooperation and 4) edge processing/artificial intelligence (AI). The use of the semantic approach is another important step with respect to interoperability in smart environments that fixes the common data terminology enabling the seamless and vendor independent operation. Automatic node discovery is also supported by SmartBAN. The use of forward error correction (FEC) coding provides added robustness. Additionally, a key feature of SmartBAN today, which differentiates it with respect to its main competitors, is the support for operations across heterogeneous networks with enhanced interoperability and connectivity options. This feature is exploited in all defined data, network and semantic IoT interoperability levels.

Connectivity for portable and wearable devices is not the only thing that SmartBAN can provide for IoT. SmartBAN can be used as our secured personal interface towards the wider digital world; in particular, in the paradigm of the future healthcare system. Our goal is to provide a BAN standard guaranteeing reliable communications, low complexity and low power consumption with open data format. Moreover, the reasoning of the development comes via simpler and more robust implementation than the other existing BAN standards, like BLE and IEEE 802.15.6, are providing.

At the time of writing this article, 22 TC meetings have been held. So far, the group has released five technical specifications (TS) [9], [11], [13]–[15] and two technical reports (TR) [6], [16]. Further, to increase its impact,

TC SmartBAN is collaborating with and contributing to, e.g., oneM2M [18] and the ITEA3 CareWare project demonstrator for elderly support at their homes [19]. In parallel, clinical tests in partnership with Office d’Hygiène Sociale based in Nancy, France, are ongoing. Liaisons with International Electrotechnical Commission (IEC) were established in SyC AAL (Active Assisted Living) [33] and TC124 (Wearable electronic devices and technologies) [34]. Additionally, TC SmartBAN has liaisons with IEEE [35] and the Alliance for Internet of Things Innovation (AIOTI) [36].

III. ETSI TC SMARTBAN

This chapter examines the main features of SmartBAN protocols, focusing mainly on PHY and MAC. The ultimate goal of the PHY-MAC activities in TC SmartBAN is to develop a standard for energy efficient, reliable wireless BAN. In addition, high security and secrecy features for end-to-end communications chain must be taken into account to protect human’s personal vital data.

The core device of the SmartBAN system is a hub, which is controlling all the operations of the whole BAN. We envision SmartBAN as a smart solution in the sense that it merges most of its operations to hub and is utilizing smart coordinator functionalities allowing node implementation to be very simple. This also means lower implementation cost and energy consumption for the nodes. Smartness will also provide heterogeneity management, semantic interoperability and IoT compliance to mention few SmartBAN specific features being available.

A. SMARTBAN PHY

The SmartBAN PHY structure consists of two different types of logical channels operating in the 2.4 GHz unlicensed industrial, scientific and medical (ISM) frequency band; Control Channels (CCH) and Data Channels (DCH). CCH is utilized only for broadcasting CCH beacon (C-Beacon) by the Hub, whereas bidirectional data, and control and management information between the Hub and the nodes are transmitted using the DCH. These two channels can be implemented in one RF chain. The utilized spectrum is divided into 40 channels, each having 2 MHz bandwidth. The 40 center frequencies are equally distributed between 2.402 GHz and 2.480 GHz. Three of these channels are dedicated for CCHs and the other 37 channels are reserved for DCHs. One CCH and one DCH are used within one SmartBAN and are selected by the Hub. In other words, all communications between the nodes and the Hub is carried out using the same DCH. Currently, different DCHs are used by different, i.e., neighbouring Hubs/SmartBANs, for coexistence management. In SmartBAN network, frequency hopping is not supported, which deviates it, e.g., from BLE. [11]

SmartBAN utilizes Gaussian frequency shift keying (GFSK) with a modulation index $h = 0.5$ and a bandwidth-bit period duration $BT = 0.5$ [4]. To improve transmission reliability, SmartBAN uses FEC coding but also repetition coding. The standard defines mandatory

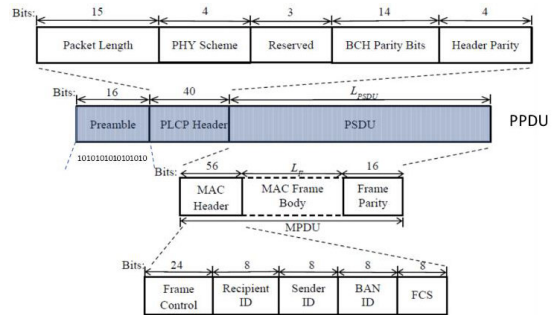


FIGURE 1. Packet format at PHY layer.

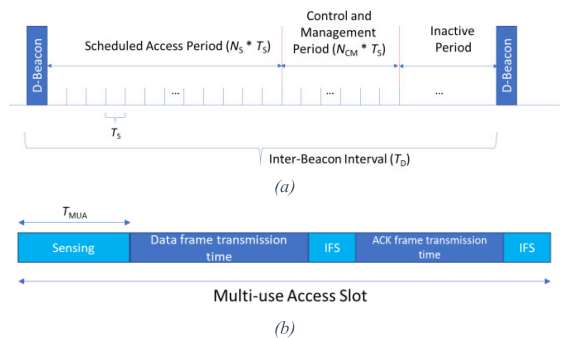


FIGURE 2. a) IBI structure in DCH and b) slot structure for multi-use channel access.

BCH(36, 22, 2) coding to protect *Physical Layer Convergence Protocol* (PLCP) Header. The *MAC Protocol Data Unit* (MPDU) is encoded using BCH(127,113,2), but in this case, the coding is not obligatory. The coded or uncoded MPDU forms the *Physical layer Service Data Unit*, and together with the Preamble and the PLCP Header, they form the *Physical layer Protocol Data Unit* (PPDU), which is the basic entity in the transmission. More details on the frame formats can be found from [9] and are also presented in Fig. 1, which merges the different data units described in [5].

For repetition coding, SmartBAN has three options: no repetition and 2- or 4-times repetitions. In the case of the SmartBAN repetition coding, the whole PPDU block is repeated. This differentiates SmartBAN, e.g., from the IEEE 802.15.6 Std., which uses the more commonly deployed bit-level repetition coding.

B. SMARTBAN MAC

The SmartBAN superframe, called as an inter-beacon interval (IBI), is divided into three channel access periods, as shown in Fig. 2a: scheduled access period (SAP); control and management period (C/M); and inactive period.

For medium access control, SmartBAN provides three different mechanisms. The SAP is dedicated for data traffic only and it is utilizing TDMA (time division multiple access) for contention free channel access. C/M period is essentially introduced for control and management messages between

TABLE 1. Payload sizes in bytes for different slot sizes and payload repetition modes.

L_{slot}	Field Value in C-Beacon	T_s (ms)	No Repetition	2 Repetition	4 Repetition
1	000	0.625	8	N/A	N/A
2	001	1.25	86	35	9
4	010	2.5	243	113	48
8	011	5	555	269	126
16	100	10	1180	582	283
32	101	20	2430	1207	595

the nodes and the control hub, and it is utilizing slotted ALOHA channel access. In addition, if SAP does not provide sufficient resources for data transmission, C/M period can be used as a reserve. C/M period is available for all the nodes who are willing to transmit data. In Fig. 2a, T_s and T_D are depicting the durations of the time slot and the inter-beacon interval, respectively. N_s and N_{CM} are representing the number of available slots in SAP and C/M period, respectively.

The entire SmartBAN IBI is divided into the slots of equal durations, T_s . From connection establishment for data transmission, all types of communications take place into the pre-defined fixed slot size, T_{slot} . The minimum allowed slot length in SmartBAN is $T_{\text{min}} = 0.625$ ms and the maximum limit is 20 ms. Smaller slot sizes are more favourable for low latency applications with smaller payloads while longer slot durations facilitate higher throughput due to the transmission of more payload at once. Table 1 summarizes the payload sizes for different slot sizes and PPDU repetition scenarios in SmartBAN. These payload sizes are computed for uncoded MPDU transmissions and further details about the calculations are given in [7].

A unique channel access solution introduced in the SmartBAN is the *Multi-use Channel Access* (MCA), which can be used in SAP, as well as in C/M period. MCA provides very low-latency emergency/high-priority messaging, called as *Priority Channel Access*. MCA allows also utilization of the scheduled but unused time slots by secondary users. This method is called as *Re-use Channel Access* and can be utilized when the channel is not used by the primary user. Thus, MCA can significantly increase the channel capacity and decrease the latency. The above-mentioned features are enabled by the unique slot structure introduced for the SmartBAN MAC Std. and are shown in Fig. 2b, where T_{MUA} depicts the total duration of a sensing period in MCA. [9]

The MCA slot introduces a sensing period at the beginning of each slot for Clear Channel Assessment (CCA) with two different purposes. When MCA is enabled, all nodes in the SmartBAN shall perform a CCA before transmitting data in their scheduled slot during SAP, or before transmitting a data or control and management information during the C/M period, in order to detect a possible emergency transmission. In addition, nodes having outstanding packet in their queue can access the channel during every time slot in the SAP, i.e., before the slots scheduled for them. In this case, the nodes shall perform two CCAs; one for the possible

emergency transmission, and one for the possible slot owner transmission.

For busy channel case, the standard defines a back-off mechanism for transmission reattempt. *Inter-frame spaces* (IFS) are used to separate data and acknowledgement (ACK) frames, and consecutive slots as seen from Fig. 2b. [9]

From the deployment point-of-view, the Hub shall always support MCA, but the support is optional for the nodes. However, if MCA is used though, all the devices connected to that sub-network must support MCA functionality. [9]

According to the first released SmartBAN MAC standard [9], every node is connected to a hub via one-hop star network topology. However, the work on an amendment to the MAC Std. is currently ongoing and the coming revision will provide definitions for two-hop relay and hub-to-hub communications still remaining the backward compatibility.

IV. ETSI TC SMARTBAN INTEROPERABILITY

One of the main objectives of ETSI TC SmartBAN is to provide solutions for heterogeneity and interoperability management for BANs. In particular, data/informational interoperability, technical interoperability (i.e., network and syntactic) and semantic interoperability should be guaranteed. The aim is therefore to develop and standardize a SmartBAN-dedicated global framework. This framework is provided with associated enablers/facilitators and application protocol interfaces. There will be a support for interoperability management, which includes cooperation between different SmartBANs and cross-domain use cases. The procedures for secure and unified interaction and access to any BAN data/information/entities are specified. For these purposes, the proposed SmartBAN solution concerns to the following aspects:

- The specification, formalization and standardization of an open reference semantic model for BAN data, entities and environment, associated with corresponding unified metadata and reference modular ontology [14]: Measurements and control/monitoring data are included in the proposal. The SmartBAN Reference Model is a key element for BAN's data/information, device and semantic interoperability handling. It will also enable embedded semantic analytics, and thus, ease the implementation of automated monitoring and control strategies.
- The specification and formalization of a SmartBAN service/application layer reference model extension, associated with the corresponding sub-ontology [14]: This SmartBAN reference service model, coupled with a Web of Things (WoT) approach, will in particular enable management of the full semantic interoperability, device discovery, data sharing in application level, and cross domain application handling.
- The specification and validation of generic Multi-Agent based enablers and global IoT reference architecture with technical and semantic interoperability management, and embedded semantic analytics

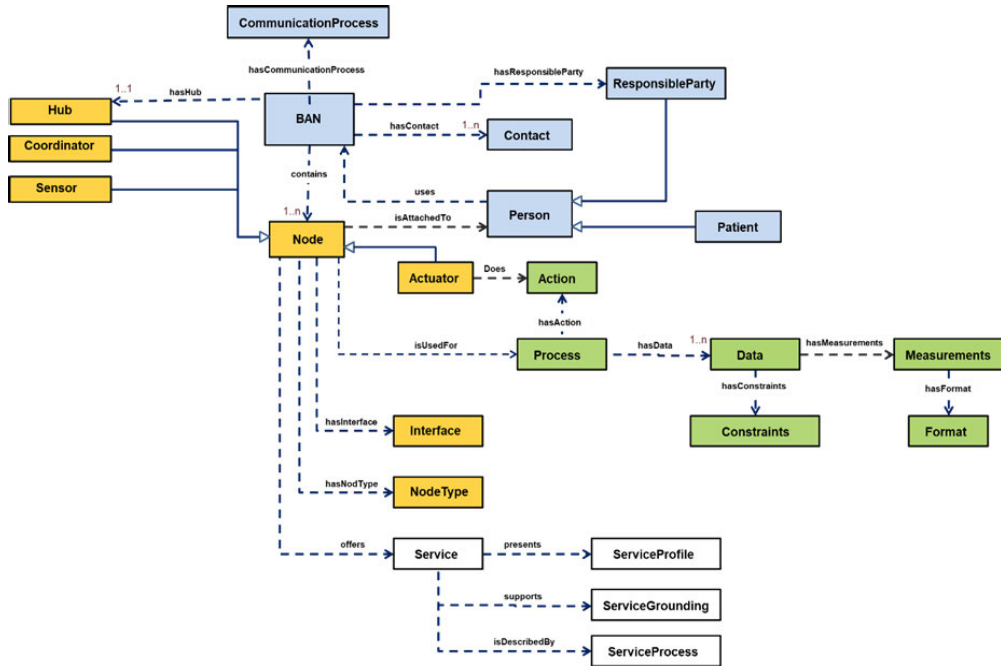


FIGURE 3. High-level view of SmartBAN reference model.

handling [15]: This SmartBAN reference architecture is providing generic service-level enablers for semantic data/information management, as well as distributed monitoring and control operations.

The SmartBAN reference data and service models, as well as reference IoT architecture, are described in the following sub-sections in more details.

A. SMARTBAN REFERENCE MODEL

Fig. 3 presents the high-level view of SmartBAN semantic Reference Model and ontology under discussion in [9], [10], i.e., the associated main modelled concepts (objects or classes) with their links (object properties). Within Fig. 3, the following conventions are used:

- Concepts, i.e. objects or classes, are denoted by rectangles.
- Sub-class relations are denoted by plain arrows with white triangles (the arrow origin is the sub-class of the class being the arrow destination).
- Relations between objects (concepts) are called object properties and are denoted by dashed arrows labelled by the object properties identifiers.

SmartBAN semantic Reference Model was designed by using the modularity principle and the associated SmartBAN ontology and thus it has been modularized in the following fully decoupled modules:

- BAN module that models all the concepts related to BANs (blue classes drawn in Fig. 3). A BAN logically contains nodes and has both a predefined

communications process (periodic, event driven or on demand) and one or multiple contacts, as depicted in Fig. 3. A contact is a person, i.e. the one that uses the BAN and whose node can be attached to. This person can mainly be a responsible party (legal entity responsible for the BAN) or a patient, etc.

- Node module that models all the concepts related to BAN nodes (orange classes drawn in Fig. 3). A BAN node can mainly be a sensor, an actuator, the BAN hub or the BAN coordinator. This node has an interface and a type, as depicted in Fig. 3 (Interface and NodeType classes).
- Process module that models all the concepts related to measurement/actuation process and measures (green classes depicted in Fig. 3). A process has Action and Data, as depicted in Fig. 3, and finally, a Service module that models all concepts related to services that are offered by the SmartBAN nodes (white classes depicted in Fig. 3).

Those modules are less complex to process in an embedded device than the full SmartBAN ontology, thus opening a door for device-embedded semantic data analytics and edge computing. This is also mandatory for local alarm management and caregiver/patient/helper support tools' implementation.

Fig. 3 shows that the SmartBAN ontology first introduces unified metadata (i.e., additional information of data, data meaning) for describing the data, which typically are measurements' results provided by different sensor/wearable nodes through dedicated processes for which these nodes

are being used. Data mainly has the following properties (see Fig. 3):

- Measurements. Measurement has both a format (i.e., the unit of measure, such as beats per minute [bpm] for a heartbeat measurement) and corresponding values (decimal ones) that are directly modelled as data properties of the class Measurements.
- Constraints, such as validity (e.g., minimum and maximum allowable values) or legal (privacy related) ones.

SmartBAN unified metadata (green classes depicted in Fig. 3) is mandatory since it provides a unique and unambiguous understanding of a measurement for any processes, applications or end users (e.g., caregivers and helpers). It already allows simple and automated data analytics and alarms' management, like detection of a body temperature or a heart rate fall above/below a predefined threshold, etc. SmartBAN unified metadata is fully aligned with BLE profiles of medical devices that were specified and formalized by Personal Connected Health Alliance (ex-Continua Health Alliance) [16].

Fig. 3 shows that the SmartBAN Reference Model is also extended with additional information, such as which device (BAN node) provides a measurement data (see orange classes depicted in Fig. 3), which BAN contains this device and which use that BAN (see blue classes depicted in Fig. 3), etc. This enables more complex semantic data analytics, like which collocated patients have the same pathology and so on.

As already aforementioned, a WoT strategy was in particular retained for SmartBAN, and the corresponding service model (i.e., upper level ontology) was specified as depicted in Fig. 3 (white classes). This in particular allows full semantic interoperability handling, (medical) device or BAN node discovery and data sharing at application level, as well as cross domain use cases handling (e.g., patient on the move, healthy lifestyles for citizens, emergency situation detection and warning, elderly at home, etc.). Indeed, if one, e.g., view a sensor as a service that is described/represented through a common reference model (white classes in Fig. 3), then whatever a sensor is (a medical, an automotive, a home- or a city-related one), it can always be viewed as a service (cross-domain common concept). As shown in Fig. 3 (white classes), this service:

- Presents a service profile that models what the service does and enables its automatic discovery.
- Supports service grounding that models how the service is accessed (i.e., through which communications protocol).
- Is described by a service process that models the way to invoke a service (e.g., input/output modalities). This service process is related to the process for which a BAN node can be used (e.g., a measurement or an actuation, an alarm sending, a patient guideline, etc.)

B. SMARTBAN GLOBAL IoT REFERENCE ARCHITECTURE

The SmartBAN IoT reference architecture has been introduced for providing both system interoperability manage-

ment (i.e., being multi-platform enabled) and secure and generic interaction/access to any BAN devices/entities and data/information (including measurements). This reference architecture fully relies on the SmartBAN Reference Model and ontology (see sub-section IVA) for offering a BAN - dedicated and more integrated global IoT platform with data, device, network and semantic interoperability management and embedded semantic analytics. The SmartBAN IoT Reference Architecture's high-level view is presented in Fig. 4.

As shown in Fig. 4, the SmartBAN IoT reference architecture follows the oneM2M specifications [14] and thus it consists of three main layers: Network Layer (also called SmartBAN data provisioning layer), Service Layer (also called IoT Layer and composed of SmartBAN semantic and service sub-Layers), and Application Layer. The SmartBAN IoT reference architecture is also directly mappable with AIOTI (Alliance for Internet of Things Innovation) IoT High Level Architecture [17] (see Fig. 4). Note that oneM2M entities are not described in this sub-section for redundancy purposes since their full specifications are already available in [14].

As also shown in Fig. 4, the SmartBAN Data Provision Layer (i.e., oneM2M Network Layer) consists of physical entities and things (sensors, actuators, wearables, hub, BAN coordinator, gateway, smartphone, etc.), users (i.e., person, such as caregivers, or patient and helpers) and human-machine interfaces. In other words, this layer covers any person/ device/process delivering raw data and using/controlling BAN-related mechanisms (such as physical entities and systems). Within this layer, interworking agents, called as Data Scanner Agents, are also provided for allowing interworking of non-SmartBAN enabled environment with SmartBAN. Those Agents were mainly designed for device discovery and associated raw data real time retrieval/ notification purposes, thus masking heterogeneity of medical devices/data to any process, application or end user (patient, caregiver, etc.). For example, a BLE Data Scanner Agent was specified and integrated since currently most of the existing wireless medical devices being on market are either utilizing BLE or IEEE 802.11 based technology.

The SmartBAN Semantic Data Sub-Layer depicted in Fig. 4 is a part of the SmartBAN IoT layer (i.e., oneM2M Service Layer) that comprises IoT entities (or oneM2M Common Service Element, CSE) mainly providing SmartBAN ontology and semantic information distributed storage and management functionalities (e.g., semantic search/query/annotation, reasoning and semantic analytics, rule handling, eventing, and so on.) Therefore, this sub-layer extends standard BAN systems with the additional embedded intelligence (device/ edge/fog levels) for allowing automated alarm management and control operations (e.g., stroke or fall detection, etc.), as well as advanced decision support (e.g., in caregivers side critical situations detection, measurements similarity detection, etc.) and assisted living (patients side, e.g., patient reminders and warnings).

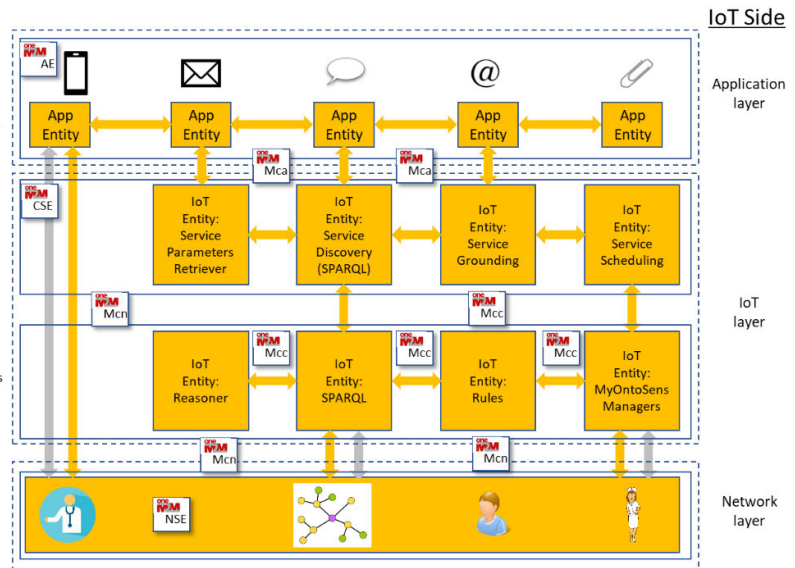
SmartBAN/oneM2M Side

SmartBAN/oneM2M Application layer
Application entities implementing a given SmartBAN application logic (e.g., data monitoring, patient evaluation result, patient notification, ...)

SmartBAN/oneM2M Service layer
Generic entities related to service management functionalities

SmartBAN Semantic Data layer
Entities mainly providing semantic and ontologies management functionalities + additional embedded intelligence related functionalities

SmartBAN Data Provision layer
OneM2M Network layer



IoT Side

Application layer

IoT layer

Network layer

FIGURE 4. High level view of SmartBAN IoT reference architecture.

The SmartBAN Service sub-Layer depicted in Fig. 4 is also a part of the SmartBAN IoT layer (i.e., oneM2M Service Layer). It mostly provides generic IoT entities or agents (or oneM2M CSEs) related to service management functionalities, such as service registration, discovery and scheduling. Those agents are directly deriving the strategy adopted for the WoT, and they offer full semantic interoperability handling [9], [10]. The services are semantically described through the SmartBAN ontology service module already introduced in sub-section IVA and specified in [9], [10]. This module provides BAN devices/data (sensors, wearables, actuators, etc.) automatic discovery and sharing, as services and via dedicated agents of the SmartBAN Service sub-Layer (see Fig. 4).

Finally, the SmartBAN application layer depicted in Fig. 4 consists of several IoT application entities. Those entities are implementing SmartBAN application logic, such as monitoring of vital data, evaluation results of certain patient, caregiver decision support or patient notification.

V. SMARTBAN PERFORMANCE EVALUATION

This section elaborates the SmartBAN performance evaluation under two different interference and channel models; one, which is based on the measurement campaigns [12], [13] and the other one using biomechanical mobility for emulating the realistic channel effects.

First, Table 2 gives a high level summary of the different functionalities between SmartBAN and two of its main competitors, namely BLE [24] and IEEE 802.15.6 [8]. The main topological difference comes from the coming support for smart relays, which distinguishes SmartBAN from BLE and IEEE 802.15.6, which are conventional one hub star

topology-based networks. However, it should be noted that in IEEE 802.15.6 there is also support for relay functionality and since the Bluetooth version 5.0, there is also support for mesh topology. As the parameter values depend on the overall system settings, we do not provide absolute numbers in Table 2.

As allowing smart channel access, SmartBAN is a perfect solution for emerging messaging. In addition, re-use of the unused timeslots improves the spectral efficiency, as well as reduces the latency in the case of critical communications needs. The biggest deviation comes from the semantic approach, which is used only by the SmartBAN. This functionality makes SmartBAN really smart. The other two technologies do not provide this kind of approach.

A. USING THE INTERFERENCE-BASED CHANNEL MODEL

The comparative analysis between SmartBAN and BLE v4.0 with the measurement-based interference model was studied under the ETSI Specialist Task Force (STF) 511 project.

The STF 511 group developed a simulator using MATLAB Simulink environment, implementing both the physical and MAC layers of SmartBAN and BLE. MATLAB multi-path fading channel model for indoor environment was used and 2.4 GHz ISM band was considered. Additionally, STF 511 has included into the simulator a block that simulates the interference in an hospital environment. The analytical model of the interference was developed by part of the authors in [12], based on the measurement campaigns in a real modern hospital. In particular, the lowest and highest interference scenarios were implemented into the interference block of the simulator. SmartBAN and BLE were

TABLE 2. High-level feature comparison between SmartBAN, BLE and IEEE802.15.6 standards.

Parameter	SmartBAN	BLE	IEEE 802.15.6™
General system specs	System Architecture	Hub + smart relay coordination	One hub
	Networking communication interoperability	Yes	No
	Smart relay	Yes	No
PHY/MAC	FEC (forward error correction)	Yes	No
	Initial set up time	Fast	Less fast
	Spread spectrum hopping	No	Yes
	Channel reassignment	Yes	No
	Very low latency emerging messaging	Very fast (timeslot)	No
	Reutilization of scheduled unused time slots (efficiency parameter)	Yes	No
	Energy consumption/efficiency	Low (e.g. long sleep times)	Low
	Network complexity	Star concept + multi hub relay (planned)	Star concept
Smarts	Semantic approach, semantic interoperability, heterogeneity management, IoT compliance	Yes	No
	Additional semantic and data analytic enablers (e.g. semantic discovery, reasoning/rules)	Yes	No
	Automatic node discovery (e.g. semantic discovery of nodes, composition)	Yes	Partially
	Coexistence management by coordinator	High	Low

compared in terms of bit error rate (BER) and frame error rate (FER), and varying additional parameters, such as frame size (50, 250, 500), signal-to-interference ratio (SIR = 0, 3, 9), repetition rate (PPDU = 1, 2), and retransmission (ReTx = on, off).

The stochastic interference models used in the studies were based on several one-week long measurements carried out in different environments at the Oulu University Hospital, Finland, and at the hospital in Florence, Italy. Within a one week, the samples of the electromagnetic (EM) spectrum were taken every 22 ms using Agilent E4440a spectrum analyser. These experiments gave a good and statistically reliable view on the EM characteristics within the frequency band of interest in those environments. Part of the authors of this paper were also involved in the experiments and data post-processing. References [12] and [13] report the generated models in more details. The overall SmartBAN simulator is detailed in [22].

As a conclusion, it can be summarized that the repetition coding, being either 1 or 2, would be required when operating SmartBAN in a highly interfered environment. In [23], the corresponding performance evaluation of the SmartBAN system is done by considering the interference, as well as the applicable radio channel model taken from literature.

Fig. 5 shows the performance comparison in terms of BER as a function of signal-to-noise ratio (E_b/N_0) between SmartBAN and BLE v4.2. The results have been carried out by the simulator mentioned above. The simulation parameters are the following: frame rate = 50 bytes; SIR = 0, 3, 9 dB; repetition coding with PPDU = 1, 2; retransmission ReTx = OFF. From the reported interference models,

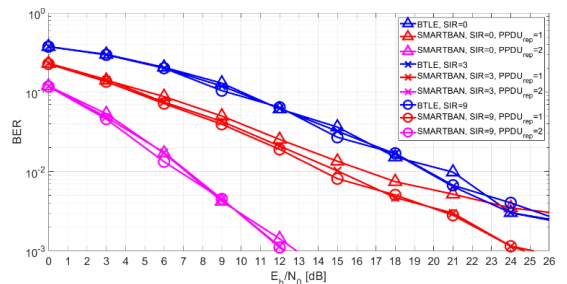


FIGURE 5. BER comparison between SmartBAN and BLE v4.2. Parameters: PPDU = {1, 2}, ReTx = OFF, Frame = 50 bytes, SIR = {0, 3, 9}dB, low interference.

low-interference frequency is considered [16]. The simulations consider hospital environment and fading radio channel. As it can be seen, SmartBAN outperforms BLE v4.2 in all studied cases. In particular, when a PPDU = 2 is used, SmartBAN obtains a FER two magnitude orders lower than BLE at $E_b/N_0 = 7$ dB.

Figs. 6 and 7 show the FER performance comparison of SmartBAN and BLE v4.2 when the retransmission is ON and the interference scenario changes from LOW (Fig. 6) to HIGH (Fig. 7). These results show how much the retransmission capability is able to decrease the FER of SmartBAN, even in high interference scenario. The gain of SmartBAN is about 15 dB over BLE at $FER = 10^{-1}$.

Fig. 8 lets us appreciate the impact of increasing the frame size from 50 to 500 bytes. A short frame size seems to be a suitable choice for reduced FER in SmartBAN.

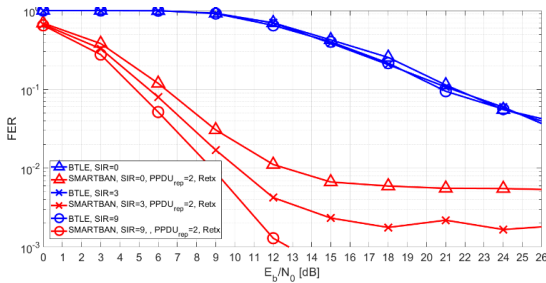


FIGURE 6. FER comparison between SmartBAN and BLE v4.2. Parameters: PPDU = 2, Retx = ON, Frame = 50 bytes, SIR = {0, 3, 9}dB, low interference.

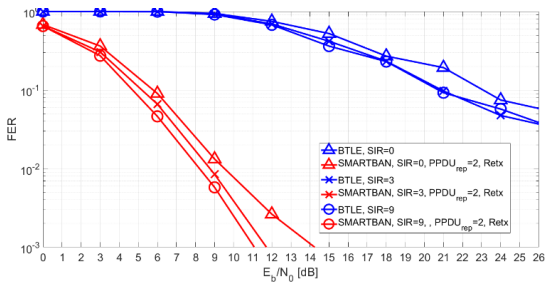


FIGURE 7. FER comparison between SmartBAN and BLE v4.2. Parameters: PPDU = 2, Retx = ON, Frame = 50 bytes, SIR = {0, 3, 9}dB, high interference.

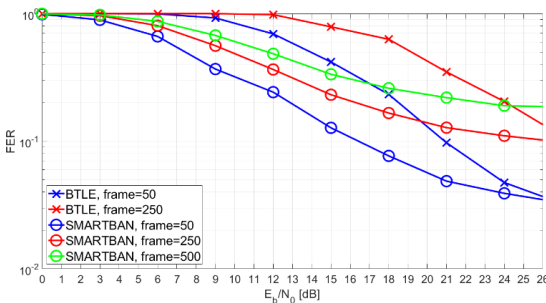


FIGURE 8. FER comparison between SmartBAN and BLE. Parameters: PPDU = 0, Retx = OFF, Frame = {50, 250, 500} bytes, SIR = 3dB, low interference.

B. USING THE BIOMECHANICAL MOBILITY MODEL

The biomechanical mobility model is based on the CM3B channel model, proposed by IEEE in [4]. However, model integrates the impact of human body shadowing, caused by the mobility, in the pathloss calculations. In biomechanical mobility model, dynamic distances and link types are generated for different on-body links using biomechanical mobility trace files. Dynamic distances and link types, as defined by a specific mobility pattern, like walking, running or sit-stand, are taken as inputs for the pathloss calculations. The space-time varying link types identify a particular on-body link as being either line-of-sight (LOS) or non-line-of-sight (NLOS). An additional NLOS component of 13% is added to the resultant pathloss values with time-varying distances for

NLOS link status, otherwise the pathloss remains unchanged. After computing the pathloss values, radio link modelling is performed including SNR, BER and packet error rate (PER) computations. Further details about biomechanical mobility-based channel model can be found from [37].

For evaluating the SmartBAN performance with biomechanical mobility model, a precise athlete monitoring use-case is considered. This is a real-time monitoring application. The performance is evaluated in terms of packet reception rate (PRR), throughput and latency. PRR can be defined as the fraction of packets received and decoded successfully at the Hub. The effective throughput of an individual BAN node can be calculated by N times of the ratio of successfully received packets at the given node-Hub link and duration of the mobility/pathloss trace file, where N is the maximum possible payload size, as given in Table 1. The packet latency is calculated as the time difference between the data packet generation at the MAC layer and its successful reception at Hub. The precise athlete monitoring use-case has one electromyography (EMG) sensor for measuring the electrical activity in muscles and four accelerometers for monitoring the body motion and posture. An EMG requires a data rate of 100 kbps – 600 kbps, while data rates required by accelerometers range from 640 bps to 16 kbps, determined by the sampling rate and bit resolution. Therefore, the aggregated data rate requirement for this use-case is 102.6 kbps – 664 kbps. For a real-time use-case, the latency should be below 10 ms and PRR is supposed to be above 90% [29]. The IBI is made of a single scheduled access slot per sensor node, and two slots in both C/M and inactive periods. We consider the slot sizes of 0.625 ms, 1.25 ms and 2.5 ms, and an information rate of 1000 kbps. The evaluations are also conducted for single PPDU transmissions with uncoded and BCH coded MPDU, with two and four PPDU repetitions. The transmission power levels are varied from -10 dBm to 0 dBm, while a receiver sensitivity of -92.5 dBm is assumed [29].

Fig. 9 illustrates the PRR performance under the biomechanical mobility-based channel model for the given use-case. Single PPDU transmission, and two and four PPDU repetitions are represented by $REP = 1$, $REP = 2$ and $REP = 4$, respectively. The smallest slot duration of 0.625 ms can achieve the required PRR (above 90%) for the transmission power levels of more than -5 dBm with uncoded MPDU transmission while with BCH coded MPDU, a transmission power level of -7.5 dBm is enough to achieve the required PRR. PPDU repetitions with 0.625 ms slot duration are not possible because the amount of related PHY-MAC overheads to constitute a complete PPDU cannot be transmitted more than once. For 1.25 ms and 2.5 ms slot durations, the transmission power should be -7.5 dBm or above to obtain the required PRR for single PPDU transmission with BCH coded MPDU. The PPDU repetitions for these slot durations improve PRR performance but BCH encoding over MPDU results in a significant improvement, compared to the repetition coding. Overall, the transmission

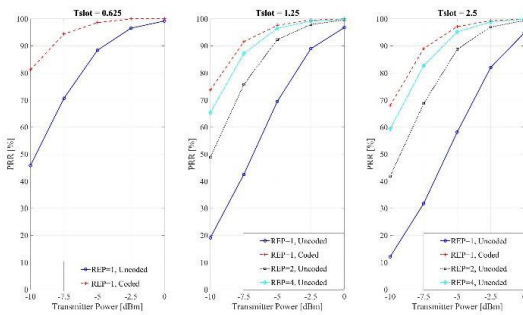


FIGURE 9. PRR (%) w.r.t transmission power (dBm).

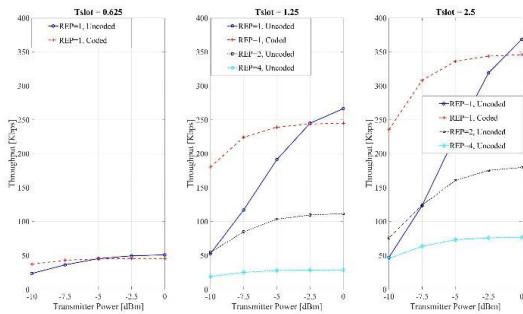


FIGURE 10. Throughput (kbps) w.r.t transmission power (dBm).

power levels of -2.5 dBm or above are required in larger slot durations and uncoded MPDU to obtain the required PRR. Larger slot durations, despite carrying more payload with less PHY-MAC overheads, can have decreased PRR because of the increase in the overall packet size [37].

Fig. 10 depicts the aggregated throughput results of all the sensor nodes in the given use-case. It can be observed that the longer slot durations result in higher throughput for the same transmission power level. The increase in throughput with the increase in slot duration can be explained by the phenomenon that the longer slots allow the transmission of more payload with the same PHY-MAC overheads, as compared to the shorter slots in a single transmission. The aggregated throughput decreases for two and four PPDU repetitions because of the duplicate transmissions of the similar payload multiple times for improving the error performance. Overall, single PPDU transmissions with the BCH coded MPDU provide the best throughput results at all transmission powers except at 0 dBm, at which the single PPDU transmission with uncoded MPDU results in the highest throughput. In this use-case, 2.5 ms slot duration with single PPDU transmission and BCH coded MPDU serves as the best option for attaining a high aggregated throughput since it enables the transmission of more payload at once.

The average latency values for the given use-case and the resulting IBI with 0.625 ms, 1.25 ms and 2.5 ms slots durations are observed to be 3.1 ms, 6.3 ms and

12.5 ms, respectively. The latency values increase with the increase in slot durations because larger slot durations have longer IBIs. A detailed analysis about the PRR, throughput and latency characteristics of SmartBAN is provided in [29] for different use-cases. The paper concludes that in low data rate applications, smaller slot durations will give a better performance than the usage of longer slots. On the contrary, better throughput is achieved with longer slot sizes. This study does not consider MCA, which would reduce the attained latency for emergency nodes.

VI. DISSEMINATION AND MOVING AHEAD

A first workshop on SmartBAN, Connected Things for Well-being and Health, was kept on Oct 25, 2018 at ETSI headquarters, Sophia-Antipolis, France. At this workshop, SmartBAN technology, including semantic interoperability and SmartBAN reference IoT/oneM2M platform for remote monitoring and control applications, and the SmartBAN 2.4 GHz PHY were jointly demonstrated. In addition, a dedicated SmartBAN Workshops were organized in-conjunction with the 9th International Symposium on Medical Information and Communication Technology (ISMICT2015) in Kamakura, Japan on 2015 and with the Bodynets 2018 conference in Oulu, Finland on 2018.

Due to the COVID-19 pandemic, the following planned SmartBAN dissemination activities at 2020 were postponed: SmartBAN Workshop for ETSI Week 2020 with demo and “Smart Body Area IoT in the era of Beyond 5G/6G” at URSI GASS 2020, Rome, were both moved to year 2021. However, dissemination of SmartBAN is continuously ongoing process.

Moving Ahead: To increase SmartBAN coverage, revision work for MAC layer specification [5] to support hub-to-hub and relaying has started. The results are planned to be published in RTS/SmartBAN-005r1 (TS 103 325) by 2021.

In Q1/2018, a new work item on implant communications was initiated in cooperation with ETSI ERM TG 30. This work is focusing on ultra wideband communications for ultra-low power medical devices. The main targeted application is a swallowable wireless capsule endoscope, which is a way to study human’s gastro-intestine (GI) track in a user-friendly way. A pill-like device is swallowed, and the endoscope, which contains camera, wireless communications and battery, is providing visual information (image/video) of the GI-track’s status. In addition to transferring visual data, the localization of the capsule inside a GI-track is an important feature. SmartBAN is aiming to contribute to this technology development by providing standardized technology reference. The ongoing work is done under DTR/SmartBAN-003 (TR 103 751) thus providing a Technical Report as a first output.

A work item on SmartBAN security, privacy and trust was also initiated in 2018. This work targets the development of computationally light security mechanisms for smart BANs. Due to the sensitive medical information handled by smart BANs, it is necessary to provide for a high security across all

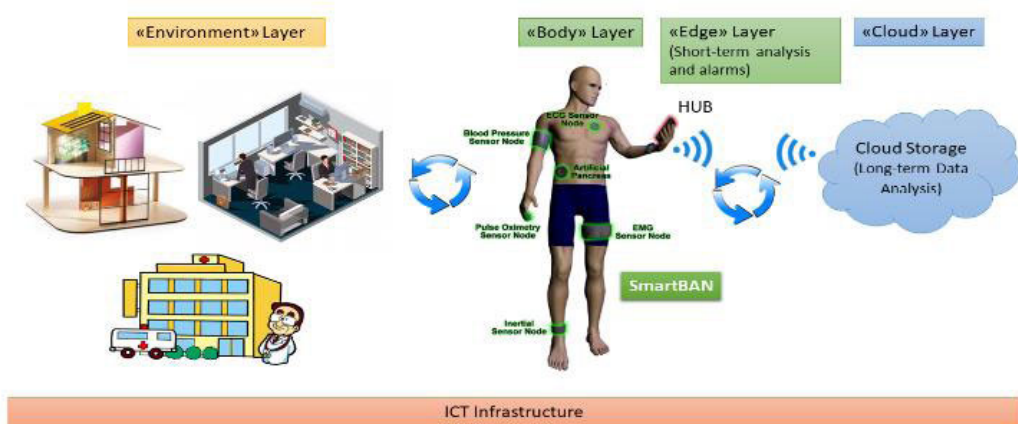


FIGURE 11. SmartBAN in the IoT domain.

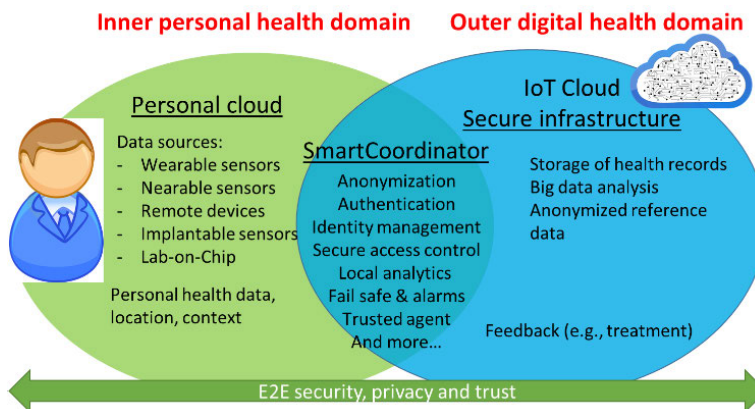


FIGURE 12. Open end-to-end security and privacy platform.

levels of data security and wireless connectivity. This work belongs to DTR/SmartBAN-0010 (TR 103 638). By reviewing first the possible threats SmartBAN can face, it could further protect itself against them.

A joint group between ETSI TC SmartBAN and ETSI TC SmartM2M is collaborating to merge and/or align the SmartBAN ontology with the corresponding Smart Appliances REFERENCE ontology (SAREF) [31] and oneM2M [32] ontologies. SAREF4EHAW [34] is an extension of SAREF ontology for the eHealth Ageing Well domain for which a minimal core version is being standardized also within ETSI TC SmartM2M. SAREF4EHAW is a priori promised to be one of the most accomplished ontology for the eHealth Ageing Well vertical. However, it is not yet fully standardized and validated, fully aligned and mapped with the aforementioned SmartBAN Reference Model, and not yet complying with all the requirements already listed in [35].

However, collaboration and contribution to [34] and [35] will significantly increase the impact of SmartBAN by

extending the utilization of the SmartBAN ontology to various application fields.

Beyond this, we envision SmartBAN solutions to be available in a wider and more general IoT context, as illustrated in Fig. 11. In this environment, SmartBAN could be the standard used jointly with smart, secure environments, providing seamless connectivity between heterogeneous sensors, wireless installations and, more broadly, the cloud, allowing SmartBAN enabled solutions to serve as a secure and trusted interface for future Digital Health. In addition, the recent advances in AI and machine learning (ML) technologies can drive the long-term analysis of health data acquired by SmartBANs far more successful than ever before.

In addition, to be our trusted interface to the digital world, the smart coordinator must maintain the security and privacy of our personal information. To do so, we envision the realization and embedding of an open and modular end-to-end (E2E) security, privacy and trust platform within the smart coordinator (e.g., mobile, watch or wristband). This solution

would provide efficient, robust and secure communications in the local domain. Moreover, it provides useful functionalities in outer domain and helps patients/users to maintain high confidence in the security and privacy of their personal data.

The functionalities of the E2E security platform is shown in Fig. 12 within the intersection of our personal cloud and the IoT cloud secure infrastructure. They include, e.g., anonymization, authentication, identity management, secure access control, local analytics, fail safe & alarms and lots of more functionalities. We envision the coordinator in this sense as our personal interface to the healthcare system of the future. Our “avatar” is effectively an artificial intelligence. We rely on our trusted smart coordinator to perform anything from low level radio adaptation to high level functionalities related to filtering and processing of personal information and security.

Our smart coordinator (and the other capable edge devices) may process this data locally and provide us with tailored feedback. The feedback is based on the knowledge of our personal case and the collective wisdom established via AI-based analysis of big data gathered over years from all the persons in the system. It may also perform predictive simulations and projections in reply to “what if” questions that we may pose, or which it poses on our behalf, and it supports personalized medicine (e.g., monitoring of dosage and drug combinations). The smart coordinator receives reference data from the system and returns anonymized data to the system, enabling it to continuously refine and update the global database.

The smart coordinator is also capable of interacting with sensors in the environment and cooperating with other AI-based devices. It can also serve as a “fail safe” as storing recent personal history and confirming that incoming data and requests are consistent with expectations, which is potentially important in the event of the system corruption (e.g., spoofing or falsification of reference data.)

The realization of the smart coordinator of the future requires an unprecedented combination of intelligence embedded in a miniaturized, energy efficient processing platform with trusted and dependable connectivity to the cloud 24/7.

In this way, SmartBAN is “our edge” and personal interface to the digital healthcare system of the future and the smart coordinator can be our trusted personal guardian and interface in an increasingly complex digital society.

VII. CONCLUDING REMARKS

In this paper, the work and current status of ETSI TC SmartBAN towards a global standard for smart body area networks were presented. SmartBAN aims to provide low power, low latency reliable wireless communications strategy especially, but not limited to, health and wellness related data transmission. Utilizing different channel access mechanisms and priority levels, the latency of communications can be substantially reduced compared to the current level. SmartBAN introduces fast channel reassignment and association for new nodes. Semantic ontology and unified data formats improve

interoperability and utilization of heterogeneous networks. The technical specifications defining physical and medium access control layers, as well as open data models and semantic ontology are published and ready for implementation. Lot of potential is seen in the utilization of smart coordinator in the near future’s personal and wearable IoT and WoT applications. This work has just started.

The future work is also providing SmartBAN recommendations for wireless communications with capsule endoscopy. In addition, TC SmartBAN has recognized the importance of security, privacy and trust in the target operation domain and is developing computationally light mechanisms to support these requirements.

REFERENCES

- [1] S. Ullah, H. Higgins, B. Braem, B. Latre, C. Blondia, I. Moerman, S. Saleem, Z. Rahman, and K. S. Kwak, “A comprehensive survey of wireless body area networks,” *J. Med. Syst.*, vol. 36, pp. 1065–1094, Jun. 2012, doi: 10.1007/s10916-010-9571-3.
- [2] R. Cavallari, F. Martelli, R. Rosini, C. Buratti, and R. Verdona, “A survey on wireless body area networks: Technologies and design challenges,” *IEEE Commun. Surveys Tuts.*, vol. 16, no. 3, pp. 1635–1657, 3rd Quart., 2014, doi: 10.1109/SURV.2014.012214.00007.
- [3] M. Ghamari, B. Janko, R. Sherratt, W. Harwin, R. Piechockic, and C. Soltanpur, “A survey on wireless body area networks for eHealthcare systems in residential environments,” *Sensors*, vol. 16, no. 6, p. 831, Jun. 2016.
- [4] E. Jovanov, “Wearables meet IoT: Synergistic personal area networks (SPANs),” *Sensors*, vol. 19, no. 19, p. 4295, Oct. 2019.
- [5] *ETSI TC SmartBAN Technical Committee*. Accessed: Aug. 5, 2020. [Online]. Available: <https://portal.etsi.org/tb.aspx?tbid=804&SubTB=804>
- [6] *Smart Body Area Networks (SmartBAN); System Description*, document ETSI TR 103 394 V1.1.1, Jan. 2018. [Online]. Available: https://www.etsi.org/deliver/etsi_tr/103300_103399/103394/01.01.01_60/tr_103394v010101p.pdf
- [7] M. Hamalainen, T. Paso, L. Mucchi, M. Girod-Genet, J. Farserotu, H. Tanaka, W. H. Chin, and L. N. Ismail, “ETSI TC SmartBAN: Overview of the wireless body area network standard,” in *Proc. 9th Int. Symp. Med. Inf. Commun. Technol. (ISMICT)*, Kamakura, Japan, Mar. 2015, pp. 24–26.
- [8] (2012). *IEEE Standard for Local and Metropolitan Area Networks: Part 15.6: Wireless Body Area Networks*. [Online]. Available: <https://ieeexplore.ieee.org/document/6161600>
- [9] *Smart Body Area Network (SmartBAN); Low Complexity Medium Access Control (MAC) for SmartBAN*, document ETSI TS 103 325 V1.1.1 (2015-04), 2015. [Online]. Available: https://www.etsi.org/deliver/etsi_ts/103300_103399/103325/01.01.01_60/ts_103325v010101p.pdf
- [10] T. Paso, H. Tanaka, M. Hamalainen, W. H. Chin, R. Matsuo, S. Subramani, and J. Haapola, “An overview of ETSI TC SmartBAN MAC protocol,” in *Proc. 9th Int. Symp. Med. Inf. Commun. Technol. (ISMICT)*, Kamakura, Japan, Mar. 2015, pp. 24–26.
- [11] *Smart Body Area Network (SmartBAN); Enhanced Ultra-Low Power Physical Layer*, document ETSI TS 103 326 V1.1.1 (2015-04), 2015. [Online]. Available: https://www.etsi.org/deliver/etsi_ts/103300_103399/103326/01.01.01_60/ts_103326v010101p.pdf
- [12] W. H. Chin, H. Tanaka, T. Nakanishi, T. Paso, and M. Hamalainen, “An overview of ETSI TC SmartBAN’s ultra low power physical layer,” in *Proc. 9th Int. Symp. Med. Inf. Commun. Technol. (ISMICT)*, Kamakura, Japan, Mar. 2015, pp. 24–26.
- [13] *Smart Body Area Network (SmartBAN); Unified Data Representation Formats, Semantic and Open Data Model*, document ETSI TS 103 378 (V1.1.1) (10-2015), 2015. [Online]. Available: https://www.etsi.org/deliver/etsi_ts/103300_103399/103378/01.01.01_60/ts_103378v010101p.pdf
- [14] *Smart Body Area Network (SmartBAN); Unified Data Representation Formats, Semantic and Open Data Model*, document ETSI TS 103 378r1, 2019. [Online]. Available: https://portal.etsi.org/webapp/WorkProgram/Report_WorkItem.asp?WKI_ID=50078

- [15] *Smart Body Area Network (SmartBAN): Service and Application Standardized Enablers and Interfaces; APIs and Infrastructure for Interoperability Management*, document ETSI TS 103 327, 2019. [Online]. Available: https://portal.etsi.org/webapp/WorkProgram/Report_WorkItem.asp?WKI_ID=42935
- [16] *Measurements and Modelling of SmartBAN Radio Frequency (RF) Environment*, document ETSI TR103 395 Ver. 1.1.1, 2016. [Online]. Available: https://www.etsi.org/deliver/etsi_tr/103300_103399/103395/01_01_01_60/tr_103395v010101p.pdf
- [17] L. Mucchi, R. Vuoltoniemi, H. Virk, A. Conti, M. Hamalainen, J. Inatti, and M. Z. Win, "Spectrum occupancy and interference model based on network experimentation in hospital," *IEEE Trans. Wireless Commun.*, early access, Jun. 1, 2020, doi: [10.1109/TWC.2020.2995116](https://doi.org/10.1109/TWC.2020.2995116).
- [18] *OneM2M—Standards for M2M and the Internet of Things*. Accessed: Aug. 5, 2020. [Online]. Available: <http://www.onem2m.org/>
- [19] *CareWare—Smart Wearable Sport and Health Solutions*. Accessed: Aug. 5, 2020. [Online]. Available: <https://itea3.org/project/careware.html>
- [20] *Personal Connected Health Alliance*. Accessed: Aug. 5, 2020. [Online]. Available: <https://www.pchalliance.org/>
- [21] (Jun. 2018). *AIOTI High Level Architecture (HLA) Release 4.0, AIOTI WG03*. [Online]. Available: <https://aioti.eu/wp-content/uploads/2018/06/AIOTI-HLA-R4.0.7.1-Final.pdf>
- [22] H. Viitala, L. Mucchi, M. Hamalainen, and T. Pasa, "ETSI SmartBAN system performance and coexistence verification for healthcare," *IEEE Access*, vol. 5, pp. 8175–8182, 2017, doi: [10.1109/ACCESS.2017.2697502](https://doi.org/10.1109/ACCESS.2017.2697502).
- [23] H. Viitala, L. Mucchi, and M. Hämäläinen, "Performance of the ETSI SmartBAN system in the interfered IEEE 802.15.6 channel," in *Proc. 11th Int. Symp. Med. Inf. Commun. Technol. (ISMICT)*, Lisbon, Portugal, Feb. 2017, pp. 15–18.
- [24] *Bluetooth Core Specification*. Accessed: Aug. 5, 2020. [Online]. Available: <https://www.bluetooth.com/specifications/bluetooth-core-specification/>
- [25] *IEEE Standard for Information Technology—Telecommunications and Information Exchange Between Systems Local and Metropolitan Area Networks—Specific Requirements—Part 11: Wireless LAN Medium Access Control (MAC) and Physical Layer (PHY) Specifications*, Standard 802.11-2016, 2016. [Online]. Available: <https://ieeexplore.ieee.org/document/7786995>
- [26] *IEEE Standard for Low-Rate Wireless Personal Area Networks (WPANs)*, IEEE Standard 802.15.-2015, Dec. 2015.
- [27] E. Karapistoli, N. Pavlidou, I. Gragopoulos, and I. Tsetsinas, "An overview of the IEEE 802.15.4a standard," *IEEE Commun. Mag.*, vol. 48, no. 1, pp. 47–53, Jan. 2010.
- [28] M. Hämäläinen and J. Inatti, *Academic Press Library in Biomedical Applications of Mobile and Wireless Communications: Wireless UWB Body Area Networks: Using the IEEE802.15.4-2011*. Amsterdam, The Netherlands: Elsevier, 2014.
- [29] R. Khan, M. M. Alam, "SmartBAN performance evaluation for diverse applications," in *Proc. EAI Int. Conf. Body Area Netw.*, Florence, Italy, 2019, pp. 239–251.
- [30] V. Niemela, J. Haapola, M. Hamalainen, and J. Inatti, "An ultra wide-band survey: Global regulations and impulse radio research based on standards," *IEEE Commun. Surveys Tuts.*, vol. 19, no. 2, pp. 874–890, 2nd Quart., 2017, doi: [10.1109/COMST.2016.2634593](https://doi.org/10.1109/COMST.2016.2634593).
- [31] *ETSI—Smart Appliances*. Accessed: Aug. 5, 2020. [Online]. Available: <https://www.etsi.org/technologies/smart-appliances>
- [32] ETSI. *One Machine-to-Machine Partnership Project (oneM2M)*. Accessed: Aug. 5, 2020. [Online]. Available: <https://www.etsi.org/committee/onem2m>
- [33] International Electrotechnical Commission. *SyC AAL Active Assisted Living*. Accessed: Aug. 5, 2020. [Online]. Available: https://www.iec.ch/dyn/www/?p=103:186:0:::FSP_ORG_ID:11827
- [34] International Electrotechnical Commission. *TC 124 Wearable Electronic Devices and Technologies*. Accessed: Aug. 5, 2020. [Online]. Available: https://www.iec.ch/dyn/www/?p=103:7:0:::FSP_ORG_ID,FSP_LANG_ID:20537
- [35] *Institute of Electrical and Electronic Engineers*. Accessed: Aug. 5, 2020. [Online]. Available: <https://www.ieee.org/>
- [36] *Alliance for Internet of Things Innovations*. Accessed: Aug. 5, 2020. [Online]. Available: <https://aioti.eu/>
- [37] M. M. Alam and E. B. Hamida, "Towards accurate mobility and radio link modeling for IEEE 802.15. 6 wearable body sensor networks," in *Proc. 10th WiMob Conf.*, Oct. 2014, pp. 298–305.

[38] P. Murdock et al., "Semantic interoperability for the Web of Things," Aug. 2016, doi: [10.13140/RG.2.2.25758.13122](https://doi.org/10.13140/RG.2.2.25758.13122).

[39] H. Baqa, M. Bauer, S. Bilbao, A. Corchero, L. Daniele, I. Fernández, Ö. Franberg, R. García-Castro, M. Girod-Genet, P. Guillemín, A. Gyrard, C. E. Kaed, A. Kung, J. Lee, M. Lefrançois, W. Li, D. Raggett, I. Esnaola-Gonzalez, and M. Wetterwald, "Towards semantic interoperability standards based ontologies," Oct. 2019, doi: [10.13140/RG.2.2.26825.29282](https://doi.org/10.13140/RG.2.2.26825.29282).



MATTI HÄMÄLÄINEN (Senior Member, IEEE) received the M.Sc. and Dr.Sc. degrees from the University of Oulu, Finland, in 1994 and 2006, respectively. From 2016 to 2018, he was nominated as an Institute of Advanced Science Visiting Professor at Yokohama National University, Japan. He is currently a University Researcher and an Adjunct Professor at the Centre for Wireless Communications, University of Oulu. He holds one patent. His research interests include radio channel modelling, UWB systems, BANs, and medical ICT. He is a member of the External Advisory Board of Macquarie University's WiMed Research Centre, Australia, and the Co-Chair for the International Steering Committee of ISMICT Conference. He is also an Active Member at ETSI TC SmartBAN. He is an Associate Editor of IEEE Access and *Frontiers in Communications and Networks*—the Non Conventional Communications and Networking Section and a member of the Editorial Board of *Annals of Telecommunications*. According to Google Scholar, his current H-index is 26. He is an EAI Community Fellow.



LORENZO MUCCHI (Senior Member, IEEE) was a Visiting Researcher at the Centre for Wireless Communications, University of Oulu, Finland, in 2000. He is currently an Associate Professor at the Department of Information Engineering, University of Florence, Italy. He is also the Founder and the Scientific Coordinator of two Joint Research Laboratories: one on Visible Light Communications and another on Medical ICTs. His research interests include theory and experimentation of wireless systems and networks, including physical-layer security, visible light communications, localization and tracking, body area networks, and molecular communications. Since 2013, he has been a member of the Smart Body Area Network Group, European Telecommunications Standard Institute (ETSI), where he leads items on security, coexistence, and interference mitigation. He chaired IEEE and EAI international conferences. He is serving as an Associate Editor for the IEEE COMMUNICATIONS LETTERS and IEEE ACCESS. He has been the Editor-in-Chief for Elsevier Academic Press.



MARC GIROD-GENET (Member, IEEE) received the Engineering degree from the EPITA Engineering School, Paris, France, in 1994, the M.Sc. degree in computer science from the Stevens Institute of Technology, Hoboken, NJ, USA, in 1995, and the Ph.D. degree in computer science from the University of Versailles. He is currently an Associate Professor at the Institut Mines-Télécom (IMT)-Télécom SudParis, Evry, France, and an Associate Researcher at CNRS (UMR 5157 SAMOVAR).

His current research interests include interoperability management (data, informational, device, system, and semantic levels), knowledge representation and modelling, modular ontology engineering, and embedded data analytics, applied in particular for eHealth and smart energy verticals. He has published over 40 conference papers and holds a patent in machine learning granted. He serves as a Rapporteur and/or a Contributor of ETSI: SmartBAN TC, SmartM2M TC, and EP eHealth. He also represents IMT inside Alliance for Internet of Things Innovation (AIOTI).



TUOMAS PASO received the M.Sc. degree from the University of Oulu, Finland, in March 2010, where he is currently pursuing the Ph.D. degree with the Centre for Wireless Communications. He is also a Research Scientist with the Centre for Wireless Communications, University of Oulu. His research interests include MAC protocols and PHY/MAC/NET cross-layer techniques in MANETs and wireless sensor networks, such as BANs and WPANs. The main focus areas of

his research are healthcare/medical ICT and security/defense. He has been serving as a Reviewer for IEEE journals and conferences and as a Technical Program Committee Member of the IEEE PIMRC, since 2014. He is a member of the European Telecommunications Standard Institute (ETSI) Technical Committee Smart Body Area Network (SmartBAN), in which he is currently the Rapporteur for the work item Low Complexity Medium Access Control (MAC) for SmartBAN.



JOHN FARSEROTU (Senior Member, IEEE) received the B.S.E.E. degree from the University of Maryland, in 1983, the M.S.E.E. degree from George Washington University, in 1985, and the Ph.D. degree from the Delft University of Technology, in 1998. He is currently the Head of the Wireless Program at the Integrated and Wireless Systems Division, Swiss Center for Electronics and Microtechnology (CSEM), Switzerland. He is also the Chair of the ETSI TC SmartBAN and

a Research Coordinator of the Hermes Partnership, a network of leading European organizations in wireless. He was the Principal Investigator of the Swiss WiseSkin nano-tera research project on the development of an artificial skin embedded with wireless sensors for tactile prosthetics and has been the Coordinator of various European projects. He is an author of over 100 publications, a co-applicant of three patents, and a coauthor of a book on *Mobile Satellite over IP/Asynchronous Transfer Mode (ATM) Networks*. He taught a course on the subject at the Ecole Polytechnique Federale de Lausanne (EPFL), from 2002 to 2019.



HIROKAZU TANAKA (Senior Member, IEEE) received the B.E. and Ph.D. degrees in communications engineering from Osaka University, Suita, in 1989 and 2001, respectively, and the second Ph.D. degree in information sciences from Hokkaido University, Sapporo, in 2015. He joined Toshiba Corporation as a Researcher, in 1989. Since 2013, he has been a Visiting Fellow at Toshiba Research Europe, Ltd. Since 2015, he has also been a Professor with Hiroshima City University. His research interests include theory and applications of modulation, error control coding, and access control and video coding, with an emphasis on mobile communications, broadcasting and dependable communications, and body area network for IoT systems. Since 1997, he has been involved with international standardization activities in the field of mobile multimedia systems in ITU-T, 3GPP, 3GPP2, and Bluetooth. Since 2013, he has been serving as the Vice Chair for TC Smart BAN in ETSI.



DAISUKE ANZAI received the B.E., M.E., and Ph.D. degrees from Osaka City University, Osaka, Japan, in 2006, 2008, and 2011, respectively. Since 2011, he has been with the Graduate School of Engineering, Nagoya Institute of Technology, Nagoya, Japan, as an Assistant Professor, where he is currently an Associate Professor. He is also a Guest Scientist at Friedrich-Alexander Universität Erlang-Nürnberg, Germany, in which role he contributes to ETSI TC SmartBAN work. He has

engaged in the research of biomedical communication systems and localization systems in wireless communications networks. He received many awards, including the IEEE 2015 IEEE MTT-S Japan Young Engineer Award and the Telecommunications Technology Award from the Telecommunications Advancement Foundation.



LAURA PIERUCCI (Senior Member, IEEE) received the Graduation degree in electronics engineering from the University of Florence, Florence, Italy, in 1987. She has been with the Department of Information Engineering, University of Florence, as an Assistant Professor, since 2000. She co-invented a patent on the use of RFID for health application. She has been involved in several national and European research projects on satellite communications, tele-medicine systems,

wireless systems, and radar signal processing. She has been the Scientific Coordinator of the EU COST Action 252. She has served as an Expert for the European Committee in the area of satellite communications. She has coauthored several international articles. Her current research interest includes wireless communication systems, especially in the topics of 4G/5G systems, resource management, D2D communications, multiple-input multiple-output antenna systems, cooperative communications, and security for wireless sensor networks and IoT. She was a recipient of the IWCMC 2016 Best Paper Award and the Globecom 2016 Best Paper Award. She is currently serving as an Associate Editor for *Telecommunication Systems*, the *IEEE Communications Magazine*, and the *IEEE INTERNET OF THINGS JOURNAL*.



RIDA KHAN (Student Member, IEEE) received the B.E. degree in telecommunication engineering from the Mehran University of Engineering and Technology, Pakistan, in 2013, and the M.Sc. degree in electronics and communication engineering from Istanbul Technical University, Turkey, in 2017. She is currently pursuing the Ph.D. degree in information and communication technology with the Tallinn University of Technology, Estonia. Her research interests include wear-

able wireless networks, network coding, and energy-efficient modulation techniques. She is a Student Member of the IEEE Standards Association and is currently serving as the Secretary of the Energy Efficient Communications Hardware (EECH) Standards Working Group. In addition, she is contributing the ETSI SmartBAN work item: DTR/SmartBAN-0014, "Applying SmartBAN MAC (TS 103 325) for various use cases."



MUHAMMAD MAHTAB ALAM (Senior Member, IEEE) received the M.Sc. degree in electrical engineering from Aalborg University, Denmark, in 2007, and the Ph.D. degree in signal processing and telecommunication from the University of Rennes1 France (INRIA Research Center), in 2013. He joined the Swedish College of Engineering and Technology, Pakistan, in 2013, as an Assistant Professor. He did his postdoctoral research at the Qatar Mobility Innovation Center,

Qatar, from 2014 to 2016. In 2016, he joined the Thomas Johann Seebeck Department of Electronics, Tallinn University of Technology, as the European Research Area Chair and an Associate Professor, where, later, in 2018, he was elected as a Professor. Since 2019, he has been the Communication Systems Research Group Leader. He has over 15 years of combined academic and industrial multinational experience while working in Denmark, Belgium, France, Qatar, and Estonia. He has several leading roles as a PI in multimillion Euros international projects funded by the European Commission (H2020-ICT-2019-3, “951867,” NATO-SPS (G5482), Estonian Research Council (PRG424), and Telia Industrial Grant). He has authored or coauthored more than 85 research publications. He is also a Contributor in two standardization bodies (ETSI SmartBAN and IEEE-GeeenICT-EECH), including “Rapporteur” of work item: DTR/SmartBAN-0014, “Applying SmartBAN MAC (TS 103 325) for various use cases.” His research interests include wireless communications—connectivity, NB-IoT 5G/B5G services and applications, and low-power wearable networks for SmartHealth. He is an Associate Editor of IEEE ACCESS journal and *Frontier in Communications and Networks*—IoT and Sensor Networks.



PHILIPPE DALLEMAGNE (Member, IEEE) received the Ph.D. degree in computer science from the Université Henri Poincaré of Nancy, France, in 1998. He joined the Swiss Center for Electronics and Microtechnology (CSEM), in 1999. He is an Expert in ultra-low power wireless systems. He is currently managing projects at CSEM in the domains of energy-autonomous wireless sensor networks, real-time communication and smart, edge computing, and complex

and collaborative systems. Before joining CSEM, he worked for the IBM Analysis and Design Tools Laboratory, Paris. He was the Leader of the ETSI Project Team 49 for the Videotext Enhanced Man-Machine Interface (VEMMI). He has an extensive experience of the software design and development in the context of wireless technologies for the Internet of things, robust and reconfigurable embedded software, and high-performance real-time communication. He is the author of several articles in international conferences and workshops. He took part in several EU projects in the FP6, FP7, and now H2020 EC programmes. He is also the Swiss Representative and Secretary of the IFIP Technical Committee 5.

...

Appendix 3

R. Khan and M. M. Alam. Joint throughput and channel aware MAC scheduling for SmartBAN. In *EAI International Conference on Body Area Networks*, pages 49–64, 2018

Joint Throughput and Channel Aware MAC Scheduling for SmartBAN^{*}

Rida Khan, and Muhammad Mahtab Alam

Thomas Johann Seebeck Department of Electronics, Tallinn University of
Technology, Tallinn, Estonia
{rikhan, muhammad.alam}@ttu.ee

Abstract. In this paper, a joint throughput and channel aware medium access control (MAC) scheduling scheme is presented and evaluated for Smart body area network (SmartBAN) standard, developed by European Telecommunication Standard Institute (ETSI). At first, various mobility patterns are generated which provide dynamic space-time variations in distance and link types for different on-body links. These space-time varying links help in realistic pathloss values calculation under dynamic environment, which subsequently provides signal to noise ratio (SNR), bit error rate (BER) and packet error rate (PER) results for further performance evaluations. Subsequently, the presented algorithm utilizes the radio link SNR to select the appropriate nodes for a given time slot in the first phase. While, in the second phase, the slot is assigned to one of the chosen nodes based on their priority level and data packet availability. We use m-periodic scheduling technique in which the nodes are considered for slot assignment according to their data packet generation rates during the second phase. For performance comparison, we carry out reference SmartBAN MAC scheduling with and without repetitions for the same m-periodically generated data. The simulation results indicate significant performance gain of the presented scheduling algorithm in terms of packet reception rate (PRR) and energy efficiency over the reference SmartBAN MAC scheduling with and without repetition. The average improvement in PRR results is found to be more than 60% whereas a maximum enhancement of 92% is observed in terms of energy efficiency. However, the performance gain is compromised by an average of 40% increase in latency for sit-stand posture.

Keywords: WBAN · MAC · throughput and channel aware scheduling · SmartBAN · PRR · energy consumption · latency.

1 Introduction

Wireless body area networks (WBANs) are becoming self-evident and a well-known research discipline due to numerous potential applications in future, rang-

^{*} This research was supported by the Estonian Research Council through the Institutional Research Project IUT19-11, and by the Horizon 2020 ERA-chair Grant Cognitive Electronics COEL H2020-WIDESPREAD-2014-2 (Agreement number: 668995; project TTU code VFP15051).

ing from health-care environments to mission critical operations [1]. A typical WBAN consists of various sensor nodes for measuring diverse set of biomedical data and a coordinator or hub node to monitor and regulate those sensor nodes. Standardized protocols are required to ensure proper functionality at the desired quality level in WBANs as well. Among several standards dedicated to WBANs, IEEE 802.15.6 was the first officially recognized standard to provide guidelines about WBAN operation [2]. However, European Telecommunication Standards Institute (ETSI) introduced another WBAN specific standard termed as Smart Body Area Network (SmartBAN) [3] with a comparatively simplified and efficient physical (PHY) and medium access control (MAC) structure [4].

SmartBAN supports a significantly high symbol rate of 1 MSymbols/s [5] with many different options for payload sizes, that are pre-defined in control channel beacon by hub [6]. However, the packet reception rate (PRR) performance starts degrading for transmission power levels below -5 dBm and increased packet sizes as the WBAN links are shadowed by human body [7]. In order to provide PHY-MAC performance gain, the provision of data packet repetition is supported at the SmartBAN PHY layer [5]. The importance of this repetition is highlighted in [8] in which data repetition is deemed necessary to get the acceptable 1% frame error rate under high interference scenario.

One of the most common MAC approach in WBAN is scheduled access mechanism in which every sensor node is assigned a dedicated time slot for data transmission to the BAN coordinator. But, for any given application, every sensor node requires different data transmission rate [9], therefore, the slot allocation to WBAN sensor nodes should be adapted according to their prescribed data transmission intervals. Moreover, an average difference of 10 dBs is reported in the path loss measurements of a space-time varying WBAN communication link [10], leading to the conclusion that variations in radio link quality can have a considerable effect on PRR performance. These phenomena motivate the research on dynamic slot scheduling to enhance the effective throughput, energy efficiency and PHY-MAC performance. Many noteworthy research contributions have been made in this domain but most of them focus on either minimizing energy consumption while keeping higher PRR or proposing channel estimation techniques to enhance PRR under dynamic environments. Addressing the throughput, energy efficiency and PRR performance requirements of emerging wearable applications, a joint throughput and channel aware dynamic scheduling algorithm was proposed in [11] in compliance with the IEEE 802.15.6 scheduled access mechanism. The algorithm was demonstrated to be successful in providing better PRR performance keeping the transmission power, and hence the energy consumption levels substantially low. Our initial simulation results on SmartBAN indicated that even the repetition was not able to achieve above 90 % PRR at lower transmission power, which is often favored in WBAN communications for energy efficiency and reduced interference for multiple co-located BANs. Therefore this study is dedicated to the performance analysis of SmartBAN in the context of required throughput and channel aware scheduling for prospective WBAN applications.

This paper addresses the effective throughput, energy consumption and reliability concern of potential WBAN applications under dynamic and realistic conditions in SmartBAN. A joint throughput and channel aware dynamic MAC scheduling algorithm is presented incorporating the SmartBAN proposed scheduled access technique. Various mobility patterns, including walking, sitting, standing and running, are generated using bio-mechanical mobility modeling to analyze the performance at different channel conditions for several sensor-hub links. The primary contributions of this paper are: 1) Enhancing the throughput and channel aware MAC scheduling algorithm for SmartBAN complaint scheduled access method. 2) Evaluating the reference SmartBAN MAC scheduled access mechanism with and without repetitions for performance comparison. 3) Providing performance gain in terms of PRR and energy consumption, with possible effects on latency.

The remainder of the paper is organized in the following way: section II provides an overview of the mobility and radio link modeling while section III explains SmartBAN MAC superframe format considered in simulations. Section VI elaborates the reference SmartBAN MAC scheduling with and without repetitions as well as throughput and channel aware MAC scheduling for SmartBAN. In section V, performance results are presented and discussed comprehensively whereas section VI concludes the paper.

2 Mobility and Radio Link Modeling

The underlying mobility and radio link modeling for PHY-MAC performance analysis is presented in this section.

2.1 Channel Model

We use IEEE 802.15.6 proposed CM3-B channel model in order to compute pathloss values for space-time varying distances and link types, as shown

$$PL_{dB} = -10\log_{10}(P_0e^{-m_0d} + P_1) + \sigma_P n_P [dB], \quad (1)$$

where $P_0 = -25.8$ dB, $m_0 = 2.0$ dB/cm, $P_1 = -71.3$ dB, $\sigma_P = 3.6$ dB, n_P is the Gaussian random variable with zero mean and unity variance, d is the distance in cm and PL_{dB} is the pathloss in dBs [12].

2.2 Mobility Modeling

Bio-mechanical mobility modeling, as proposed in [13], is used to generate dynamic distances and link types for various on-body links between sensor nodes and coordinator. The dynamic distances serve as input distances in the CM3-B model to provide pathlosses for dynamic mobility scenarios. Furthermore, the space-time varying link types are used to characterize the given link as line of sight (LOS) or non-line of sight (NLOS). In case of NLOS link status, an additional NLOS factor of 13% is added to the calculated pathloss [14] otherwise the pathloss remains the same.

2.3 Radio Link Modeling

The precise mobility and channel modeling of dynamic links is followed by accurate radio link modeling. This modeling consists of SNR, bit error rate (BER) and packet error rate (PER) computations. We utilize the similar approach as performed in [13] for radio link modeling with few modifications in BER calculations for SmartBAN.

BER with no Repetition SmartBAN standard proposes Gaussian Frequency Shift Keying (GFSK) modulation technique at the physical layer with the bandwidth-bit period product BT and modulation index h of 0.5 [5]. According to [15], for $h = 0.5$ frequency shift keying modulation becomes minimum shift keying modulation and therefore, the corresponding BER expression becomes

$$P_e \left(\frac{E_b}{N_0} \right) = Q \left(\sqrt{2\epsilon \frac{E_b}{N_0}} \right), \quad (2)$$

where $\frac{E_b}{N_0}$ is signal-to-noise ratio for a bit, ϵ is a constant [16] and for BT of 0.5, is equal to 0.79 [17]. The detailed calculation of $\frac{E_b}{N_0}$ using pathloss and SNR values can be found in [13].

BER with Repetition BER for this case is computed using the similar BER expression as provided in the previous sub-section but SNR calculations are made in accordance with the diversity technique used for evaluating the repetition gain. Since maximal ratio combining (MRC) provides the best performance over all diversity combining techniques, therefore, we assume MRC diversity scheme for evaluating the best case scenario performance that SmartBAN can provide with repetition. In MRC with statistically independent transmission channels, the output SNR is equal to the addition of instantaneous SNRs at the individual links [15].

3 SmartBAN MAC Superframe Format

This section provides a detailed explanation about the SmartBAN MAC superframe format that is considered for MAC scheduling in this paper, as illustrated in Fig. 1. The transmissions between node and hub take place on data channels and the data channel used for transmission is partitioned into inter-beacon intervals or superframe durations. The beginning of each superframe is marked by a data channel beacon (D-Beacon), followed by scheduled access period for data transmissions by sensor nodes and corresponding acknowledgements. Control and management period is used for management and control signaling by hub and/or sensor nodes and the entire superframe duration ends with an inactive period [6]. Each scheduled access slot is made of physical-layer protocol data unit (PPDU) transmissions and PPDU acknowledgements separated by inter-frame spacing (IFS). The actual payload is found in MAC frame body, that

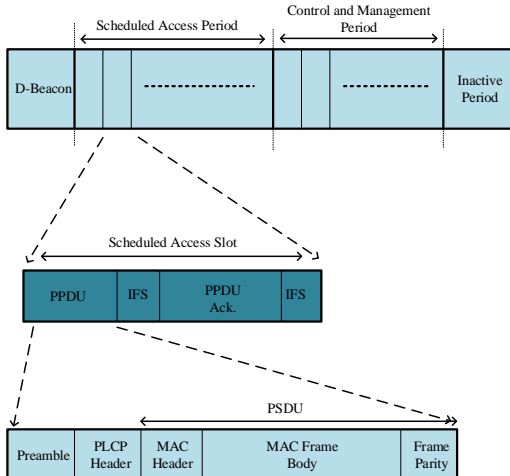


Fig. 1. SmartBAN MAC superframe format.

along with MAC header and frame parity constitutes a MAC protocol data unit (MPDU). Since, we assume uncoded MPDU in our case, therefore, the resultant MPDU becomes physical-layer service data unit (PSDU). PSDU, after the addition of physical-layer convergence protocol (PLCP) header and preamble, creates a complete PPDU [5], as depicted in Fig. 1.

For superframe duration computation, it is necessary to first calculate the beacon duration, time slot duration and the number of time slots in scheduled access period, time slot duration and the number of time slots in control and management period and the duration of inactive period. D-beacon duration is found as

$$T_{Beacon} = \frac{N_{Beacon}}{R_{Sym}}, \quad (3)$$

where, N_{Beacon} is the number of bits in D-beacon and R_{Sym} is the symbol rate. The duration of each time slot in scheduled access period is found according to a pre-defined parameter L_{SLOT} [6], as under

$$T_{SLOT} = T_{min} \times L_{SLOT}, \quad (4)$$

where T_{min} is the minimum duration for any scheduled access slot. We do not assume any inactive period in our simulations while the calculations for control and management period will be provided in the later sections for each case of SmartBAN MAC scheduling.

Within a single time slot during scheduled access period, there is acknowledgement and IFS duration as well. IFS duration is fixed and the duration for acknowledgement is written as

$$T_{ACK} = \frac{N_{preamble} + N_{PLCPheader} + N_{parity} + N_{MACheader}}{R_{Sym}}, \quad (5)$$

where $N_{preamble}$, $N_{PLCPheader}$, N_{parity} and $N_{MACheader}$ are the number of bits in physical-layer preamble, PLCP header, MAC frame parity and MAC frame header respectively. After the computation of T_{ACK} , the effective duration for PPDU transmission is given as

$$T_{TX} = \frac{T_{SLOT} - T_{ACK} - 2 \times T_{IFS}}{REP}, \quad (6)$$

where REP is the number of PPDU repetitions. The calculation of T_{TX} is followed by the computation of maximum allowed MAC frame body size for uncoded MPDU, as under

$$Payload = T_{TX} \times R_{Sym} - N_{preamble} - N_{PLCPheader} - N_{parity} - N_{MACheader}. \quad (7)$$

4 MAC Scheduling with m-Periodicity

This section discusses SmartBAN MAC scheduling with m-periodic slot assignment for reference MAC with and without repetition as well for traffic and channel aware MAC.

4.1 SmartBAN MAC Scheduling without Repetition

For applications with sensor nodes having a variety of data generation rates, it becomes unnecessary to allocate a fixed time slot for every node inside MAC superframe. Therefore, the time slots inside the scheduled access period are assigned based on their data generation rates. The m-periodic slot assignment considered in this case is depicted in Fig. 2. In the given scheme, the priority node P, based on high data generation rate and/or emergency traffic, is assigned time slot in consecutive superframes while the other low traffic nodes periodically wake up to send their data after a fixed number of m superframes, defined by their required data rate. As shown in Fig. 2, we assume only scheduled access period along with data beacons in superframe duration, unless stated otherwise, in order to evaluate the performance for transmitted data packets only. It should be noted that all the sensor nodes are assumed to have their respective time slots pre-assigned by coordinator based on the packet generation rates. Therefore, under reference SmartBAN m-periodic MAC scheduling without repetitions, each time slot consists of PPDU transmission followed by PPDU acknowledgement and both separated by IFS. Each inter-beacon duration comprises of time slots assigned on the basis of m-periodicity principle.

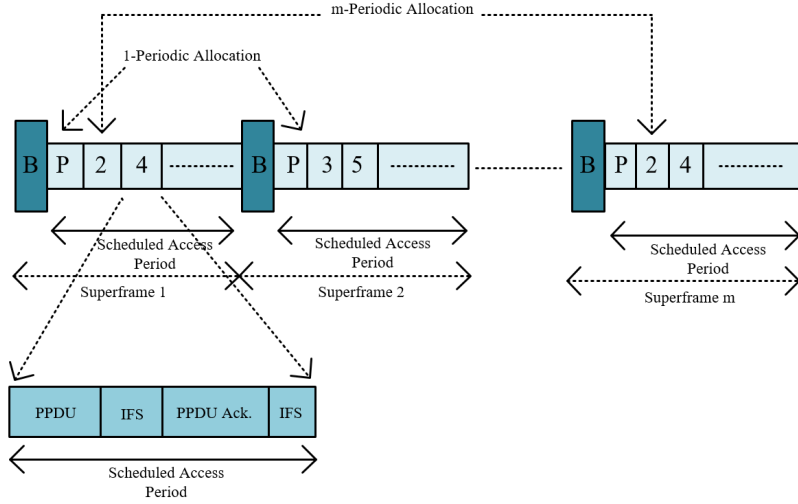


Fig. 2. m-Periodic MAC scheduling and scheduled access slot without repetition for SmartBAN.

4.2 Scheduled Access Slot with Repetition for SmartBAN

In this scenario, the transmitted PPDU is repeated within the assigned time slot for each node, so the effective payload size for a given slot length is reduced. Consequently, for sending the same amount of data, sensor nodes would be required to assign time slots more often with reduced payload sizes. At reception, the repeated PPDU's are combined using MRC technique. Fig. 3 illustrates the scheduled access time slot structure with repetition for SmartBAN. The remaining m-periodic scheduled access method is the same as described in sub-section 4.1.

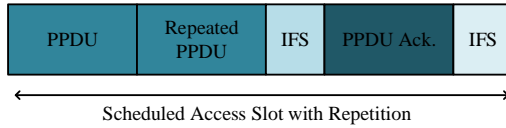


Fig. 3. Scheduled access slot with 2 repetitions for SmartBAN.

4.3 Throughput and Channel Aware MAC Scheduling for SmartBAN

This scheduled access mechanism has slightly different superframe structure from the previous scheduling strategies since the time slots are dynamically assigned based on the SNR level and the availability of data packet. As indicated in Fig. 4, superframe now includes control and management period as well in which hub dynamically assigns time slots to sensor nodes for data transmission during scheduled access period in the next superframe. Every sensor node periodically wakes up during the control and management period which contains the slot re-assignments for every node. The slot goes to sleep mode for energy conservation if it is not assigned any slot otherwise the node remains in low power mode and wakes up for data transmission just before the start of the slot. The flow chart

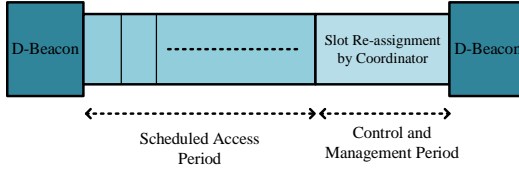


Fig. 4. Superframe format for joint throughput and channel aware scheduled access MAC.

of the algorithm for slot assignment is given in Fig. 5. During the first step, each time slot is checked for the SNR conditions of every node-hub link and a set of sensor nodes is defined for which the link SNR is greater than a pre-defined threshold value. In the second step, the set of sensor nodes with good links is checked for priority node. If priority node is among the candidate sensor nodes and it has data packet to send, it is assigned the time slot else other low priority nodes are assigned the given slot based on their data packet status. In order to define the SNR threshold for the first phase, a PER value of 0.1 is considered to obtain the PRR above 90% and reverse radio link computations are performed to acquire the corresponding SNR threshold. The required PER value of 0.1 gives the resultant BER value using the relation $PER = 1 - \left(1 - P_e \left(\frac{E_b}{N_0}\right)\right)^N$, where N is the packet size in bits, which in turn provides $\frac{E_b}{N_0}$ after evaluation in (2). The required SNR can be obtained using the equation $\frac{E_b}{N_0}[dB] = SNR[dB] + 10 \times \log_{10} \left(\frac{BW}{R}\right)$, where BW is the channel bandwidth which is 2MHz and R is the information rate which is 1MSymbols/s for SmartBAN. The appropriate SNR threshold found for SmartBAN standard using this method is 7dB or higher to get a resulting PRR above 90%.

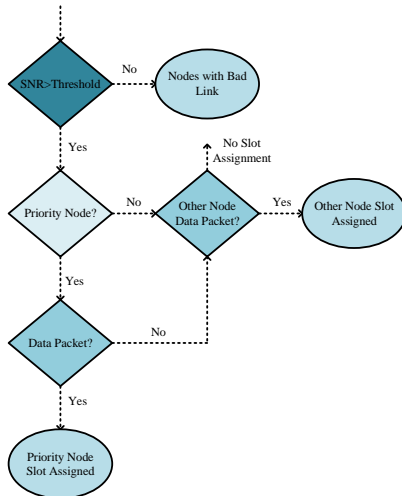


Fig. 5. Throughput and channel aware MAC scheduling algorithm.

5 Performance Evaluation

This section analyzes the performance results of the reference SmartBAN MAC scheduling with and without repetition and the presented throughput and channel aware MAC scheduling in terms of PRR, energy consumption and latency.

5.1 Simulation Setup

For the performance assessment of the above mentioned scheduled access mechanisms, we consider a rescue and emergency management application scenario [18] with six sensors and a coordinator node located on chest. Each sensor collects information about different parameters which include body temperature, pulse rate, GPS coordinates, blood pressure, user mobility and voice commands, with their corresponding data rate requirements of 2.4kbps, 48kbps, 96kbps, 1.2kbps, 4.8kbps and 100kbps [14]. These sensors are respectively placed on the right wrist, left wrist, right knee, left elbow, left knee and right shoulder, as shown in Fig. 6. In order to have better energy efficiency and reduced interference over the surrounding WBANs, we consider rather low transmission power levels of -10.9dBm, defined for RN4020 bluetooth low energy (BLE) devices [19]. Three mobility patterns (walking, sit-stand and running) are assumed in all simulations and $L_{SLOT} = 4$ is taken to define T_{SLOT} . According to the calculations made in section 3, T_{SLOT} is found to be equal to 2.5ms while T_{Beacon} is 128 μ s.

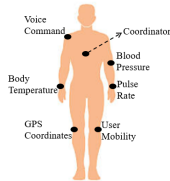


Fig. 6. Coordinator and sensor nodes placements.

Since the reference SmartBAN MAC scheme is not assumed to have control and management period, therefore 66 superframes can be transmitted every second while for throughput and channel aware SmartBAN MAC scheduling scheme, 65 superframes are sent every second. Table 1 summarizes all the major simulation setup parameters. The voice communication node is given priority status

Table 1. Simulation Setup Parameters.

RF Parameters	
Transmitter Power (dBm)	-10.9
Receiver Sensitivity (dBm)	-92.5
Current Consumption Tx (mA)	15
Current Consumption Rx (mA)	16
Bandwidth per channel (MHz)	2
PHY/MAC Parameters	
Minimum slot length (T_{min})	$625\mu s$
Slot duration (T_{SLOT})	2.5ms
Beacon duration (T_{Beacon})	$128\mu s$
Interframe spacing (IFS)	$150\mu s$
Symbol Rate (R_{Sym})	10^6

because of its higher data generation rate and assigned time slot in every consecutive superframe for all scheduling scenarios. For reference SmartBAN MAC, body temperature, pulse rate, blood pressure and GPS sensor nodes are allocated time slot after every 65 superframes while the motion sensor node is provided time slot after every 21 superframes. For reference smartBAN MAC scheduling with 2 repetitions ($REP=2$), the maximum allowed payload size is reduced and body temperature, pulse rate and GPS sensor nodes send their packets after every 65 superframes. Blood pressure node is allocated time slot after every 32 superframes whereas the motion sensor node is assigned a time slot after every 10 superframes. For reference SmartBAN MAC with 4 repetitions ($REP=4$), body temperature, pulse rate and GPS sensor nodes are given time slots after every 65 superframes, blood pressure sensor node is assigned a time slot after

every 15 superframes and motion sensor node can send data after every 4 superframes. Finally, for throughput and channel aware SmartBAN MAC, body temperature, pulse rate, blood pressure and GPS sensor nodes have slot allocation after every 64 superframes while the motion sensor node sends data after every 20 superframes.

5.2 Simulation Results

Packet Reception Rate (PRR) Fig. 7 summarizes the PRR results for each link between different sensor nodes and the coordinator node, under walking, sit-stand and running mobility scenarios. In this scenario, links corresponding to the voice communication, pulse rate, body temperature, motion detection, positioning and blood pressure are respectively identified as Link1, Link2, Link3, Link4, Link5 and Link6. It can be observed that throughput and channel aware MAC scheduling in SmartBAN outperforms the reference smartBAN MAC schemes with and without repetition due to appropriate slot assignment. Despite using packet repetitions with MRC technique, a significant improvement in performance is not observed because of data transmission under poor channel conditions. Moreover, SmartBAN reference MAC scheduling gives severely degraded PRR performance for some links under certain mobility patterns primarily because of shadowing by body posture. For example, Link4 and Link5 in which sensor nodes are placed on left and right knees, experience the worst performance in sit-stand posture as they are shadowed by human torso most of the time. Also, in running scenario, the links corresponding to wrists and knees have lower PRR for reference SmartBAN MAC without any repetition and with 2 repetitions because of the higher pathloss associated with higher mobility.

Energy Consumption The energy consumption in joules for each transmitted packet by a sensor node is given as

$$E_J = T_{TX} \times 3V_{olts} \times I_{mA}, \quad (8)$$

where I_{mA} is the current consumption in mA. Fig. 8 illustrates the energy consumption profile for various links under the given mobility scenarios. These results are computed for the total number of packets transmitted in a given duration for all links, mobility profiles and the previously discussed MAC-layer scheduling schemes, as given in Table 2. The energy consumption is generally the highest for priority node-hub link since this node sends data packet the most often, however, the implementation of throughput and channel aware scheduling leads to better energy efficiency because of opportunistic data transmission over good links. The energy consumption observations for reference SmartBAN MAC with and without repetition do not have any noticeable dissimilarities, except for Link1 which has an average energy consumption difference of 1.2J between reference MAC without repetition and reference MAC with 4 repetitions scheduling schemes. Also, the energy consumption with repetitions is slightly increased for the links having higher data rates as their related nodes send data more frequently.

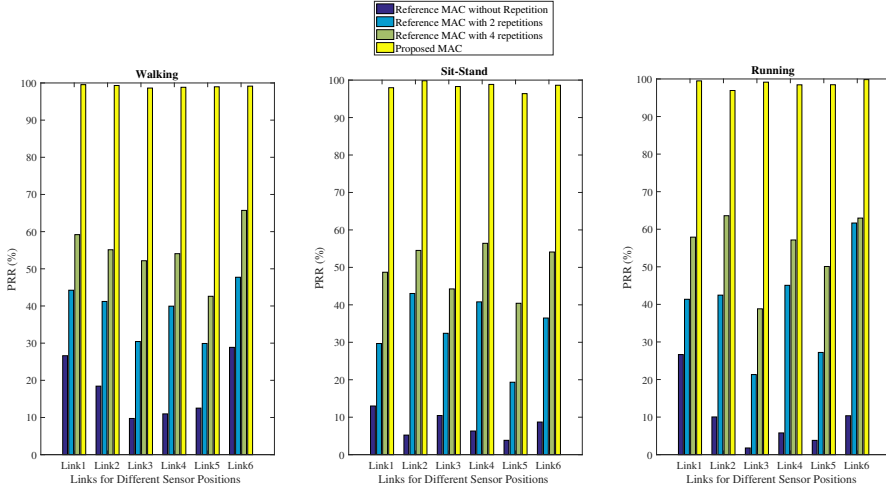


Fig. 7. Packet Reception Rate (PRR) in % under: walking, sit-stand and running mobility profiles.

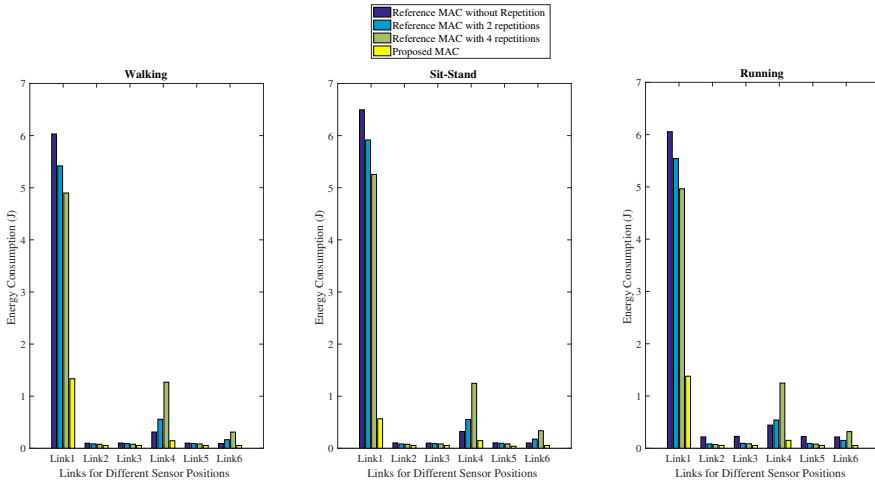


Fig. 8. Energy Consumption in joules under: walking, sit-stand and running mobility profiles.

Table 2. Number of Packets Transmitted.

SmartBAN Reference MAC without Repetition			
	Walking	Sit-Stand	Running
Link1	37312	37250	37464
Link2	575	574	1235
Link3	575	574	1235
Link4	1777	1774	2453
Link5	575	574	1235
Link6	575	574	1235
SmartBAN Reference MAC with 2 Repetitions			
	Walking	Sit-Stand	Running
Link1	37312	37250	37464
Link2	575	574	577
Link3	575	574	577
Link4	3732	3726	3747
Link5	575	574	577
Link6	1167	1165	1171
SmartBAN Reference MAC with 4 Repetitions			
	Walking	Sit-Stand	Running
Link1	37312	37250	37464
Link2	575	574	577
Link3	575	574	577
Link4	9328	9313	9366
Link5	575	574	577
Link6	2488	2484	2498
Throughput and Channel Aware SmartBAN MAC			
	Walking	Sit-Stand	Running
Link1	14256	5960	14718
Link2	583	583	586
Link3	583	582	586
Link4	1548	1565	1606
Link5	583	415	586
Link6	583	582	586

Latency The packet latency is found as the time difference between the generated and the received data packet. Fig. 9 provides latency results for each link considering the given MAC scheduling schemes. Link1 has the lowest latency in all mobility profiles since it is associated with the priority node which sends data in consecutive superframes. In addition, the links having lower data generation rates generally seem to have higher latencies in all mobility scenarios. Latency is also dependent on the link quality as the links having poor SNR usually do not lead to successful packet receptions, resulting in higher latencies. Therefore, the links with lower PRRs for reference SmartBAN MAC schemes are observed to have higher latencies as well. For example, Link3 has the worst PRR performance in running posture which is reflected in its associated latency result as well. The latency for throughput and channel aware SmartBAN MAC is also no-

ticeably higher for Link2, Link3, Link5, and Link6 in sit-stand mobility scenario which can be traced back to their corresponding lower PRR values and lower data generation rates.

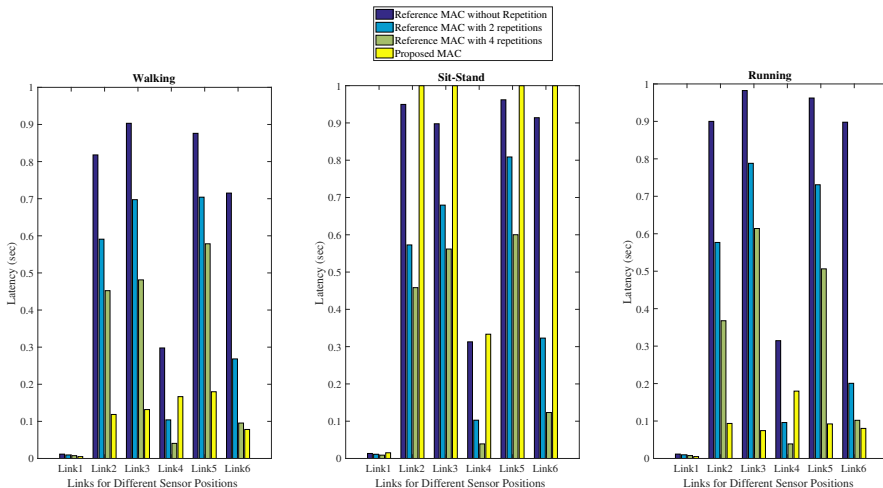


Fig. 9. Latency in seconds under: walking, sit-stand and running mobility profiles.

6 Conclusion

This paper provides an overview about the effectiveness of different SmartBAN MAC scheduling strategies considering PRR, energy consumption and latency as criteria. The conventional SmartBAN scheduled access MAC schemes with and without repetition as well as a throughput and channel aware dynamic MAC scheduling scheme are evaluated in this context for multiple on-body links. The simulation results in terms of PRR and energy consumption certainly recommend the dynamic scheduling, based on channel and data packet availability, for reliable and energy efficient data transmission.

References

1. Movassaghi, S., Abolhasan, M., Lipman, J., Smith, D., Jamalipour, A.: Wireless Body Area Networks: A Survey. *IEEE Commun. Surveys and Tutorials* **16**(3), 1658–1686 (2014)

2. IEEE Xplore Digital Library Homepage, <https://ieeexplore.ieee.org/document/6161600>. Last accessed 26 May 2018
3. Hamalainen, M., Paso, T., Mucchi, L., Girod-Genet, M., Farserotu, J., Tanaka, H., Chin, W. H., Ismail, L. N.: ETSI TC SmartBAN: Overview of the wireless body area network standard. In: Proc. IEEE 9th Int. Symp. on Medical Info. and Commun. Tech., pp. 1–5. IEEE, Japan (2015)
4. ETSI SmartBAN Homepage, http://www.etsi.org/deliver/etsi_tr/103300-103399/103394/01.01.01.60/tr_103394v010101p.pdf. Last accessed 26 May 2018
5. ETSI SmartBAN Homepage, http://www.etsi.org/deliver/etsi_ts/103300-103399/103326/01.01.01.60/ts_103326v010101p.pdf. Last accessed 26 May 2018
6. ETSI SmartBAN Homepage, http://www.etsi.org/deliver/etsi_ts/103300-103399/103325/01.01.01.60/ts_103325v010101p.pdf. Last accessed 26 May 2018
7. Khan, R., Alam, M. M.: Joint PHY-MAC Realistic Performance Evaluation of Body-to-Body Communication in IEEE 802.15.6 and SmartBAN. In: Proc. IEEE 12th Int. Symp. on Medical Info. and Commun. Tech., IEEE, Australia (2018)
8. Viittala, H., Mucchi, T., Hamalainen, M.: Performance of the ETSI SmartBAN System in the Interfered IEEE 802.15.6 Channel. In: Proc. IEEE 11th Int. Symp. on Medical Info. and Commun. Tech., pp. 15–18. IEEE, Portugal (2017)
9. Alam, M. M., Hamida, E. B.: Strategies for Optimal MAC Parameters Tuning in IEEE 802.15.6 Wearable Wireless Sensor Networks. *Journal of Medical Systems* **39**(9), 1–16 (2015)
10. Alam, M. M., Hamida, E. B.: Performance evaluation of IEEE 802.15.6 MAC for Wearable Body Sensor Networks using a Space-Time dependent radio link model. In: Proc. IEEE/ACS 11th Int. Conf. on Computer Systems and Applications (AICCSA), pp. 441–448. IEEE, Qatar (2014)
11. Alam, M. M., Arbia, D. B., Hamida, E. B.: Joint throughput and channel aware (TCA) dynamic scheduling algorithm for emerging wearable applications. In: Proc. IEEE Wireless Comm. and Networking Conf. (WCNC), pp. 1–6. IEEE, Qatar (2016)
12. Martelli, F., Buratti, C., Verdone, R.: On the performance of an IEEE 802.15.6 Wireless Body Area Network. In: Proc. 11th European Wireless Conference, pp. 1–6. IEEE, Austria (2011)
13. Alam, M. M., Hamida, E. B.: Towards Accurate Mobility and Radio Link Modeling for IEEE 802.15.6 Wearable Body Sensor Networks. In: Proc. 10th WiMob Conference, pp. 298–305. IEEE, Cyprus (2014)
14. Alam, M. M., Hamida, E. B., Arbia, D. B., Maman, M., Mani, F., Denis, B., D'Errico, R.: Realistic Simulation for Body Area and Body-To-Body Networks. *Sensors* **16**(4), art. 561 (2016)
15. Simon, M. K., Alouini, M. S.: *Digital Communication over Fading Channel*. 2nd edn. John Wiley & Sons Inc., New York (2005)
16. Ziong, F.: *Digital Modulation Techniques*. 2nd edn. Artech House Inc., London (2006)
17. Anane, R., Bouallegue, M., Raouf, K., Bouallegue, R.: Achieving Energy Efficient and Reliable Communication in WSN with Coded GMSK System under various Channel Conditions. In: Proc. IEEE Int. Conf. on Wireless Comm. and Mobile Computing, pp. 769–775. IEEE, Croatia (2015)
18. Alam, M. M., Hamida, E. B.: Surveying wearable human assistive technology for life and safety critical applications: standards, challenges and opportunities. *Sensors* **14**(5), 9153–9209 (2014)
19. Microchip Homepage, <https://www.mouser.com/ds/2/268/50002279A-515512.pdf>. Last accessed 29 May 2018

Appendix 4

R. Khan, M. M. Alam, T. Paso, and J. Haapola. Throughput and channel aware MAC scheduling for SmartBAN standard. *IEEE Access*, 7:63133–63145, 2019

Received March 31, 2019, accepted April 29, 2019, date of publication May 10, 2019, date of current version May 28, 2019.

Digital Object Identifier 10.1109/ACCESS.2019.2916159

Throughput and Channel Aware MAC Scheduling for SmartBAN Standard

RIDA KHAN¹, (Student Member, IEEE), MUHAMMAD MAHTAB ALAM¹, (Member, IEEE), TUOMAS PASO², AND JUSSI HAAPOLA², (Member, IEEE)

¹Thomas Johann Seebeck Department of Electronics, Tallinn University of Technology, 19086 Tallinn, Estonia

²Centre for Wireless Communications, University of Oulu, FI-90014 Oulu, Finland

Corresponding author: Rida Khan (rikhan@ttu.ee)

This work supported in part by the European Union's Horizon 2020 Research and Innovation Program under Grant 668995, in part by the European Union Regional Development Fund through the framework of the Tallinn University of Technology Development Program 2016–2022, in part by the Estonian Research Council under Grant PUT-PRG424, and in part by the Academy of Finland 6Genesis Flagship under Grant 318927.

ABSTRACT In this paper, a throughput- and channel-aware (TCA) medium access control (MAC) scheduling scheme is presented and evaluated for smart body area network (SmartBAN) standard, developed by the European Telecommunication Standard Institute (ETSI). The presented algorithm utilizes the radio link signal-to-noise ratio (SNR) to select the candidate nodes for a given time slot in the first phase, while, in the second phase, the slot is assigned to one of the chosen nodes based on their priority level and data packet availability. The algorithm uses an m-periodic scheduling technique, in which the nodes are considered for slot assignment according to their data packet generation rates during the second phase. Subsequently, a comprehensive explanation of the TCA algorithm execution through the slot reassignment method in SmartBAN is provided. For performance comparison, we use four key performance indicators (KPIs), which include packet reception rate (PRR), latency, energy consumption per successful transmission, and throughput. The simulation results indicate a significant performance gain of the SmartBAN-compliant TCA algorithm in terms of PRR and energy efficiency over the reference SmartBAN MAC scheduling with and without repetition. The average improvement in the PRR results is approximately 40%, whereas a maximum enhancement of 66% is observed in terms of energy efficiency while satisfying the throughput and latency requirements of the use case considered during simulations. Furthermore, we introduce some enhancements in the primary TCA to decrease the frequency of TCA execution via slot re-assignment frames transmission for reducing energy consumption, which results in a slight improvement of energy efficiency.

INDEX TERMS Energy consumption, enhanced TCA, latency, MAC, PRR, SmartBAN, TCA, throughput, WBAN.

I. INTRODUCTION

With the growing trends in ubiquitous networking and contemporary evolution in ultra-low-power wireless technologies, there have been significant research efforts dedicated to the utilization of wireless networks around human bodies. Wireless body area networks (WBANs) are the wearable monitoring systems, consisting of interconnected low-power and energy efficient tiny nodes such as sensors, actuators and coordinators for WBAN management, to realize numerous applications in the domain of health-care, athletic monitoring and training, public safety networks, and consumer electronics [1]–[3]. To deal with the

requirements set forth by WBAN applications, IEEE standards association came up with the first officially recognized operational guidelines, termed as IEEE 802.15.6 [4], for WBAN functioning. A low-complexity and flexible WBAN standard, known as SmartBAN, was introduced by European Telecommunication Standards Institute (ETSI). SmartBAN defines more efficient system specifications to facilitate faster initial set up times, hub-to-hub communication, better co-existence management and many additional features over IEEE 802.15.6 standard [5], [6].

The significant changes in the pathloss measurements of space-time varying WBAN channels result in a considerable degradation of error performance at low transmission power levels [7]. Due to human body shadowing, the packet reception rate (PRR) performance is shown to severely decrease for

The associate editor coordinating the review of this manuscript and approving it for publication was Tawfik Al-Hadhrami.

transmission power levels below -5 dBm and increased packet sizes [8]. At the physical (PHY) layer, SmartBAN provides the options for Bose-Chadhuri Hocquenghem (BCH) error correction codes and frame repetitions for enhanced error performance [9], [10]. In [11], authors highlight the importance of this repetition to get the acceptable 1% frame error rate under high interference scenario. But at very low transmission power and realistic WBAN channels, even the repetition was not able to achieve above 90% PRR.

A. RELATED WORK AND MOTIVATION

For mitigating the packet losses due to poor radio link quality, several channel variations-based dynamic medium access control (MAC) schemes have been proposed in the literature. Authors in [12] propose a scheduling algorithm which contemplates the success or failure status of packet transmissions using the two-state Gilbert's model of wireless links to improve the packet loss rate. Considering the context-specific temporal correlation properties of WBAN channels, authors in [13] determine the WBAN channel state during the upcoming transmission trials and suggest the variations in transmission power levels accordingly, resulting in improved energy consumption outcomes. BANMAC protocol in [14] first detects that whether the WBAN node is mobile or stationary. For nodes on the mobile limbs, the transmissions are made when the received signal strength (RSS) is likely to be higher whereas the remaining available time is used in transmissions from stationary nodes. In [15], a channel-aware polling-based MAC protocol for WBANs is presented in which the sensors are triggered for polling and packet transmission when the channel conditions become favorable. Since WBAN channel quality is also affected by the co-channel interference, therefore, authors in [16] suggest an interference avoidance algorithm which employs carrier sense multiple access with collision avoidance (CSMA/CA) between sources and relays and a flexible time division multiple access between relays and coordinator. The scheme allows low interfering nodes to send their messages using primary channel and the high interfering nodes double their contention windows coupled with the possible usage of a switched orthogonal channel. Using the correlation properties of the on-body links, a prediction-based dynamic relay transmission method is suggested in [17] in which WBAN relay transmissions are made depending upon the recently obtained channel states.

To sum up, the above mentioned research efforts primarily consider the channel characteristics of the WBAN links for dynamic MAC scheduling while either minimizing the energy consumption at higher PRR or providing better channel estimation to improve PRR performance. The emerging wearable applications have diverse data rate requirements for various sensor nodes [18] which constitute another important metric in dynamic MAC scheduling techniques. Addressing the data rate, energy efficiency and PRR performance requirements of WBAN applications, a joint throughput and channel aware dynamic scheduling algorithm is suggested

in [7]. The IEEE 802.15.6 complaint algorithm is shown to boost the PRR performance while maintaining the energy consumption levels substantially low. Motivated by these factors, this article thoroughly explores the implementation of SmartBAN-complaint joint throughput and channel aware (TCA) dynamic MAC scheduling algorithm. In TCA, first the channel conditions are examined for each scheduled access slot and later the data rate considerations of the selected nodes (with favorable radio link quality) are taken into account for slot assignments to a given node.

B. SUMMARY OF CONTRIBUTIONS

The fully-complaint execution of TCA with SmartBAN is based on the slot re-assignment operation defined in SmartBAN MAC [19] at alternate inter-beacon intervals (IBIs), followed by the acknowledgement of the updated slot assignments. In slot reassignment, the hub re-allocates the unused scheduled access slots to sensor nodes for efficiently utilizing the MAC resources [19]. Executing TCA this way comes with its own set of limitations in terms of PRR and throughput performance. For some on-body links under a certain mobility scenario (walking, sit-stand, running), the channel state may change from the moment slot re-assignment packet is sent until the updated assignments are actually executed which leads to a decrease in performance. In other words, the channel SNR conditions for few links under a given mobility change significantly fast and as a result the assigned slots to the nodes do not give good performance. Whereas for some WBAN links and mobility cases, the slot re-assignment for TCA execution is not required to be performed at the alternate IBIs due to relatively stable channel conditions. Based on this discussion, the key contributions for this article include:

- Implementation of TCA MAC algorithm in full compliance with the SmartBAN standard. TCA improves the error performance of reference SmartBAN MAC by scheduling and re-allocating time slots to certain nodes when their channel conditions are favorable. But performing slot reassignment at alternate IBIs leads to an increase in overall energy consumption. However the energy used up this way is utilized in successful data packet receptions, thus enhancing the overall energy efficiency.
- Presentation of results for the SmartBAN complaint TCA algorithm in terms of four key performance indicators (KPIs), i.e., PRR, Latency, Throughput and energy consumption evaluation against reference SmartBAN MAC with and without repetitions. Moreover, both the reference SmartBAN MAC and SmartBAN complaint TCA are compared in terms of all these KPIs with respect to varying transmission power levels. A comprehensive analysis of the PRR, energy consumption, latency and throughput results generated this way, is given in Table 3.
- Since the baseline TCA execution may increase the overall energy consumption by performing slot reassignments at alternate IBIs, therefore the third contribution

includes the proposal of an enhanced TCA MAC algorithm. Enhancing the TCA execution only when the channel SNR severely degrades or when the packet status at the sensor nodes changes, improves the energy consumption profile by lowering the frequency of slot reassignments. A performance comparison of the generic and enhanced TCA is also given, taking PRR and energy consumption as the evaluation metrics.

The remainder of the paper is arranged as given. Section II presents the detailed description of the reference SmartBAN MAC characteristics while Section III explains the TCA algorithm basics, TCA execution in SmartBAN and the enhancements in the TCA algorithm. Section IV describes the systems model and parameters used in simulation setup. The section also discusses the simulation results for the given KPIs under different mobilities. Finally, concluding remarks are provided in Section V.

II. SMARTBAN MAC SPECIFICATIONS

This section provides a detailed explanation about the reference SmartBAN MAC superframe format MAC details with and without repetition in scheduled access mode. Additionally the slot-reassignment method in SmartBAN MAC is also given.

A. REFERENCE SMARTBAN MAC WITHOUT REPETITION

The data channel used for packet transmission between the coordinator and sensor nodes is partitioned into IBIs. A data channel beacon (D-Beacon) marks the IBI beginning, followed by scheduled access period for data transmissions by sensor nodes and the corresponding data packet acknowledgements. Management and control signaling by hub and/or sensor nodes is communicated in control and management (C/M) period and the entire IBI duration ends with an inactive period [19], [20]. Every scheduled access slot consists of physical-layer protocol data unit (PPDU) transmissions and PPDU acknowledgements with inter-frame spacing (IFS) in between. MAC frame body contains the actual payload, that along with MAC header and frame parity creates a MAC protocol data unit (MPDU). For uncoded transmissions, the resultant MPDU becomes physical-layer service data unit (PSDU). PSDU, after the addition of physical-layer convergence protocol (PLCP) header and preamble, constitutes a complete PPDU [19], [20]. The entire IBI duration is made of beacon duration, time slot duration and the number of time slots in scheduled access period, time slot duration and the number of time slots in control and management period and the duration of inactive period, as depicted in Fig. 1. The duration of each time slot in the entire IBI is found according to a pre-defined parameter L_{Slot} [19], as follows

$$T_{Slot} = T_{min} \times L_{Slot}, \quad (1)$$

where T_{min} is the minimum slot duration defined in SmartBAN MAC specifications [19]. Beacon period, scheduled access period, control and management period and inactive

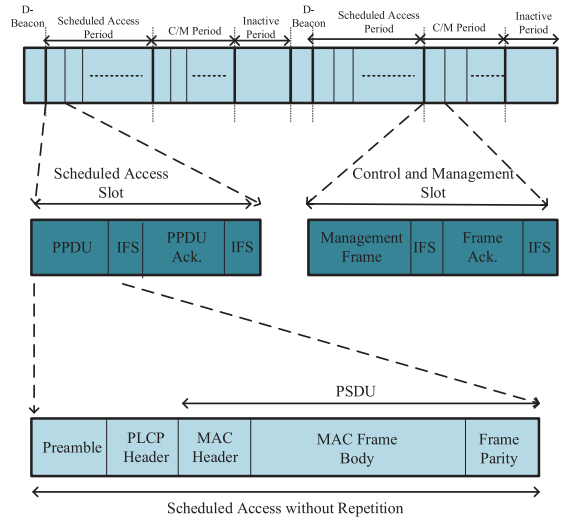


FIGURE 1. Reference smartBAN MAC without repetition.

period are made of the identical slot duration T_{Slot} throughout the IBI.

During the scheduled access period of each time slot, there is acknowledgement and IFS duration as well [19]. IFS duration is fixed and the duration for acknowledgement is computed as

$$T_{Ack} = \frac{N_{preamble} + N_{PLCP} + N_{par} + N_{MAC}}{R_{Sym}}, \quad (2)$$

where $N_{preamble}$, N_{PLCP} , N_{par} and N_{MAC} are the number of bits in physical-layer preamble, PLCP header, MAC frame parity and MAC frame header respectively. After the calculation of T_{Ack} , the effective duration for PPDU transmission becomes

$$T_{Tx} = T_{Slot} - T_{Ack} - 2 \times T_{IFS}. \quad (3)$$

After finding T_{Tx} , the maximum allowed MAC frame body size for uncoded MPDU can be found as

$$Payload = T_{Tx} \times R_{Sym} - N_{preamble} - N_{PLCP} - N_{par} - N_{MAC}. \quad (4)$$

In scheduled access duration, all the sensor nodes are assumed to have their respective time slots pre-assigned by hub and the mandatory C/M period is also present within IBI. For applications with diverse data rate requirements, it becomes inefficient for sensor nodes to wake up at every IBI for data transmission, therefore, the low rate nodes are assumed to employ m-periodicity in which they only wake up for transmission when data is available, and remain in the sleep mode otherwise.

B. REFERENCE SMARTBAN MAC WITH REPETITION

In scheduled access mode with repetition, the sensor node repeats the PPDU transmission within the assigned time slot. This alters the effective PPDU transmission time as under

$$T_{Tx} = \frac{T_{Slot} - T_{Ack} - 2 \times T_{IFS}}{REP}, \quad (5)$$

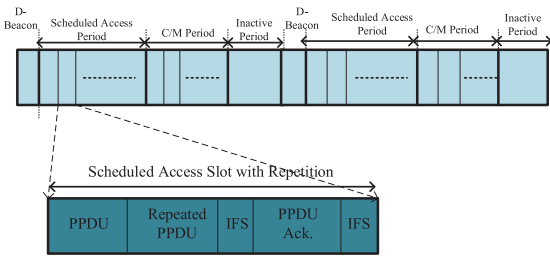


FIGURE 2. Reference smartBAN MAC with repetition.

where REP is the number of times a PPDU is repeated. The effective payload size is also reduced, as per (4), which results in more frequent transmissions by sensor nodes to send the same amount of data. SmartBAN proposes two and four repetitions for improving the error performance [9] but it leads to the reduced amount of transmitted payload in a given duration, lowering the effective throughput. The rest of the IBI operation in scheduled access MAC with repetition is similar to the reference SmartBAN MAC without repetition and is illustrated in Fig. 2.

C. SLOT REASSIGNMENT

Slot reassignment operation in SmartBAN is performed to inform sensor nodes of their newly allocated slots in scheduled access duration. In order to perform slot reassignment, the hub indicates in D-Beacon about the execution of slot reassignment during the C/M period and the list of nodes for which slot re-assignment would be performed. The hub then sends slot reassignment frame in the C/M period with the highest level user priority employing the slotted ALOHA channel access mechanism. The procedure is repeated again in the next IBI if the transmission of slot reassignment frame fails in the current IBI. The slot reassignment frame contains the timing information specifying the starting and ending time slot allocated to the node. The nodes, upon successful reception of slot re-assignment frame during the C/M period, acknowledge hub in the MAC header of the data frame during the following IBI. The complete procedure of slot

reassignment in SmartBAN is depicted in Fig. 3. The new slot allocation comes into practice for data transmission by nodes in the next IBI, making the slot reassignment procedure take at least two IBIs to be completed.

III. THROUGHPUT AND CHANNEL AWARE MAC

This section elaborates TCA basics, details of the TCA execution in SmartBAN and enhancements within the existing TCA algorithm.

A. TCA DESCRIPTION

TCA algorithm is based on the principle of m-periodic scheduling recommended by IEEE 802.15.6 standard. In m-periodic allocation, time slots within the scheduled access duration are assigned based on the data generation rates of individual sensor nodes. Therefore, high rate or emergency nodes can be defined as the priority nodes which are assigned time slots at consecutive IBIs while low data rate nodes are assigned scheduled access slots m-periodically only when they have data packets to send [7]. This concept of m-periodic allocation is exploited in TCA mechanism, along with the information about the channel conditions between coordinator and sensor nodes. TCA algorithm comprises of two main steps; slot allocation based on the WBAN link SNR conditions and a final slot assignment based on m-periodicity.

The input of the algorithm consists of the estimated pathloss values, transmission power and noise power. In this paper, the deterministic pathloss values are used which are obtained from the experimental traces of the motion capture system and biomechanical modeling [21] as one of the inputs. The obtained pathloss is used for the computation of signal-to-noise ratio (SNR) threshold for the first step. For defining the SNR threshold during the first phase, a packet error rate (PER) value of 0.1 is considered to acquire the PRR above 90% and reverse radio link computations are made to obtain the corresponding SNR threshold [21]. For the required PER value of 0.1, the resultant bit error rate (BER) value is computed using the relation $PER = 1 - \left(1 - P_e \left(\frac{E_b}{N_0}\right)\right)^N$, where N is the packet size in bits, which subsequently provides $\frac{E_b}{N_0}$ after being evaluated in

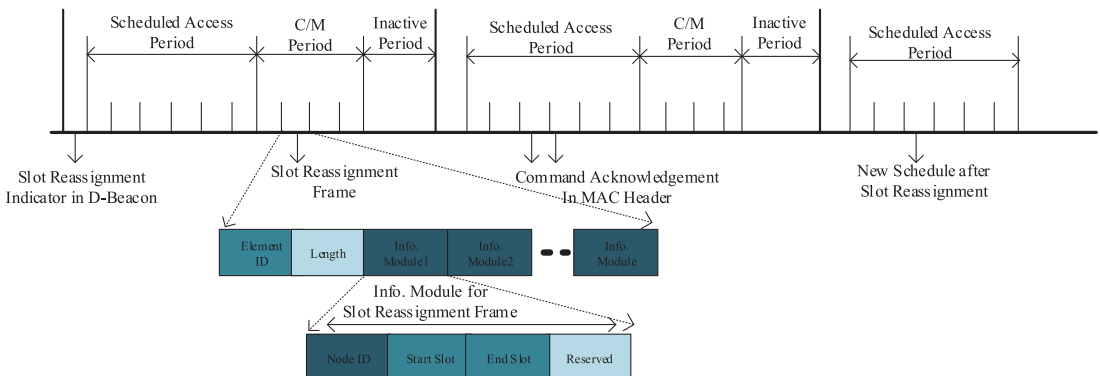


FIGURE 3. Slot reassignment operation in smartBAN.

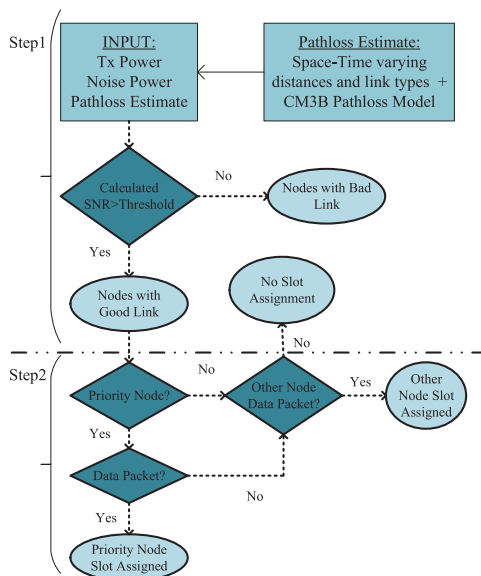


FIGURE 4. Throughput and channel aware MAC algorithm.

the BER expression. SmartBAN defines Gaussian frequency shift keying (GFSK) modulation at the physical layer [9], therefore the corresponding BER expression will be used for $\frac{E_b}{N_0}$ computations. The required SNR can be obtained using the equation $\frac{E_b}{N_0} [dB] = SNR [dB] + 10 \times \log_{10} \left(\frac{BW}{R} \right)$, where BW is 2MHz channel bandwidth and R is 1MSymbols/s information rate, specified for SmartBAN [9]. The pertinent SNR threshold found for TCA execution in SmartBAN using this method is 7dB or higher for a packet length of 86 bytes in order to obtain a PRR above 90%.

During the first step, the SNR conditions of each time slot are checked for every node-hub link and if the link SNR is greater than the pre-defined threshold value, the node is considered as a candidate node for slot assignment in the next step. The resulting set of sensor nodes, in the second step, is checked for priority node and if priority node is among the candidate sensor nodes with data packet available, it is allocated the given time slot. If priority node does not have good SNR conditions at the radio link or is already allocated the slot, other low priority nodes are assigned the given slot based on their data packet status. The flow chart representation of TCA algorithm is shown in Fig. 4.

B. TCA EXECUTION IN SMARTBAN

A reasonable way of executing TCA in SmartBAN is the implementation of slot reassignment operation at the alternate IBIs. Initially, the hub checks the SNR conditions between itself and the sensor nodes for the given time slot in the scheduled access period and finds the most suitable candidate nodes for packet transmission, with their link-SNR values greater than the per-defined threshold. Depending upon the channel state and data packet availability of the

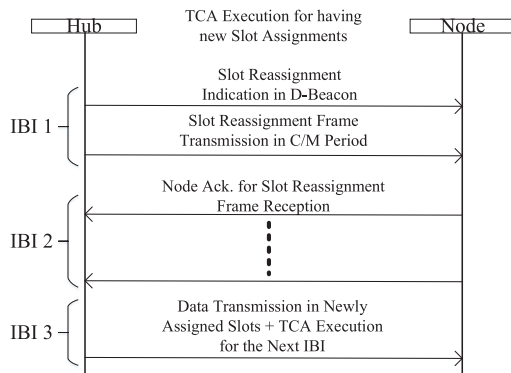


FIGURE 5. TCA execution in smartBAN.

candidate nodes, the given slot is allocated to one of the sensor nodes. Based on TCA algorithm, a list of the assigned slots is created for all the nodes present in WBAN. At the beginning of each IBI in D-Beacon, hub sends the information about the possible slot reassignment operation during the C/M period. Later in the C/M period, hub sends slot reassignment frames to all the nodes that are meant to perform packet transmission. If the hub fails to send slot reassignment frame within the current IBI, it attempts to perform the slot reassignment for TCA scheduling in the successive IBI. All the sensor nodes which receive slot reassignment frame perform mandatory command acknowledgement via MAC header in the scheduled access period of the following IBI. The new slot assignment, as suggested by coordinator, comes into operation in the next IBI while the coordinator simultaneously analyzes the current WBAN link SNR conditions to perform the TCA scheduling via slot reassignment method again. Fig. 5 summarizes the details of the TCA execution and the related frame exchange in SmartBAN. This way TCA algorithm can be carried out by sending the slot reassignment frames at the most in the alternate IBIs.

C. ENHANCED TCA FOR SMARTBAN

The conventional TCA scheme mentioned in sub-section III-B proposes the slot reassignment performed at every alternate IBI after creating the list of assigned slots using TCA algorithm. The recurrence of slot reassignment at alternate IBIs can be decreased by executing TCA only when required, depending upon the channel conditions and the packet availability of the previous slot assignments. Therefore, the enhanced TCA algorithm consists of the following main steps before carrying out the slot reassignment at alternate IBIs

- At first, hub checks that whether TCA was executed and a slot reassignment frame was sent in the preceding IBI or not since TCA execution through slot reassignment is not possible at the consecutive IBIs. If TCA execution was carried out in the last IBI, the algorithm stops and repeats the same procedure during the next IBI, else the algorithm proceeds to the next step.

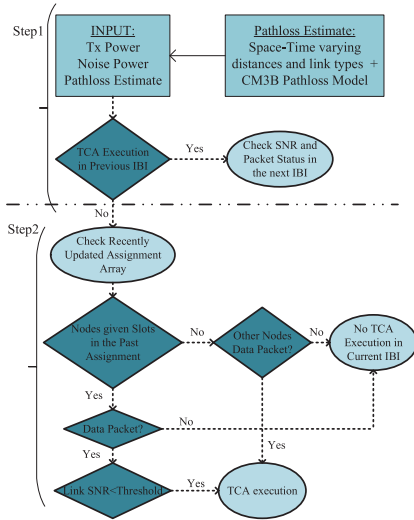


FIGURE 6. Enhanced TCA modifications.

- The hub checks the past assignment array having the details of the assigned slots to sensor nodes. The hub executes the generic TCA and implements slot reassignment if i) SNR values of all the nodes in the previous assignment array, having data packet to send, go below the pre-defined threshold for the current IBI. OR ii) some other sensor node, not included in the past assignment array, has data packet to send. Otherwise the next IBI is checked for possible changes in the channel conditions of the hub-node links or packet status of the sensor nodes.

Fig. 6 summarizes the modifications done in TCA algorithm for performance enhancements.

IV. PERFORMANCE EVALUATION

This section, at first, describes the inherent system model and the simulation parameters utilized in performance evaluation of various WBAN applications. Then a comprehensive analysis of the acquired simulation results, in terms of PRR, energy consumption per successful transmission and latency, is presented.

A. SYSTEM MODEL

The system model to provide PHY-MAC performance analysis consists of mobility modeling for dynamic links generation, channel models for finding realistic pathloss values, and radio link modeling. Bio-mechanical mobility modeling, as suggested in [21], provides space-time varying distances and link types, classified as line of sight (LOS) or non-line of sight (NLOS), between sensor nodes and the central hub. Both the dynamic distances and link types serve as inputs to generate pathlosses for dynamic mobility scenarios.

In order to compute pathloss values for space-time varying distances and link types, IEEE 802.15.6 proposed CM3-B

TABLE 1. Simulation setup parameters. [9], [19], [25].

RF Parameters	
Transmitter Power (dBm)	-10.9, -6.9, -2.5
Receiver Sensitivity (dBm)	-92.5
Current Consumption Tx (mA)	15, 15.9, 17.6
Current Consumption Rx (mA)	16
Bandwidth per channel (MHz)	2
Receiver Sensitivity (dBm)	-92.5
Information Rate (kbps)	1000
PHY/MAC Parameters	
Minimum slot length (T_{min})	625 μ s
Slot duration (T_{SLOT})	1.25ms
Interframe spacing (IFS)	150 μ s
Symbol Rate (R_{Sym})	10 ⁶
MAC header (N_{MAC})	7 octets
Frame Parity (N_{par})	2 octets
PLCP header (N_{PLCP})	5 octets
PLCP Preamble ($N_{preamble}$)	2 octets

channel model [22] is used. An additional NLOS term of 13% is added to the calculated pathloss value for the NLOS categorized links. Radio link modeling involves the successive computations of SNR, bit energy-to-noise ratio, BER and PER from the obtained realistic pathlosses [21].

GFSK modulation, with the bandwidth-bit period product BT and modulation index h of 0.5, is used at the physical layer described by SmartBAN [9]. Frequency shift keying modulation becomes minimum shift keying modulation for $h = 0.5$ [23] and therefore, the corresponding BER expression becomes

$$P_e \left(\frac{E_b}{N_0} \right) = Q \left(\sqrt{2\epsilon \frac{E_b}{N_0}} \right), \quad (6)$$

where $\frac{E_b}{N_0}$ is signal-to-noise ratio for a bit, ϵ is a constant and for BT of 0.5, equals 0.79 [24]. Further details about the radio link modeling performed in this paper are given in [21]. For obtaining BER with repetition, SNR is found according to the diversity technique employed at the receiver. We assume maximal ratio combining (MRC) diversity scheme for assessing the maximum achievable gain that SmartBAN can provide with repetition. In MRC, the instantaneous SNRs of individual transmissions are directly added if statistically independent transmission channels are assumed [23].

B. SIMULATION SETUP

The parameters considered in the simulation setup are summarized in Table 1. We evaluate the performance at three different transmission power levels of -10.9 dBm, -6.9 dBm and -2.5 dBm, defined for RN4020 Bluetooth low energy (BLE) devices [25]. For three distinct mobility patterns, which include walking, sit-stand and running, $L_{SLOT} = 2$ is assumed to give T_{Slot} in all the simulations. From the calculations performed according to (1), T_{SLOT} equals 1.25ms.

For the performance assessment of the reference SmartBAN as well as TCA scheduled access mechanisms, we consider precise athlete monitoring application scenario, as given in Table 2, along with the sensor node data rate requirements. In precise athlete monitoring application scenario, hub is located on the right shoulder, ECG and respiratory nodes

TABLE 2. Use case scenario for performance evaluation. [5], [26]–[28].

Precise Athlete Monitoring	
Sensor Type	Required Data Rates (kbps)
ECG (1 node)	6-48
IMU (4 nodes)	4.8-35
Respiratory Rate (1 node)	0.24-0.8
Sensor Placement	
Sensor Type	Location
ECG	Chest
IMU1	Left elbow
IMU2	Right elbow
IMU3	Left knee
IMU4	Right knee
Respiratory Rate	Upper chest

are respectively placed on the lower and upper chest and four IMU sensors are positioned on left and right, knees and elbows. In the reference SmartBAN MAC, ECG node sends packets at every IBI due to its potentially high data rate requirement while IMU and respiratory node may transmit data after a few IBIs and remain in sleep mode for energy preservation because of their relatively low data rate specifications. However, for reference SmartBAN MAC with repetition, these low rate nodes make transmissions more often to accommodate their throughput requirements. TCA MAC performs slot assignments depending upon the channel conditions as well as the sensor nodes packet generation rates and transmissions are made only when both scheduling factors are in agreement. For all scheduling scenarios, we assume mandatory scheduled access and C/M periods with an IBI duration on 11.25ms, resulting in the transmission of 88 IBIs per second.

C. SIMULATION RESULTS

We define the KPIs for performance evaluation, mentioned in sub-section IB, as under

- PRR, for each sensor node, is the ratio of successfully decoded packets and the total number of packets transmitted by each node throughout the trace duration.

- Latency is the amount of time elapsed between the data packet generation at a particular node and its successful reception at coordinator.
- We define the total energy consumed as the summation of energy utilized during transmission and reception at the circuitry as well as the amplifier, according to the energy consumption model given in [29]. For sensor nodes, energy consumption per successful transmission becomes $\frac{E_i}{n_i}$, where E_i is the total energy consumed at node i and n_i is the number of successful transmissions made by the particular node. In case of hub, the energy consumption equals $\frac{E_h}{n_{total}}$, where E_h is the total energy utilized by hub and n_{total} is the total number of successful transmissions made by all sensor nodes.
- The attained throughput is defined as the number of bits successfully transmitted by a node per second, and can be written as $\frac{n_i \times N}{T_{IBI} \times n_{IBI}}$, where T_{IBI} is complete IBI duration in seconds and n_{IBI} is the number of IBIs elapsed throughout the trace file.

1) SIMULATION RESULTS FOR SMARTBAN COMPLAINT TCA

Fig. 7 sums up the PRR results for each link between different sensor nodes and the hub, under walking, sit-stand and running mobility scenarios at -10.9dBm transmission power. Link1, link2, link3, link4, link5 and link6 respectively correspond to the nodes placed on chest, left knee, right knee, left elbow, right elbow and upper chest. Under walking scenario, TCA scheduling in SmartBAN outperforms the reference SmartBAN MAC schemes with and without repetition due to link SNR-based appropriate slot assignment for all the WBAN links. Despite using packet repetitions with MRC combining, a considerable improvement in performance is not observed because of repeated data transmission under poor channel conditions. The similar remarks can be made about the PRR performance under running scenario. The related mobility and body shadowing due to posture changes under walking and running scenarios severely

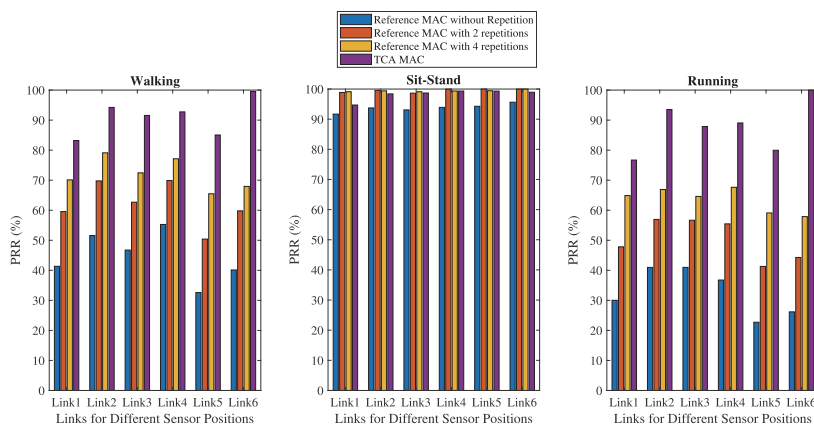


FIGURE 7. Packet reception rate (PRR) (%) under: Walking, sit-stand, and running mobility profiles.

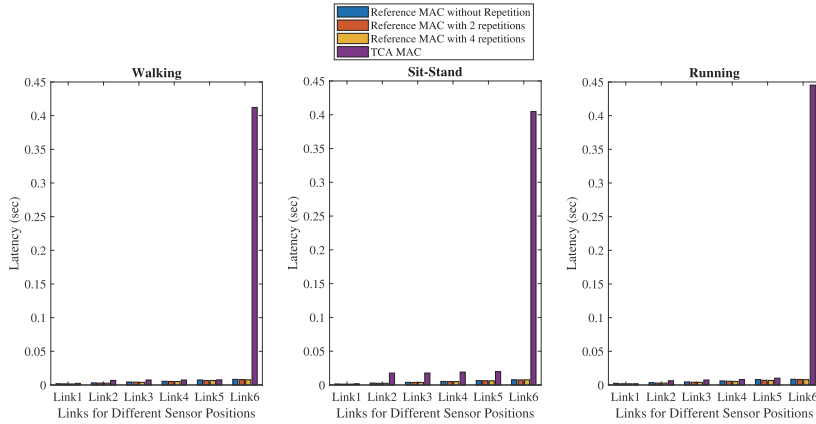


FIGURE 8. Latency (sec) under: Walking, sit-stand, and running mobility profiles.

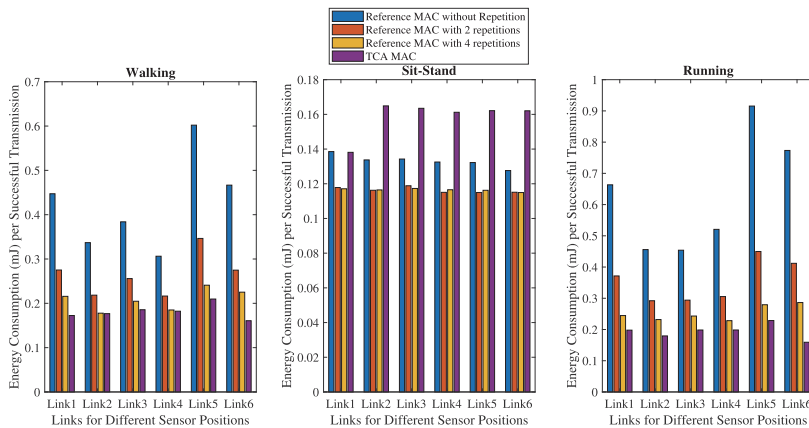


FIGURE 9. Energy consumption per successful transmission (mJ) under: Walking, sit-stand, and running mobility profiles.

degrades the PRR performance. However, SmartBAN reference MAC scheduling gives good performance under sit-stand posture for all the links due to reduced mobility. On average under walking conditions, SmartBAN compliant TCA gives a respective PRR performance gain of about 40%, 25% and 12% over the reference SmartBAN without repetition, SmartBAN MAC with 2-repetitions and 4-repetitions. The similar trends in performance enhancement can be seen under running mobility scenario.

Fig. 8 summarizes the latency results for each link under the given mobility conditions at -10.9dBm transmission power. TCA, being based on the concept of m-periodicity and sensor node packet generation rates, compromises the latency metric while still not exceeding the maximum allowable latency limits of 125ms, mentioned under SmartBAN standard [5]. This is evident from the results provided in Fig. 8. The latency outcomes for links 1-5 do not increase more than the latency limits of few tens of milliseconds under all

mobility conditions. But for link6, which corresponds to the respiratory rate node with a single packet generated per second, the latency is increased but is still under the given latency requirements of the respiratory rate application. However, TCA MAC does not meet the 125ms latency constraints of SmartBAN standard for respiratory rate application. Additionally, link1 has the lowest latency for all the scheduled techniques in all mobility profiles since it is associated with the priority node which makes transmissions in consecutive IBIs.

Fig. 9 and Fig. 10 depict the energy consumption profile for various links and the hub respectively, under the given mobility scenarios at -10.9dBm transmission power. Energy consumption during **transmission**, for **sensor** node mainly includes, i) data packet transmission energy and ii) slot reassignment acknowledgement transmission energy in case of TCA MAC. For **hub**, the transmission energy consists of i) D-Beacon ii) data packet acknowledgement and

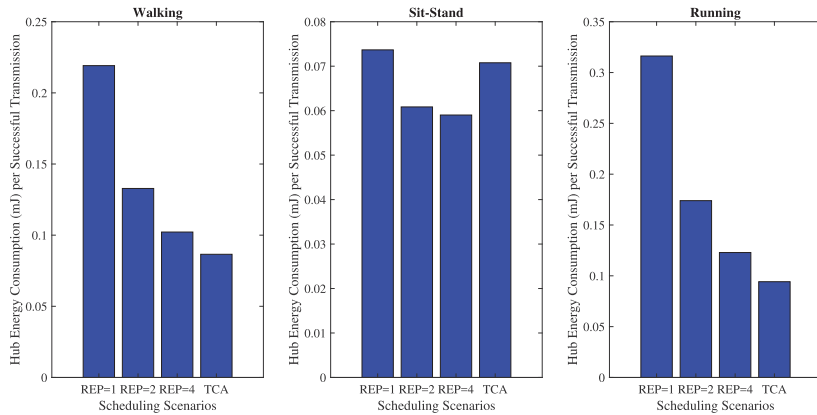


FIGURE 10. Hub energy consumption per successful transmission (mJ) under: Walking, sit-stand, and running mobility profiles.

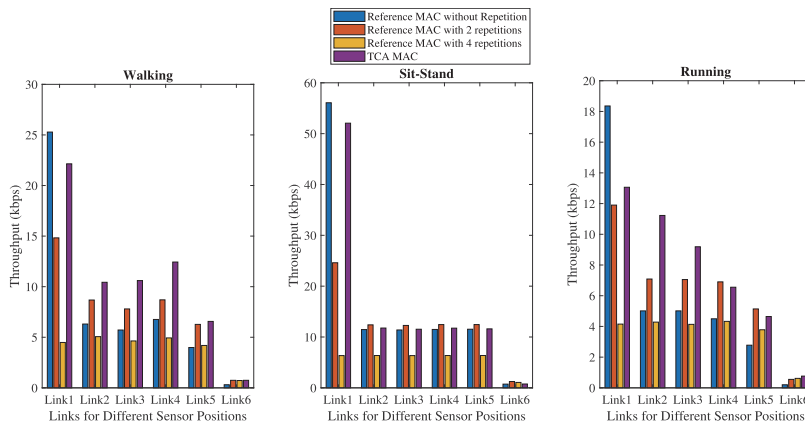


FIGURE 11. Throughput (kbps) under: Walking, sit-stand, and running mobility profiles.

iii) slot reassignment frame transmission energy in case of TCA MAC. During the **reception**, the corresponding energy consumption for **sensor** and **hub** respectively becomes i) D-Beacon ii) data packet acknowledgement iii) slot reassignment frame reception energy in case of TCA MAC and i) data packet reception energy and ii) slot reassignment acknowledgement reception energy in case of TCA MAC. This could increase the overall energy consumption for TCA MAC in SmartBAN but the energy is actually utilized in the successful transmissions of data packets. TCA scheduling in SmartBAN has overall higher energy consumption but due to the higher rate of successful packet reception, the energy consumption per successful transmission is significantly reduced under walking and running scenarios. Under sit-stand mobility, a good PRR performance was observed even with the reference SmartBAN MAC, and therefore this metric increases for TCA due to the unnecessary transmission of slot reassignment frames by the coordinator and their

reception by the sensor nodes. TCA MAC reduces the energy consumption by 50% and 60% on average as compared to the reference MAC with no repetitions under walking and running mobility scenarios respectively. For 4-repetitions, the increase in energy efficiency is not very evident because of the resulting higher PRR, as shown in Fig. 7, however, this could decrease the attained throughput at the sensor nodes, as will be investigated later. TCA also decreases the energy consumption at the hub by 60% and 66% in comparison with the reference MAC with no repetitions under walking and running conditions respectively.

Fig. 11 illustrates the attained throughput results for various sensor nodes under the given mobility conditions at -10.9dBm transmission power. TCA slightly decreases the throughput as compared to the reference SmartBAN with no repetitions for link1 (corresponding to the priority node) because of the selective transmissions under good channel conditions only. The obtained throughput for link1 is fairly

TABLE 3. Performance evaluation results with respect to transmission power levels.

Mobility	Tx Power (dBm)	Hub Energy (mJ)				Link	Node Energy (mJ)				PRR (%)	Latency (ms)				Throughput (kbps)			
		R1	R2	R4	TCA		R1	R2	R4	TCA		R1	R2	R4	TCA	R1	R2	R4	TCA
Walking	-2.5	0.17, 0.14, 0.13, 0.17	1	0.61, 0.54, 0.52, 0.57	92.4, 97.8, 99.3, 95.8	1.5, 1.3, 1.3, 1.7	56.5, 24.3, 6.36, 53.9												
			2	0.56, 0.52, 0.51, 0.64	96.9, 99.3, 99.9, 98.3	2.7, 2.5, 2.5, 6.5	11.8, 12.3, 6.39, 21.8												
			3	0.57, 0.53, 0.52, 0.64	95.7, 99, 99.3, 98.6	4.1, 3.8, 3.8, 6.7	11.7, 12.3, 6.35, 21.1												
			4	0.58, 0.53, 0.52, 0.65	94.3, 98.9, 99, 98	5.2, 5, 5, 7.3	11.5, 12.3, 6.3, 21.8												
			5	0.61, 0.53, 0.52, 0.65	93.1, 98.7, 99.5, 98	6.6, 6.3, 6.3, 8.1	11.3, 12.3, 6.3, 20.4												
			6	0.6, 0.53, 0.51, 0.62	93.5, 98.9, 99.9, 100	7.8, 7.5, 7.5, 418.4	0.71, 1.2, 1.06, 0-6												
	-6.9	0.16, 0.1, 0.08, 0.11	1	0.44, 0.28, 0.25, 0.3	67, 88.2, 92.9, 86.2	1.9, 1.5, 1.3, 2.2	40.9, 21.9, 5.9, 34.5												
			2	0.35, 0.25, 0.23, 0.32	77.7, 92.4, 96.3, 92.1	3, 2.7, 2.6, 6.6	9.5, 11.5, 6.1, 16.4												
			3	0.4, 0.28, 0.24, 0.32	70.9, 88.3, 94.9, 91.9	4.3, 4, 3.9, 7.5	8.6, 10.9, 6.07, 16.8												
			4	0.36, 0.27, 0.24, 0.32	75.7, 89.9, 95.2, 92.2	5.4, 5.2, 5.1, 7.3	9.3, 11.1, 6.09, 16.5												
			5	0.49, 0.3, 0.25, 0.32	62.8, 85.1, 92.7, 92.5	7.2, 6.5, 6.4, 8.5	7.6, 10.6, 5.9, 12.6												
			6	0.45, 0.29, 0.25, 0.28	65.3, 85.7, 92.8, 99.3	7.9, 7.8, 7.7, 0.42	0.5, 1.06, 0.99, 0.75												
	-10.9	0.21, 0.13, 0.1, 0.086	1	0.44, 0.27, 0.21, 0.17	41.4, 59.3, 70.1, 83.2	1.9, 1.6, 1.5, 2.4	25.3, 14.7, 4.48, 22.1												
			2	0.33, 0.21, 0.17, 0.17	51.8, 69.9, 79.2, 94.2	3.1, 2.9, 2.7, 6.8	6.3, 8.7, 5.07, 10.4												
			3	0.38, 0.25, 0.2, 0.18	47.1, 62.8, 72.4, 91.4	4.5, 4.2, 4, 7.4	5.7, 7.8, 4.63, 10.6												
			4	0.3, 0.21, 0.18, 0.18	54.9, 69.7, 77.1, 92.8	5.5, 5.3, 5.2, 7.4	6.7, 8.6, 4.93, 12.4												
			5	0.59, 0.35, 0.24, 0.21	32.8, 50.2, 65.5, 84.8	7.4, 6.8, 6.7, 7.6	4, 6.2, 4.19, 6.5												
			6	0.46, 0.28, 0.22, 0.16	40.4, 58.7, 67.7, 99.3	8, 8, 7.7, 412.9	0.3, 0.73, 0.72, 0.74												
Sit-Stand	-2.5	0.15 0.14 0.13 0.15	1	0.51, 0.51, 0.51, 0.52	100, 100, 100, 100	1.3, 1.3, 1.3, 1.3	61.1, 24.8, 6.4, 61.1												
			2	0.51, 0.51, 0.51, 0.62	100, 100, 100, 100	2.5, 2.5, 2.5, 16.9	12.2, 12.4, 6.4, 12.2												
			3	0.51, 0.51, 0.51, 0.62	100, 100, 100, 100	3.8, 3.8, 3.8, 18.1	12.2, 12.4, 6.4, 12.2												
			4	0.51, 0.51, 0.51, 0.62	100, 100, 100, 100	5, 5, 5, 19.4	12.2, 12.4, 6.4, 12.2												
			5	0.51, 0.51, 0.51, 0.62	100, 100, 100, 100	6.3, 6.3, 6.3, 20.6	12.2, 12.4, 6.4, 12.2												
			6	0.51, 0.51, 0.51, 0.62	100, 100, 100, 100	7.5, 7.5, 7.5, 0.4	0.76, 1.2, 1.06, 0.76												
	-6.9	0.08 0.08 0.076 0.089	1	0.22, 0.22, 0.22, 0.23	99.2, 100, 100, 99.3	1.3, 1.3, 1.3, 1.3	60.7, 24.8, 6.4, 60.7												
			2	0.22, 0.22, 0.22, 0.28	99.3, 100, 100, 100	2.5, 2.5, 2.5, 16.8	12.1, 12.4, 6.4, 12												
			3	0.22, 0.22, 0.22, 0.28	99.2, 100, 100, 100	3.8, 3.8, 3.8, 18	12.1, 12.4, 6.4, 12												
			4	0.22, 0.22, 0.22, 0.28	99.3, 100, 100, 100	5, 5, 5, 19.2	12.1, 12.4, 6.4, 12.2												
			5	0.22, 0.22, 0.22, 0.28	99.4, 100, 100, 100	6.3, 6.3, 6.3, 20.5	12.1, 12.4, 6.4, 12.2												
			6	0.22, 0.22, 0.22, 0.28	98.9, 100, 100, 98.9	7.5, 7.5, 7.5, 0.404	0.75, 1.2, 1.06, 0.756												
	-10.9	0.07, 0.06, 0.06, 0.07	1	0.13, 0.11, 0.11, 0.13	91.6, 98.8, 99.1, 94.8	1.5, 1.3, 1.3, 1.8	56, 24.6, 6.34, 52.1												
			2	0.13, 0.11, 0.11, 0.16	93.7, 99.6, 99.4, 98.4	2.9, 2.5, 2.5, 17.5	11.4, 12.4, 6.36, 11.7												
			3	0.13, 0.11, 0.11, 0.16	92.7, 98.6, 99.1, 98.6	4, 3.8, 3.8, 17.7	11.3, 12.3, 6.34, 11.5												
			4	0.13, 0.11, 0.11, 0.16	93.9, 99.9, 99.3, 99.3	5.3, 5, 5, 19.1	11.5, 12.4, 6.36, 11.7												
			5	0.13, 0.11, 0.11, 0.16	93.8, 100, 99.4, 99.3	6.5, 6.3, 6.3, 19.9	11.4, 12.4, 6.36, 11.6												
			6	0.12, 0.11, 0.11, 0.16	96, 100, 100, 98.9	7.7, 7.5, 7.6, 404.6	0.73, 1.2, 1.06, 0.756												
Running	-2.5	0.17, 0.14, 0.13, 0.17	1	0.55, 0.51, 0.51, 0.54	97.6, 100, 100, 99.1	1.6, 1.3, 1.3, 1.7	59.7, 24.8, 6.4, 52.9												
			2	0.56, 0.51, 0.51, 0.63	97.3, 100, 100, 99.2	2.9, 2.5, 2.5, 6.3	11.9, 12.4, 6.4, 21.9												
			3	0.56, 0.52, 0.51, 0.63	96.8, 98.9, 99.9, 99.5	4, 3.8, 3.8, 7.1	11.8, 12.3, 6.4, 21.9												
			4	0.6, 0.52, 0.51, 0.62	93.5, 99.1, 100, 99.9	5.3, 5.1, 5, 8.3	11.4, 12.3, 6.4, 22.4												
			5	0.66, 0.53, 0.51, 0.64	88.6, 98.4, 100, 98.6	6.6, 6.4, 6.3, 8.2	10.8, 12.2, 6.4, 18.3												
			6	0.64, 0.55, 0.53, 0.62	90.1, 97, 98.4, 100	7.8, 7.6, 7.5, 0.44	0.69, 1.2, 1.04, 0.764												
	-6.9	0.18, 0.1, 0.086, 0.12	1	0.51, 0.27, 0.23, 0.32	61.5, 89.9, 96.7, 83.4	2.3, 1.6, 1.3, 3	37.6, 22.3, 6.18, 29.7												
			2	0.44, 0.29, 0.24, 0.3	67.7, 86.4, 95.6, 95.6	3.2, 2.7, 2.7, 6.5	8.3, 10.7, 6.12, 16.6												
			3	0.47, 0.27, 0.23, 0.35	64.3, 89.4, 96.6, 87.9	4.4, 4, 3.9, 7.2	7.8, 11.1, 6.18, 14.6												
			4	0.46, 0.28, 0.24, 0.35	65.4, 87.1, 94, 87.9	5.8, 5.2, 5.1, 8.4	8, 10.8, 6.01, 14.6												
			5	0.58, 0.31, 0.27, 0.35	55.9, 82.9, 88.8, 87.08	7.4, 6.8, 6.3, 9.7	6.8, 10.3, 5.68, 10.1												
			6	0.58, 0.3, 0.26, 0.27	55.8, 84.2, 91.2, 100	8.3, 7.8, 7.6, 0.445	0.42, 1.04, 0.97, 0.764												
	-10.9	0.31, 0.17, 0.12, 0.094	1	0.66, 0.37, 0.24, 0.19	30, 47.8, 64.8, 76.7	2.5, 1.8, 1.8, 1.9	18.4, 11.8, 4.14, 13.06												
			2	0.46, 0.29, 0.23, 0.18	40.8, 56.7, 66.9, 93.6	3.5, 2.9, 2.8, 6.3	4.9, 7.06, 4.28, 11.2												
			3	0.45, 0.29, 0.24, 0.19	41.1, 56.8, 64.6, 87.6	4.5, 4.1, 4, 7.4	5, 7.07, 4.13, 9.1												
			4	0.52, 0.3, 0.22, 0.19	36.5, 55.4, 67.7, 88.7	6, 5.6, 5.4, 8.1	4.4, 6.9, 4.3, 6.5												
			5	0.91, 0.45, 0.28, 0.22	22.8, 41.1, 58.9, 79.9	8.2, 7, 6.8, 10.1	2.8, 5.1, 3.77, 4.6												
			6	0.78, 0.41, 0.28, 0.16	25.8, 43.7, 57.8, 100	8.4, 8.1, 7.9, 445.4	0.19, 0.54, 0.61, 0.76												

decreased because of the repetitions in reference SmartBAN MAC under all the given mobility cases, giving a trade-off between the effective throughput results and the energy consumption per successful transmission. TCA outperforms the reference SmartBAN MAC in terms of throughput under the walking mobility while the performance of TCA and reference SmartBAN MAC is comparable under the sit-stand mobility for the remaining links. TCA gives the best throughput performance of all the scheduling strategies for link2, 3 and 6 whereas the reference SmartBAN MAC with 2-repetitions imparts the best throughput results for link4 and 5 under the running mobility. Overall, TCA seems to meet the individual throughput requirements of all the sensor nodes,

as given in Table 2, while cutting down the energy consumption and enhancing the PRR.

In Table 3, the performance comparison of all KPIs for the reference SmartBAN MAC and TCA MAC is given with respect to varying transmission power levels. TCA is meant to provide good error performance even at extremely low transmission power, therefore we compare the TCA performance results at -10.9dBm transmission power with the with reference SmartBAN MAC results at higher transmission power levels. Reference SmartBAN MAC gives good PRR performance at higher transmission power which in turn increases the energy consumption per successful transmission for both the hub and nodes under all the mobility scenarios.

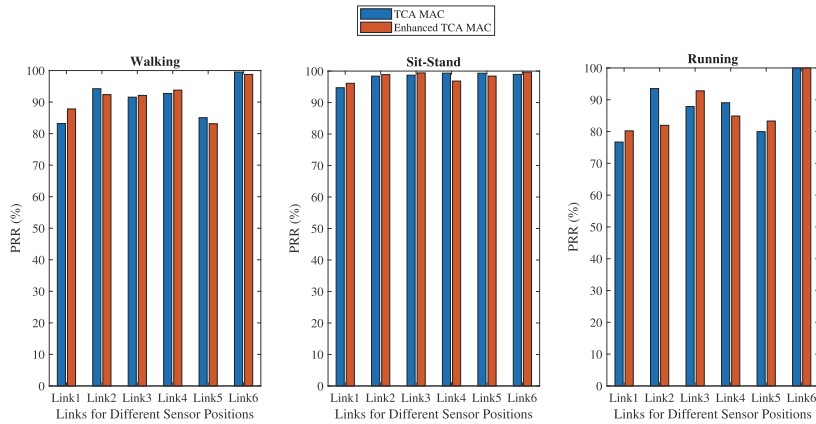


FIGURE 12. Packet reception rate (PRR) (%) under: Walking, sit-stand, and running mobility profiles (TCA and enhanced TCA).

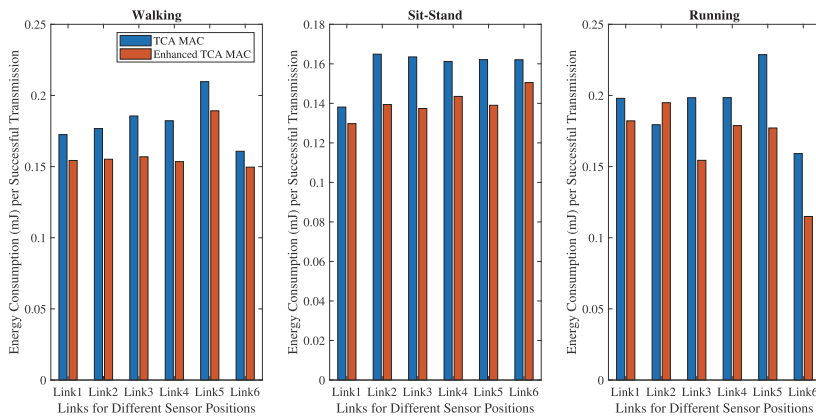


FIGURE 13. Energy consumption per successful transmission (mJ) under: Walking, sit-stand, and running mobility profiles (TCA and enhanced TCA).

For example, TCA MAC gives an average PRR of above 90% under the walking scenario at -10.9dBm as compared to the reference SmartBAN MAC which delivers an average PRR of around 93% at -2.5dBm transmission power, resulting in increased energy consumption with the reference MAC scheduling with and without repetition. In short, TCA provides the best trade-off between the PRR and energy consumption over the reference MAC, specially under walking and running mobility cases, while meeting the throughput and latency constraints of the individual sensor applications.

2) SIMULATION RESULTS FOR ENHANCED TCA

In order to make TCA more energy efficient for both hub and sensor nodes, we propose some enhancements in the existing TCA algorithm, as mentioned in sub-section IIIC. Fig. 12 provides a comparison of the basic and enhanced TCA in terms of PRR, under the given mobility scenario for all hub-node links. It can be observed that enhanced TCA gives

a PRR performance comparable to the basic TCA for most of the links related to the different sensor positions under consideration. But from the energy consumption profile, illustrated in Fig. 13, an average decrease of 11.7% in energy consumption per successful transmission can be observed under the walking scenario. For sit-stand and running mobilities, enhanced TCA cuts down the energy consumption by 13% on average. This reduction in energy consumption is due to the selective execution of TCA via slot reassignment procedure only when the hub-node link SNR goes below the given threshold or sensors' packet availability status changes. The energy consumption variations for individual links are more prominent under the running and walking scenarios rather than sit-stand because of the expected rapid changes in the individual links channel conditions, which in turn alters the SNR as well. A similar trend can also be seen in the hub energy consumption profile, as depicted in Fig. 14. Under the walking and running scenario, enhanced TCA

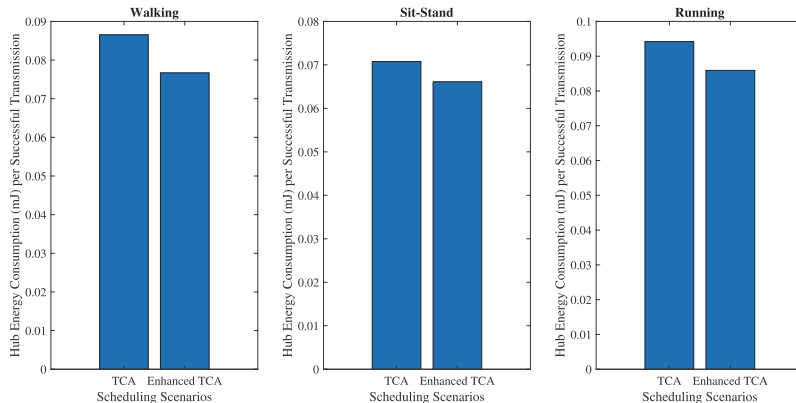


FIGURE 14. Hub energy consumption per successful transmission (mJ) under: Walking, sit-stand, and running mobility profiles (TCA and enhanced TCA).

again decreases the energy consumption per successful transmission by 11% while under sit-stand position, both the basic and enhanced TCA give almost identical energy consumption performance.

V. CONCLUSION

In this paper, we present the SmartBAN complaint Throughput and Channel Aware (TCA) and its execution through slot reassignment method. The algorithm performance is analyzed in terms of four KPIs, Packet Reception Rate (PRR), latency, energy consumption per successful transmission and throughput and compared with the reference SmartBAN MAC with and without repetitions. On the whole, SmartBAN complaint TCA improves the PRR and energy consumption over the reference SmartBAN MAC while satisfying the latency and throughput constraints of the application considered. Additionally, enhancements in the baseline TCA are performed which result in the reduction of energy consumption by the sensors and hub.

ACKNOWLEDGMENT

This material reflects only the authors view and the EC Research Executive Agency is not responsible for any use that may be made of the information it contains.

REFERENCES

- [1] S. Movassaghi, M. Abolhasan, J. Lipman, D. Smith, and A. Jamalipour, "Wireless body area networks: A survey," *IEEE Commun. Surveys Tuts.*, vol. 16, no. 3, pp. 1658–1686, Jan. 2014.
- [2] H. Cao, V. Leung, C. Chow, and H. Chan, "Enabling technologies for wireless body area networks: A survey and outlook," *IEEE Commun. Mag.*, vol. 47, no. 12, pp. 84–93, Dec. 2009.
- [3] M. Chen, S. Gonzalez, A. Vasilakos, H. Cao, and V. C. M. Leung, "Body area networks: A survey," *Mobile Netw. Appl.*, vol. 16, no. 2, pp. 171–193, 2011. doi: 10.1007/s11036-010-0260-8.
- [4] *IEEE Standard for Local and Metropolitan Area Networks—Part 15.6: Wireless Body Area Networks*, IEEE Standard 802.15.6-2012, Feb. 2012, pp. 1–271.
- [5] *Smart Body Area Networks (SmartBAN): System Description*, document ETSI TR 103 394 V1.1.1, Jan. 2018, pp. 1–20.
- [6] M. Hämmäläinen *et al.*, "ETSI TC SmartBAN: Overview of the wireless body area network standard," in *Proc. 9th Int. Symp. Med. Inf. Commun. Technol.(ISMICT)*, Mar. 2015, pp. 1–5.
- [7] M. M. Alam, D. Ben Arbia, and E. Ben Hamida, "Joint throughput and channel aware (TCA) dynamic scheduling algorithm for emerging wearable applications," in *Proc. IEEE Wireless Commun. Netw. Conf.*, Apr. 2016, pp. 1–6.
- [8] R. Khan and M. M. Alam, "Joint PHY-MAC realistic performance evaluation of body-to-body communication in IEEE 802.15.6 and SmartBAN," in *Proc. 12th Int. Symp. Med. Inf. Communication Technol.(ISMICT)*, Mar. 2018, pp. 1–6.
- [9] *Smart Body Area Network (SmartBAN): Enhanced Ultra-Low Power Physical Layer*, document ETSI TS 103 326 V1.1.1, Apr. 2015, pp. 1–13.
- [10] W. H. Chin, H. Tanaka, T. Nakanishi, T. Paso, and M. Hämmäläinen, "An overview of ETSI TC SmartBAN's ultra low power physical layer," in *Proc. 9th Int. Symp. Med. Inf. Commun. Technol.(ISMICT)*, Mar. 2015, pp. 6–9.
- [11] H. Viittala, L. Mucchi, M. Hämmäläinen, and T. Paso, "ETSI SmartBAN system performance and coexistence verification for healthcare," *IEEE Access*, vol. 5, pp. 8175–8182, 2017.
- [12] Y. Tselishchev, A. Boulis, and L. Libman, "Variable scheduling to mitigate channel losses in energy-efficient body area networks," *Sensors (Basel)*, vol. 12, no. 11, pp. 14692–14710, Nov. 2012.
- [13] S. Archasantisuk, T. Aoyagi, M. Kim, and J.-I. Takada, "Transmission power control in WBAN using the context-specific temporal correlation model," in *Proc. IEEE 27th Annu. Int. Symp. Pers., Indoor, Mobile Radio Commun. (PIMRC)*, Sep. 2016, pp. 1–6.
- [14] K. S. Prabh, F. Royo, S. Tennina, and T. Olivares, "BANMAC: An opportunistic mac protocol for reliable communications in body area networks," in *Proc. IEEE 8th Int. Conf. Distrib. Comput. Sensor Syst.*, May 2012, pp. 166–175.
- [15] C.-H. Lin, K. C.-J. Lin, and W.-T. Chen, "Channel-aware polling-based MAC protocol for body area networks: Design and analysis," *IEEE Sensors J.*, vol. 17, no. 9, pp. 2936–2948, May 2017.
- [16] M. J. Ali, H. Mungla, and A. Mehaoua, "Interference avoidance algorithm (IAA) for multi-hop wireless body area network communication," in *Proc. 17th Int. Conf. E-Health Netw., Application Services (HealthCom)*, Oct. 2015, pp. 540–545.
- [17] H. Feng, B. Liu, Z. Yan, C. Zhang, and C. W. Chen, "Prediction-based dynamic relay transmission scheme for wireless body area networks," in *Proc. IEEE 24th Annu. Int. Symp. Pers., Indoor, Mobile Radio Commun. (PIMRC)*, London, U.K., Sep. 2013, pp. 2539–2544.
- [18] M. M. Alam, E. B. Hamida, O. Berder, D. Menard, and O. Sentieys, "A heuristic self-adaptive medium access control for resource-constrained WBAN systems," *IEEE Access*, vol. 4, pp. 1287–1300, 2016.
- [19] *Smart Body Area Network (SmartBAN): Low Complexity Medium Access Control (MAC) for SmartBAN*, document ETSI TS 103 325 V1.1.1, Apr. 2015, pp. 1–36.

- [20] T. Paso et al., "An overview of ETSI TC SmartBAN MAC protocol," in *Proc. 9th Int. Symp. Med. Inf. Commun. Technol. (ISMICT)*, Mar. 2015, pp. 10–14.
- [21] M. M. Alam and E. B. Hamida, "Towards accurate mobility and radio link modeling for IEEE 802.15.6 wearable body sensor networks," in *Proc. IEEE 10th Int. Conf. Wireless Mobile Comput., Netw. Commun. (WiMob)*, Oct. 2014, pp. 298–305.
- [22] F. Martelli, C. Buratti, and R. Verdone, "On the performance of an IEEE 802.15.6 wireless body area network," in *Proc. 17th Eur. Wireless Sustain. Wireless Technol.*, Apr. 2011, pp. 1–6.
- [23] M. K. Simon and M.-S. Alouini, *Digital Communication over Fading Channels*, 2nd ed. New York, NJ, USA: Wiley, 2005. [Online]. Available: <https://cds.cern.ch/record/994549>
- [24] R. Anane, M. Bouallegue, K. Raoof, and R. Bouallegue, "Achieving energy efficient and reliable communication in WSN with coded GMSK system under various channel conditions," in *Proc. Int. Wireless Commun. Mobile Comput. Conf. (IWCMC)*, Aug. 2015, pp. 769–775.
- [25] *RN4020 Bluetooth Low Energy Module*. Accessed: Mar. 25, 2019. [Online]. Available: <http://ww1.microchip.com/downloads/en/DeviceDoc/50002279B.pdf>
- [26] M. M. Alam, H. Malik, M. I. Khan, T. Pardy, A. Kuusik, and Y. L. Moullec, "A survey on the roles of communication technologies in IoT-based personalized healthcare applications," *IEEE Access*, vol. 6, pp. 36611–36631, 2018.
- [27] S. Arnon, D. Bhastekar, D. Kedar, and A. Tauber, "A comparative study of wireless communication network configurations for medical applications," *IEEE Wireless Commun.*, vol. 10, no. 1, pp. 56–61, Feb. 2003.
- [28] S. Farshchi, A. Pesterev, P. H. Nuyujukian, I. Mody, and J. W. Judy, "Bi-Fi: An embedded sensor/system architecture for remote biological monitoring," *IEEE Trans. Inf. Technol. Biomed.*, vol. 11, no. 6, pp. 611–618, Nov. 2007.
- [29] E. Shih et al., "Physical layer driven protocol and algorithm design for energy-efficient wireless sensor networks," in *Proc. 7th Annu. Int. Conf. Mobile Comput. Netw.*, New York, NY, USA, 2001, pp. 272–287. doi: 10.1145/381677.381703.



RIDA KHAN (S'18) received the B.E. degree in telecommunication engineering from the Mehran University of Engineering and Technology, Pakistan, in 2013, and the M.Sc. degree in electronics and communication engineering from Istanbul Technical University, Turkey, in 2017. She is currently pursuing the Ph.D. degree in information and communication technology with the Tallinn University of Technology, Estonia.

Her research interests include wearable wireless networks, network coding, and energy-efficient modulation techniques. She is a Student Member of the IEEE Standards Association and is currently serving as the Secretary of the Energy Efficient Communications Hardware Standards Working Group.



MUHAMMAD MAHTAB ALAM (M'07) received the M.Sc. degree in electrical engineering from Aalborg University, Denmark, in 2007, and the Ph.D. degree from the University of Rennes1 (INRIA Research Center), France, in 2013.

He conducted postdoctoral research with the Qatar Mobility Innovations Center, from 2014 to 2016. In 2016, he was elected as the European Research Area Chair in the cognitive electronics project and an Associate Professor with the Thomas Johann Seebeck Department of Electronics, Tallinn University of Technology, Estonia. In 2018, he obtained tenure professorship to chair Telia Professorship under the cooperation framework between Telia and the Tallinn University of Technology. He has authored or coauthored over 60 research publications. His research interests include self-organized and self-adaptive wireless sensor and body area networks specific to energy-efficient communication protocols and accurate energy modeling, the Internet of Things, public safety and critical networks, embedded systems, digital signal processing, and software-defined radio.



TUOMAS PASO received the M.Sc. degree in telecommunications engineering from the University of Oulu, Finland, in 2010, where he is currently pursuing the Ph.D. degree and also a Research Scientist with the Centre for Wireless Communications. His research interests include MAC protocols and PHY/MAC/NET cross-layer techniques in MANETs and wireless sensor networks, such as WBANs and WPANs. The main focus areas of his research are healthcare/medical

ICT and security/defense. He has been serving as a Reviewer for the IEEE journals and conferences, and a Technical Program Committee Member for the IEEE PIMRC, since 2014. He is a member of the European Telecommunications Standard Institute (ETSI) Technical Committee Smart Body Area Network (SmartBAN), in which he is currently the Rapporteur for the work item—Low Complexity Medium Access Control (MAC) for SmartBAN.



JUSSI HAAPOLA received the M.Sc. degree in physical sciences and the Ph.D. degree in telecommunications engineering from the University of Oulu, Finland, in 2002 and 2010, respectively. He joined the Centre for Wireless Communications, University of Oulu, in 2001, where he is currently a Postdoctoral Researcher. In 2011, he made a Postdoctoral Fellow visit to Tohoku University, Sendai, Japan, and from 2012 to 2015, he was with the University of Oulu Research Institute Japan—

CWC-Nippon Ltd., as a Deputy Manager. His recent works include major contributions to two IEEE 802.15 standard amendments and research on smart infrastructure and energy grids.

...

Appendix 5

R. Khan, M. M. Alam, and A. Kuusik. Channel prediction based enhanced throughput and channel aware MAC in SmartBAN standard. In *2019 16th International Symposium on Wireless Communication Systems (ISWCS)*, pages 463–468. IEEE, 2019

Channel Prediction based Enhanced Throughput and Channel Aware MAC in SmartBAN Standard

Rida Khan, Muhammad Mahtab Alam, Alar Kuusik
{rikhan, muhammad.alam, alar.kuusik}@taltech.ee

Abstract—Throughput and Channel Aware (TCA) Medium Access Control (MAC) scheduling scheme works effectively in compliance with the SmartBAN standard in enhancing the Packet Reception Rate (PRR) performance and reducing the node energy consumption per successful transmission over the reference SmartBAN MAC scheme. The algorithm uses the radio link SNR and the data packet generation rates, corresponding to different sensor nodes, to assign the scheduled access slots for data packet transmission. TCA algorithm in SmartBAN can be executed by slot reassignment method but sending slot reassignment frames and their node acknowledgements for TCA execution at alternate inter-beacon intervals may lead to poor energy efficiency. For decreasing the frequent occurrence of TCA execution via slot reassignment frame transmission, further enhancements can be introduced in baseline TCA. Therefore, this paper proposes a channel prediction based enhanced TCA MAC for SmartBAN standard. We take PRR as well as the node and hub energy consumption per successful transmission as key performance indicators for performance comparison. The simulation results indicate a maximum PRR performance improvement of 25% over the primary TCA whereas a maximum enhancement of 44.44% is observed in terms of energy efficiency.

Index Terms—Channel prediction, energy consumption, enhanced TCA, MAC, PRR, SmartBAN, WBAN.

I. INTRODUCTION

Wireless Body Area Network (WBAN) has emerged as a vital technology that facilitates numerous applications from different sectors of everyday life. WBAN consists of interconnected low-powered tiny sensor nodes to monitor the human body vital signs, a central hub for WBAN management and operations, and actuators for feedback provision [1]. For WBAN functioning, several other low power and reduced data rate standards, like ZigBee [2], [3], were considered but IEEE standards association defined the first officially recognized WBAN standard, known as IEEE 802.15.6 [4]. Later, European Telecommunication Standards Institute (ETSI) came up with a relatively flexible and low-complexity WBAN standard, called SmartBAN. SmartBAN yields several additional features over IEEE 802.15.6 standard such as faster initial setup times, convenient hub-to-hub communication and better coexistence management [5].

Rida Khan, Muhammad Mahtab Alam and Alar Kuusik are with Thomas Johann Seebeck Department of Electronics, Tallinn University of Technology, Tallinn, Estonia. This project has received funding partly from European Union's Horizon 2020 Research and Innovation Program under Grant 668995, European Union Regional Development Fund in the framework of the Tallinn University of Technology Development Program 2016-2022 and Estonian Research Council Grant PUT-PRG424. This material reflects only the authors view and the EC Research Executive Agency is not responsible for any use that may be made of the information it contains.

The error performance in WBANs severely degrades at transmission power levels below -5dBm and large packet sizes due to human body shadowing [6]. In SmartBAN, Bose-Chadhuri Hocquenghem (BCH) error correction codes and frame repetitions are defined at the physical (PHY) layer to improve the error performance [7] but a channel variation-based scheduling method provides the desired reliability for WBANs [8]. The diverse data rate requirements for WBAN sensor nodes provide another paramount metric for dynamic medium access control (MAC) scheduling. Taking the WBAN channel and data rate as the MAC layer scheduling parameters, a joint throughput and channel aware (TCA) dynamic scheduling algorithm is proposed in [9], in compliance with the IEEE 802.15.6 standard which enhances the PRR performance and energy efficiency significantly. The channel conditions are examined for each scheduled access slot and later the data rate requirements of the chosen nodes, with good radio link quality, are taken into account for MAC scheduling in TCA algorithm.

The execution of TCA with SmartBAN is based on the slot re-assignment operation defined in Smart-BAN MAC [10] at alternate inter-beacon intervals (IBIs), followed by the acknowledgement of the updated slot assignments from WBAN nodes. Slot reassignment implicates the re-allocation of the unused scheduled access slots by hub to sensor nodes for efficiently utilizing the MAC resources [10]. In [11], the SmartBAN complaint TCA performance is evaluated against the reference SmartBAN MAC with and without frame repetitions, at the PHY layer. SmartBAN complaint TCA is shown to give better performance than the reference SmartBAN MAC in terms of PRR and energy utilized in successful transmissions. However, sending the slot reassignment frame at alternate IBIs by the hub and reception of corresponding acknowledgements from the sensors become unnecessary when WBAN channels or packet status at the sensor nodes remain unchanged for multiple IBIs. To counteract this phenomenon, authors in [11] suggest some enhancements in TCA which propose the TCA execution through slot reassignment only when the WBAN channel conditions are altered or packet status at the sensor nodes is updated.

TCA execution using slot reassignment method in SmartBAN still involves two major drawbacks which are: 1) Slot reassignment in SmartBAN cannot be executed at the consecutive IBIs and the transmission of slot reassignment frame in one IBI is followed by the node acknowledgments reception in the next IBI. Therefore, the updated assignments based on the

channel states are executed after one entire IBI is elapsed. For some on-body links under a certain mobility scenario (walking, sit-stand, running), the channel state may change from the moment slot reassignment packet is sent until the updated assignments are actually executed which may lead to a decrease in error performance. 2) Transmission of acknowledgements by the sensor nodes at slot reassignment frame reception may result in WBAN energy resources wastage. It should be noted that this energy is actually consumed in successful data packet transmissions as opposed to the reference SmartBAN MAC in which the fixed scheduled access slot allocation (irrespective of WBAN channel states) causes frequent packet errors and hence, an increased energy consumption per successful transmission. Motivated by these facts, in this paper, a channel prediction based enhanced TCA algorithm is introduced for SmartBAN which utilizes auto-regressive (AR) channel modeling to predict the channel states in the upcoming IBI. Based on this discussion, the key contributions for this article include:

- Proposal of AR modeling for WBAN channel predictions under various mobility scenarios such as walking, sit-stand and running. Depending upon the channel prediction at the IBI beginning, TCA is either executed or not for the given IBI. Upon TCA execution, the newly assigned scheduled access slots are broadcast to WBAN sensor nodes as downlink information rather than slot reassignment procedure.
- Performance analysis of the SmartBAN complaint baseline TCA, enhanced TCA and channel prediction based enhanced TCA algorithms in terms of PRR as well as energy consumption per successful transmission at the nodes and the hub.

The rest of the paper is organized as: Section II explains the SmartBAN complaint TCA, enhanced TCA and channel prediction based TCA details. Section III elaborates the simulation setup and the underlying performance evaluation for the above mentioned TCA variants. Finally, section IV concludes the paper.

II. THROUGHPUT AND CHANNEL AWARE MAC

This section discusses the primary TCA execution in SmartBAN, MAC layer enhancements in the existing TCA and the channel prediction-based enhanced TCA.

A. SmartBAN complaint TCA

TCA algorithm employs the principle of m-periodic scheduling recommended by IEEE 802.15.6 standard. M-periodic allocation refers to the assignment of scheduled access time slots in every m th beacon period for servicing low duty cycle periodic traffic [4]. The priority nodes, which are generally high rate or emergency nodes, are assigned time slots at consecutive IBIs while low data rate nodes are assigned scheduled access slots m-periodically only when a new data packet is generated [9]. TCA exploits the primary notion of m-periodic allocation along with the information about the channel conditions between the hub and sensor

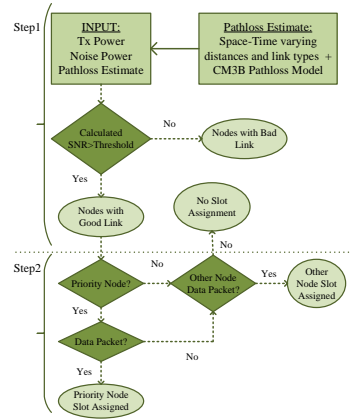


Fig. 1. Throughput and channel aware MAC algorithm.

nodes. TCA algorithm consists of two steps: 1) slot allocation based on the SNR conditions at WBAN links and 2) a final slot assignment based on m-periodicity. The input of the algorithm includes estimated pathloss values (obtained using the experimental traces of the motion capture system and biomechanical modeling [12]), transmission power and noise level. The estimated pathloss is used for the computation of signal-to-noise ratio (SNR) threshold during the first step. Further details about the calculation of SNR threshold, to achieve a PRR above 90%, are given in [11]. In the first step, the SNR condition at each node-hub link is examined and if the link SNR is higher than the pre-defined threshold value, the node is included into the list of candidate nodes for the final slot assignment in the next step. During the second step, the resulting batch of sensor nodes is checked for priority node presence. If priority node is found among the candidate sensor nodes with data packet available, it is assigned the given time slot. If priority node does not have favorable SNR value at the radio link or is already allocated the slot, other low priority nodes are given the particular slot based on their data packet status. The flow chart representation of TCA algorithm is depicted in Fig. 1.

TCA in SmartBAN is carried out by implementing the slot reassignment procedure at the alternate IBIs. At first, the hub performs the TCA algorithm execution and creates an array of the assigned slots for all the nodes present in WBAN with data packet available for transmission. At the IBI beginning in D-Beacon, hub sends the information about the possibility of slot reassignment frame transmission during the control and management (C/M) period. Later in the C/M period, hub transmits the slot reassignment frame, with the highest priority, to all the nodes that are supposed to make packet transmissions. If the hub fails to make the slot reassignment frame transmission within the current IBI, it attempts to perform the slot reassignment in the successive IBI [10] for TCA scheduling. All the sensor nodes, which receive slot reassignment frame,

reply with a mandatory command acknowledgement in the frame MAC header transmitted during the scheduled access period of the subsequent IBI, with or without data payload from MAC layer. The new slot assignment, as recommended by the hub, comes into operation in the next IBI while the hub simultaneously investigates the current WBAN links' SNR values to carry out the TCA scheduling via slot reassignment procedure again. Fig. 2 summarizes the description of the TCA execution and the relevant frame exchange in SmartBAN.

B. Enhanced TCA for SmartBAN

The baseline TCA algorithm mentioned in sub-section II-A suggests the slot reassignment implementation at each alternate IBI after generating the array of assigned slots. The periodic transmission of slot reassignment frame at alternate IBIs can be decreased by executing TCA and recreating the assignment array only when necessary, depending upon the channel states and the data packet status of the past slot allocations. Therefore, the enhanced TCA algorithm comprises of some additional steps before TCA execution through slot reassignment method.

Initially, hub checks that whether TCA was executed and slot reassignment frame was sent in the preceding IBI or not since TCA execution through slot reassignment is not allowed at the consecutive IBIs. If TCA execution was performed in the previous IBI, the algorithm stops and repeats the similar procedure during the next IBI, else the algorithm continues to the next step. The hub then examines the past assignment array having the details of the assigned slots to sensor nodes. The hub proceeds with the conventional TCA execution and the implementation of slot reassignment if i) SNR values of all the nodes in the past assignment array, having data packet to send, go below the pre-defined threshold for the current IBI. OR ii) Some other sensor node, excluding the previous assignment array, has data packet to send. Otherwise the next IBI is checked for potential changes in the channel conditions of the hub-node links or packet status of the sensor nodes. Fig. 3 shows the modifications made in the TCA algorithm for performance enhancements.

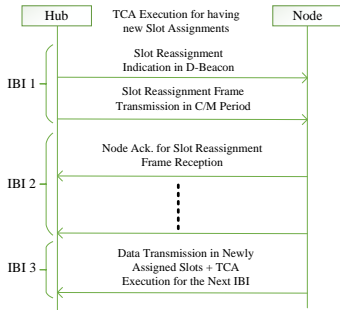


Fig. 2. TCA execution in SmartBAN.

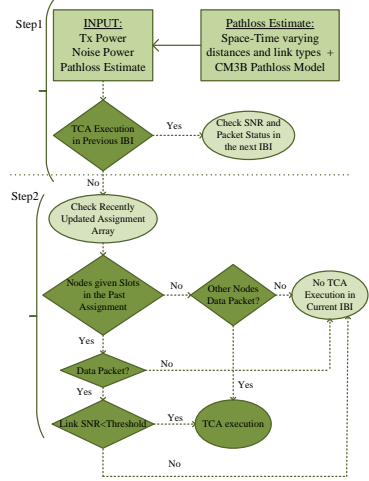


Fig. 3. Enhanced TCA modifications.

C. AR model based Enhanced TCA

The primary TCA and its enhanced version are implemented in SmartBAN using the slot reassignment procedure. Although, the enhanced TCA decreases the frequency of recurrent slot reassignment frame transmission at alternate IBIs and the corresponding node acknowledgements, it still involves the flaws of the mandatory node acknowledgements upon slot reassignment frame reception and a delayed execution of the updated slot assignments. In order to prevent these issues, we introduce an AR modeling channel prediction based enhanced TCA for SmartBAN in this paper. It is safe to assume that the channel characteristics for WBAN communication are highly correlated due to the repetitive human body movements such as respiration, walking, running and sit-stand mobilities and predominantly include human body shadowing. Therefore, AR modeling offers an adequate approach for exploiting the space-time dependent behavior of WBAN channels [13]. AR modeling enables the future generation of time series related to the on-body channel traces using the auto-correlation function (ACF) for on-body channels. The ACFs for different mobility scenarios additionally give insight into the time-dependency of on-body propagation and a theoretical basis for WBAN channel prediction.

We consider the WBAN channel as an AR process of order p in which the current output $x(t)$ is dependent on the past p inputs at equidistant time instants t . The estimated output process $\hat{x}(t)$ can be represented as an AR(p) process by

$$\hat{x}(t) = \sum_{i=1}^p \alpha_i \times \hat{x}(t-i) + \sigma(t), \quad (1)$$

where $\{\alpha_1, \alpha_2, \dots, \alpha_p\}$ are the AR coefficients to give the previous samples weightage and σ is a zero mean uncorrelated

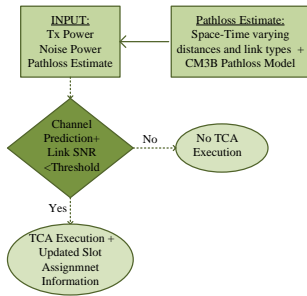


Fig. 4. Channel prediction based enhanced TCA.

Gaussian noise process. Multiplying (1) by $\hat{x}(t)$ at time lag k and taking the expectation yields

$$\delta(k) = \sum_{i=1}^p \alpha_i \times \delta(k-i), \quad (2)$$

where $\delta(k) = E[\hat{x}(t)\hat{x}(t+k)]$ and $k > 0$. The autocorrelation at time lag k can be found using the relation $\rho_k = \frac{\delta(k)}{\delta(0)}$ which transforms (2) into the form (for $k > 0$)

$$\rho_k = \sum_{i=1}^p \alpha_i \times \rho_{k-1}. \quad (3)$$

Replacing $k = 1, 2, \dots, p$ for the selected order of AR model produces Yule-Walker equations [14]. These Yule-Walker equations are recursively solved using the Levinson-Durbin algorithm [13] for obtaining the weighted AR coefficients α_i .

Using this procedure, the filter coefficients to build the required AR model for the desired on-body channel are generated and the channel states for the given WBAN links in the upcoming IBI are estimated. These predicted channel states are followed by the pathloss computations which helps in estimating the SNR conditions of the individual WBAN links. As given in Fig. 4, if the SNR value corresponding to any of the WBAN links goes below the pre-defined threshold level, TCA algorithm is executed at the hub and new channel assignments are broadcast in the form of downlink information to all sensor nodes in a pre-allocated scheduled access slot. The execution of channel prediction based enhanced TCA, using the downlink information broadcast during the scheduled access period, rather than the generic slot reassignment method, not only eliminates the necessity of sending the node acknowledgements in response to the slot reassignment frame but also permits the TCA execution at consecutive IBIs if WBAN channel conditions change rapidly at successive IBIs. This helps in boosting the error performance of TCA variants executed using the slot reassignment method.

III. PERFORMANCE EVALUATION

This section, at first, describes the inherent simulation parameters utilized in performance evaluation and then a

TABLE I
SIMULATION SETUP PARAMETERS [7], [10], [15].

RF Parameters	
Transmitter Power (dBm)	-10.9, 0 (for TCA-related information)
Receiver Sensitivity (dBm)	-92.5
Current Consumption Tx/Rx (mA)	16
Bandwidth per channel (MHz)	2
Receiver Sensitivity (dBm)	-92.5
Information Rate (kbps)	1000
PHY/MAC Parameters	
Minimum slot length (T_{min})	625 μ s
Slot duration (T_{SLOT})	1.25ms
Interframe spacing (IFS)	150 μ s
Symbol Rate (R_{Sym})	10^6
MAC header (N_{MAC})	7 octets
Frame Parity (N_{par})	2 octets
PLCP header (N_{PLCP})	5 octets
PLCP Preamble ($N_{preamble}$)	2 octets

thorough analysis of the acquired simulation results, in terms of PRR and energy consumption per successful transmission for both the hub and sensor nodes, is presented.

A. Simulation Setup

The system model to provide PHY-MAC performance results consists of mobility modeling for dynamic links generation, channel models for finding the realistic pathloss values, and radio link modeling [12]. The additional details about the system model considered in this paper are similar to those given in [11]. The parameters assumed in the simulation setup are given in Table I. We assume a transmission power level of -10.9dBm for RN4020 BLE device [15] in all the cases except for sending the slot reassignment frames (for TCA and enhanced TCA execution) or the downlink information by hub (for channel prediction based enhanced TCA execution). For conveying the TCA-related slot assignment information in both the cases, hub uses 0dBm transmission power to ensure successful reception by the sensor nodes. For three distinct mobility patterns, which include walking, sit-stand and running, a slot duration of 1.25ms is assumed in all the simulations. For the performance assessment of the SmartBAN complaint baseline TCA, enhanced TCA and

TABLE II
USE CASE SCENARIO FOR PERFORMANCE EVALUATION [5], [16], [17]

Rescue and Emergency Management	
Sensor Type	Required Data Rates (kbps)
Voice command (1 node)	50-100
IMU (2 nodes)	4.8-35
GPS (1 node)	0.096
Temperature sensor (1 node)	0.12
Pulse rate (1 node)	0.048
Sensor Placement	
Sensor Type	Location
Coordinator/Hub	Chest
Voice command	Left shoulder
IMU1, IMU2	Left knee, Right knee
GPS	Left elbow
Temperature sensor	Right wrist
Pulse rate	Left wrist

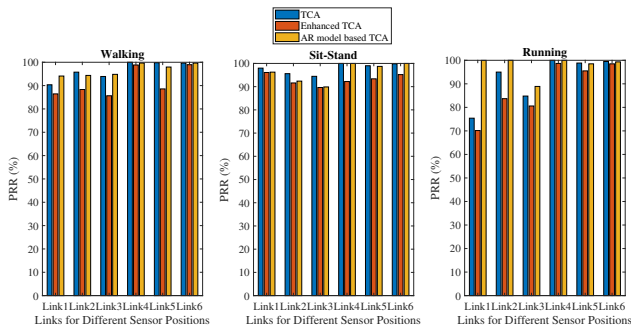


Fig. 5. Packet reception rate (PRR) (%) under: walking, sit-stand and running mobility profiles.

channel prediction based enhanced TCA, we consider a rescue and emergency management application scenario, as given in Table II, along with the sensor node data rate requirements and on-body placements. For all scheduling scenarios, we assume mandatory scheduled access and C/M periods and an IBI duration of 11.25ms, resulting in the transmission of 88 IBIs per second. All the simulations are carried out using the MATLAB script files.

B. Simulation Results

We define PRR, for each sensor node, as the ratio of successfully decoded packets and the total number of packets transmitted by each node throughout the trace duration. The total energy consumed is defined as the summation of energy utilized during transmission and reception at the circuitry as well as the amplifier, according to the energy consumption model given in [18]. For sensor nodes, energy consumption per successful transmission equals $\frac{E_i}{n_i}$, where E_i is the total energy consumed at node i and n_i is the number of successful transmissions made by the particular node. In case of hub, the energy consumption becomes $\frac{E_h}{n_{total}}$, where E_h is the total energy utilized by hub and n_{total} is the total number of successful transmissions made by all the sensor nodes.

Fig. 5 sums up the PRR results for each link between different sensor nodes and the hub, under walking, sit-stand and running mobility scenarios. Link1, link2, link3, link4, link5 and link6 respectively correspond to the nodes placed on left shoulder, left knee, right knee, left elbow, right wrist and left wrist. Under walking scenario, channel prediction based TCA scheduling in SmartBAN outperforms all the TCA variants for every link except link5 but maintains a desired PRR above 90% for all the sensor nodes. The channel conditions under sit-stand mobility are generally static, so the performance gain for channel prediction based TCA is not quite evident, yet the suggested TCA variant preserves the required PRR greater than 90% at most of the links. However, under the running mobility, the severe degradation in PRR performance at link1 and link3 is mitigated by the channel prediction based TCA technique which results in a maximum PRR performance gain of about 25%.

Fig. 6 and Fig. 7 depict the energy consumption profile for various links and the hub respectively, under the given mobility scenarios. Energy consumption during **transmission**, for **sensor** node mainly includes, i) data packet transmission energy and ii) slot reassignment acknowledgement transmission energy in case of baseline and enhanced TCA. For **hub**, the transmission energy consists of i) D-Beacon ii) data packet acknowledgement iii) slot reassignment frame transmission energy in case of baseline and enhanced TCA and iv) downlink information transmission energy in case of channel prediction based TCA. During the **reception**, the corresponding energy consumption for **sensor** and **hub** respectively becomes i) D-Beacon ii) data packet acknowledgement iii) slot reassignment frame reception energy in case of baseline and enhanced TCA iv) downlink information reception energy in case of channel prediction based TCA and i) data packet reception energy and ii) slot reassignment acknowledgement reception energy in case of baseline and enhanced TCA. By cutting down the energy consumption used for mandatory node acknowledgement transmission and reception in baseline and enhanced TCA versions, channel prediction based TCA enhances the energy efficiency. The suggested TCA variant imparts a maximum 44.44% reduction of energy consumption over the other TCA variants at the sensor nodes. However rapid changes in channel conditions under walking and running mobilities lead to more frequent transmissions of downlink information frames, resulting in a slight increase in hub energy consumption. To sum up, the channel prediction based TCA gives the best trade-off between the PRR and energy efficiency metrics under all the given mobility cases.

IV. CONCLUSION

In this paper, we propose a channel prediction based enhanced TCA algorithm for SmartBAN and compare it with the slot-reassignment based primary and enhanced TCA schemes in terms of PRR and energy consumption per successful transmission. AR modeling is used in channel prediction for deciding the possibility of TCA execution at each IBI and the suggested changes yield an overall improvement in the baseline TCA PRR and node energy efficiency results.

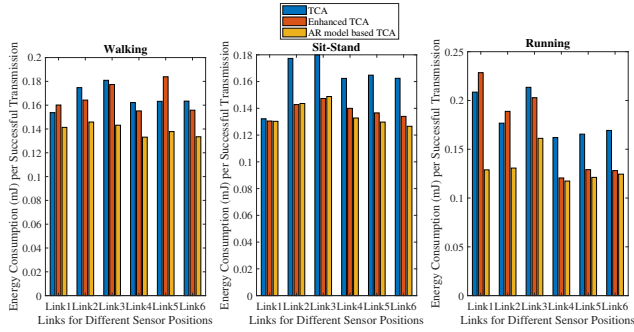


Fig. 6. Energy consumption per successful transmission (mJ) under: walking, sit-stand and running mobility profiles.

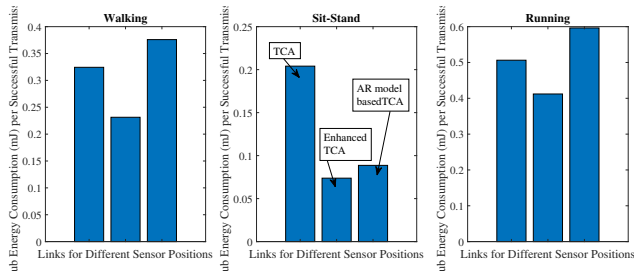


Fig. 7. Hub energy consumption per successful transmission (mJ) under: walking, sit-stand and running mobility profiles.

REFERENCES

- [1] R. Cavallari, F. Martelli, R. Rosini, C. Buratti, and R. Verdone, "A Survey on Wireless Body Area Networks: Technologies and Design Challenges," *IEEE Communications Surveys Tutorials*, vol. 16, pp. 1635–1657, March 2014.
- [2] D. Scazzoli, A. Kumar, N. Sharma, M. Magarini, and G. Verticale, "Fault recovery in time-synchronized mission critical zigbee-based wireless sensor networks," *International Journal of Wireless Information Networks*, vol. 24, no. 3, pp. 268–277, 2017.
- [3] D. Scazzoli, A. Kumar, N. Sharma, M. Magarini, and G. Verticale, "A novel technique for ZigBee coordinator failure recovery and its impact on timing synchronization," in *2016 IEEE 27th Annual International Symposium on Personal, Indoor, and Mobile Radio Communications (PIMRC)*, pp. 1–5, IEEE, 2016.
- [4] "IEEE Standard for Local and metropolitan area networks - Part 15.6: Wireless Body Area Networks," *IEEE Std 802.15.6-2012*, pp. 1–271, Feb 2012.
- [5] "Smart Body Area Networks (SmartBAN); System Description," *ETSI TR 103 394 V1.1.1*, pp. 1–20, Jan 2018.
- [6] R. Khan and M. M. Alam, "Joint PHY-MAC Realistic Performance Evaluation of Body-to-Body Communication in IEEE 802.15.6 and SmartBAN," in *2018 12th International Symposium on Medical Information and Communication Technology (ISMICT)*, pp. 1–6, March 2018.
- [7] "Smart Body Area Network (SmartBAN); Enhanced Ultra-Low Power Physical Layer," *ETSI TS 103 326 V1.1.1*, pp. 1–13, Apr 2015.
- [8] M. Salayma, A. Al-Dubai, I. Romdhani, and Y. Nasser, "New dynamic, reliable and energy efficient scheduling for wireless body area networks (wban)," in *2017 IEEE International Conference on Communications (ICC)*, pp. 1–6, May 2017.
- [9] M. M. Alam, D. Ben Arbia, and E. Ben Hamida, "Joint throughput and channel aware (TCA) dynamic scheduling algorithm for emerging wearable applications," in *2016 IEEE Wireless Communications and Networking Conference*, pp. 1–6, April 2016.
- [10] "Smart Body Area Network (SmartBAN); Low Complexity Medium Access Control (MAC) for SmartBAN," *ETSI TS 103 325 V1.1.1*, pp. 1–36, Apr 2015.
- [11] R. Khan, M. M. Alam, T. Paso, and J. Haapola, "Throughput and channel aware mac scheduling for smartban standard," *IEEE Access*, vol. 7, pp. 63133–63145, 2019.
- [12] M. M. Alam and E. Ben Hamida, "Towards accurate mobility and radio link modeling for IEEE 802.15.6 wearable body sensor networks," in *2014 IEEE 10th International Conference on Wireless and Mobile Computing, Networking and Communications (WiMob)*, pp. 298–305, Oct 2014.
- [13] S. L. Cotton, G. A. Conway, and W. G. Scanlon, "A time-domain approach to the analysis and modeling of on-body propagation characteristics using synchronized measurements at 2.45 ghz," *IEEE Transactions on Antennas and Propagation*, vol. 57, pp. 943–955, April 2009.
- [14] G. E. Box, G. M. Jenkins, G. C. Reinsel, and G. M. Ljung, *Time series analysis: forecasting and control*. John Wiley & Sons, 2015.
- [15] "RN4020 Bluetooth Low Energy Module." (Date last accessed 25-Mar-2019).
- [16] M. M. Alam, E. B. Hamida, M. Rehmani, and A. Pathan, "Wearable wireless sensor networks: Applications, standards, and research trends," in *Emerging Communication Technologies Based on Wireless Sensor Networks: Current Research and Future Applications*, pp. 59–88, CRC Press, 2016.
- [17] C. Chakraborty, B. Gupta, and S. K. Ghosh, "A review on telemedicine-based wban framework for patient monitoring," *Telemedicine and e-Health*, vol. 19, no. 8, pp. 619–626, 2013.
- [18] E. Shih, S.-H. Cho, N. Ickes, R. Min, A. Sinha, A. Wang, and A. Chandrakasan, "Physical layer driven protocol and algorithm design for energy-efficient wireless sensor networks," in *Proceedings of the 7th Annual International Conference on Mobile Computing and Networking, MobiCom '01*, (New York, NY, USA), pp. 272–287, ACM, 2001.

Appendix 6

R. Khan, M. M. Alam, and M. Guizani. A flexible enhanced throughput and reduced overhead (FETRO) MAC protocol for ETSI SmartBAN (Accepted). *IEEE Transactions on Mobile Computing (Early Access)*

A Flexible Enhanced Throughput and Reduced Overhead (FETRO) MAC Protocol for ETSI SmartBAN

Rida Khan, *Student Member, IEEE*, Muhammad Mahtab Alam, *Senior Member, IEEE*, and Mohsen Guizani, *Fellow, IEEE*

Abstract—Smart body area networks (SmartBAN) is an emerging wireless body area networks (WBAN) standard proposed by the European Telecommunications Standards Institute (ETSI). This paper first examines the potential of SmartBAN medium access control (MAC) layer with scheduled access to support a myriad of WBAN applications, having diverse data rate requirements. Extra scheduled access slots can be allocated to high data rate sensor nodes for managing their data rate requirements. High data rate sensor nodes can also be re-assigned to use the available time slots of low data rate sensor nodes in Inter-Beacon Interval (IBI) by the central hub. But these two schemes incorporate different physical (PHY) and MAC layer overheads related to frame transmission, frame acknowledgement and slot re-assignment. This redundant overhead transmission results in high overhead energy consumption and reduced effective throughput. Therefore, an innovative and flexible enhanced throughput and reduced overhead (FETRO) MAC protocol for scheduled access is proposed in this article. In the proposed scheme, the sensor node data rate requirements are considered while assigning the scheduled access slot duration by allowing minimal changes in the base-line standard implementation. This infers the provision of scheduled access slots with variable slot durations within an IBI. We also evaluate the existing techniques of extra slot allocation and slot re-assignment in SmartBAN as well as the proposed FETRO MAC protocol with variable slot length. The proposed FETRO MAC scheme results in optimizing both the overall throughput and normalized overhead energy consumption per kilo bits per second (Kbps). Additionally, the impact of various WBAN channel models over these throughput management approaches is also investigated. The proposed FETRO MAC protocol with variable slot duration gives an average reduction of 65.5% and 59.16%, respectively, in the hub and nodes normalized overhead energy consumption per Kbps outcomes, as compared to the de-facto SmartBAN MAC scheduling strategies.

Index Terms—Energy consumption, FETRO, MAC, overheads, scheduled access, SmartBAN, throughput.

I. INTRODUCTION

WIRELESS body area networks (WBANs) have gained significant popularity among research and innovation communities in both academia and industry because of their potential in realizing many different applications. Smart body area network (SmartBAN) is among several standards which define WBAN operation at the physical (PHY) and medium

access control (MAC) layers. It is distinguished for its low complexity, energy efficient network structure, faster channel acquisitions, interoperability and data semantic models, hub-to-hub communication or inter-hub transmission and coexistence management by the central hub [1]. WBAN applications involve diverse fields such as health care, military, rescue and emergency management, sports and entertainment [2]. These applications may include the monitoring of vital signs such as electrocardiogram (ECG) and electromyograph (EMG) signals which require very high throughput as well as body temperature and blood oxygen level signals which are characterized by their low data rates. WBAN MAC should be designed to manage these massive variations in data transmission rates while maintaining a reduced energy consumption especially on overheads transmission as well as better quality of service (QoS).

A. Related Work and Motivation

In order to efficiently accommodate WBAN throughput requirements within the energy constraints, several dynamic MAC strategies have been proposed in the existing literature. One such study was conducted in [3] in which authors presented a traffic aware dynamic MAC (TAD-MAC) protocol. The TAD-MAC algorithm is heuristically modeled to comprehend its convergence patterns, resulting in the network nodes wake-up intervals with minimal energy consumption at the receiving end. Authors in [4] suggest a traffic priority aware MAC (TraPy-MAC) protocol which is based on the classification of WBAN traffic into emergency and non-emergency categories. Emergency data are allocated slots without contention while non-emergency data are again categorized for contention depending upon their priority levels. In [5], dynamic adjustments in the sensor nodes transmission order and transmission duration (number of scheduled access slots) are considered in the baseline time division multiple access (TDMA) protocol. The channel status (using Markov model) and application context are taken as scheduling criteria to yield minimum energy consumption by sensor nodes. A context aware MAC (CA-MAC) is proposed in [6] which defines a new hybrid contention/TDMA superframe structure, consisting of four parts: beacon, contention access slots, TDMA scheduled-based slots and TDMA polling-based slots. The superframe and the beacon durations remain unchanged while the duration allocated to contention or TDMA part

R. Khan and M. M. Alam are with Thomas Johann Seebeck Department of Electronics, Tallinn University of Technology, Tallinn, Estonia, 12616. Mohsen Guizani is with Department of Computer Science and Engineering, Qatar University, Qatar. e-mail: {rikhan, muhammad.alam}@taltech.ee, mguizani@gmail.com.

can be modified depending upon the application requirements. Also, the polling-based TDMA slots are used to manage time-critical contexts. Complying with the channel conditions and data traffic requirements, authors in [7] propose a context aware and channel-based WBAN resource allocation scheme. The WBAN data are separated into non-medical, constant bit rate medical and emergency medical types and the intervals of consecutive transmission are adaptively changed depending upon the channel conditions. Similar approach is adopted in [8] in which the TDMA based technique is improved to provide reliability and energy efficiency while synchronizing the sensor nodes for packet transmission based on their predicted link status. A priority-based adaptive MAC (PA-MAC) protocol for WBANs is suggested in [9] in which different channels are allocated for beacon frame and data frames. The algorithm incorporates traffic prioritization, simultaneous usage of parallel data transmission channels and the presence of both the contention access and contention free periods to accommodate various data traffic categories with minimum energy resources. In order to exclusively manage the WBAN emergency traffic, a MEB MAC protocol is provided in [10] which dynamically inserts listening windows in the contention free period of beacon-enabled IEEE 802.15.6 superframe.

The SmartBAN standard defines low complexity PHY and MAC layers for managing both the periodic and emergency WBAN traffic. SmartBAN PHY layer specifies separate channels for control signals and data packet transmissions. The data channel is partitioned into Inter-Beacon Intervals (IBIs). All IBIs are divided into distinct time slots that constitute data beacon (D-Beacon) period, scheduled access duration, control and management (CM) duration and inactive duration. D-Beacons mark the boundaries of IBI and are broadcast by hub for communicating specific information about SmartBAN. Scheduled access duration is reserved for data transmission by sensor nodes and CM period is used for control information exchange between hub and sensor nodes. Finally inactive duration is provided for employing duty cycling in SmartBAN for energy preservation [11]. Authors in [12] suggest a time-optimized MAC framework in which the IBI, scheduled access period, CM period and inactive duration are optimized for minimizing both delay and energy consumption. Authors in [13] propose a resource allocation scheme for SmartBAN in which IBI duration and single slot durations are optimized depending upon the delay requirements of periodic uplink transmissions. The proposed optimization also allows sensor nodes to remain in the longest possible sleep mode to minimize the energy consumption while maintaining the delay constraints. In [14], variations in both the channel and data traffic are taken into account to adapt the time slot allocation in reference SmartBAN standard. The algorithm, termed as joint throughput and channel aware (TCA) scheduling, adopts m-periodic scheduling approach. The sensor nodes are assigned slots depending upon the wireless channel conditions as well as data packet availability using slot reassignment procedure at alternate IBIs. Another MAC scheduling scheme for improving channel utilization and better throughput management is provided in [15] which suggests the usage of managed access phase (MAP) and random access phase (RAP) for pre-

allocated and un-allocated time slots respectively. In MAP, the emergency data is sent by high priority sensor nodes immediately without the prior channel sensing. If no transmissions are detected for emergency traffic upon channel sensing, slot owner nodes make their transmissions. If none of these node types send data, the remaining sensor nodes in BAN contend for transmission. In RAP with unassigned time slots, this procedure takes place only between high priority sensor nodes and other transmission entities. However this method of channel sensing and contention at subsequent slots may lead to higher energy consumption, leading to the notion that scheduled access methods yield better outcomes in terms of energy efficiency.

SmartBAN defines a parameter L_{Slot} to imply the single slot duration within every IBI. L_{Slot} is broadcast in the control channel beacon (C-Beacon) by hub and it remains essentially the same in each IBI. The connected sensor nodes transmit their data at this pre-defined slot duration, irrespective of their particular data rate requirements. Slot duration is changed only when the coordinator node broadcasts a different L_{Slot} value in its C-Beacon and the connection is re-established with all the sensor nodes [11]. A longer slot length can accommodate more payload, with the same PHY-MAC and acknowledgement overheads, and facilitates higher throughput while shorter slot duration is sufficient to support low data rate sensor nodes. The allocation of fixed longer slot durations in the presence of low data rate sensor nodes leads to the wastage of scheduled access resources. Whereas the throughput requirements of high data rate sensors cannot be met with fixed smaller slot durations. For better throughput management in existing SmartBAN standard with scheduled access, extra slots can be allocated to high data rate sensor nodes. Another option for handling data traffic with scheduled access method is slot re-assignment in which the unused slots of low data rate sensor nodes are reassigned to high data rate sensor nodes within an IBI. Both of these throughput management techniques in scheduled access MAC are the proposed as part of the ETSI SmartBAN MAC layer specifications [11]. While these options with fixed slot durations may accommodate the throughput requirements of a WBAN system, their related PHY-MAC overheads, acknowledgement transmissions and re-assignment procedures lead to high overhead energy consumption in overheads and relatively decreased throughput. In order to encounter these shortcomings, the assignment of slot durations in scheduled access MAC should be flexible enough to adapt according to the throughput requirements of the individual sensor nodes, at minimized overhead energy consumption.

B. Summary of Contributions

In the view of the above discussion, we aim to make the following contributions.

- First, we numerically evaluate the conventional SmartBAN MAC performance in the presence of constant bit rate sensor nodes with distinct data rate requirements. The two primary methods of throughput management proposed in ETSI SmartBAN MAC layer specifications [11] for scheduled access, i.e., extra slot allocation and

TABLE I: Summary of Symbols and Notations.

Symbols	Notations	Symbols	Notations
$3V$	3 volts supply voltage.	BT	Bandwidth-bit period product of GFSK.
h	Modulation index of GFSK.	E_{OHnode}	PHY-MAC overhead energy consumption at sensor node.
E_{OHhub}	PHY-MAC overhead energy consumption at hub.	E_{PLnode}	Data payload transmission energy consumption at sensor node.
E_{PLhub}	Data payload reception energy consumption at hub.	$E_{SRaNode}$	Slot Reassignment energy consumption at sensor node.
$E_{SRaShub}$	Slot Reassignment energy consumption at hub.	I_{mA}^{idle}	Current consumption in idle mode (mA).
I_{mA}^{Rx}	Current consumption at the receiving end (mA).	I_{mA}^{Tx}	Current consumption at the transmitting end (mA).
$K_{Preamble}$	Number of bits in preamble.	K_{PHY}	Number bits in of PHY header.
K_{Parity}	Number of bits in frame parity.	K_{MAC}	Number of bits in MAC header.
$K_{Overhead}$	Number of bits in complete PHY-MAC overhead.	K_{ID}	Number of bits in element ID field of information unit.
K_L	Number of bits in length field of information unit.	K_{SRas}	Number of bits in slot reassignment information module.
L_{IM}	Information module size in bits.	L_{Slot}	Parameter to indicate slot duration in C-Beacon.
N_{Min}	Number of minimum length units in IBI.	N_{Slot}	Number of slots in IBI.
N_{IBI}	IBIs transmitted in one second.	N_{SA}	Number of slots in scheduled access duration.
N_{CM}	Number of slots in CM duration.	N_{IA}	Number of slots in inactive duration.
N_{Rx}	Total number of received bits for the given sensor node.	N_{SRas}	Number of slot reassignment information modules.
PL	Data payload size in bits.	PL^i	Data payload size in bits with T_{Slot}^i .
REP	Number of PPDU repetitions.	R_{Sym}	Symbols per second.
T_{Slot}	Slot duration.	T_{Min}	Minimum possible slot duration.
T_{IBI}	IBI duration.	T_{Beacon}	Slot duration of D-Beacon in IBI.
T_B	D-Beacon transmission duration.	T_{SA}	Scheduled access duration in IBI.
T_{CM}	CM duration in IBI.	T_{IA}	Inactive duration in IBI.
T_{Tx}	PPDU transmission duration.	T_{Ack}	PPDU acknowledgement duration.
T_{IFS}	IFS duration.	T_{PL}	Data payload transmission duration.
T_{Trace}	Trace duration of the pathloss file.	T_{Slot}^i	Slot duration for the i th slot.
T_{Tx}^i	PPDU transmission duration with T_{Slot}^i .	TP_{Th}	Theoretical MAC throughput in Kbps.
TP_{Pr}	Effective MAC throughput under the given channel in Kbps.	TP_{Th}^{FETRO}	FETRO MAC theoretical throughput in Kbps.

slot reassignment, are considered to satisfy the high data rate requirements of some particular sensor nodes.

- Second, an innovative and “flexible” enhanced throughput and reduced overhead (FETRO) scheduled access MAC protocol with variable slot length is introduced. In the proposed algorithm, slot duration is assigned based on the individual traffic demands of each sensor node. So in every IBI, the slot durations are distinctive to the data rate requirements of the individual sensors. The FETRO MAC with variable slot length can be executed by making few changes in the connection request and the connection assignment information modules of the existing SmartBAN standard, as further discussed in section IV. A flexible L_{Slot} will help satisfy the throughput demands of high data rate sensor nodes in the presence of nominal data traffic nodes. It will also prevent the under-utilization of SmartBAN resources when low throughput sensor nodes are allocated larger slot durations due to the presence of high data rate sensor nodes. To the best of our knowledge, this is the first dynamic MAC protocol proposed to enhance the performance of ETSI SmartBAN MAC in which individual slot duration is varied within IBI to manage the data rate requirements of each sensor node at the same time reducing the associated overheads with each slot allocation.
- Both of these MAC strategies with fixed and variable

slot durations are assessed taking effective throughput and normalized energy consumption per kilo bits per second (Kbps) as the key performance indicators. The proposed FETRO MAC protocol with variable slot duration retains the base structure of SmartBAN MAC and is shown to outperform the conventional methods. Four different WBAN channel models which are widely considered in WBAN performance evaluations, are also integrated in the simulation setup for better understanding of the results associated with both methods. These channel models include the standard IEEE CM3B model [16], CM3B model with Rician fading [16], dynamic IEEE CM3B (deterministic) channel model [17] and deterministic channel model with fading.

The remainder of the paper is organized as follows: SmartBAN PHY-MAC layer specifications and functional details are provided in section II. The throughput and energy consumption analysis with SmartBAN specifications is elaborated in section III and the proposed FETRO MAC scheduling algorithm with variable slot length is explained in section IV. Section V comprehensively discusses the simulation setup and simulation results whereas section VI concludes the paper. For ease of reference, the symbols and notations used in this paper are summarized in Table I.

II. SMARTBAN MAC SPECIFICATIONS AND FUNCTIONING

SmartBAN standard defines a relatively low complexity and efficient MAC structure. This section elaborates the key characteristics and functioning of SmartBAN MAC layer.

A. Channel Structure and MAC Frame Format

A SmartBAN coordinator uses a separate control channel to transmit C-Beacons for channel acquisition and connection initialization by sensor nodes that intend to join the network. C-Beacon mainly defines the data channel parameters such as slot duration T_{Slot} indicated by L_{Slot} in C-Beacon, number of slots in IBI N_{Slot} , hub address and data channel number. The minimum allowed slot duration in SmartBAN is T_{Min} which equals 0.625ms and T_{Slot} equals $L_{Slot} \times T_{Min}$. L_{Slot} increases as an exponent of two, therefore the possible slot durations (T_{Slot} values) in SmartBAN become 0.625ms, 1.25ms, 2.5ms, 5ms, 10ms and 20 ms. After the initialization of connection establishment, data channel is used for transmitting both control as well as data frames. Both the control channel and data channel structures along with the general MAC frame format are depicted in Fig. 1(a) and 1(b) respectively.

The beginning of IBI at the data channel is marked by D-Beacon, followed by scheduled access period, CM period and inactive period at the end. Each of these access periods is divided into the individual slots of duration T_{Slot} , broadcast in C-Beacon. D-Beacon communicates the number of slots in IBI N_{Slot} , slot numbers at which CM and Inactive periods start and other fields to indicate the MAC functioning within the current IBI. A scheduled access period is mainly used for data transmission by sensor nodes to the hub. Each slot of duration T_{Slot} within the scheduled access period contains a data frame transmission duration, a subsequent inter-frame spacing (IFS), acknowledgement transmission by the receiver node and another IFS. A CM period involves the transmission of control frames for initiating and regulating the SmartBAN MAC functioning. A CM period generally has a similar slot structure as the scheduled access period.

Every data or a CM transmission time contains the actual payload appended with the MAC header and frame parity which jointly create a MAC protocol data unit (MPDU). The entire MPDU is optionally encoded to formulate a Physical-Layer Service Data unit (PSDU) which after the inclusion of PHY header and preamble, constitutes the Physical-Layer Protocol Data Unit (PPDU). The information about the local clock of hub device is broadcast in D-Beacon and then preamble further synchronizes the transmission between the sensor nodes and hub. PHY header provides information about the PPDU repetition and encoding [11], [18]. This PPDU is transmitted during the data or CM frame transmission times in either scheduled access or CM slot respectively. Further information about the SmartBAN MAC and PHY layer structure and functioning is correspondingly provided in [11] and [18].

B. Connection Request and Connection Assignment Frames

The connection request and connection assignment frames are the CM frames for connection establishment between the

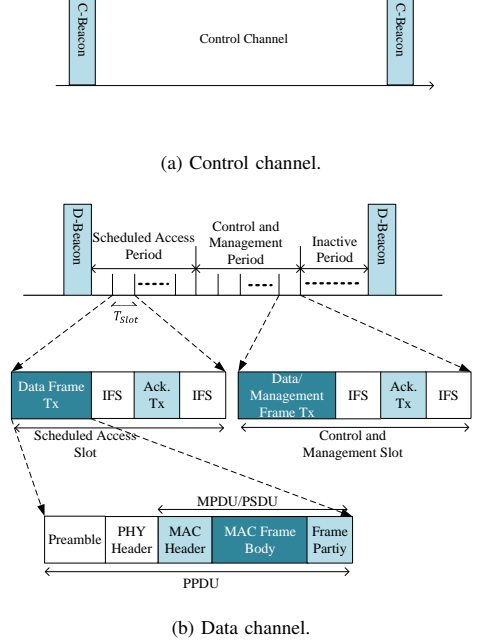
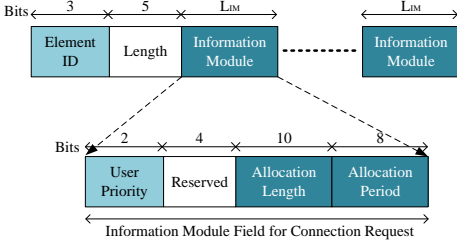


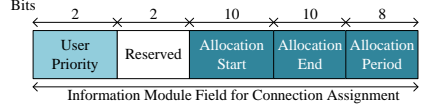
Fig. 1: Channel structure and general MAC frame format. Control channel involves the transmission of C-Beacon. Data channel has D-Beacon, scheduled access, CM and inactive periods. Scheduled access and CM period slot structure consists of PPDU and its acknowledgement set apart by IFS. Each PPDU has PHY-MAC layer overheads along with the data or control information payload.

hub and sensor nodes. These frame types use information units as the payload to communicate the relevant information specific to their procedures. Each information unit contains the element ID which indicates the category of information unit such as the connection request or connection assignment category. Length field represents the number of information modules of length L_{IM} inside the information unit. Fig. 2(a) and 2(b) depict the information modules corresponding to the connection request and connection assignment frames respectively. In Fig. 2(a), the allocation length denotes the total number of time slots requested in every IBI and allocation period represents the sequence number of D-Beacon at which the allocation may start. The allocation start and allocation end fields in Fig. 2(b) respectively depict the numbers at which the slot allocation starts and ends. The allocation period in Fig. 2(b) again denotes the sequence number of D-Beacon at which the allocation starts [11].

The allocation length field in the connection request information module only indicates the number of requested slots of fixed duration T_{Slot} , such that each allocated scheduled access slot has the slot structure shown in Fig 1(b). Similarly, the allocation start and allocation end fields in connection assignment



(a) Information module for connection request information unit.



(b) Information module for connection assignment information unit.

Fig. 2: Information modules for (a) connection request and (b) connection assignment. Each of these information modules is appended with “Element ID” and “Length” fields to generate the information unit. Connection request and connection assignment frames send information units as their payloads.

information module represent the number of allocated slots of pre-defined length T_{Slot} . Therefore, the connection request and connection assignment information modules in the existing SmartBAN standard cannot modify T_{Slot} as per the sensor node traffic demands.

C. Connection Establishment and Data Transmission Procedures

For connection initialization, the unconnected node monitors the C-Beacon at the control channel from which the data channel parameters such as slot length parameter (indicated by L_{Slot}) and the number of slots in IBI are acquired. The parameter L_{Slot} specifies the IBI slot duration T_{Slot} beforehand and each data or control frame transmission along with its acknowledgement should take place within this pre-defined slot duration T_{Slot} . The data channel is monitored for D-Beacon which provides the CM period and inactive period start. The connection request frame, as mentioned in sub-section IIB, is transmitted by the unconnected sensor node during the CM period. The frame is acknowledged by the hub upon a successful reception in the given slot. The hub then sends the connection assignment frame in the upcoming slot or the next IBI during the CM period which is acknowledged by the targeted sensor node in a similar way.

After the connection establishment, data communication between the given node and the hub takes place during scheduled access period [11]. Scheduled access period in IBI is generally contention-free and data PPDU can be transmitted by the sensor node in the allocated scheduled access slot(s) after the connection establishment. The transmission of data PPDU is acknowledged by the hub within the same slot. Both the PDU transmissions and acknowledgements are separated by IFS, as discussed in sub-section IIA.

III. MAC THROUGHPUT AND ENERGY CONSUMPTION ANALYSIS

The MAC throughput associated with each sensor node is defined by its total number of bits transmitted per second. The theoretical MAC throughput TP_{Th} can be found by the multiplication of the number of IBIs sent in one second N_{IBI}

and the total data payload size PL sent by the given node in each IBI, as

$$TP_{\text{Th}} = N_{\text{IBI}} \times PL. \quad (1)$$

The first term can be found by the reciprocal of the IBI duration T_{IBI} , therefore (1) becomes

$$TP_{\text{Th}} = \frac{1}{T_{\text{IBI}}} \times PL. \quad (2)$$

The IBI duration for the SmartBAN includes the D-Beacon, scheduled access, CM period and inactive durations and can be written as

$$T_{\text{IBI}} = T_{\text{Beacon}} + T_{\text{SA}} + T_{\text{CM}} + T_{\text{IA}}, \quad (3)$$

where T_{Beacon} is the duration of D-Beacon slot which equals T_{Slot} . T_{SA} , T_{CM} and T_{IA} are scheduled access, CM and inactive durations respectively. Since the entire IBI duration T_{IBI} is divided into the slots of equal size T_{Slot} , so T_{IBI} can also be represented as

$$T_{\text{IBI}} = T_{\text{Beacon}} + N_{\text{SA}} \times T_{\text{Slot}} + N_{\text{CM}} \times T_{\text{Slot}} + N_{\text{IA}} \times T_{\text{Slot}}, \quad (4)$$

or

$$T_{\text{IBI}} = N_{\text{Slot}} \times T_{\text{Slot}}, \quad (5)$$

where N_{SA} , N_{CM} and N_{IA} are the number of slots in scheduled access, CM and inactive durations respectively. N_{Slot} is the total number of slots in the entire IBI duration. Substituting T_{IBI} from (4) or (5) in (2), the expression for TP_{Th} becomes

$$TP_{\text{Th}} = \frac{1}{\left(T_{\text{Beacon}} + N_{\text{SA}} \times T_{\text{Slot}} + N_{\text{CM}} \times T_{\text{Slot}} + N_{\text{IA}} \times T_{\text{Slot}} \right)} \times PL, \quad (6)$$

or

$$TP_{\text{Th}} = \frac{1}{N_{\text{Slot}} \times T_{\text{Slot}}} \times PL. \quad (7)$$

The SmartBAN is intended to facilitate a maximum throughput of up-to 1000Kbps [1].

TABLE II: Payload size (bytes) for different L_{Slot} values and repetition modes.

L_{Slot}	Field Value in C-Beacon	T_{Slot} (ms)	Payload (bytes) No Repetition	Payload (bytes) 2 Repetitions	Payload (bytes) 4 Repetitions
1	000	0.625	8	NA	NA
2	001	1.25	86	35	9
4	010	2.5	243	113	48
8	011	5	555	269	126
16	100	10	1180	582	283
32	101	20	2430	1207	595

The data payload transmitted by a sensor node depends upon the number of slots allocated to it in each IBI as well as the slot duration T_{Slot} . Since each slot includes PPDU transmission duration T_{Tx} , two IFS of length T_{IFS} and acknowledgement duration T_{Ack} , therefore

$$T_{\text{Tx}} = \frac{T_{\text{Slot}} - T_{\text{Ack}} - 2 \times T_{\text{IFS}}}{\text{REP}}, \quad (8)$$

where REP is the number of times an identical PPDU is repeated. Within T_{Tx} , the PHY and MAC overheads are also transmitted along with the data payload. Hence, the effective payload size in bits for a single slot becomes

$$PL = T_{\text{Tx}} \times R_{\text{Sym}} - K_{\text{Overhead}}, \quad (9)$$

where R_{Sym} is the symbol rate. For uncoded SmartBAN transmissions, $K_{\text{Overhead}} = K_{\text{Preamble}} + K_{\text{PHY}} + K_{\text{Parity}} + K_{\text{MAC}}$. K_{Preamble} , K_{PHY} , K_{Parity} and K_{MAC} respectively denote the number of bits in preamble, PHY header, frame parity and MAC header. [11] and [18] can be referred for the computation of PHY-MAC overheads, T_{Ack} and T_{IFS} .

Table II summarizes the payload size in bytes for different L_{Slot} values and repetition scenarios, calculated using (8) and (9). It can be observed that the amount of payload transmitted in a single slot decreases with the reduction in slot length. The minimum slot length T_{Min} provides the PPDU transmissions only once. No PPDU repetitions are allowed because with 0.625ms slot duration, the amount of related PHY-MAC overheads to constitute a complete PPDU cannot be transmitted more than once. According to (6) and (7), TP_{Th} decreases with the increase in IBI duration which in turn increases due to the higher number of slots N_{Slot} and/or longer slot duration T_{Slot} . However (6) and (7) also reflect that the throughput increases if more PL is accommodated per IBI transmission. Since larger slot durations allow the transmission of more

payload in a single round therefore, the MAC throughput theoretically improves for increased slot durations, keeping N_{Slot} constant. This is depicted in Fig. 3 which provides the aggregated theoretical MAC throughput TP_{Th} , found using (6), (7), (8) and (9), with respect to the number of slots in scheduled access duration. One D-Beacon slot, two slots in CM period and one slot in inactive duration are assumed in the IBI duration for plotting these results. The throughput results provided in Fig. 3 indicate that with the increase in individual slot durations T_{Slot} , the payload PL increases which in turn increases the theoretical throughput TP_{Th} . But increasing the number of slots in IBI (N_{Slot}) beyond a certain limit does not result in higher throughput because of the corresponding increase in IBI duration. Moreover is no significant difference in the throughput attained with longer slot durations of 5ms and 10ms compared to the 2.5ms slot. The reason for this is that as the slot size increases to 5ms or 10ms, the IBI duration also increases significantly. Therefore, less number of IBIs are transmitted in one second, thus saturating the overall increase in throughput.

The total energy consumed during the active transmission and reception at both the sensor nodes and hub is the summation of energies utilized in the data payload and overheads communication. While the energy consumed during the data payload transmission leads to the enhanced effective throughput, the frequent transmission of PHY-MAC overheads and data acknowledgements results in high overhead energy consumption. The primary source of overheads in each scheduled access time slot consists of PHY-MAC layer headers and the subsequent acknowledgements sent by the hub. Therefore, the resulting energy consumption at each sensor node due to overheads in scheduled access time slot can be written as

$$E_{\text{OHnode}} = 3V \times T_{\text{B}} \times I_{\text{mA}}^{\text{Rx}} + 3V \times \frac{K_{\text{Overhead}}}{R_{\text{Sym}}} \times I_{\text{mA}}^{\text{Tx}} + 3V \times T_{\text{Ack}} \times I_{\text{mA}}^{\text{Rx}}, \quad (10)$$

where $I_{\text{mA}}^{\text{Tx}}$ and $I_{\text{mA}}^{\text{Rx}}$ are the current consumptions in mA at the transmission and reception respectively. T_{B} is the beacon transmission duration. The first term in (10) denotes the energy consumption due to the reception of D-Beacon at the IBI beginning. The second term corresponds to the energy consumption during the PHY-MAC layer overheads transmission by the sensor node. The third term represents the energy consumption due to the reception of packet acknowledgement sent by the hub. $3V$ represents the hub or sensor node's supply voltage. It is chosen as 3 volts because for the nRF52832 BLE device [19], considered in simulations throughout the article, the supply voltage range is 1.7 volts to 3.6 volts.

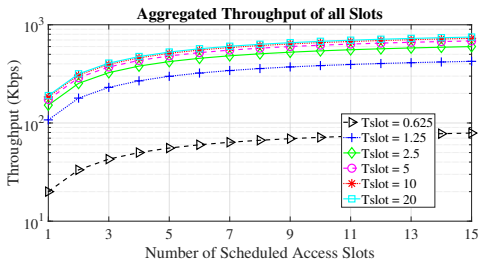
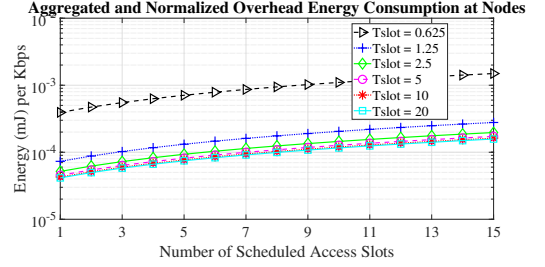
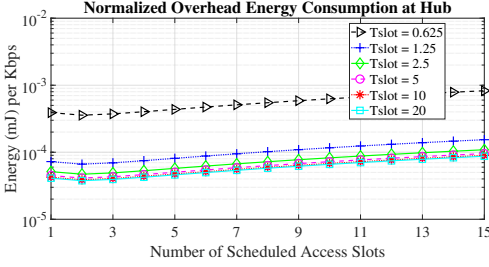


Fig. 3: Aggregated theoretical MAC throughput (Kbps) with respect to the number of scheduled access slots.



(a) Normalized PHY-MAC overhead energy consumption (mJ) at the hub. (b) Aggregated and normalized PHY-MAC overhead energy consumption (mJ) at the sensor nodes.

Fig. 4: PHY-MAC overhead energy consumption (mJ) normalized to the aggregated theoretical MAC throughput (Kbps) with respect to the number of scheduled access slots.

Moreover, the values of supply voltages are generally taken the same for all the transceivers in a given WBAN [20]. Subsequently, the overhead energy consumption at the hub in scheduled access communication is due to the transmission of D-Beacon and packet acknowledgements and the reception of PHY-MAC layer overheads appended with the payload. It can be mentioned as

$$E_{OH_{hub}} = 3V \times T_B \times I_{mA}^{Tx} + \sum_{N_{SA}} \left\{ 3V \times \frac{K_{Overhead}}{R_{Sym}} \times I_{mA}^{Rx} + 3V \times T_{Ack} \times I_{mA}^{Tx} \right\}. \quad (11)$$

According to (10) and (11), each time a node is assigned an extra slot for data transmission, the related PHY-MAC headers, preamble and acknowledgement overhead energy is also consumed by both the hub as well as the sensor nodes. We calculated overhead energy consumption results for both the hub and sensor nodes and normalized them to the effective theoretical throughput, shown in Fig. 3 (per Kbps). These results are illustrated in Fig. 4(a) and 4(b) respectively. Generally the energy consumption is normalized to the total number of bits or bytes transmitted. But we provide the energy consumption results normalized to the throughput for two reasons. 1) The energy utilized in transmission and reception is meant to increase the overall data throughput as well. 2) The normalization of energy consumption to the effective throughput also serves the same purpose with better analysis because the throughput, by definition, refers to the number of bits transmitted in one second. It can be observed that the normalized overhead energy consumption at both the hub and sensor nodes becomes higher as the number of slots in IBI increase and the slot size decreases.

One of the methods for managing the throughput requirements, without allocating the extra slots to high data rate sensor nodes and increasing the IBI size as well as the frequent transmissions of PHY-MAC overheads and acknowledgements, is slot reassignment. Slot reassignment refers to the periodic allocation of the unused slots of low data rate sensor nodes to the high data rate sensor nodes. The slot reassignment frames are also transmitted as information units appended with PHY-MAC overhead, from the hub to the

sensor nodes, as discussed in sub-section IIB. During slot reassignment procedure, the hub first informs all the sensor nodes of possible slot re-allocations in D-Beacon and then sends the slot re-assignment frame during the CM period of the IBI [11]. So, the additional energy consumption at each sensor node because of the slot reassignment during the run time can be described as

$$E_{SRaNode} = 3V \times \frac{\left(K_{Overhead} + K_{ID} + K_L + N_{SRas} \times K_{SRas} \right)}{R_{Sym}} \times I_{mA}^{Rx}, \quad (12)$$

where K_{ID} , K_L , K_{SRas} and N_{SRas} represent the element ID field size in bits, length field size in bits, slot re-assignment information module size in bits and the number of sensor nodes which receive the slot reassignment frame [11] respectively. In a similar manner, the related extra energy consumption at the hub due to slot reassignment frame transmission becomes

$$E_{SRaShub} = 3V \times \frac{\left(K_{Overhead} + K_{ID} + K_L + N_{SRas} \times K_{SRas} \right)}{R_{Sym}} \times I_{mA}^{Tx}. \quad (13)$$

Consequently the execution of slot reassignment also leads to extra energy consumption at both the sensor nodes and the hub.

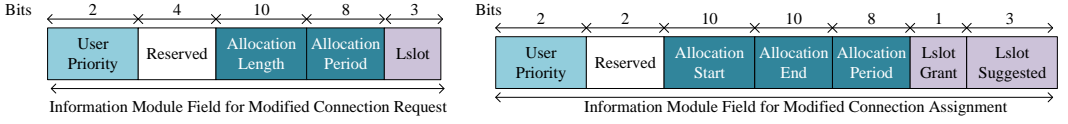
The energy consumptions at the nodes and the hub associated with the payload transmission during the scheduled access period are given as

$$E_{PLnode} = 3V \times T_{PL} \times I_{mA}^{Tx}, \quad (14)$$

and

$$E_{PLhub} = \sum_{N_{SA}} 3V \times T_{PL} \times I_{mA}^{Rx}, \quad (15)$$

where T_{PL} is the time duration for payload transmission and equals $\frac{PL}{R_{Sym}}$.



(a) Information module for modified connection request information unit. (b) Information module for modified connection assignment information unit.

Fig. 5: Suggested information modules for connection request and connection assignment in FETRO MAC. Additional fields associated with the requested and granted L_{slot} are added.

IV. FETRO MAC SCHEME WITH VARIABLE SLOT LENGTH

In view of the results given in Fig. 3, 4(a) and 4(b) as well as the discussion provided in section III, the main issues with the base-line scheduled access MAC are: i) Allocating extra slots to high data rate sensor nodes for throughput management not only decreases the throughput (due to long T_{IBI}) but also increases the PHY-MAC overhead and acknowledgement energy consumption, ii) Performing slot reassignment periodically also results in the extra overhead energy consumption due to slot reassignment frame transmission, and iii) Increasing the overall slot duration to accommodate the high data rate sensor nodes also increases the IBI duration which in turn results in the throughput saturation as shown in Fig. 3. These phenomena motivate the design of a MAC algorithm in which high data rate sensor nodes make data transmissions in longer slots while the slot durations assigned to low data rate sensor nodes should be small. It should be noted that the existing connection request or connection assignment frames can only notify about the number of allocated slots, whose duration T_{slot} is already defined and broadcast in C-Beacon. The existing frame format cannot modify slot duration (T_{slot}) depending upon the sensor node data rate requirements on the run-time. To overcome these issues with fixed slot duration scheduled access MAC in SmartBAN, this section elaborates on the FETRO MAC protocol. The variable slot length execution in the SmartBAN reduces the PHY-MAC and slot reassignment overheads as well as frequent acknowledgement transmissions for subsequently enhancing the throughput at a reduced overhead energy consumption.

In the proposed FETRO scheme, the slot durations are primarily allocated based on the amount of payload an individual node intends to send. The payload is determined by the sensor node's sampling rate and bit resolution. For example, an inertial measurement unit (IMU) sensor samples data at the rate of 1KHz and uses a bit resolution of 16 bits per sample, so a payload of 16 kilo bits shall be generated per second [1] which is also the data rate requirement of the given sensor. If the sampling rate and bit resolution of the same sensor type are decreased, the payload and the required sensor data rate shall also be reduced. As discussed in section III, the longer slot duration can carry more payload in a single transmission and smaller slot duration is sufficient to carry smaller payloads. Therefore, each sensor node provides its own required L_{slot} value at the time of connection establishment, depending upon

the sensor node's data rate requirement, sampling rate and bit resolution. For high data rate sensor nodes, more number of minimum slot units can be combined to create a longer T_{slot} which communicates more data payload simultaneously with less PHY-MAC and acknowledgement overheads. While for low data rate sensor nodes, shorter T_{slot} can be allocated which prevents the wastage of scheduled access resources and does not increase T_{IBI} unnecessarily.

The hub sends its response, indicating the acceptance (grant) of the requested L_{slot} , retainment of its own L_{slot} or the suggestion of another L_{slot} value. The hub decision and response in this context is again determined by the available resources like available energy, duty cycling status, number of connected sensor nodes and the presence of relay node. For example, if the hub is operating on low power mode and has to retain a duty cycling of less than 50%, it may reject a slot duration which increases the duty cycle of the hub. It should be noted that the FETRO MAC is effective if there are massive variations in the data rate requirements of the different sensor nodes in a given use case. The example applications would be "Precise Athlete Monitoring" use case in which both the EMG (hundreds of Kbps) and IMU (upto 16Kbps) measurements are taken for the athlete and "Rescue and Emergency Monitoring" use case in which both low data rate measurements like GPS and pulse monitoring (few bps data rate) as well as high data rate voice communication (upto 100Kbps) are required [21]. In such scenario, the proposed FETRO MAC will optimize the throughput by allocating the suitable slot duration to each sensor node and shall also reduce the overhead energy consumption, resulting due to extra slot allocation and slot reassignments for throughput management.

A. FETRO MAC Connection Request and Connection Assignment Frames

FETRO MAC is implemented by providing the few necessary modifications in the primary SmartBAN MAC frame format which are: i) Rather than broadcasting the number of slots in IBI N_{slot} within C-Beacon and D-Beacon at the beginning, the number of minimum slot duration (T_{Min}) units, i.e., N_{Min} should be broadcast by the hub, ii) The allocation length field in connection request information module, as given in Fig. 2(a), should indicate the number of minimum slot units (of length T_{Min}) requested by the sensor node, and iii) The allocation start and allocation end fields in connection assignment information module, as shown in Fig. 2(b), should

respectively represent the numbers at which the minimum slot unit allocation starts and ends. These modifications will ensure the necessary synchronization between the hub and the sensor nodes when the individual slot duration of each sensor node is different.

The FETRO MAC with variable slot length is executed by providing a minor ad-on to the connection request and the connection assignment information modules in the existing SmartBAN, as given in Fig. 2(a) and 2(b) respectively. The modified information modules for connection request and connection assignment information units are illustrated in Fig. 5(a) and 5(b) respectively. A three-bit field L_{Slot} is added in the modified connection request information module. The L_{Slot} field along with the element ID field, length field and PHY-MAC overheads constitutes the connection request frame, as mentioned in sub-section IIA. This added field is necessary to indicate the slot duration assigned to a particular sensor node. Using the L_{Slot} parameter in modified connection request and connection assignment information modules, the way of combining the given number of minimum slot duration T_{Min} units is determined.

B. Connection Establishment Procedure and IBI operation in FETRO MAC

Similar to the default connection establishment mechanism in SmartBAN, the sensor node trying to connect monitors the C-Beacon over the control channel and acquires the information about the data channel and other network parameters. Later, the sensor node monitors the data channel and D-Beacon for the CM period start to send its connection request frame. The node requests the L_{Slot} value, required by its payload, in the modified connection request frame which is acknowledged by the hub. Then the hub responds with a connection assignment frame, which includes an “ L_{Slot} Grant” field to signify the allocation status of the requested L_{Slot} value, with “1” referring the provision of the requested L_{Slot} value and “0” depicting the refusal of the requested L_{Slot} . In the second scenario, the hub either suggests its own “ L_{Slot} ” to satisfy the node throughput requirements or retains the L_{Slot} broadcast in the C-Beacon. The “ L_{Slot} Suggested” field is only present when the hub suggests its own slot length. The entire procedure for connection establishment in FETRO MAC with variable slot length is embodied in Fig. 6. The received connection assignment frame by the node is acknowledged and the communication starts taking place from the mutually agreed IBI between the sensor node and the hub.

The synchronization among other sensor nodes which are allocated different slot durations and the hub in FETRO MAC can be maintained with the help of the fact that the slot durations T_{Slot} for the increasing L_{Slot} values are the integer multiples of the T_{Min} , as can be seen in Table II. The proposed idea in FETRO MAC focuses on having a flexible and dynamic T_{Slot} assignment by keeping intact the existing integer multiple characteristic of slot durations represented by L_{Slot} values. The strategy here is that the D-beacon would broadcast the number of minimum length units N_{Min} , that are present within the IBI, in its “inter-beacon interval field” [11], where T_{Min} is

the minimum time slot duration possible in SmartBAN MAC. This would allow the sensor nodes to adjust their wake-up intervals irrespective of the L_{Slot} broadcast in the C-Beacon and the remaining slot sizes which are exclusively allocated to the other sensor nodes. An illustration of the IBI in the FETRO MAC scheme is shown in Fig. 7 in which the slots “1”, “2” and “4” follow the L_{Slot} broadcast in the C-Beacon whereas the slot number “3” has a duration equal to the twice of default slot length. Slot “5” has the duration equal to T_{Min} . Every slot has the frame transmission duration, acknowledgement duration and two IFS. The D-Beacon broadcasts the N_{Min} , i.e. the number of minimum time slot duration T_{Min} units in its “inter-beacon interval field” for the sensor nodes to adjust their wake-up intervals accordingly.

C. FETRO MAC Throughput and Energy Consumption Analysis

With the scheduled access slot duration distinctive to each node, the related throughput at every node in FETRO MAC technique also changes as every node sends a different payload, defined by its slot duration. The IBI with several distinct slot durations becomes

$$T_{\text{IBI}} = T_{\text{Beacon}} + \sum_{i=1}^{N_{\text{SA}}} T_{\text{Slot}}^i + T_{\text{CM}} + T_{\text{IA}}, \quad (16)$$

where T_{Slot}^i is the duration of individual scheduled access slots and $i = 1, 2, \dots, N_{\text{SA}}$. The FETRO MAC throughput associated with the slot duration T_{Slot}^i will therefore be written as

$$TP_{\text{Th}}^{\text{FETRO}} = \frac{1}{\left(T_{\text{Beacon}} + \sum_{i=1}^{N_{\text{SA}}} T_{\text{Slot}}^i + T_{\text{CM}} + T_{\text{IA}}\right)} \times PL^i, \quad (17)$$

where PL^i is the payload size which is defined by the scheduled access slot duration T_{Slot}^i . The data frame transmission duration and the effective payload size in bits for a single slot also change accordingly as

$$T_{\text{Tx}}^i = \frac{T_{\text{Slot}}^i - T_{\text{Ack}} - 2 \times T_{\text{IFS}}}{REP}, \quad (18)$$

and

$$PL^i = T_{\text{Tx}}^i \times R_{\text{Sym}} - K_{\text{Overhead}}, \quad (19)$$

respectively. The above equations indicate that allocating the slot duration according to the sensor nodes’ data rates in FETRO MAC leads to a better repletion of the individual data rate requirements at each sensor node.

The overhead energy consumption for the sensor nodes and hub in FETRO MAC strategy can be easily computed using (10) and (11) respectively. The energy consumption associated with the payload transmission in scheduled access period can be calculated using (14) and (15) respectively for the sensor nodes and hub. Note that the transmission of additional fields to define L_{Slot} in the modified connection request and connection assignment frames leads to a slight increase in energy consumption only at the time of connection establishment (as mentioned in sub-sections IvA and IVB)

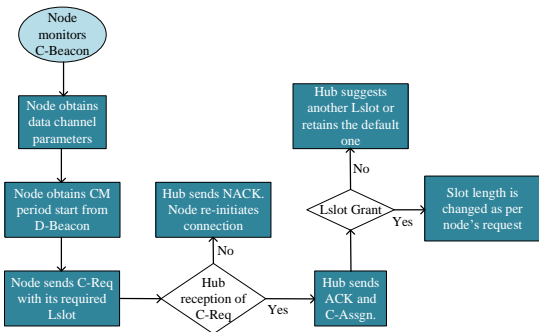


Fig. 6: Connection initialization in FETRO MAC protocol. The modified connection request frame by the node indicates the desired L_{Slot} and the modified connection assignment frame by the hub responds with the grant or refusal of the requested L_{Slot} .

in FETRO MAC. However, it can significantly reduce the overhead energy consumption which occurs periodically and frequently because of the “extra slot allocation” and “slot reassignment” techniques in conventional SmartBAN MAC for accommodating the high data rate sensor nodes’ throughput requirements.

V. PERFORMANCE EVALUATION

This section evaluates the performance of the existing SmartBAN MAC schemes for throughput management, such as the provision of extra slots and slot re-assignment, as well as the proposed FETRO MAC technique. The channel models and radio link modeling assumed in the simulation setup and the application use-case scenario are described as well.

A. Radio Link and Channel Modeling

We assume four different channel models for computing the pathloss values, i.e., static IEEE CM3B model with additive white Gaussian noise (AWGN) [16], dynamic IEEE CM3B (deterministic) channel model with AWGN [22], static IEEE CM3B model with fading [16] and deterministic channel model with fading. The static AWGN and Fading channel models are the standard for WBAN communication developed over the ISM 2.4GHz frequency band, widely termed as IEEE CM3B [16]. The static channel models (both AWGN and fading) are derived using the measurement campaigns in which nodes are placed on a static human body and the received signal is then modeled mathematically. Therefore, the static channel models do not take into account the human body mobility in pathloss calculations [22].

The integration of the effects of human body mobility in pathloss computation considers all the losses that occur due to human body shadowing under non-line of sight (NLOS) links. The biomechanical mobility traces are used to provide the on-body link distances and link types which are line of sight (LOS) or NLOS. Therefore deterministic channel model is considered for evaluating the realistic pathloss values. In the

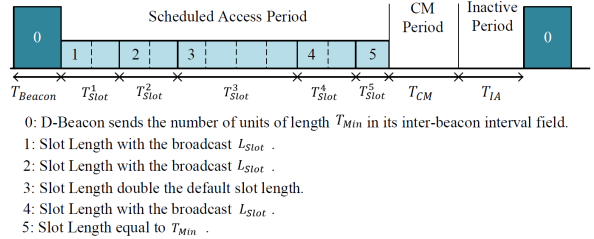


Fig. 7: IBI operation with different slot duration in FETRO MAC. Each slot has frame transmission duration and acknowledgement duration separated by IFS in scheduled access period. The duration of each slot T_{Slot} is an integer multiple of T_{Min} for retaining the synchronization at each node.

deterministic channel model with AWGN, dynamic distances and link types are generated for several on-body links between the sensor nodes and hub. As opposed to the static IEEE CM3B model dynamic distances are taken as input distances for pathloss calculation in the deterministic model. The space-time varying link types identify the given link as either LOS or NLOS links. An additional NLOS factor of 13% is added to the computed pathloss value with time-varying distances, for NLOS link condition, otherwise the pathloss remains unchanged [22]. The realistic channel model with fading can be derived by taking the CM3B channel model with fading [16] as the baseline, integrating the dynamic distances and adding the space-time varying link-related pathloss values. The deterministic channel model with fading, therefore, includes all the losses that occur due to short-term fading and the human body shadowing under mobility.

After determining the pathloss results, a radio link modeling is performed which includes the computation of signal-to-noise ratio (SNR), bit error rate (BER) and packet error rate (PER) calculations. For the radio link modeling, an identical approach is followed in this article as was proposed in [17] with slight modifications in the BER expressions. The Gaussian Frequency Shift Keying (GFSK) modulation technique with the bandwidth-bit period product BT and modulation index h of 0.5 [18] is used at SmartBAN PHY layer. Therefore, the theoretical expression to compute the BER at the SmartBAN PHY layer is given by [23, eq. (10)] under AWGN channel. Whereas the upper bound to calculate the BER at the SmartBAN PHY layer under fading channel is written as [23, eq. (11)]. The details of the computations from the BER to the PER and the packet reception status can be found in [17].

B. Use Case Description

We assume a health monitoring application scenario for the performance assessment of the conventional SmartBAN MAC and the proposed MAC protocol. It is a health and fitness

TABLE III: Use Case Scenario for Performance Evaluation [25]–[27].

Health and Fitness Monitoring Application	
Sensor Type	Throughput Requirements
EMG (1 channel)	240Kbps
ECG (3 channels)	7.5Kbps
Pulse Oximeter Sensor	1.92Kbps

monitoring use case which involves simultaneous monitoring of ECG, EMG and pulse oximetry signals. Similar type of patient monitoring use cases are extensively discussed in the section II of [24]. The sensor nodes in the given medical use-case generate constant bit rate traffic which is deterministic and therefore, the scheduled access MAC schemes are the most suitable ones for handling this traffic category. Both the MAC schemes in the existing SmartBAN standard as well as the proposed FETRO MAC are based on the scheduled access.

The ECG node contains three channels with ten bits resolution at 750Hz sampling rate, leading to 7.5Kbps data rate per channel [25], [26]. The EMG sensor consists of a single channel sampled at 30KHz rate with eight bits of precision [25], [26], giving a data rate of 240Kbps. For pulse oximetry measurement, a sensor module with a total data rate of 1.92Kbps is considered [27]. The total throughput required by this health and fitness monitoring application, therefore, sums upto 264.42Kbps. Given the individual data rate requirements of the sensor nodes, a slot duration of 0.625ms would be enough to support the data rates of the majority nodes except of the EMG sensor. However for performance evaluation, we consider three different values of T_{slot} in the conventional SmartBAN MAC which are 0.625ms, 1.25ms and 2.5ms. Furthermore, the slot durations of 5ms, 10ms and 20ms are not considered in the performance analysis because there is no significant difference in the theoretical throughput results with these slot sizes compared to the 2.5ms slot, as depicted in Fig. 3. The sensor types, number of nodes and their throughput requirements for the given use-case are summarized in Table III.

For each considered slot duration, we assume three different conventional SmartBAN MAC strategies to manage the throughput requirements of the health and fitness monitoring application. The first one is the reference scheme, in which each channel/node is allocated a single scheduled access slot, and hence there would be five slots in the scheduled access period. There are two slots in the CM period for management operations and one slot in inactive duration in all MAC strategies. This results in the IBI period of 5.625ms and 178 IBIs per second with 0.625ms slot, 11.25ms IBI and 89 IBIs per second with 1.25ms slot and 22.5ms IBI and 44 IBIs per second with 2.5ms slot. In the reference scheme with 0.625ms slot, each ECG and EMG channel sends data at every IBI while the pulse oximeter makes transmission after every 5 IBIs. The EMG node sends data at every IBI in the reference scheme with 1.25ms and 2.5ms slot durations. ECG channels send data after every 8 and 11 IBIs with 1.25ms and 2.5ms slot durations respectively. While the pulse oximeter node makes transmissions after 22 and 29 IBIs with 1.25ms and 2.5ms slot

durations correspondingly.

In the second strategy, extra slots are provided to the high data rate sensor nodes. With 0.625ms, 1.25ms and 2.5ms slot durations, the high data rate EMG node is allocated three, one and one extra slots respectively. Whereas the slot allocations for ECG and pulse oximeter nodes remain the same. This results in the entire IBI duration of 7.5ms and 133 IBIs per second with 0.625ms slot, 12.5ms IBI duration and 80 IBIs per second with 1.25ms slot length and 25ms IBI duration and 40 IBIs per second with 2.5ms slot. The ECG and EMG nodes make transmission at every IBI whereas the pulse oximeter node sends data after every 4 IBIs with the slot duration of 0.625ms. The EMG node makes transmissions at every IBI when extra slots are assigned with 1.25ms and 2.5ms slot durations. The intervals between the successive transmissions for ECG channels become 7 and 10 respectively with 1.25ms and 2.5ms slot durations. Whereas the pulse sensor sends data after every 26 and 20 IBIs with 1.25ms and 2.5ms slots respectively. It should be noted that the number of extra slots assigned to the high data rate sensor node are not increased beyond one for longer slot durations because it increases the IBI duration which in turn would decrease the throughput, according to the theoretical throughput results indicated in Fig. 3.

The slot reassignment strategy has a similar IBI duration as the reference SmartBAN MAC scheme but the unused slots of ECG channels and pulse oximeter node are strategically reassigned to manage the EMG channel transmissions. Finally, in the proposed FETRO MAC with variable slot length, a slot duration of 2.5ms is assumed for EMG channel while the remaining nodes retain a slot length of 0.625ms since this slot length is enough to manage their throughput requirements. With an IBI of 7.5ms, EMG and ECG nodes send data at subsequent IBIs. While the pulse oximeter node keeps a

TABLE IV: Simulation Setup Parameters.

RF Parameters [19]	
Transmitter Power (dBm)	0
Receiver Sensitivity (dBm)	-96
Current Consumption Tx ($I_{\text{mA}}^{\text{Tx}}$)	5.3
Current Consumption Rx ($I_{\text{mA}}^{\text{Rx}}$)	5.4
Current Consumption (idle) ($I_{\text{mA}}^{\text{idle}}$)	1.2
Bandwidth per channel (MHz)	2
Information Rate (Kbps)	1000
Modulation type	GFSK ($h = 0.5$ and $BT = 0.5$)
PHY/MAC Parameters [11] [18]	
Minimum slot length (T_{Min})	625 μs
Interframe spacing (IFS)	150 μs
Acknowledgement Duration (T_{Ack})	128 μs
Beacon Duration (T_{B})	104 μs
Beacon Duration with slot reassignment (T_{B})	128 μs
Symbol Rate (R_{Sym})	10^6
MAC header (K_{MAC})	7 octets
PHY header (K_{PHY})	5 octets
Preamble (K_{Preamble})	2 octets
Frame Parity (K_{Parity})	2 octets
Element ID and Length fields ($K_{\text{ID}} + K_{\text{L}}$)	1 octet
Slot Reassignment information module (K_{SRas})	4 octets
Number of slots in CM period (N_{CM})	Two
Number of slots in inactive period (N_{IA})	One

transmission periodicity of 4 IBIs in the suggested FETRO MAC protocol.

C. Simulation Setup

The trace file that provides space-time varying distances and link types for the deterministic channel models (with and without fading) assessment of this application scenario is about 59 seconds long and contains several mobility patterns such as walking, sitting and hand motions. The pathloss values for the static CM3B channel models (with and without fading) are repeated for the identical duration to give the performance evaluation at a similar time span. The simulation with this trace file is repeated 100 times to give more reliable results. For the performance assessment of conventional SmartBAN MAC strategies and FETRO MAC, we consider transmission power levels of “0dBm”, defined for nRF52832 BLE device [19]. The sensor nodes and the hub go into an idle mode while not performing any active transmission or reception, except during the T_{Tx} of the scheduled access and CM slots when the hub has to remain in the active mode for any other possible frame reception. The other relevant RF specifications and PHY-MAC parameters are summarized in Table IV. All the simulations are performed using the MATLAB script files.

D. Simulation Results

This sub-section elaborates the simulation results for the given simulation setup and the use-case scenario in terms of the throughput attained at the receiving end as well as normalized the energy consumption per Kbps due to payload transmission and overheads. The throughput results under ideal channel conditions for the baseline SmartBAN and FETRO MAC schemes can be calculated using (4) and (17) respectively. But the practical WBAN channels greatly impact the effective throughput attained at the receiver. The effective throughput under the given channel conditions, such as AWGN or fading and static or deterministic, can be computed as

$$Th_{Pr} = \frac{N_{Rx}}{T_{Trace}}, \quad (20)$$

where N_{Rx} is the total number of received bits for each node in the given time span and the T_{Trace} is complete duration of the pathloss file, as given in sub-section IVC.

1) *Throughput Analysis*: The aggregated throughput results of all the sensor nodes in the given health and fitness monitoring applications for the given 59 seconds trace duration are presented in Fig. 8. We refer to the “static AWGN channel” as “C1”, deterministic AWGN channel” as “C2”, “static fading channel” as “C3” and the “deterministic fading model” as “C4” in all the performance evaluation results. This is the effective throughput attained by the packet transmissions of all the sensor nodes for different channel types with several slot durations compared against the proposed FETRO MAC strategy. The throughput results of the extra slot and the slot reassignment cases are better than the reference SmartBAN case under all channel conditions and MAC slot durations. Also, the throughput outcomes for all the MAC scenarios with fixed slot durations, i.e., reference, extra slot allocation

and slot re-assignment cases, are not significantly changed under different channel types for 0.625ms slot duration. This is because with smaller slot durations of 0.625ms, the payload size is also very small (8bytes, as mentioned in Table II), leading to lower PER values even under extremely poor channel conditions [23]. This leads to the reception of almost all the transmitted bits, resulting in higher throughput under static as well as dynamic channels, with and without fading. But all the MAC scenarios with fixed slot durations fail to achieve a total throughput of 264.42Kbps using the 0.625ms slot length.

For 1.25ms slot duration, the reference SmartBAN MAC and the SmartBAN MAC with extra slots fail to attain the throughput requirements under all the channel conditions because of the transmission of insufficient payload and increased IBI duration respectively. However the throughput is significantly improved with slot reassignment strategy under the static and deterministic AWGN channels. It is because the unused slots of other nodes/channels are re-allocated to the EMG for maximum resource utilization within the smaller IBI duration. The same trends in throughput can be observed with 2.5ms slot duration under the static and deterministic AWGN channels. The throughput results degrade under the static and deterministic fading channels with 1.25ms and 2.5ms slot durations because of the transmission of large payload at once which results in higher PER values under poor channel conditions [23].

Referring to (17), with an IBI of 7.5ms and the allocated slot size of 2.5ms in FETRO MAC, EMG can achieve a total throughput of 258.55Kbps in total (243 bytes in a single transmission, $243 \times 8 \times 133$). Each of the 3 ECG channels can obtain a total throughput of 8.5Kbps (8 bytes in a single transmission, $8 \times 8 \times 133$). While the pulse oximeter which makes transmission after every 5 IBIs achieves a throughput of 2.128Kbps (8 bytes in a single transmission, $8 \times 8 \times 133/4$). This leads to a total theoretical throughput of 286.178Kbps in FETRO MAC which is certainly within the bounds as shown by Fig. 8. Both the static CM3B and the deterministic AWGN channels have considerably high throughput of more than 275Kbps for the proposed FETRO MAC protocol with variable slot length. It clearly demonstrates the potential of the suggested MAC scheme in fulfilling the total throughput requirements of the use-case considered. The effective throughput results for FETRO MAC respectively become 195Kbps and 110Kbps for the static CM3B and the realistic channel models with fading. This phenomenon can be explained by the two facts. One is the transmission of larger payload size (234bytes) in the slot allocated to the EMG node. Other is the BER calculation on Rician fading channel, taking an upper bound expression [23, eq. (11)] which gives the highest possible error rate results. With the upper bound results of BER, the related PER also takes the maximum values which in turn decreases the total number of received bits N_{Rx} and the attained throughput Th_{Pr} under the fading channels.

The provision of variable slot durations within an IBI makes the scheduled access MAC highly adaptable according to the throughput requirements of the individual sensor nodes in FETRO MAC. For example, with 0.625ms slot length extra

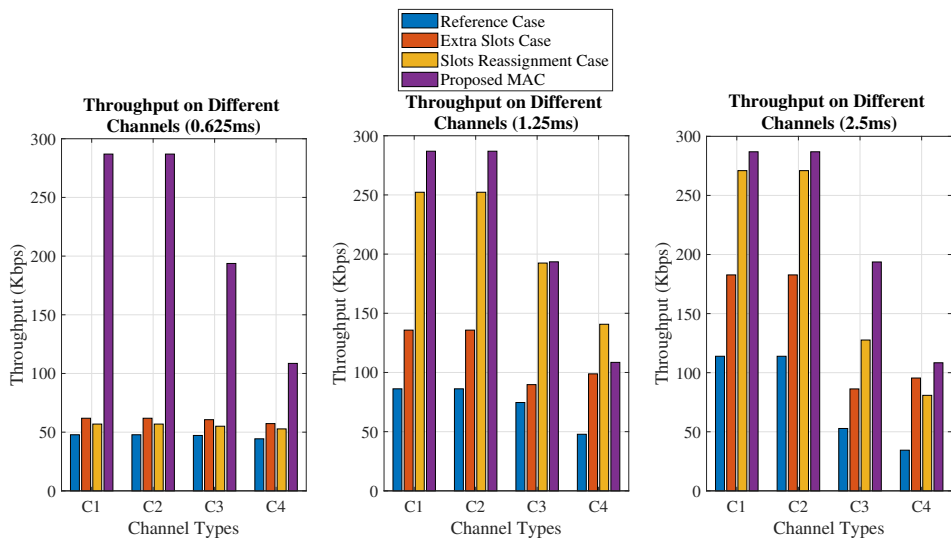


Fig. 8: Throughput on different channel types (Kbps), health and fitness monitoring applications. C1: Static AWGN channel, C2: Deterministic AWGN channel, C3: Static fading channel, C4: Deterministic fading channel.

slot allocation SmartBAN scheme, EMG is allocated 4 slots in total with 3 of them as extra slots. There are 133×4 ACK transmissions and 133×4 overhead transmissions (for 133 IBI per second) for transmitting the EMG payload. Also there are 2 IFS within each slot which results in 8 IFS for a single EMG transmission with extra slots and 133×8 IFS per second. In FETRO MAC, these numbers are reduced to 133 ACK transmissions, 133 overhead transmissions, and 133×2 IFS per second for EMG node. Therefore, there is an overall reduction of extra 399 ACK transmissions, 399 packet overhead transmissions and 798 IFS which collectively lead to a significantly high throughput with the proposed scheme. FETRO MAC also helps preventing the wastage of scheduled access resources due to the allocation of unnecessary longer slot durations to low data rate sensor nodes.

2) *Node Energy Consumption Analysis:* The aggregated and normalized energy consumption per Kbps can be found as the ratio of total energy utilized in the entire trace duration (mentioned in sub-section VC) and the attained effective throughput. Fig. 9 illustrates the aggregated payload and overhead energy consumption per Kbps results for all the sensor nodes. The aggregated energy of all the sensor nodes is summed up for the entire trace duration and normalized to the effective throughput, as shown in Fig. 8. The energy can also be normalized to the number of bits or bytes transmitted successfully in the entire trace duration. But here the energy is normalized to the effective throughput which again refers to the number of bits transmitted successfully per second. The results are presented for the similar channel types and slot durations, as mentioned in sub-sections VA and VB. Furthermore, the energy consumption results of the conventional SmartBAN MAC scheduling strategies with 0.625ms, 1.25ms

and 2.5ms slot durations are compared against the proposed FETRO MAC. Since the motivation behind FETRO MAC is the reduction of overhead energy consumption, therefore we provide comparison taking overhead energy consumption per Kbps as the primary metric.

For 0.625ms slot duration and under all the given channel types, employing FETRO MAC decreases the normalized overhead energy consumption by 84.6%, 80.9% and 83% in comparison with the reference, extra slot allocation and slot reassignment SmartBAN MAC schemes respectively on average. The allocation of three extra slots to manage the EMG node throughput requirements incorporates the additional PHY-MAC layer and acknowledgement overhead energy consumption at node, as given by (10). The slot reassignment strategy has high overhead energy consumption with 0.625ms slot because of more frequent slot re-allocations to handle high data rate EMG sensor node.

The overhead energy consumption per Kbps is significantly decreased in all three conventional SmartBAN MAC schemes (reference, extra slot, slot reassignment) with 1.25ms and 2.5ms slot durations because of the transmission of relatively higher payload with less overheads. Nevertheless, the proposed FETRO MAC reduces the normalized energy consumption per Kbps by 65%, 53.3% and 49% as compared to the reference, extra slot allocation and slot reassignment SmartBAN MAC scheduling methods respectively, on average, with 1.25ms slot length. With 2.5ms slot, the proposed FETRO MAC results in an average decrease of 42.8% in overhead energy consumption per Kbps outcomes in contrast to the conventional SmartBAN MAC scheduling methods. The normalized overhead energy consumption per Kbps results for FETRO MAC are increased under the deterministic fading channel because of the related

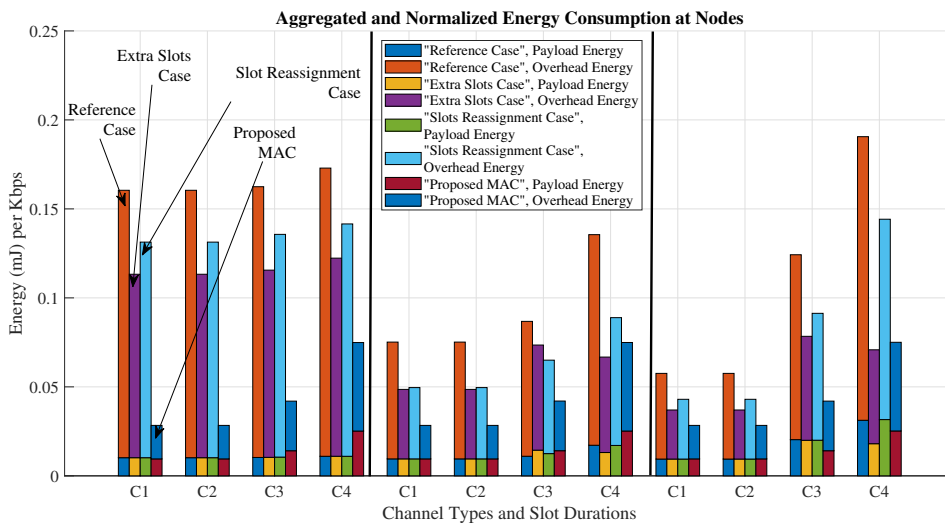


Fig. 9: Node energy consumption (mJ) per Kbps, health monitoring and fitness applications. C1: Static AWGN channel, C2: Deterministic AWGN channel, C3: Static fading channel, C4: Deterministic fading channel.

decrease in FETRO MAC throughput results, as previously shown in Fig. 8.

It can also be observed that the normalized overhead energy consumption is much higher than the normalized payload energy consumption but decreases with the increase in slot size. It is because all three base-line SmartBAN MAC strategies utilize a lot of energy in transmitting and receiving overheads (PHY-MAC, acknowledgement, slot reassignment and others) while attaining comparatively low effective throughput. The energy is also consumed when the sensor nodes and hub are in the active state during the CM period for the possible reception of control frames by the other WBAN nodes. So, the longer the slot duration, the higher is the energy to keep the device in the active state. Furthermore the normalized overhead (or payload) energies are much higher for the deterministic fading channel because the corresponding effective throughput is considerably declined under the static and deterministic fading channels.

3) *Hub Energy Consumption Analysis*: The normalized energy consumption results for hub are depicted for the conventional SmartBAN MAC strategies and compared against the proposed FETRO MAC in Fig. 10 for the identical channel types and slot durations. The hub energy consumption is summed up for the entire trace duration and normalized to the effective throughput, as shown in Fig. 8. The payload and overhead energy consumption per Kbps outcomes for the hub follow a similar pattern as the aggregated and normalized energy consumption per Kbps results for the nodes. Employing the FETRO MAC cuts down the overhead energy consumption per Kbps by 75%, 62.5% and 40% as compared to the conventional SmartBAN scheduling methods with 0.625ms, 1.25ms and 2.5ms slot durations respectively.

The aggregated and normalized payload energy consump-

tion, as shown in Fig. 9 and Fig. 10 for the nodes and hub respectively, is related to the actual data payload transmission by the sensor nodes. The larger the payload transmitted per unit time, the higher shall be the payload energy consumption. However all of the transmitted payload is not received successfully because of the channel losses. The fading channel types (both static and deterministic) have more packet losses compared to the AWGN channel types, resulting in the reduced effective throughput. This phenomenon is also illustrated in the throughput results (Fig. 8) in which the attained effective throughput is comparatively higher under AWGN channel types while the throughput decreases under fading channels for the same MAC procedures. If the aggregated payload energy consumption (at both the sensor nodes and hub) for some MAC algorithm is high and there are negligible channel losses, the higher effective throughput shall normalize it to the same level because all the consumed energy is utilized in the successful packet reception. Likewise, if some MAC technique transmits less payload with more overheads, the lower effective throughput normalizes that low (aggregated) payload energy to yield the same level of normalized energy usage. But under the fading channel types, the effective throughput decreases because of the higher channel losses although the same payload transmission energy is consumed for the given method (at both the sensor nodes and hub) as in the AWGN channels. Therefore, the normalized payload energy consumption performance varies under fading channels for the different methods compared. This throughput degradation under the fading channel types is more obvious for 1.25ms and 2.5ms slot durations, as shown in Fig. 8. Therefore, the changes in normalized payload energy consumption (of the methods compared) are also more observable for 1.25ms and

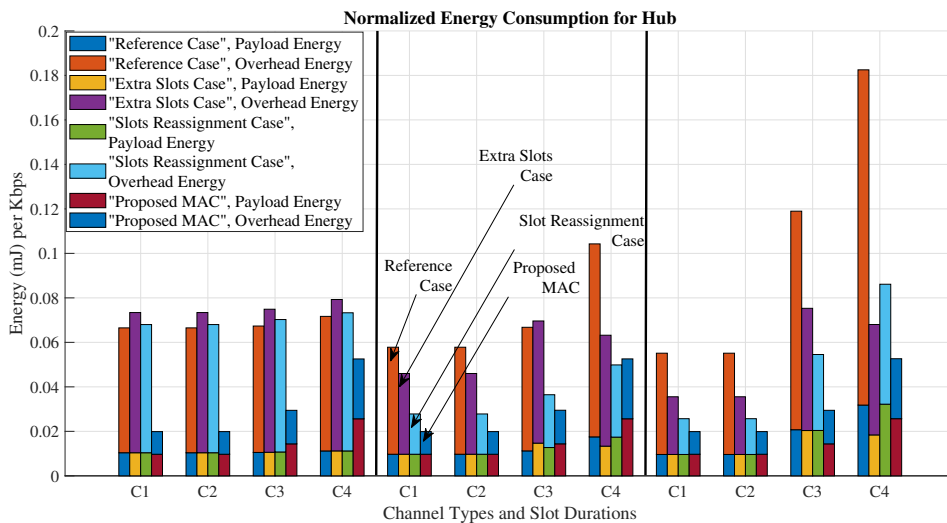


Fig. 10: Hub energy consumption (mJ) per Kbps, health monitoring and fitness applications. C1: Static AWGN channel, C2: Deterministic AWGN channel, C3: Static fading channel, C4: Deterministic fading channel.

2.5ms slots.

VI. CONCLUSION

This paper thoroughly discusses the potential of SmartBAN MAC layer to collectively manage the throughput requirements of the sensor nodes with varying data rates. In this regard, both extra slots allocation and slot reassignment methods are investigated for health and fitness monitoring applications. Either additional slots are allocated to high data rate sensors or empty slots within an IBI are utilized to regulate the proper data transmission in a slot reassignment method. Both of these strategies in existing SmartBAN MAC require more PHY-MAC overheads. The provision of longer slot durations in the simultaneous presence of low and high data rate sensors may lead to the under-utilization of SmartBAN scheduled access resources due to fixed slot length allocation. An innovative FETRO MAC technique with variable slot length is proposed in this article which requires minimal changes in the baseline SmartBAN structure. The suggested variable slot length MAC scheme is based on the adaptation of the slot durations according to the sensors data rate requirements. The proposed FETRO MAC scheme counters the extra energy consumption by reducing the required transmission of several PHY-MAC overheads and offers the best trade-off between the effective throughput and overhead energy consumption per Kbps outcomes.

ACKNOWLEDGMENT

This work is supported in part by the European Union's Horizon 2020 Research and Innovation Program under Grant 668995, in part by the European Union Regional Development Fund through the framework of the Tallinn University of

Technology Development Program 2016–2022, and in part by the Estonian Research Council under Grant PUT-PRG424.

REFERENCES

- [1] "Smart Body Area Networks (SmartBAN); System Description," *ETSI TR 103 394 V1.1.1*, pp. 1–20, Jan 2018.
- [2] S. Movassaghi, M. Abolhasan, J. Lipman, D. Smith, and A. Jamalipour, "Wireless Body Area Networks: A Survey," *IEEE Communications Surveys Tutorials*, vol. 16, pp. 1658–1686, Mar 2014.
- [3] M. M. Alam, E. Ben Hamida, O. Berder, D. Menard, and O. Sentieys, "A Heuristic Self-Adaptive Medium Access Control for Resource-Constrained WBAN Systems," *IEEE Access*, vol. 4, pp. 1287–1300, 2016.
- [4] F. Ullah, A. H. Abdullah, O. Kaiwartya, and Y. Cao, "TraPy-MAC: Traffic Priority Aware Medium Access Control Protocol for Wireless Body Area Network," *Journal of Medical Systems*, vol. 41, p. 93, May 2017.
- [5] B. Liu, Z. Yan, and C. W. Chen, "Medium Access Control for Wireless Body Area Networks with QoS Provisioning and Energy Efficient Design," *IEEE Transactions on Mobile Computing*, vol. 16, pp. 422–434, Feb 2017.
- [6] B. Liu, Z. Yan, and C. W. Chen, "MAC protocol in wireless body area networks for E-health: challenges and a context-aware design," *IEEE Wireless Communications*, vol. 20, pp. 64–72, August 2013.
- [7] S. Rezvani and S. A. Ghorashi, "Context aware and channel-based resource allocation for wireless body area networks," *IET Wireless Sensor Systems*, vol. 3, pp. 16–25, March 2013.
- [8] M. Salayma, A. Al-Dubai, I. Romdhani, and Y. Nasser, "New dynamic, reliable and energy efficient scheduling for wireless body area networks (WBAN)," in *2017 IEEE International Conference on Communications (ICC)*, pp. 1–6, May 2017.
- [9] S. Bhandari and S. Moh, "A priority-based adaptive MAC protocol for wireless body area networks," *Sensors*, vol. 16, no. 3, p. 401, 2016.
- [10] M. A. Huq, E. Dutkiewicz, and R. Vesilo, "MEB MAC: Improved channel access scheme for medical emergency traffic in WBAN," in *2012 International Symposium on Communications and Information Technologies (ISCIT)*, pp. 371–376, Oct 2012.
- [11] "Smart Body Area Network (SmartBAN); Low Complexity Medium Access Control (MAC) for SmartBAN," *ETSI TS 103 325 V1.1.1*, pp. 1–36, Apr 2015.

- [12] Lihua Ruan, M. P. I. Dias, and E. Wong, "Time-optimized MAC for low latency and energy-efficient SmartBANs," in *2016 IEEE Conference on Computer Communications Workshops (INFOCOM WKSHPS)*, pp. 1089–1090, April 2016.
- [13] J. Ramis-Bibiloni and L. Carrasco-Martorell, "An energy-efficient and delay-constrained resource allocation scheme for periodical monitoring traffic in SmartBANs," in *2017 IEEE Biomedical Circuits and Systems Conference (BioCAS)*, pp. 1–4, Oct 2017.
- [14] R. Khan, M. M. Alam, T. Paso, and J. Haapola, "Throughput and Channel Aware MAC Scheduling for SmartBAN Standard," *IEEE Access*, pp. 1–1, 2019.
- [15] J. Haapola, P. Tuomas, and R. Kohno, "Method of improving channel utilization," Feb. 7 2017. US Patent 9,565,692.
- [16] D. Smith and L. W. Hanlen, *Channel Modeling for Wireless Body Area Networks*, pp. 25–55. 01 2015.
- [17] M. M. Alam and E. Ben Hamida, "Towards accurate mobility and radio link modeling for IEEE 802.15.6 wearable body sensor networks," in *2014 IEEE 10th International Conference on Wireless and Mobile Computing, Networking and Communications (WiMob)*, pp. 298–305, Oct 2014.
- [18] "Smart Body Area Network (SmartBAN); Enhanced Ultra-Low Power Physical Layer," *ETSI TS 103 326 V1.1.1*, pp. 1–13, Apr 2015.
- [19] *nRF52832: Multiprotocol Bluetooth low energy, ANT/ANT+ and 2.4GHz proprietary System-on-Chip*. Available at <https://www.nordicsemi.com/Products/Low-power-short-range-wireless/nRF52832>. [last accessed: Oct 2020].
- [20] M. T. I. ul Huque, K. S. Munasinghe, and A. Jamalipour, "Body Node Coordinator Placement Algorithms for Wireless Body Area Networks," *IEEE Internet of Things Journal*, vol. 2, no. 1, pp. 94–102, 2015.
- [21] R. Khan and M. M. Alam, "SmartBAN Performance Evaluation for Diverse Applications," in *EAI International Conference on Body Area Networks*, pp. 239–251, Springer, 2019.
- [22] M. M. Alam, E. B. Hamida, D. B. Arbia, M. Maman, F. Mani, B. Denis, and R. D'Errico, "Realistic Simulation for Body Area and Body-To-Body Networks," *Sensors*, vol. 16, no. 4, 2016.
- [23] R. Khan and M. M. Alam, "Joint PHY-MAC Realistic Performance Evaluation of Body-to-Body Communication in IEEE 802.15.6 and SmartBAN," in *2018 12th International Symposium on Medical Information and Communication Technology (ISMICT)*, pp. 1–6, March 2018.
- [24] M. M. Alam, H. Malik, M. I. Khan, T. Pardy, A. Kuusik, and Y. Le Moulec, "A Survey on the Roles of Communication Technologies in IoT-Based Personalized Healthcare Applications," *IEEE Access*, vol. 6, pp. 36611–36631, 2018.
- [25] S. Arnon, D. Bhastekar, D. Kedar, and A. Tauber, "A comparative study of wireless communication network configurations for medical applications," *IEEE Wireless Communications*, vol. 10, pp. 56–61, Feb 2003.
- [26] C. Chakraborty, B. Gupta, and S. Ghosh, "A Review on Telemedicine-Based WBAN Framework for Patient Monitoring," *Telemecine journal and e-health : the official journal of the American Telemedicine Association*, vol. 19, 07 2013.
- [27] S. Farshchi, A. Pesterev, P. H. Nuyujukian, I. Mody, and J. W. Judy, "Bi-Fi: An Embedded Sensor/System Architecture for Remote Biological Monitoring," *IEEE Transactions on Information Technology in Biomedicine*, vol. 11, pp. 611–618, Nov 2007.



Rida Khan (S'18) received the B.E. degree in Telecommunication Engineering from the Mehran University of Engineering and Technology, Pakistan, in 2013 and the M.Sc. degree in Electronics and Communication engineering from Istanbul Technical University, Turkey, in 2017. She is currently pursuing the Ph.D. degree in Information and Communication Technology with the Tallinn University of Technology, Estonia.

Her research interests include wearable wireless networks, network coding, and energy efficient modulation techniques. She is a Student Member of IEEE Standards Association and is currently serving as the Secretary of the Energy Efficient Communications Hardware (EECH) Standards Working Group. In addition, she is contributing the ETSI SmartBAN work item: DTR/SmartBAN-0014, "Applying SmartBANMAC (TS 103 325) for various use cases".



Muhammad Mahtab Alam (M'07, SM'19) received the M.Sc. degree in electrical engineering from Aalborg University, Denmark, in 2007, and the Ph.D. degree in signal processing and telecommunication from the University of Rennes I France (INRIA Research Center), in 2013. He joined the Swedish College of Engineering and Technology, Pakistan, in 2013, as an Assistant Professor. He did his postdoctoral research (2014–2016) at the Qatar Mobility Innovation Center, Qatar. In 2016, he joined as the European Research Area Chair and

as an Associate Professor with the Thomas Johann Seebeck Department of Electronics, Tallinn University of Technology, where he was elected as a Professor in 2018. Since 2019, he has been the Communication Systems Research Group Leader. His research focuses on the fields of wireless communications—connectivity, NB-IoT 5G/B5G services and applications, as well as low-power wearable networks for SmartHealth. He has over 15 years of combined academic and industrial multinational experiences while working in Denmark, Belgium, France, Qatar, and Estonia. He has several leading roles as principal investigator (PI) in multimillion Euros international projects funded by European Commission (H2020-ICT-2019-3, "951867", NATOSPS (G5482), Estonian Research Council (PRG424), Telia Industrial Grant. He is an author and co-author of more than 80 research publications. He is actively supervising a number of Ph.D. and Postdoc Researchers. He is also a contributor in two standardization bodies (ETSI SmartBAN, IEEE-GreenCT-EECH), including "Rapporteur" of work item: DTR/ SmartBAN-0014, "Applying SmartBAN MAC (TS 103 325) for various use cases." He is an Associate Editor of IEEE Access.



Mohsen Guizani (S'85, M'89, SM'99, F'09) received his B.S. (with distinction) and M.S. degrees in electrical engineering, and M.S. and Ph.D. degrees in computer engineering from Syracuse University, New York, in 1984, 1986, 1987, and 1990, respectively. He is currently a professor in the Computer Science and Engineering Department at Qatar University. Previously, he served in different academic and administrative positions at the University of Idaho, Western Michigan University, the University of West Florida, the University of Missouri-Kansas

City, the University of Colorado-Boulder, and Syracuse University. His research interests include wireless communications and mobile computing, computer networks, mobile cloud computing, security, and smart grid. He is currently the Editor-in-Chief of IEEE Network, serves on the Editorial Boards of several international technical journals, and is the Founder and Editor-in-Chief of the Wireless Communications and Mobile Computing journal (Wiley). He is the author of nine books and more than 500 publications in refereed journals and conferences. He has guest edited a number of Special Issues in IEEE journals and magazines. He has also served as a TPC member, Chair, and General Chair of a number of international conferences. Throughout his career, he received three teaching awards and four research awards. He also received the 2017 IEEE Communications Society WTC Recognition Award as well as the 2018 AdHoc Technical Committee Recognition Award for his contribution to outstanding research in wireless communications and ad hoc sensor networks. He was the Chair of the IEEE Communications Society Wireless Technical Committee and the Chair of the TAOS Technical Committee. He served as a IEEE Computer Society Distinguished Speaker and is currently an IEEE ComSoc Distinguished Lecturer. He is a Senior Member of ACM.

Appendix 7

R. Khan and M. M. Alam. Joint PHY-MAC realistic performance evaluation of body-to-body communication in IEEE 802.15. 6 and SmartBAN. In *12th International Symposium on Medical Information and Communication Technology (ISMICT)*, pages 1–6. IEEE, 2018

Joint PHY-MAC Realistic Performance Evaluation of Body-to-Body Communication in IEEE 802.15.6 and SmartBAN

Rida Khan, Muhammad Mahtab Alam
Thomas Johann Seebeck Department of Electronics
Tallinn University of Technology
Tallinn, Estonia
Email: {rikhan, muhammad.alam}@ttu.ee

Abstract—This paper presents the joint physical-medium access control (PHY-MAC) performance analysis of inter-BAN communication systems using realistic body-to-body (B2B) wireless channel model in IEEE 802.15.6 and smartBAN standards. The time-varying distances for the space-time B2B link variations are generated by real-time motion capture traces which are then introduced into already established B2B wireless channel model to give the actual path-loss values in dynamic environments. The SNR (Signal to Noise Ratio), BER (Bit Error Rate) and PER (Packet Error Rate) computations are briefly discussed to give an overview of the radio link modeling employed in the simulations. Using the mobility and the proposed radio link models, a more tangible performance assessment of B2B systems with IEEE 802.15.6 and SmartBAN specifications is achieved. Consequently, transmission power, packet length and data rate variations are investigated and the obtained results of packet reception rate (PRR) identify “head” as the best position to place the coordinator nodes for B2B communication.

Keywords—WBANs; inter-BAN; mobility modeling; radio link modeling; IEEE 802.15.6; SmartBAN; PRR.

I. INTRODUCTION

Wireless body area networks (WBANs) refer to a network of sensors (and/or actuators) placed on, inside or around the human body in order to serve a variety of emerging applications [1]. WBANs not only offer a wide scope of research and development but also represent a new generation of personal area networks, with their own unique set of challenges for implementation. The vital issues encountered by WBAN technology include the mobility of WBAN nodes, reliable low power operation, security and privacy of WBAN data and coexistence of multiple WBANs in the same environment [2]. WBANs have different types of communication scenarios based on the relative positions of WBAN nodes. The placement of communicating BAN nodes on multiple bodies is attributed to body-to-body Networks (BBNs) [3]. BBNs provide innovative solutions for a wide range of applications such as remote health care, precision monitoring of athletes, search and rescue operations in disastrous situations and coordination of soldiers on a battlefield [3].

Most of the efforts in channel characterization of WBANs have been dedicated to on-body communications and the contribution of research efforts in body-to-body (B2B) channel

modeling is quite limited. Nonetheless, many noteworthy contributions exist in the literature which attempt to discuss B2B channel characteristics [4]-[6]. But these channel models assume very limited mobility scenarios and for the realistic performance evaluation of BBNs on the higher layers such as medium access control (MAC) and network, accurate mobility and radio link modeling should be taken into account. A comprehensive analysis of the MAC layer performance evaluation is presented in [7] for on-body communication scenario, after measuring the channel characteristics when the nodes are placed on a walking subject. The notion of integrating realistic mobility traces with IEEE 802.15.6 channel models for accurate performance analysis of on-body communication at the MAC layer was proposed in [8]. Considering other co-located WBAN signals as interference and jointly exploiting on-body and B2B realistic channel models, a comprehensive MAC level performance analysis of intra-BAN communication is given in [9], [10]. However, to the best of our knowledge, no research work has been dedicated so far to study the joint physical-MAC (PHY-MAC) layer performance evaluation of inter-BAN communication systems under realistic/unrestricted mobility scenarios.

This research work is focused on the joint PHY-MAC performance assessment of B2B communication over a dedicated frequency channel with realistic channel models, using IEEE 802.15.6 and smartBAN standards specifications. The primary contributions of this paper include the identification of suitable positions to place the BAN coordinators for B2B communication and the examination of appropriate transmission power levels under different packet sizes and data rates. With the help of real time motion capture data, mobility traces are generated for multiple co-located BANs which provide dynamic distances with space-time variations. These dynamic distances serve to provide the realistic path-losses for B2B links under various mobility profiles (e.g., walking, running, standing etc.) using the B2B channel model derived by the real time measurement campaign. Subsequently, a detailed radio link modeling, based on the B2B channel characteristics, is implemented in which signal to noise ratio (SNR), bit error rate (BER) and packet error rate (PER) are computed using

the generated path-losses. The performance is examined in terms of packet reception rate (PRR) and the PHY-MAC layer specifications of both IEEE 802.15.6 as well as SmartBAN are considered in this context. A thorough investigation of PRR reveals that the relative coordinator nodes position is crucial for reliable data transmission over B2B links under real time dynamic environments.

The rest of the paper is arranged in the following way: section II elaborates the system model whereas IEEE 802.15.6 and smartBAN PHY-MAC layer parameters are described in section III. In section IV, the simulation results are presented and discussed while section V gives the concluding remarks.

II. SYSTEM MODEL

This section explains the underlying system model used in performance evaluation, as given:

A. B2B Channel Model

We use B2B channel model derived in [11], [12], using real time measurement campaigns under restricted mobility scenarios. This channel model provides channel gain, long term (LT) and short term (ST) fading components to estimate the path-loss values and the channel characteristics are a function of inter-body distance (d) and mutual body orientation (α) for various inter-BAN links. These links include head-to-head, belt-to-belt, wrist-to-wrist, head-to-belt, head-to-wrist, belt-to-wrist and vice versa, as depicted in Fig. 1, and are in-line with the links investigated in [11], [12]. In this model, shadowing effects by the bodies are primarily dealt with the distance and orientation-dependent channel gain, LT effects caused by the environment are represented by LT fading and ST fading is the outcome of the constructive and destructive interference resulting from multi-path propagation. According to [11], the distance (d) and orientation (α) dependent channel gain can be stated in dB as

$$G(d, \alpha) = G_0(\alpha) - 10n(\alpha)\log_{10}\left(\frac{d}{d_0}\right), \quad (1)$$

where n corresponds to the path-loss exponent and G_0 represents the gain at the reference distance d_0 , equal to 1m. $G_0(\alpha)$ and $n(\alpha)$ show different characteristics for various links between the relative node positions over different BANs. For example, n and G_0 do not exhibit mutual orientation dependence for head-to-head links between two different BANs so, distance-based channel gain can be calculated with the fixed values of n and G_0 . But mutual orientation α is crucial in determining n and G_0 values for other links mentioned previously. Further information about $G_0(\alpha)$ and $n(\alpha)$ calculations for obtaining the channel gains corresponding to other links can be found in [11]. The LT fading component in dB scale can be characterized with a zero-mean normal distribution [11] as

$$f(z_{LT}) = \frac{1}{\sigma_{LT}\sqrt{2\pi}} \exp\left(-\frac{z_{LT}^2}{2\sigma_{LT}^2}\right), \quad (2)$$

where z_{LT} is the LT fading component in dB and σ_{LT} is the standard deviation, whose values for different B2B links

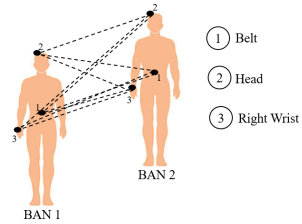


Fig. 1: B2B Channels.

are indicated in [11, Tab. 5]. The ST fading envelope can be typically represented by Rice distribution [11], [12], as given

$$f(z_{ST}) = \frac{z_{ST}}{\sigma^2} \exp\left(-\frac{z_{ST}^2 - A^2}{2\sigma^2}\right) I_0\left(\frac{z_{ST}A}{\sigma^2}\right), \quad (3)$$

where z_{ST} is the ST fading envelope, A is the non-centrality parameter and σ represents the scale parameter. Rice K -factor, the power ratio between the direct path and the multi-paths, is given as $K = \frac{A^2}{2\sigma^2}$. The characteristics of head-to-head links again do not show mutual orientation-dependence in estimating A and σ values whereas for other links, A and σ values are mainly described by mutual orientation α [11], [12]. A comprehensive discussion of ST fading properties for other B2B links is presented in [11], [12].

B. Realistic Mobility Modeling

The space-time variations of wireless links under unrestricted mobility are often not fully considered while developing path-loss models using measurement campaigns [8]. The B2B channel model proposed in [11], [12] assumes restricted mobility scenarios (close and far crossing and parallel walking) and can be enhanced to give more practical inter-BAN performance by the integration of dynamic distances with unrestricted mobility. This can be accomplished by exploiting real-time body motion capture traces which include various mobility scenarios (walking, running, sitting, exercising etc.) [8]. This real-time motion capture data when combined with geometrical transformation and analysis methods helps in actual performance evaluation of BANs and BBNs. The details of the entire process for intra-BAN communication are illustrated in [8], [10] but the major changes in algorithm to modify it for B2B communication are mentioned as

- The determined body constructed by motion capture traces is replicated in multiple human bodies for simulating dynamic inter-BAN links.
- The impact of body shadowing is mainly considered in the distance and orientation-dependent channel gain for the links between various relative node positions, as discussed in sub-section II-A, so, it is not important to characterize such links as LOS or NLOS. But wrist-related channels can be line of sight (LOS) or non-line of sight (NLOS) for the same body orientation because for the same α , the two nodes may either be shadowed or not by the torso [11], [12]. Therefore, geometrical analysis is

applied to ensure the accuracy of link types in inter-BAN wrist-related channels. In this case, the intersection of the link with single or multiple human body torso cylinders declares the given B2B link as NLOS for the wrist-related channels.

- Space-time varying inter-BAN links and mobility traces are generated to give the appropriate dynamic distances for the B2B channels mentioned in sub-section II-A. The mutual orientation between two separate BANs is taken the same throughout the mobility trace duration since a coordinated movement scenario is simulated in this paper and the variations in α are within a range of 10° . Furthermore, the classification of dynamic link types as LOS or NLOS is performed for B2B wrist-related channels.

After obtaining the dynamic distances and link types for the given inter-BAN scenario, the channel behavior is accurately modeled with unrestricted mobility. The inter-BAN dynamic distances and mutual orientation are used to obtain channel gain values while ST fading parameters for different links are a function of mutual orientation only. The channel gain, LT fading and ST fading for wrist-related channels are computed differently for LOS and NLOS link types so, the knowledge of dynamic link types is important in this context. It should be noted that mobility modeling provides higher and more accurate space-time variations which help in estimating more accurate path-loss results in comparison to the restricted mobility based channel models [8], [10] for B2B channels. Subsequently, the obtained path-loss values are utilized in radio link modeling to calculate the SNR, BER and PER. The entire system model with mobility modeling, B2B channel modeling and radio link modeling is illustrated in Fig. 2.

C. Radio Link Modeling

The realistic mobility modeling of inter-BAN communication and the resultant space-time varying channels are followed by the significance of accurate radio link modeling, which

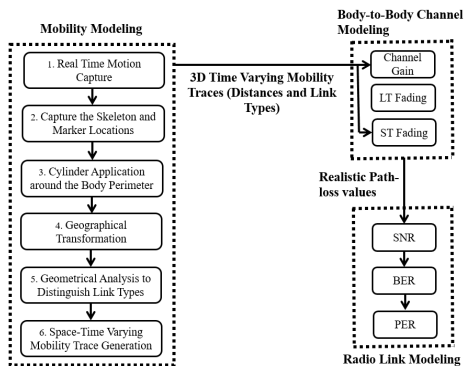


Fig. 2: Mobility, channel and radio link modeling for B2B communication.

includes SNR, BER and PER evaluation. The PER estimation using threshold based method is not an accurate approach [8], so an extensive approach and a practical method is presented in this sub-section to calculate PER for B2B links. The SNR between the two nodes i and j on two different BANs over the time index t can be written as

$$SNR_{i,j,t}^{dB} = P_{Tx}^{dBm} + PL_{i,j,t}^{dB} - P_N^{dBm}, \quad (4)$$

where P_{Tx} is the transmit power, P_N is the noise power and $PL_{i,j,t}^{dB}$ is the path-loss between i and j over the time t .

The exact formulation of the energy per bit to noise power spectral density ratio E_b/N_0 and BER is done depending upon the frequency and exact data rate at the physical layer. According to IEEE 802.15.6 physical layer specifications, differential binary phase shift keying (DBPSK) modulation is used for low data rates and differential quadrature phase shift keying (DQPSK) modulation is employed for high data rates at 2.45 GHz frequency [1]. The value of E_b/N_0 in dB, based on the current $SNR_{i,j,t}^{dB}$, bandwidth BW in Hz and data rate R in bps can be written as

$$E_b/N_0[dB] = SNR_{i,j,t}^{dB} + 10\log_{10}\left(\frac{BW}{R}\right), \quad (5)$$

Since Rice type ST fading is assumed in the channel model, therefore the corresponding DBPSK BER for low data rate between the inter-BAN links i and j over the time t can be calculated as

$$BER_{i,j,t}^{DBPSK} = \frac{K+1}{2(1+K+\Gamma)} \exp\left(-\frac{K\Gamma}{1+K+\Gamma}\right). \quad (6)$$

where Γ is the average SNR given as $\Gamma = E\{z_{ST}^2\} \frac{E_b}{N_0}$ [13]. The DQPSK BER expression for high data rate is derived using the Rice density equation as a function of instantaneous SNR γ_b and the DQPSK additive white Gaussian noise (AWGN) error equation which are respectively written as

$$p(\gamma_b) = \frac{K+1}{\Gamma} \exp\left(-\frac{\gamma_b(K+1)+K\Gamma}{\Gamma}\right) I_0\left(\sqrt{\frac{4(K+1)K\gamma_b}{\Gamma}}\right), \quad (7)$$

$$P_e(\gamma_b) = Q\left(\sqrt{1.112\gamma_b}\right). \quad (8)$$

Substituting $p(\gamma_b)$ and $P_e(\gamma_b)$ into the average error probability expression $P_e = \int_0^\infty P_e(\gamma_b)p(\gamma_b)d(\gamma_b)$ [13] and integrating using the Chernoff bound for Gaussian Q-function $Q(\gamma_b) \leq \frac{1}{2}\exp^{-\frac{\gamma_b}{2}}$ [14], the upper bound on the respective DQPSK BER for high data rate between the inter-BAN links i and j over the time t can be described as

$$BER_{i,j,t}^{DQPSK} \leq \frac{\Gamma}{2(1+K+0.556\Gamma)} \left(\frac{K+1}{\Gamma}\right) \exp\left(-K + \frac{K(K+1)}{1+K+0.556\Gamma}\right). \quad (9)$$

The smartBAN standard defines the usage of Gaussian minimum shift keying (GMSK) with the bandwidth-bit period product (BT) of 0.5 and modulation index (h) of 0.5 as the key modulation technique at the physical layer [15]. The upper bound on GMSK BER under Rice fading is acquired using the procedure discussed above and taking $P_e(\gamma_b)$ as

$$P_e(\gamma_b) = Q\left(\sqrt{2\epsilon\gamma_b}\right), \quad (10)$$

where ϵ is the GMSK constant and for BT of 0.5 is equal to 0.79 [16]. The upper bound on the corresponding GMSK BER between the given B2B links i and j over the time t is therefore mentioned as

$$BER_{i,j,t}^{GMSK} \leq \frac{\Gamma}{2(1+K+0.79\Gamma)} \left(\frac{K+1}{\Gamma}\right) \exp\left(-K + \frac{K(K+1)}{1+K+0.79\Gamma}\right). \quad (11)$$

Consequently, the PER is computed based on the packet length N in bits and the adequate $BER_{i,j,t}$ expression as

$$PER_{i,j,t} = 1 - (1 - BER_{i,j,t})^N. \quad (12)$$

Finally, the obtained PER values which are based on the dynamic space-time dependent channel measurements and the accurate radio link modeling, are given to the high level packet-oriented simulation environment for the MAC layer performance evaluation.

III. PHY/MAC LAYER PARAMETERS

In this work, the joint PHY-MAC layer performance evaluation in terms of both IEEE 802.15.6 and smartBAN standards is performed. Therefore, this section highlights the physical and the MAC layer specifications of IEEE 802.15.6 and smartBAN used in the PRR simulations.

A. IEEE 802.15.6 PHY/MAC Layer

We consider time division multiple access (TDMA)-based scheduled access mechanism with beacon-enabled superframe format [1] since the priority is the investigation of the impact of accurate channel modeling on MAC layer performance. The variable-length MAC frame body is appended with MAC frame header and frame check sequence (FCS) to form physical layer service data unit (PSDU), which is spread using the spreading factor determined by the data rate. The resulting PSDU is added with physical layer convergence protocol (PLCP) preamble for timing synchronization, channel offset recovery and packet detection and with PLCP header for conveying information about the physical and MAC parameters required at the receiver side. The PLCP header spreading is additionally done and the combination of PLCP preamble, PLCP header and PSDU forms a physical layer protocol data unit (PPDU) which represents the information transmitted through the propagation medium [17]. Guard duration is used to separate PPDU's sent by different BBN nodes in different time slots. The additional information on guard duration formulation using the synchronization interval, inter-frame spacing and turnaround time, as well as the maximum

packet transmission duration and packet size calculations can be found in [1], [17].

B. SmartBAN PHY/MAC Layer

Again TDMA-based scheduled access method is used in this context and each time slot comprises of data frame transmission and ACK frame transmission periods separated by inter-frame spacing. Each BBN node transmits its data in data frame transmission period while the receiving node shall send an ACK frame (successful transmission) or a NACK frame (unsuccessful transmission) in the ACK frame transmission time which is ended with inter-frame spacing at the end of the slot [18].

On the MAC layer, a 56 bit MAC header and 16 bit frame parity are added to the MAC frame body to generate MAC protocol data unit (MPDU). Since we assume uncoded data transmissions for both IEEE 802.15.6 and smartBAN, MPDU will be the same as PSDU. The PSDU is further appended with 16 bit PLCP preamble and 40 bit PLCP header fields to create a PPDU structure [15]. A complete discussion on the smartBAN physical and MAC layer specifications and parameters can be explored in [15], [18].

IV. JOINT PHY-MAC PERFORMANCE RESULTS

This sections presents a thorough analysis of the results obtained using the system model and PHY/MAC layer parameters discussed in Section II and III respectively.

A. Simulation Setup

We assume three different BANs with one of them being the leader (BAN1) and the rest two being the followers (BAN2 and BAN3), receiving information from their leader for the coordinated movements over a dedicated frequency channel. Note that a separate frequency channel is used for on-body communication within each BAN and here different coordinator node positions for inter-BAN communication are investigated. The mobility scenarios considered in the simulations include walking, running, sitting and standing and therefore, represent the primary movements made in the mission critical operations and precise monitoring during sports activities. The node positions for all the BANs examined in simulations consist of head (H), belt (B) and right wrist (W). Each coordinator node on the leader BAN sends its information to all the other coordinator nodes placed on the follower BANs in its assigned time slot with an objective to identify the best coordinator

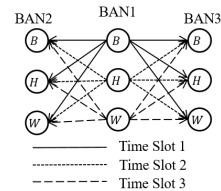


Fig. 3: TDMA for B2B communication.

location, as shown in Fig. 3. For IEEE 802.15.6 standard, MAC payload sizes of 16, 128 and 256 bytes as well as both low data rate (LDR, 121.4 kbps) and high data rate (HDR, 971.4 kbps) are considered. Whereas smartBAN assumes a data rate of 1000 kbps for all payload sizes [15] and with no data transmission repetition, MAC payload sizes of 16, 128 and 250 bytes are taken.

B. Simulation Results

The main purpose of this work is the investigation of the suitable coordinator nodes positions in inter-BAN communication using PRR as the performance criteria. For this purpose, statistical results including mean, standard deviation and correlation coefficient of path-losses corresponding to different transmitter-receiver location combinations are listed in Table I. The results are demonstrated for the running scenario since it involves the highest level of mobility. It can be seen that for every transmitter node location, the mean path-loss values are the minimum when the receiver node is placed on head. Moreover, the positioning of the transmitter node on head also results in the reduction of mean path-loss values as compared to the other coordinator positions. Furthermore, the high correlation coefficient values indicate

TABLE I: Statistical Analysis of the Channel Model with Mobility Modeling (Running Scenario)

Link Type	Mean	Standard Deviation	Correlation Coefficient
Belt-to-Belt	59.25	3.18	0.23
Belt-to-Head	54.50	2.94	0.17
Belt-to-Wrist	71.36	3.97	0.20
Head-to-Belt	54.35	2.90	0.14
Head-to-Head	42.15	2.72	0.17
Head-to-Wrist	66.41	17.09	0.67
Wrist-to-Belt	74.65	3.91	0.20
Wrist-to-Head	63.90	13.92	0.55
Wrist-to-Wrist	60.83	3.37	0.25

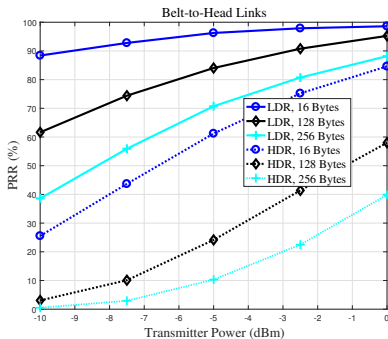


Fig. 4: PRR versus transmission power level results for belt-to-head links in BBN, $N = 16, 128$ and 256 bytes, LDR (121.4 kbps) and HDR (971.4 kbps).

that the unrestricted mobility-based path-loss model keeps the track of high mobility and temporal variations for B2B links as well, in the same manner as indicated in [8] for on-body links. It is also noticeable that the statistical values are not very different when the transmitter and the receiver node positions are interchanged. Using these observations as the basis, the MAC level performance results are further narrowed down to the links which include head as the receiver node position since these links assume comparatively lesser mean path-losses.

Fig. 4, Fig. 5 and Fig. 6 summarize the PRR results of belt-to-head, head-to-head and wrist-to-head links respectively for different transmission power levels using IEEE 802.15.6 specifications. It is quite obvious that head-to-head links outperform all the other links while wrist-to-head links give the worst performance. The PRR values degrade for all link types if the packet size and the data rate are increased. For belt-to-head links, the acceptable performance of equal or above 90 percent PRR is achieved only when 16 byte payload is sent with LDR at any given transmission power level. 128 byte payload also gives adequate performance when transmitted at higher power levels with LDR. But for head-to-head links, the PRR performance is considerably improved in comparison to the belt-to-head links. For LDR, the transmission of different payload sizes is permissible even at the lower transmission power levels. High transmission power and small payload size should be used when data is transmitted at the high rate. For wrist-to-head links, a PRR above 90 percent is achieved only at the higher transmission power levels with lower payload sizes and data rate.

Finally, the PRR performance evaluation of smartBAN is shown in Fig. 7 for the above mentioned link types. Head-to-head links again give the best results among all the link types with smartBAN specifications as well. Data can be sent with all payload sizes at almost all transmission power levels over head-to-head links. For belt-to-head links, payload of 16 bytes can be transmitted at the transmission power level of above -5 dB while the payload size of 128 bytes requires higher

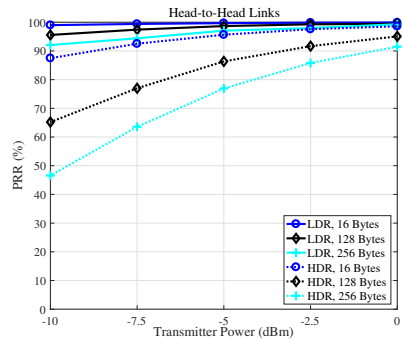


Fig. 5: PRR versus transmission power level results for head-to-head links in BBN, $N = 16, 128$ and 256 bytes, LDR (121.4 kbps) and HDR (971.4 kbps).

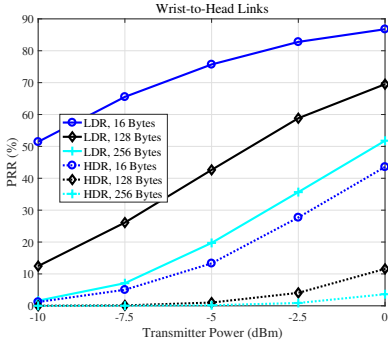


Fig. 6: PRR versus transmission power level results for wrist-to-head links in BBN, $N = 16, 128$ and 256 bytes, LDR (121.4 kbps) and HDR (971.4 kbps).

transmission power levels. Finally, wrist-to-head links do not contribute to any transmission with acceptable performance for any payload size or transmission power and might require encoded or repetitive transmissions.

V. CONCLUSION

Recently developed channel models through measurement campaigns are integrated into realistic mobility and radio link modeling and the joint PHY-MAC performance evaluation of B2B communication for IEEE 802.15.6 and smartBAN standards specifications is performed. The usage of mobility modeling facilitates more accurate performance analysis of time-varying inter-BAN links. The presented results indicate that the placement of coordinators on the head significantly reduces the required transmission power levels for inter-BAN communication, even at high data rate and payload sizes.

ACKNOWLEDGMENT

This research was supported by the Estonian Research Council through the Institutional Research Project IUT19-11, and by the Horizon 2020 ERA-chair Grant Cognitive Electronics COEL H2020-WIDESPREAD-2014-2 (Agreement number: 668995; project TTU code VFP15051).

REFERENCES

- [1] A. Astrin et al., "IEEE Standard for Local and Metropolitan Area Networks Part 15.6: Wireless Body Area Networks: IEEE Std. 802.15.6-2012," February 2012.
- [2] S. Movassaghi, M. Abolhasan, J. Lipman, D. Smith, and A. Jamalipour, "Wireless Body Area Networks: A Survey," *IEEE Commun. Surveys and Tutorials*, vol. 16, no. 3, pp. 1658-1686, Jan. 2014.
- [3] M. M. Alam and E.B. Hamida, "Surveying Wearable Human Assistive Technology for Life and Safety Critical Applications: Standards, Challenges and Opportunities," *Sensors*, vol. 14, no. 5, pp. 9153-9209, 2014.
- [4] S. L. Cotton and W. G. Scanlon, "Channel Characterization for Single- and Multiple-Antenna Wearable Systems Used for Indoor Body-to-Body Communications," *IEEE Trans. on Antennas Propag.*, vol. 57, no. 4, pp. 280-290, Apr. 2009.
- [5] Y. Wang, I. B. Bonev, J. O. Nielsen, I. Z. Kovacs, and G. F. Pedersen, "Characterization of the Indoor Multi antenna Body-to-Body Radio Channel," *IEEE Trans. on Antennas and Propag.*, vol. 57, no. 4, pp. 972-979, 2009.

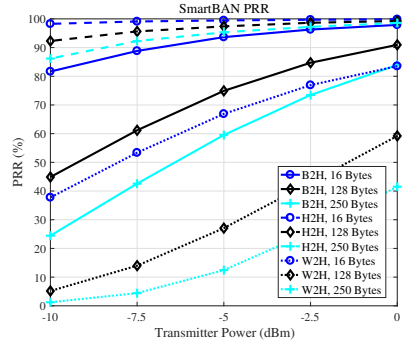


Fig. 7: PRR versus transmission power level results for smartBAN, $N = 16, 128$ and 250 bytes, belt-to-head (B2H), head-to-head (H2H) and wrist-to-head (W2H) links.

- [6] N. Bhargav, S. L. Cotton, and D. B. Smith, "An Experimental-Based Analysis of Inter-BAN Co-Channel Interference Using the κ - μ Fading Model," *IEEE Trans. on Antennas and Propag.*, vol. 65, no. 2, pp. 983-988, Dec. 2016.
- [7] R. Rosini, F. Martelli, M. Maman, R. D'Errico, C. Buratti, and R. Verdono, "On-body area networks: from channel measurements to MAC layer performance evaluation," in *Proc. 18th European Wireless Conference*, Poznan, Poland, April 2012.
- [8] M. M. Alam and E. B. Hamida, "Towards Accurate Mobility and Radio Link Modeling for IEEE 802.15.6 Wearable Body Sensor Networks," in *Proc. 10th WiMob Conference*, Oct. 2014, pp. 298-305.
- [9] M. Maman, F. Mani, B. Denis, and R. D'Errico, "Evaluation of multiple coexisting Body Area Networks based on realistic on-body and body-to-body channel models," in *Proc. 10th Int. Symp. on Medical Info. and Commun. Tech.*, Mar. 2016, pp. 1-5.
- [10] M. M. Alam, E. B. Hamida, D. B. Arbia, M. Maman, F. Mani, B. Denis, and R. D'Errico, "Realistic Simulation for Body Area and Body-To-Body Networks," *Sensors*, vol. 16, no. 4, art. 561, 2016.
- [11] F. Mani and R. D'Errico, "A Spatially Aware Channel Model for Body-to-Body Communications," *IEEE Trans. on Antennas and Propag.*, vol. 64, no. 8, pp. 3611-3618, Aug. 2016.
- [12] F. Mani and R. D'Errico, "Short term fading spatial dependence in indoor body-to-body communications," in *Proc. IEEE 26th Annual Int. Symp. on Pers. Indoor and Mobile Radio Commun. (PIMRC)*, Aug. 2015, pp. 171-175.
- [13] F. Ziong, "Digital Modulation Techniques." Artech House Inc., 2006, p. 553-559.
- [14] S. H. Chang, P. C. Cosman, and L. B. Milstein "Chernoff-Type Bounds for the Gaussian Error Function," *IEEE Trans. on Commun.*, vol. 59, no. 11, pp. 2939-2944, Nov. 2012.
- [15] W. H. Chin, H. Tanaka, T. Nakanishi, T. Paso, and M. Hamalainen, "An Overview of ETSI TC SmartBAN's Ultra Low Power Physical Layer," in *Proc. IEEE 9th Int. Symp. on Medical Info. and Commun. Tech.*, Mar. 2015, pp. 6-9.
- [16] R. Anane, M. Bouallegue, K. Raoof, and R. Bouallegue, "Achieving Energy Efficient and Reliable Communication in WSN with Coded GMSK System under various Channel Conditions," in *Proc. IEEE Int. Conf. on Wireless Comm. and Mobile Computing.*, Aug. 2015, pp. 769-775.
- [17] M. M. Alam and E. B. Hamida, "Strategies for Optimal MAC Parameters Tuning in IEEE 802.15.6 Wearable Wireless Sensor Networks," *Journal of Medical Systems*, vol. 39, no. 9, pp. 106-120, Aug. 2015.
- [18] T. Paso, H. Tanaka, M. Hamalainen, W. H. Chin, R. Matsuo, S. Subramani, and J. Haapola, "An Overview of ETSI TC SmartBAN MAC Protocol," in *Proc. IEEE 9th Int. Symp. on Medical Info. and Commun. Tech.*, Mar. 2015, pp. 10-14.

Appendix 8

R. Khan and M. M. Alam. Body-to-body communication: Applications, system design aspects and performance evaluation. In *12th International Symposium on Medical Information and Communication Technology (ISMICT)*, pages 1-2. IEEE, 2018

Body-to-Body Communication: Applications, System Design Aspects and Performance Evaluation

Rida Khan, Muhammad Mahtab Alam
Thomas Johann Seebeck Department of Electronics
Tallinn University of Technology, Tallinn, Estonia
Email: {rikhan, muhammad.alam}@ttu.ee

Abstract—Wireless body area networks (WBANs) contain set of wearable and/or implantable sensors that are located in, on, around or in immediate proximity to the human body. The fundamental concept of WBANs can be developed into future body-to-body (B2B) communication systems by attaining the existence of multiple co-located WBANs as well as their mutual coordination and communication. The huge scope of challenges and potential applications (i.e., sports and fitness, rescue and critical operations etc.) associated with B2B communication has led to many publications. On the other hand, a thorough characterization of B2B propagation channels is the foremost step whether the purpose is minimizing the interference from neighboring WBANs or maintaining a good quality communication link between adjacent WBANs. Therefore, we highlight different candidate applications of B2B communication systems and present an investigative overview of various B2B channel models. Moreover, several physical (PHY) and medium access control (MAC) parameters are enlisted and discussed with regards to their impact on packet reception rate (PRR) performance in B2B communication systems.

Keywords—WBANs; B2B; Application scenarios; channel models; PHY and MAC parameters.

I. OVERVIEW

Wireless body area networks (WBANs) are envisioned to play a significant role in providing technological assistance for improving quality of life. WBANs are attributed to the body-centric wireless communication scenario in which one of the sensor nodes is positioned inside/on human body [1]. Depending upon the placement of WBAN nodes, different WBAN communication scenarios are defined and among them, body-to-body (B2B) communication scenario refers to the placement of WBAN nodes on multiple bodies. In B2B communication, the coordinator node serves as a gateway that shares communication data with other WBANs [2]. The new paradigm of B2B communication can facilitate multitudes of applications such as ubiquitous health (U-health) monitoring, rescue and critical operations, sports and fitness etc. In this context, we provide an overview of various B2B communication prospective applications. With propagation channel modeling being the first step in evaluating a communication system quality, we also discuss B2B communication channel characterization in different perspectives. In addition, B2B communication system design aspects such as physical (PHY) and medium access control (MAC) layer parameters are also discussed in terms of their effect on packet reception rate (PRR) performance.

II. APPLICATIONS

B2B communication can serve in many different emerging applications of WBANs to ensure real social benefits. The examples span both medical and non-medical (Consumer Electronics) categories, as illustrated in Fig. 1. Wearable medical applications of WBAN like sleep monitoring, cardiovascular disease detection, remote patient monitoring, telemedicine systems etc can benefit from B2B communication not only to support generic health-monitoring in case of poor channel conditions from coordinator to access point but also to realize the notion of future ubiquitous healthcare systems for supporting distant patients. Another application related to medical domain can be precise sports monitoring, involving the provision of real time feedback to prevent sport-related injuries as well as the facilitation of athletes' vital signs monitoring. From non-medical applications' view point, mission critical operations in the unavailability or failure of network infrastructure can also utilize B2B communication. Another non-medical application of B2B communication can be activity, location and fatigue monitoring of soldiers in the battlefield to assess their readiness.

III. CHANNEL MODELING

B2B propagation channels are subjected to many complexities due to mobility at both ends of the communication link and possible dual-body shadowing events. Therefore, robust

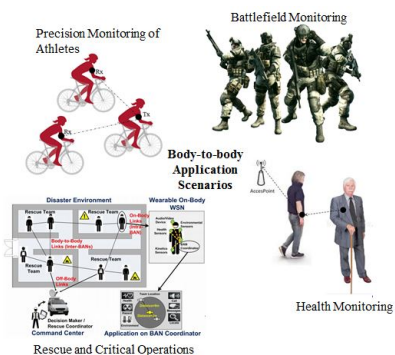


Fig. 1: Body-to-body network emerging applications.

TABLE I: Channel Modeling Approach

Real Time Measurements	Analytically Derived	Simulation Based
[3][5][6][7][8][9]		[4]

TABLE II: Mobility Profile

No Mobility	Restricted Mobility	Unrestricted Mobility
[4]	[3][5][6][8][9]	[7]

hardware and communication protocols are necessary to be proposed and designed for meeting the stringent efficiency requirements associated with B2B communication. This leads to the significance of appropriate B2B propagation channel modeling to develop a better understanding of performance evaluation at the higher layers. Table I, II and II summarize information about different B2B communication channel models, in terms of approaches considered in their proposal and development, mobility scenarios and channel characterization using different distributions and parameters. It can be observed that majority of the B2B channel models, although based on real time measurement campaigns, assume restricted mobility scenarios which might not be suitable for realistic performance assessment. Therefore, we integrate the channel model proposed in [3] with biomechanical mobility modeling tool [10] for introducing space-time varying distances and link types, i-e; line of sight (LOS) or non line of sight (NLOS), to simulate real time PHY-MAC performance in terms of PRR. More details about the biomechanical mobility modeling can be explored in [10].

IV. PHY/MAC LAYER PARAMETERS

Fig. 2 depicts the PHY-MAC performance results, interpreted using PRR, as function of payload length at the MAC layer and data transmission rate when the communicating WBAN nodes are located on different human bodies. The transmission power is taken to be 0 dBm and the mobility modeling includes different body postures like walking, running, sitting and standing. IEEE 802.15.6 standard parameters with TDMA-based scheduled access mechanism are used in the simulations and three node positions, that is head, belt

TABLE III: Channel Characterization

Path Loss	Long Term Fading	Short Term Fading	All Presented in One
[3] Distance and Orientation Dependent	[3] Zero mean Normal Distribution (dB)	[3] Rice Distribution	[5] κ - μ Distribution
[6] Distance and Orientation Dependent	[6] Mixture of two one-dimensional Normal Distributions	[6] Rice Distribution	[7] κ - μ Distribution
[8] Distance Dependent	[8] Lognormal Distribution	[8] Rice Distribution	
	[8] Gamma Distribution	[9] Rice Distribution	

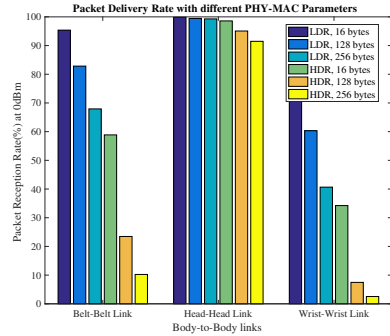


Fig. 2: PRR with different PHY-MAC Parameters.

and wrist are investigated. The results are shown for 16, 128 and 256 bytes of MAC payload while being transmitted at both low data rate (LDR) and high data rate (HDR) over belt-belt, head-head and wrist-wrist links. The results indicate a general behavior of decrease in PRR performance with increase in payload size and data rate for all given B2B links but the phenomenon is more obvious for wrist-wrist links in comparison to the more stable head-head links.

REFERENCES

- [1] A. Astrin et al., "IEEE Standard for Local and Metropolitan Area Networks Part 15.6: Wireless Body Area Networks: IEEE Std. 802.15.6-2012," February 2012.
- [2] M. M. Alam and E.B. Hamida, "Surveying Wearable Human Assistive Technology for Life and Safety Critical Applications: Standards, Challenges and Opportunities" *Sensors*, vol. 14, no. 5, pp. 9153-9209, 2014.
- [3] F. Mani and R. D'Errico, "A Spatially Aware Channel Model for Body-to-Body Communications," *IEEE Trans. on Antennas and Propag.*, vol. 64, no. 8, pp. 3611-3618, Aug. 2016.
- [4] S. L. Cotton, W. G. Scanlon, and P. S. Hall, "A Simulated Study of Co-channel Inter-BAN Interference at 2.45 GHz and 60 GHz, in *2010 European Wireless Tech. Conference*, Sept. 2012, pp. 61-64.
- [5] N. Bhargav, S. L. Cotton, and D. B. Smith, "An Experimental-Based Analysis of Inter-BAN Co-Channel Interference Using the κ - μ Fading Model," *IEEE Trans. on Antennas and Propag.*, vol. 65, no. 2, pp. 983-988, Dec. 2016.
- [6] R. Rosini, R. Verdone, and R. D'Errico, "Body-to-Body Indoor Channel Modeling at 2.45 GHz," *IEEE Trans. on Antennas and Propag.*, vol. 62, pp. 5807-5819, Nov. 2014.
- [7] S. L. Cotton and W. G. Scanlon, "Channel Characterization for Single- and Multiple-Antenna Wearable Systems Used for Indoor Body-to-Body Communications," *IEEE Trans. on Antennas Propag.*, vol. 57, no. 4, pp. 280-290, Apr. 2009.
- [8] S. L. Cotton, A. McKernan, and W. G. Scanlon, "Received signal characteristics of outdoor body-to-body communications channels at 2.45 GHz, in *Loughborough Antennas and Propagation Conference*, Nov. 2011.
- [9] Y.I. Nechayev, Z.H. Hu, and P. Hall, "Fading of the Transmission channel between two Wireless Body Area Networks in an Office at 2.45 GHz and 5.8 GHz, in *Proc. of LAPC2010 - Loughborough Antennas and Propagation Conference*, Nov. 2010.
- [10] M. M. Alam and E. B. Hamida, "Towards Accurate Mobility and Radio Link Modeling for IEEE 802.15.6 Wearable Body Sensor Networks, in *Proc. 10th WiMob Conference*, Oct. 2014, pp. 298-305.

Curriculum Vitae

1. Personal data

Name Rida Khan
Nationality Pakistani

2. Contact information

Address Tallinn University of Technology, School of Information Technology,
Thomas Johann Seebeck Department of Electronics,
Ehitajate tee 5, 19086 Tallinn, Estonia
E-mail rikhan@ttu.ee

3. Education

2017–2021 Tallinn University of Technology,
Thomas Johann Seebeck Department of Electronics,
PhD studies
2014–2016 Istanbul Technical University,
Department of Electronics and Communication Engineering,
MSc Telecommunication Engineering
2009–2012 Mehran University of Engineering and Technology,
Department of Telecommunication Engineering,
BE Telecommunication Engineering

4. Language competence

Urdu native
English fluent
Turkish fluent
Estonian basic

5. Professional employment

2020– Present Ericsson Tallinn, Product Integration Engineer
2017–2018 Tallinn University of Technology, Early Stage Researcher
2014–2016 Istanbul Technical University, Research Assistant

6. Voluntary work

2018–Present Secretary in IEEE Standard (PARs P.1923 and P.1924)

7. Publications

1. R. Khan and M. M. Alam. SmartBAN performance evaluation for diverse applications. In *EAI International Conference on Body Area Networks*, pages 239–251. Springer, 2019
2. M. Hämäläinen, L. Mucchi, M. G. Genet, T. Paso, J. Farserotu, H. Tanaka, D. Anzai, L. Pierucci, R. Khan, M. M. Alam, and P. Dallemagne. ETSI SmartBAN architecture: the global vision for smart body area networks. *IEEE Access*, 7(10):100–107, 2020

3. R. Khan and M. M. Alam. Joint throughput and channel aware MAC scheduling for SmartBAN. In *EAI International Conference on Body Area Networks*, pages 49–64, 2018
4. R. Khan, M. M. Alam, T. Paso, and J. Haapola. Throughput and channel aware MAC scheduling for SmartBAN standard. *IEEE Access*, 7:63133–63145, 2019
5. R. Khan, M. M. Alam, and A. Kuusik. Channel prediction based enhanced throughput and channel aware MAC in SmartBAN standard. In *2019 16th International Symposium on Wireless Communication Systems (ISWCS)*, pages 463–468. IEEE, 2019
6. R. Khan, M. M. Alam, and M. Guizani. A flexible enhanced throughput and reduced overhead (FETRO) MAC protocol for ETSI SmartBAN (Accepted). *IEEE Transactions on Mobile Computing (Early Access)*
7. R. Khan and M. M. Alam. Joint PHY-MAC realistic performance evaluation of body-to-body communication in IEEE 802.15. 6 and SmartBAN. In *12th International Symposium on Medical Information and Communication Technology (ISMICT)*, pages 1–6. IEEE, 2018
8. R. Khan and M. M. Alam. Body-to-body communication: Applications, system design aspects and performance evaluation. In *12th International Symposium on Medical Information and Communication Technology (ISMICT)*, pages 1–2. IEEE, 2018

Elulookirjeldus

1. Isikuandmed

Nimi Rida Khan
Kodakondsus Pakistani

2. Kontaktandmed

Address Tallinna Tehnikaülikool, Infotehnoloogia teaduskond,
Thomas Johann Seebecki elektroonikainstituut,
Ehitajate tee 5, 19086 Tallinn, Eesti
E-post rikhan@ttu.ee, rida.khanoct@yahoo.com

3. Haridus

2017–2021 Tallinna Tehnikaülikool
Doktoriõpe, elektroonika ja telekommunikatsioon
2014–2016 Istanbuli tehnikaülikool
Magister, elektroonika ja telekommunikatsioon
2009–2012 Mehran University of Engineering and Technology
Bakalaureus, telekommunikatsioon

4. Keelteoskus

Urdu keel emakeel
Inglise keel kõrgtase
Turgi keel kõrgtase
Eesti keel algtase

5. Teenistuskäik

2020– ... Ericsson Tallinn, Insener
2017–2018 Tallinna Tehnikaülikool, Nooremteadur
2014–2016 Istanbuli tehnikaülikool, Teadusassistent

ISSN 2585-6901 (PDF)
ISBN 978-9949-83-663-5 (PDF)